MDOT

Bridge Structural Analyses for Staged Construction and Constructability Reviews

FINAL REPORT – MAY 2020

Department of Civil & Environnemental Engineering
College of Engineering
Wayne State University

Intentionally left blank

1. Report No. SPR-1691	2. Government Accession No. N/A	3. MDOT Project Manager Peter Jansson P.E.	
4. Title and Subtitle Bridge Structural Analyses for Staged Construction and Constructability Reviews		**5. Report Date** 05/31/2020	
		6. Performing Organization Code N/A	
7. Author(s) Haluk M. Aktan, Ph.D., P.E. and Upul Attanayake, Ph.D., P.E.		**8. Performing Org. Report No.** N/A	
9. Performing Organization Name and Address Wayne State University College of Engineering 5050 Anthony Wayne Drive Detroit, MI 48202		**10. Work Unit No. (TRAIS)** N/A	
		11. Contract No. 2016-0070	
		11(a). Authorization No. Z3	
12. Sponsoring Agency Name and Address Michigan Department of Transportation Research Administration 8885 Ricks Road P.O. Box 30049 Lansing, MI 48909		**13. Type of Report & Period Covered** Final Report 7/01/2017 - 05/31/2020	
		14. Sponsoring Agency Code N/A	
15. Supplementary Notes			

16. Abstract

Constructability requirements need to be addressed during the design of highway bridges. However, the typical design practice is to consider the limit state stresses in structural elements of a bridge that is completed as per the project specifications. This process leaves the responsibility of analysis and design for construction stages to a contractor since the means and methods for construction are developed by the contractor. Yet, the agency engineer needs to review and approve the contractor submittals. A lack of a comprehensive program for (i) fabricated structural element quality evaluation and (ii) structural element and partially erected structural system response analysis during construction by both parties may lead to rejection by the agency, project delays, change requests by the contractor, and sometimes, to construction safety and durability issues. This report describes constructability analysis cases for each stage of construction and provides guidelines and tools for performing calculations and inspections to verify fabrication quality of PC beams and the review of contractor submittals. The calculation tools for engineers include Microsoft Excel spreadsheets with embedded VBA codes and Mathcad analysis scripts. The tools for inspectors include two constructability checklists and a post-construction review form. Finally, recommendations are provided to incorporate the guidelines and tools into MDOT bridge design and precast concrete quality assurance and quality control programs.

17. Key Words Bridge construction, calculation tools, check lists, constructability evaluation, constructability review, Mathcad, quality control and quality assurance		**18. Distribution Statement** No restrictions. This document is available to the public through the Michigan Department of Transportation.	
19. Security Classification - report Unclassified	**20. Security Classification - page** Unclassified	**21. No. of Pages** 161 (w/o appendices)	**22. Price** N/A

Intentionally left blank

Bridge Structural Analyses for Staged Construction and Constructability Reviews

Final Report

Project Manager: Peter Jansson, P.E.

Submitted to:

Submitted by:

Haluk Aktan, Ph.D., P.E.
Professor
(269) 276 – 3206
haluk.aktan@wayne.edu

Upul Attanayake, Ph.D., P.E.
Associate Professor
(269) 276 – 3217
upul.attanayake@wmich.edu

Intentionally left blank

DISCLAIMER

This publication is disseminated in the interest of information exchange. The Michigan Department of Transportation (hereinafter referred to as MDOT) expressly disclaims any liability, of any kind, or for any reason, that might otherwise arise out of any use of this publication or the information or data provided in the publication. MDOT further disclaims any responsibility for typographical errors or accuracy of the information provided or contained within this information. MDOT makes no warranties or representations whatsoever regarding the quality, content, completeness, suitability, adequacy, sequence, accuracy or timeliness of the information and data provided, or that the contents represent standards, specifications, or regulations.

This material is based upon work supported by the Federal Highway Administration under SPR OR15-181. Any opinions, findings and conclusions or recommendations expressed in this publication are those of the author(s) and do not necessarily reflect the views of the Federal Highway Administration.

ACKNOWLEDGMENTS

Intentionally left blank

EXECUTIVE SUMMARY

INTRODUCTION

The typical design practice is to consider the limit state stresses in structural elements of a bridge that is completed as per the project specifications. Highway agencies design bridges in-house or contract the design to consultants. Once the design is complete and the plans are finalized, the project related documents go through a quality assurance and quality control (QA/QC) procedure to ensure that the final contract documents are prepared free of errors and omissions. The Michigan Department of Transportation (MDOT) Bridge Design Manual (BDM) Section 2.05 describes the bridge design QA/QC procedures implemented by MDOT. This process leaves the responsibility of analysis and design for construction stages to a contractor ("the Contractor") since the means and methods for construction are developed by the Contractor. The agency engineer ("the Engineer") needs to review and approve the means and methods described in the Contractor submittals. The Contractor selects qualified suppliers to provide materials and elements for the bridge to assure constructability, safety, and durability. A lack of a comprehensive program for (i) fabricated structural element quality evaluation and (ii) structural element and partially erected structural system response analysis during construction by both parties may lead to rejection by MDOT, project delays, change requests by the contractor, and sometimes, to construction safety and durability issues.

This project was designed to assist the inspectors and designers in the verification of fabrication quality of PC girders and the review of contractor submittals by developing a comprehensive list of constructability analysis cases for each stage of construction, supported by a set of guidelines and tools for performing calculations and inspections. The objectives of the study are as follows:

1. Document the fabrication and construction issues/cases to be addressed.
2. Document key components of constructability reviews for MDOT bridge projects.
3. Provide analysis templates.
4. Provide manuals and guides with examples.
5. Provide implementation recommendations.

To satisfy the objectives, this project was organized into seven tasks: (1) review of literature and state-of-the-art practices, (2) collect input from MDOT Design, Field Services, and Construction staff and the review of typical MDOT bridge project plans and construction methods,

ix

(3) develop PC beam performance assessment guidelines and procedures, (4) identify common design and construction review scenarios that require documented guidelines, (5) develop frameworks to address the common scenarios and the Mathcad scripts, (6) develop standalone constructability review and staged construction design guidelines, and (7) produce final research deliverables.

SUMMARY

Constructability cases associated with capacity, deformation, stability, and durability of bridge beams and assemblies were documented through a comprehensive literature review. These cases were grouped under each construction activity and discussed for production and manufacturing, transportation and lifting, erection, and deck placement stages. In addition to these activities, phased construction and the associated constructability cases were documented. The design and construction best practices to avert these problems as well as available methods and tools for analyzing the constructability cases were documented. These cases were discussed with the Research Advisory Panel (RAP). The cases documented with the RAP feedback were incorporated to develop a constructability framework for prestressed concrete (PC) and steel (S) girder bridges. Together with the first and second tasks, the MDOT involvement warranted the success of this project and completion of the fourth task, which was to identify common design and construction review scenarios that need documented guidelines.

The PC beams are manufactured and produced under stringent quality control requirements. The final decision regarding beams with deficiencies is at the Engineer's discretion. To improve the QA process for PC beam performance assessment, a non-destructive testing toolkit and a PC beam capacity assessment procedure need to be defined. Defining a non-destructive testing toolkit is beyond the scope of this project. As a fulfilment of the third task, an excel spreadsheet (*Quality Assurance Load Testing.xlsx*) was developed evaluate the load capacity of a PC beam. The spreadsheet (i) checks for PC beam capacity against the stress limits defined in the AASHTO LRFD (2017), (ii) identifies the flexural failure mode during load testing, and (iii) calculates the force magnitude required for load testing using either a 3-point or 4-point loading configuration.

The fifth and sixth tasks were to identify the common constructability cases to develop constructability review and design guidelines. Microsoft Excel spreadsheets with embedded VBA

codes and Mathcad analysis scripts were developed for engineers. Two constructability checklists and a post-construction review form were developed for inspectors.

To identify the potential constructability cases based on bridge type, bridge geometry, and the construction type, the *Constructability Analysis Cases Form*, a spreadsheet with embedded VBA codes, was developed. The *Constructability Required Level of Analysis (RLOA) Selection Tools*, a separate spreadsheet with embedded VBA codes, was developed to identify the required level of analysis (1D, 2D, or 3D) for the cases obtained from the *Constructability Analysis Cases Form*. A set of Mathcad scripts was developed and linked to the *Constructability Required Level of Analysis (RLOA) Selection Tools*. These tools provide a platform to assure the constructability of a bridge through the collective effort of the Engineer, Contractor, and Inspector.

IMPLEMENTATION RECOMMENDATIONS

The bridge design QA/QC procedures implemented by MDOT are described in BDM Section 2.05. The purpose is to ensure that the bridge design final contract documents are prepared with no errors and omissions. The *Structural Precast Concrete QAI Manual* describes the QA/QC process of precast concrete members. The tools and recommendations developed in this project can be seamlessly integrated into these procedures to achieve the QA/QC objectives.

1) Employ the *Quality Assurance Load Testing* spreadsheet with data to (i) check for PC beam capacity against the stress limits defined in the AASHTO LRFD (2017), (ii) identify the flexural failure mode during load testing, and (iii) calculate the force magnitude required for load testing using either a 3-point or 4-point loading configuration. This spreadsheet can be integrated into PC beam QA process for checking the failure mode and load capacity of PC beams with major nonconformance.

2) As per BDM Section 2.05.03A., "the Designers, Checkers, and Reviewers are key personnel providing well-designed, accurate, and constructible plans for use in the construction of bridges." The Designers, Checkers, and Reviewers can use the *Constructability Analysis Cases Form* tool to identify analysis cases that need to be considered during bridge construction. These cases are grouped under activities of lifting, erection, deck placement and phased construction. *Constructability Analysis Cases Form* can be required during the design, checking, and review processes.

3) According to BDM Section 2.05.03C5, Designers and Checkers face significant challenges due to the complexity of the software programs used for bridge structural analysis and design. Also, Checkers and Reviewers may face difficulties with the content and formats of contractor submittals for review. Such difficulties can be managed by providing (i) Required Level of Analysis (RLOA) guidance for bridge elements at each stage of construction and (ii) tools for independent verification of calculations submitted by the contractor. MDOT can request contractors to follow the required level of analysis guidelines by providing access to the *Constructability Required Level of Analysis (RLOA) Selection Tools*.

4) BDM Section 2.05.03D6 indicates that Program Level Quality Assurance (PLQA) is performed by the Bridge Design Supervising Engineer (BDSE). The objective of performing PLQA is "to promote consistency and uniformity between MDOT working units and between MDOT in-house and consultant designers." The *Constructability Analysis Cases Form* will be a tool to promote consistency in constructability related calculations and the approval of the submittals.

5) For inspectors, two constructability checklists were developed. BDM Section 2.02.18 describes the process for the final constructability review. The two checklists can be introduced in this section to ensure that the items are addressed in the plans with adequate details and notes. MDOT Form 5616 *Pre and Post Pour Inspection Checklist* can also be updated by the items listed in the *Constructability Checklist for Inspectors - Prestressed Concrete Bridges*. The checklist for prestressed concrete bridges can be linked to the Wiki E-Construction Section 708. The checklist for steel I-girder bridges can be linked to Wiki E-Construction Section 707. Also, checklist items related to structural stability can be incorporated into the construction staging section of the Form 1960.

6) According to BDM Section 2.04.04, project history needs to be documented. The *Constructability Checklist for Inspectors - Post-Construction Review* form can be used to document the errors/omissions in the plans, contractor change requests, and deviations from the approved construction plans. The compilation of such information helps to convert tacit knowledge into explicit knowledge that can be used to enhance the QA/QC program outcome.

The deliverables of this project can be implemented as described below to identify and evaluate (i) the capacity and failure mode of a beam with major nonconformance and (ii) potential

constructability cases as a result of the contractor-proposed means and methods and change requests:

1) Employ the *Quality Assurance Load Testing* spreadsheet with data to identify the failure mode of the beam with major nonconformance and to calculate the load magnitude required to reach the design stress limits during load testing.

2) Employ the *Constructability Analysis Cases Form* with required input data to identify the potential constructability cases that require analysis and development of design details. The output can be used to check if contractor submittals and calculations are incomplete for all the required analysis and design. The input data for this form is simple and only includes bridge type, bridge geometry, and the construction type.

3) Employ the *Required Level of Analysis (RLOA) Selection Tools* to identify the required level of analysis (i.e., 1D, 2D, or 3D) for analyzing the cases from the *Constructability Analysis Cases Form* output. This tool helps to evaluate the suitability of the models and tools used by the contractor in representing the stress state of structural elements included in the analysis.

4) Employ the *Required Level of Analysis (RLOA) Selection Tools* to access structural analysis tools for verifying the calculations given in contractor submittals.

TABLE OF CONTENTS

LIST OF TABLES

Bridge Structural Analyses for Staged Construction and Constructability Reviews

LIST OF FIGURES

Bridge Structural Analyses for Staged Construction and Constructability Reviews

1   INTRODUCTION

1.1   OVERVIEW

The memorandum issued in 2000 by the Federal Highway Administration (FHWA) requires that all bridges in the nation should be designed as per the American Association of State Highway and Transportation Officials (AASHTO) Load and Resistance Factor Design (LRFD) Specifications. The AASHTO LRFD design philosophy requires bridges to be designed for specified limit states to satisfy constructability, safety, and serviceability requirements as well as inspectability, economy, and aesthetics.

Operational responsibilities of a bridge during its entire lifetime are undertaken by various parties. The owner's design engineer (hereinafter referred to as "the Engineer") is responsible for designing the bridge as per the AASHTO LRFD specifications and the state or agency-specific policies documented in their design manual, guides, and standard plans. Subsequently, a Contractor with sufficient expertise and experience constructs the bridge as per the project specifications. The Contractor selects qualified suppliers to provide materials and structural elements for the bridge to assure constructability, safety, and durability. Before construction, owner agencies require submittals from the Contractor for girder lifting scheme, superstructure erection plans and procedures, deck pouring sequence, and associated supporting calculations. These calculations include, but are not limited to, girder stability checks during lifting and erection, stability analysis of partially erected structures, analysis of bridge frame under component and construction loads, and the design of falsework and formwork systems used during construction stages. The contractor submittals are reviewed and approved by the Engineer before commencing construction activity. During construction, the owner's field inspector (hereinafter referred to as "the Inspector") is responsible for verifying the approved construction plans, documenting ongoing construction activities, and consulting the Engineer when the activities deviate from the approved plans and procedures. The Inspector is also responsible for reporting the contractor's change requests to the approved plans and procedures.

AASHTO LRFD Bridge Design Specifications (AASHTO 2017a), requires that constructability requirements are addressed during the design of highway bridges. However, the typical design practice is to consider the limit state stresses in structural elements of a complete structure that is constructed as per the project specifications. Analysis of construction stages is left to the Contractor with their means and methods. The Engineer needs to review and approve

1

the means and methods described in the contractor submittals. A lack of a comprehensive program to evaluate fabricated structural element quality and the structural element and partially erected structural system response during construction by both parties may lead to delays, change requests by the contractor and sometimes, to construction safety and durability issues. Subsequently, there is a need to provide a framework that outlines fabrication quality assessment needs and constructability analysis cases during every stage of construction, as well as guidelines and tools for performing required inspections and calculations. This framework will address the following cases:

- Load capacity and durability of prefabricated elements
- Adequacy of the constructability cases described in contractor submittals
- Adequacy of the level of analysis employed by the contractor for an accurate evaluation of the constructability case under consideration
- Tools for evaluating analysis and design calculations of constructability cases in contractor submittal.

The Michigan Department of Transportation (MDOT) has material quality assurance procedures and a structural element quality assurance program in place. The Structural Fabrication Quality Assurance Guidance Document (MDOT 2019e) provides procedures and tools required for Quality Assurance Inspector (QAI) to maintain consistency while conducting quality assurance (QA) verification inspection at precast concrete fabrication facilities. The structural element quality assurance program does not include procedures and tools for evaluating load capacity and durability of prefabricated elements with the significant nonconformance.

MDOT incorporates two checklists for constructability review: one for early project scoping (Form 1961) and the other for the project development phase (Form 1960). Aktan and Attanayake (2013) developed a checklist in a format similar to Forms 1960 and 1961 for evaluating the constructability of prefabricated bridge elements and systems. These forms, however, do not include instructions or guidance to evaluate the construction activities, details on constructability and stability, and the required level of structural modeling (1D, 2D, or 3D) for an accurate representation of stresses and deformations under boundary conditions and loads during each stage of construction. For this reason alone, these forms require updating with adequate instructions to guide the Engineer for evaluating the constructability and stability of structural elements and systems.

The significance of performing constructability reviews for bridges is being recognized by many agencies. As an example, the New Jersey Department of Transportation (NJDOT) developed a Constructability Manual that discusses review objectives, construction concepts, and review checklists (NJDOT 2016). Idaho DOT (2011) has a manual with detailed constructability review guidelines. FHWA developed a training course on *Engineering for Structural Stability in Bridge Construction*. This course is offered by the National Highway Institute (NHI) under the Course Number 130102. The course provides guidance to bridge erection engineers, resident/construction engineers, and design engineers for the design and evaluation of bridge superstructures during construction. The course scope includes local and global stability analysis of bridge superstructure elements and stability analysis of the superstructure.

The current constructability practice is to perform required evaluations and analyses on a case-by-case basis. This process has many drawbacks, as listed below:

- Projects are delayed due to a lack of guidance on acceptance testing and procedures for evaluating the strength and durability performance of prefabricated girders with the major nonconformance.

- Efforts are duplicated since experience gained from constructability analysis and implementation is not effectively disseminated.

- Engineers have to repeatedly evaluate change requests by the contractors.

- Bridge construction and demolition procedures are not being standardized, engineers have to deal with each case individually.

- During a project of some complexity, certain critical analysis steps may be overlooked.

- Needless efforts are put forth to evaluate cases that do not impact the constructability or stability of the structure.

- A simplified analysis is often performed because a detailed analysis of construction staging sequences requires increased time and effort. The simplified analysis might fail to capture potential member instability or deformations that result in construction difficulties and/or poor geometry of the finished structure.

To overcome the above-stated limitations in the current process, a constructability evaluation framework needs to be developed by incorporating structural element production and manufacturing, transportation and lifting, erection, deck placement, phased construction, and

bridge demolition. The framework can be the guide to develop analysis cases, as well as calculation templates, procedures, and guidelines.

1.2 PROJECT OBJECTIVES AND TASKS

The objectives of the project include developing (*i*) quality assurance testing procedure for prestressed concrete (PC) girders, (*ii*) preapproved construction staging and demolition methods and (*iii*) additional staging methods in a format to allow analysis supported with calculation templates, procedures, and guidelines. The specific objectives of the study are as follows:

1. Identify the fabrication and construction issues/cases to be addressed.
2. Identify key components of constructability reviews for MDOT bridge projects.
3. Provide analysis templates.
4. Provide manuals and guides with examples.
5. Provide implementation recommendations.

To achieve these objectives, this project was organized into seven tasks: (1) review of literature and state-of-the-art practices, (2) collect input from MDOT Design, Field Services, and Construction staff and the review of typical MDOT bridge project plans and construction methods, (3) develop PC beam performance assessment guidelines and procedures, (4) identify common design and construction review scenarios that need documented guidelines, (5) develop frameworks to address the common scenarios and the Mathcad scripts, (6) develop standalone constructability review and staged construction design guidelines, and (7) produce final research deliverables.

1.3 REPORT ORGANIZATION

This report is organized into 7 chapters.

Chapter 1 Includes the introduction and overview of the research project.

Chapter 2 Describes a list of constructability cases that are documented during (*i*) production and manufacturing of PC girders, (*ii*) transportation and lifting, (*iii*) erection, (*iv*) deck placement, and (*v*) phased construction. These cases are associated with capacity, durability, deformation, and stability. A framework was developed and presented for evaluating the constructability of typical highway bridges.

Chapter 3 Presents testing procedures to assure performance expectations of PC girders.

Chapter 4 Discusses the *Constructability Analysis Cases Form* developed for the framework presented in Chapter 2. The form identifies the list of constructability cases based on bridge type, bridge geometry, and the type of construction. The *Constructability Required Level of Analysis (RLOA) Selection Tool* presented in this chapter (i) defines the required level of analysis for evaluating the cases given in the *Constructability Analysis Cases Form* and (ii) lists *Structural Analysis Tools* for evaluating constructability cases.

Chapter 5 Offers three inspector checklists developed for the constructability cases listed in Chapter 2. This chapter provides an overview of the rationale behind the checklist and constructability cases.

Chapter 6 Presents a summary and implementation recommendations.

Chapter 7 Lists the cited references.

2 STATE-OF-THE-ART LITERATURE REVIEW

2.1 OVERVIEW

Conventional highway bridge design requires an accounting of stresses in structural elements and systems at the strength and/or service limit states assuming that the structure is constructed as per project specifications. However, during various stages of construction, structural elements and systems are subjected to loading, deformation, and boundary conditions that might not be present in the completed structure. Failure to account for the stresses in the analysis and design could result in locked-in stresses, require modifications to the structural system, trigger a failure of a bridge element or the partially erected structure, or a combination thereof. To identify these cases during construction, implementation of constructability reviews supported with analysis tools and guidelines is required. According to AASHTO Constructability Review Best Practices Guide (AASHTO 2000), constructability review is *"a process that utilizes construction personnel with extensive construction knowledge early in the design stages of projects to ensure that the projects are buildable, while also being cost-effective, biddable, and maintainable."* To assure that a bridge is buildable, cost-effective, and maintainable, the constructability review process needs to encompass the entire process and activities starting from material selection and acceptance to project completion, including documentation and effective dissemination of lessons learned.

This chapter presents a summary of constructability review forms or checklists used by various agencies. As discussed later in this chapter, the review and checklists forms do not provide the detail required to guide engineers to evaluate the impact of construction activities on constructability and stability. Also, lacking is the required level of structural modeling (1D, 2D, or 3D) for an accurate representation of stresses and deformations from the structural response of elements and systems under boundary conditions and loads that exist during construction stages. The constructability review forms need to include details to identify the need for stress analysis to evaluate the constructability and stability of bridge elements and systems. Development of review forms with detailed guidelines requires documenting constructability cases, level of analysis appropriate for evaluating stresses and deformations, and procedures and tools for such analysis.

A comprehensive review of the literature was conducted to document the constructability cases during (*i*) structural element production and manufacturing, (*ii*) transportation and lifting, (*iii*) erection, (*iv*) deck placement, and (*v*) phased construction. These constructability cases are associated with structural element production and manufacturing as well as construction stages

6

that impact capacity, durability, deformation, and stability of the structural elements and assemblages of the bridge. Figure 2-1 shows the constructability framework developed using the documented constructability cases and MDOT Research Advisory panel (RAP) feedback. The framework in Figure 2-1 includes constructability analysis objectives and cases related to prestressed concrete (PC) and steel (S) bridges. The subsequent sections of this chapter provide details of (a) constructability cases identified for each of these stages, (b) required level of analysis for the cases, (c) analysis methods, tools and procedures for calculating stresses and deformations, (d) deformation tolerances, and (e) corrective actions for maintaining bridge element and/or system stress limits, stability and tolerances.
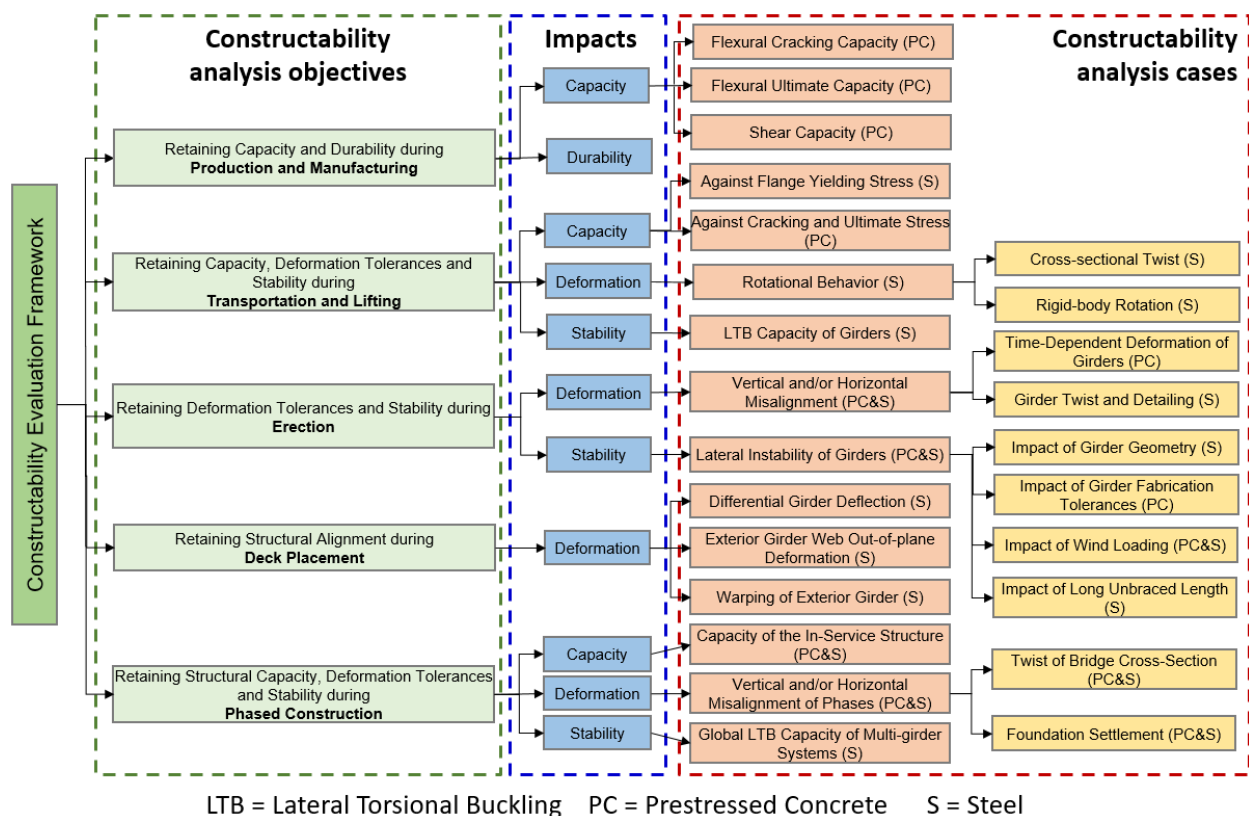
Figure 2-1. Constructability cases for conventional highway bridges

2.2 CONSTRUCTABILITY REVIEW CHECKLISTS

MDOT currently uses two constructability checklists: *Form 1961- Constructability Checklist for Early Project Scoping* (preliminary review of constructability), and *Form 1960 – Constructability Checklist for Project Development Phase* (final review of constructability). Resident engineers are accountable for completing these forms. As per Section 2.02 of the MDOT Bridge Design

7

Manual (MDOT 2019a), the design engineer requests supplementary data from various sources before the preparation of contract plans, including the completed Forms 1960 and 1961.

Form 1961 primarily checks the acquisition of permits required for initiating construction. The form includes four main sections: site investigation, right of way (R.O.W), construction staging, and maintenance of traffic. Under each section, associated permits and construction activities that could impact the surroundings, such as site, environmental, and R.O.W constraints, are discussed. Form 1961 is the preliminary constructability checklist and does not include review items that relate superstructure analysis for constructability evaluation.

Form 1960 is the final constructability review and includes schedule, special materials/conditions, and staffing categories. The content of Form 1960 is broader and addresses a variety of different aspects of the project under consideration including required permits, drainage, site survey and subsurface exploration, etc. The "construction staging" category includes the followings questions that are related to constructability of superstructure units:

- *Does staging cause special conditions (structural adequacy/stability, etc.)?*
- *Can the details as shown on the plans be constructed using standard industry practices, operations, and equipment?*

None of these forms are designed to guide the engineer to evaluate the impact of construction practices and details on constructability and stability, as well as the need for analysis.

Constructability review checklists are used by various state highway agencies. Stamatiadis et al. (2013) tabulated the similarities and differences in constructability reviews of various state highway agencies. Table 2-1 is a modified version of the content presented in Stamatiadis et al. (2013). The definitions of constructability review categories discussed in Stamatiadis et al. (2013) are provided in Appendix B.

Table 2-1. Constructability Review Checklist Items of Selected State Highway Agencies

Category	CA	CT	FL	ID	IN	MI	NJ	NY	VA
Access	✓		✓	✓			✓		
Bases and Pavements							✓		
Constructability				✓					
Construction Staging			✓	✓	✓	✓		✓	
Detours		✓		✓			✓		
Drainage	✓	✓	✓	✓	✓	✓	✓	✓	✓
Earthwork							✓		✓
Environmental	✓	✓	✓		✓				✓
Erosion Control/Landscaping	✓		✓	✓					✓
Future Work/Maintenance	✓						✓		✓
General/Incidentals		✓		✓			✓		
Guardrail				✓					
Maintenance of Traffic	✓	✓	✓	✓	✓	✓	✓	✓	✓
Pay Items					✓				
Plan Content					✓				
Railroad	✓	✓			✓				
Reconstructability			✓						
Removal/Demolition			✓	✓					✓
Right of Way	✓			✓	✓	✓		✓	
Roadway		✓		✓					
Schedule			✓	✓		✓		✓	
Signs/Signals/Electrical		✓	✓	✓			✓		✓
Site Investigation						✓		✓	
Sound Walls			✓	✓					
Special Materials/Conditions	✓					✓		✓	
Staffing						✓			
Structure Rehabilitation				✓					
Structures		✓	✓	✓			✓		✓
Surveying	✓	✓	✓		✓				
Utilities		✓	✓	✓					✓
Vertical Construction		✓							

The following references were used for Table 2-1:

CA: CALTRANS (2006)   CT: ConnDOT (2011)   FL: FDOT (2018a)

ID: Idaho DOT (2011)   IN: INDOT (2010)   MI: MDOT (2009, 2010)

NJ: NJDOT (2016)   NY: NYSDOT (2017)   VA: VDOT (2007)

The checklist items that evaluate the impacts of highway bridge construction practices on deformations, stability, and safety of superstructure elements are summarized as follows:

- FDOT (2018a), Idaho DOT (2011), NJDOT (2016), and VDOT (2007) evaluate the space available for crane swings. This item is related to constructability cases during lifting since lifting schemes (the number of cranes, number and position of the lifting points, etc.,) could impact capacity, deformation, and stability during lifting of the structural members.
- ConnDOT (2011) includes erection plans for curved and/or skewed girder or tub girder bridges for calculating differential deflections and rotations. ConnDOT also reviews the proposed deck placement sequence for multi-span bridges for constructability.
- INDOT (2010) bridge design evaluates stability during construction. INDOT requires closure pours to form longitudinal joints between construction phases when extreme deflections are anticipated during deck placement.
- VDOT (2007) checks available space for screed machine installation during each phase of construction to limit the impact of deflection during the respective construction phases.
- ConnDOT (2011) and VDOT (2007) check the need for temporary supports during phased construction.
- For phased construction projects, NYSDOT (2017) and VDOT (2007) evaluate the impact of proposed construction stages on structural safety and stability.

Even though these constructability review checklists include steps to evaluate phased construction issues, a comprehensive approach is lacking to evaluate the cases presented in Figure 2-1. The cases include capacity and durability assessment at the precast concrete fabrication facilities and analysis and guidance in prescribing the required level of analysis for constructability and stability of bridge elements and systems.

2.3 PERFORMANCE ASSESSMENT OF PRECAST ELEMENTS

2.3.1 An Overview of MDOT Practice

The bridge structural element quality affects buildability, cost-effectiveness, durability, and maintainability. MDOT has an established process to assure the quality of prestressed concrete (PC) girders, the most widely used precast/prefabricated bridge element. The process is being regularly updated in partnership with the stakeholders. The following is an abbreviated list of MDOT manuals, guides, specifications, and forms that describe the quality of materials, workmanship, and products used on their bridges:

- Bridge Design Manual (MDOT 2019a)

- Bridge Design Guides (MDOT 2019b)

- Materials Quality Assurance Procedures Manual (MDOT 2018)

- MDOT Construction Forms (MDOT 2020a)

  - Independent Assurance Concrete Tests (Form 0503)

  - Strand Tensioning Report (Form 0513)

  - Notification to the Manufacturer of an Intermediate Inspection Made of Prestressed Concrete Beams (Form 0551A)

- Special Provision for Quality Control and Acceptance of Structural Precast Concrete (MDOT 2019d)

- Standard Specifications for Construction (MDOT 2012)

- Structural Precast Concrete QAI Manual (MDOT 2019e)

- Supplier Qualification Standard for Prestressed Concrete Beams (MDOT 2020b)

The Bridge Design Manual (BDM) (MDOT 2019a) and the Bridge Design Guides (BDG) (MDOT 2019b) present MDOT policies. The bridge design quality assurance and quality control (QA/QC) procedures are described in BDM Section 2.05. The purpose is to ensure that the bridge design final contract documents are prepared with no errors and omissions. As per BDM Section 2.05.03A., "*the Designers, Checkers, and Reviewers are key personnel providing well-designed, accurate, and constructible plans for use in the construction of bridges*." As noted in BDM Section 2.05.03C5, Designers and Checkers may face challenges due to the complexity of the software programs used for bridge structural analysis and design. Checkers and Reviewers may also face difficulties with the content and formats of contractor submittals for review. These difficulties

require developing guidelines and formats for contractor/consultant submittals. BDM Section 2.05.03D6 indicates that Program Level Quality Assurance (PLQA) is performed by the Bridge Design Supervising Engineer (BDSE) "*to promote consistency and uniformity between MDOT working units and between MDOT in-house and consultant designers*." The process for the final constructability review is described in BDM Section 2.02.18. BDM Section 2.04.04 describes the need for documenting the project history, including the changes in scheduling (with the reasons, if known), to capture the tacit knowledge acquired by the design team.

The Materials Quality Assurance Procedures Manual (MQAP) (MDOT 2018) describes the scope of material QA program to assure material conformance with contract documents and the standard specifications for construction. This manual refers to additional documents such as the construction manual, materials and source guide, Michigan test methods, quality system manual, etc., for detailed procedures.

MDOT provides forms to assist with the QA of materials, structural elements, and procedures (MDOT 2020a). As an example, (i) *Form 0503 – Independent Assurance Concrete Tests* records fresh concrete properties evaluated in the field and hardened concrete properties evaluated in the lab to make acceptance or rejection decisions with justifications; (ii) *Form 0513 - Strand Tensioning Report* records the sequence of strand release, location of the strand (numbered from left to right, and from bottom to top), measured elongation, actual gauge reading, inputs and outputs of tensioning calculations with necessary corrections (including live end seating, bed shortening, thermal elongation, and thermal force corrections), and strand type (straight, draped, support, and debonded); and (iii) *Form 0551A - Notification to the Manufacturer of an Intermediate Inspection Made of Prestressed Concrete Beams* records findings of intermediate inspection performed within one working day after a beam is moved to storage, results of the shipping inspection performed at the time the beams are loaded for shipment, any work performed on the beam, and the cause for rejection.

In addition to the manuals, guides, and forms described above, MDOT has a special provision, a manual (*Structural Precast Concrete QAI Manual*), and a more recently developed standard (*MDOT Supplier Qualification Standard for Prestressed Concrete Beam*) for improving the manufacturing quality of prestressed concrete beams. The *Structural Precast Concrete QAI Manual* (MDOT 2019e) describes the QA/QC process of precast concrete members by defining the duties and responsibilities of MDOT, Contractor, Fabricator, Engineer, and Inspector to ensure

statewide consistency in performing quality assurance verification inspection at the fabrication facilities. The primary steps of the MDOT precast concrete quality assurance process are shown in Figure 2-2. The process starts with MDOT assigning a Quality Assurance Inspector (QAI) for the project and holding a pre-fabrication meeting between the Fabricator and MDOT to discuss general concerns about fabrication, duties and responsibilities of the Fabricator, and the schedule. The Fabricator prepares a Quality Control Plan (QCP) to be reviewed by a certification agency (such as the Precast/Prestressed Concrete Institute – PCI), provides a copy of QCP to MDOT, and assigns a Quality Control Inspector (QCI) to take the responsibility for implementing the QCP. QCI is responsible for the review of data and pertinent documents, an inspection of the process and the final product, and deciding on the acceptance of the products. QAI notifies MDOT when shortcomings and non-conformance are detected, and the Fabricator sends a Non-Conformance Report (NCR) to MDOT.

MDOT nonconformance policy stated in the *Structural Precast Concrete QAI Manual* (MDOT 2019e) expects the Fabricator to submit an NCR after QCI observes a nonconformance due to workmanship or material quality. PC beams with some nonconformance are accepted with a price reduction if approved for use (Figure 2-3). As an example, there is a price reduction for a beam approved for use if the strength of match cured concrete specimens is below the specified limit at the test age. Additionally, fabrication related nonconformance is documented, such as dimensional tolerance deviations, cracking, spalling, honeycombing, and curing temperature above the approved limits. The price reductions for nonconformance described in the manual are for infrequent occurrences. The price reductions are doubled "*in the event of repeated occurrences of the same defect.*" But, the manual does not provide a statistically meaningful and measurable limit to define "*repeated occurrences.*" Minor nonconformance, such as concrete air holes, can be repaired using a preapproved MDOT repair procedure and without MDOT preapproval on a case-by-case basis. Major nonconformance (such as honeycombing, voids, and damages) can be repaired following preapproved MDOT repair procedures with the prior approval of MDOT. Even though it is stated that the PC beams that are "*judged to be structurally or otherwise unacceptable by MDOT due to low strength, cracking, breakage, honeycombing, or other deficiency will be rejected and replaced,*" clear procedures and guidelines are not presented for the assessment of capacity and durability to make such decisions.

More recently, MDOT developed the *Supplier Qualification Standard for Prestressed Concrete Beams* (MDOT 2020b) that requires the fabricators to implement a regularly maintained and audited quality management system (QMS). The Precast/Prestressed Concrete Institute (PCI) certified plants can be included in the MDOT Approved Supplier List (ASL) once their QMS obtains approval from MDOT. The approval process requires a documentation audit and an onside audit. The outcome of this audit process leads to Approved, Approved-Provisional, Approved-Probation, Disqualified, Dismissed, Hiatus, and Unlisted status. Maintaining the approved status on the ASL requires the fabricators to maintain "*a functioning QMS, passing recurring MDOT audits without major or critical nonconformance[s] and by producing work without serious product nonconformance.*" As part of the QC plan, an inspection and testing plan (ITP) is required. Receipt inspection/acceptance inspection of materials, in-process inspection, final inspection of PC beams as well as the list of tests performed for QC purposes need to be included in the ITP. All products are required to be inspected before shipment. With the implementation of the standard, MDOT could collect a wealth of information and data related to each product, the PC beams. If the data collected from the suppliers is maintained in an easily retrievable format, the data can be used to predict PC girder performance, frequency of nonconformance, and setting up a data-driven schedule for the audits.
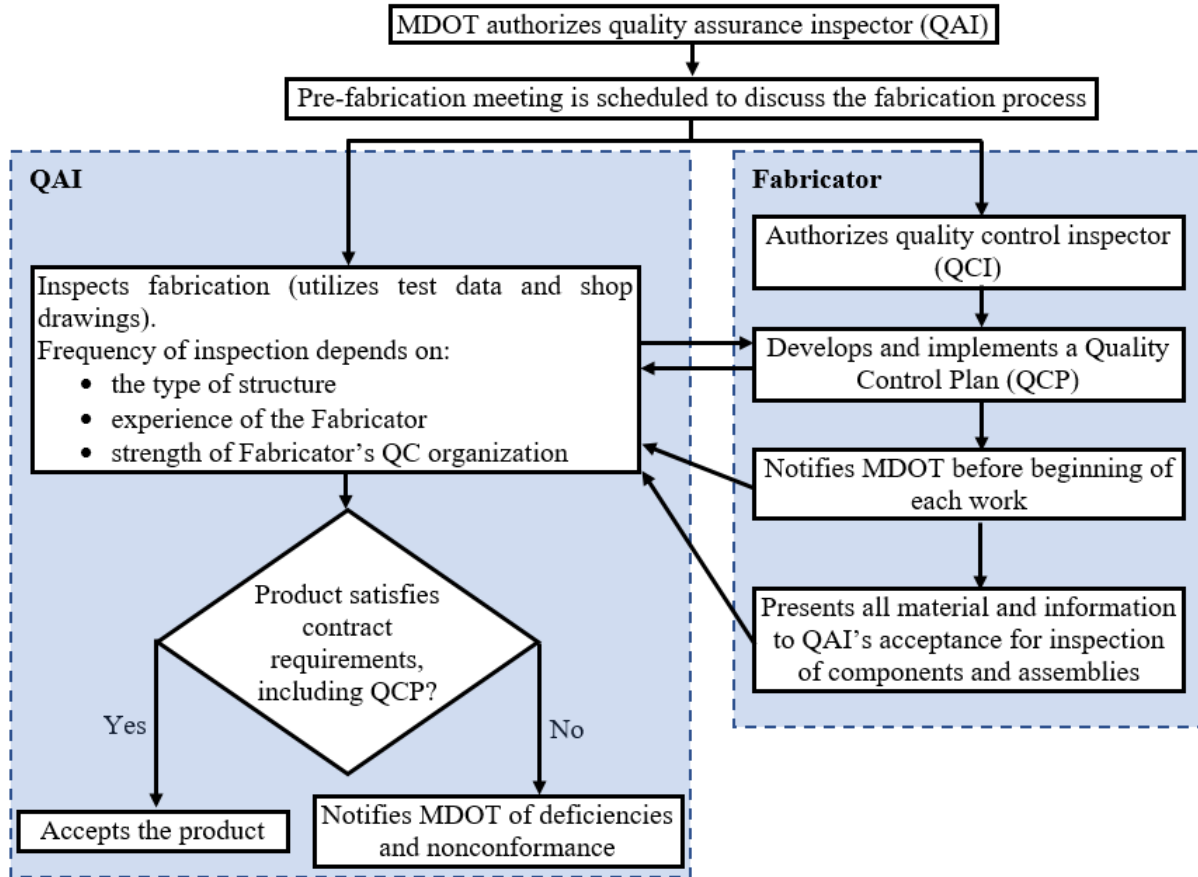
Figure 2-2: MDOT precast concrete fabrication quality assurance process
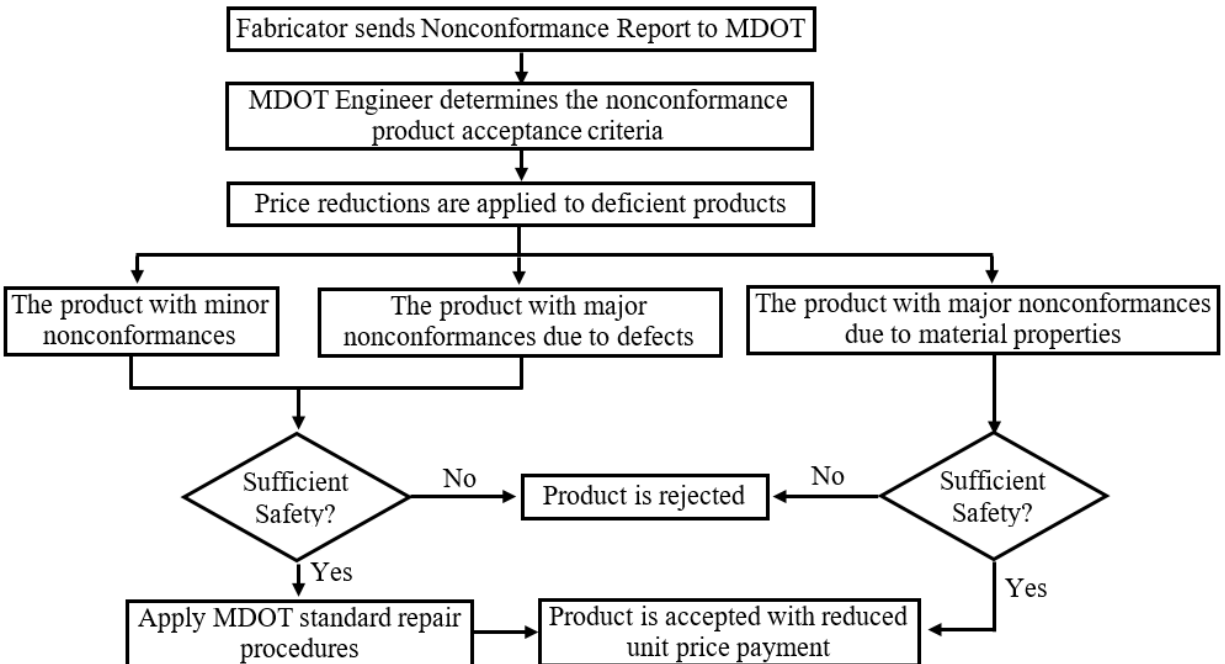
Figure 2-3: Quality control process of deficient precast concrete products

15

2.3.2 Structural Performance Evaluation of Railway Ties

The quality of PC beams fabricated for MDOT projects is evaluated by visual inspection and checking geometric tolerances. The railway industry utilizes load testing of railway ties for design approval and production QC process (AREMA 2015). A monoblock prestressed concrete railway tie is shown in Figure 2-4. The design approval process flow diagram for prestressed concrete railway monoblock ties is shown in Figure 2-5. To approve a new design, 4 ties are selected from a lot of not less than 10 ties manufactured as per the new design and labeled as Tie 1, Tie 2, Tie 3 and Tie 4. The compliance of these ties with the material, geometry (configuration and dimensions), and weight specifications are evaluated. Tie 1 and Tie 2 are load-tested for their structural and fastening capacities. Tie 3 and Tie 4 are retained for future tests and as a control for dimensional tolerances and surface appearance of ties that comes out from the subsequent production. As shown in Figure 2-5, seven tests are conducted on Tie 1 and three tests are conducted on Tie 2 to evaluate the compliance of the products with the design specifications. Only the tests conducted on Tie 1 are discussed in this section considering their relevance to the capacity assessment of PC members.
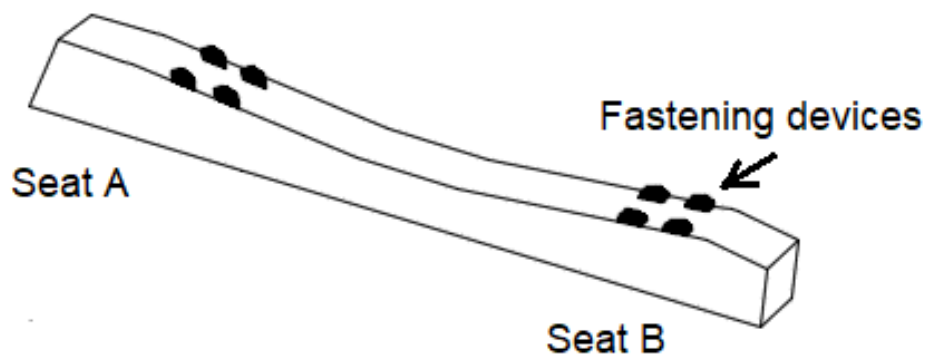
Figure 2-4. Prestressed concrete monoblock railway tie (AREMA 2015)
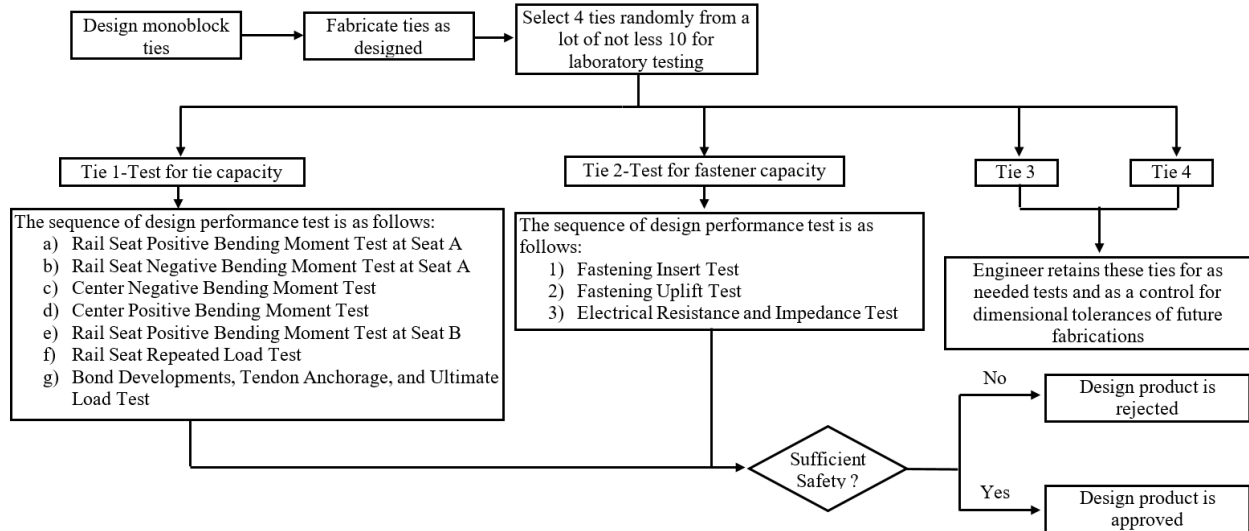
Figure 2-5. Design product approval process for prestressed concrete railway monoblock ties (AREMA 2015)

The seven tests conducted on Tie 1 are:

a) Rail Seat Positive Bending Moment Test at Seat A – see Figure 2-6a

- Load rate is controlled between 3 to 10 kips/min

- Load is increased until it reaches P, the load required to produce the specified rail seat bending moment.

- Tie is inspected for structural cracking while holding the maximum load for 3 minutes.

- The testing requirements are satisfied if the tie shows no cracking.

b) Rail Seat Negative Bending Moment Test at Seat A – see Figure 2-6b

- Load rate and the procedure are identical to the positive bending moment test.

c) Center Negative Bending Moment Test – see Figure 2-7

- Load rate is controlled between 1 to 5 kips/min.

- Load is increased until it reaches P, the load required to produce the specified midspan bending moment.

- Deflection at the center of the tie relative to the vertical support is measured.

- Tie is inspected for structural cracking while holding the maximum load for 3 minutes.

- The testing requirements are satisfied if the tie shows no cracking.

d) Center Positive Bending Moment Test – see Figure 2-7

- Load rate and the procedure are identical to the center negative bending moment test.

e) Rail Seat Positive Bending Moment Test at Seat B – see Figure 2-6

- Load rate and the procedure are identical to the positive bending moment test at Seat A.

17

f) Rail Seat Repeated Load Test – see Figure 2-8

- At the end of the positive bending moment test at Seat B, increase the load at a rate of 5 kips/min until the tie cracks from its bottom surface up to the lower layer of reinforcement or strands.
- Remove load and replace the elastomeric pad with a ¼ in. thick plywood.
- Perform a repeated load test with a total of 3 million cycles at a frequency not to exceed 600 cycles/min (10 Hz).
- Maintain a loading range of 4 kips to 1.1P during each cycle.
- At the end of 3 million cycles, increase the load to 1.5P and hold for at 3 minutes.
- The requirements of the test are satisfied if the tie can support a rail seat load of 1.5P for 3 minutes without a tendon slip of more than 0.001 in., concrete compressive failure, concrete shear cracks, or tendon failure.

g) Bond Developments, Tendon Anchorage, and Ultimate Load Test

- Support and load rail Seat A similar to positive bending moment test shown in Figure 2-6.
- Apply a total load of 1.5P, where P is the load used for the positive bending moment test at Seat A.
- Hold this load for at least 3 minutes and measure the slippage of the outermost tendons of the lower layer.
- Bond development and tendon anchorage requirements are satisfied if the slippage of the tendons is no more than 0.001 in. when measured with an extensometer reading to 1/10,000 of an inch.
- If the requirements are satisfied, increase the load at a rate not greater than 10 kips per minute and continuously measure tendon slippage until failure occurs.
- Record the load at which tendon slippage occurs as the maximum load.
- Report the failure mode at the maximum load as either tendon slip, tendon breakage, or concrete compressive failure.
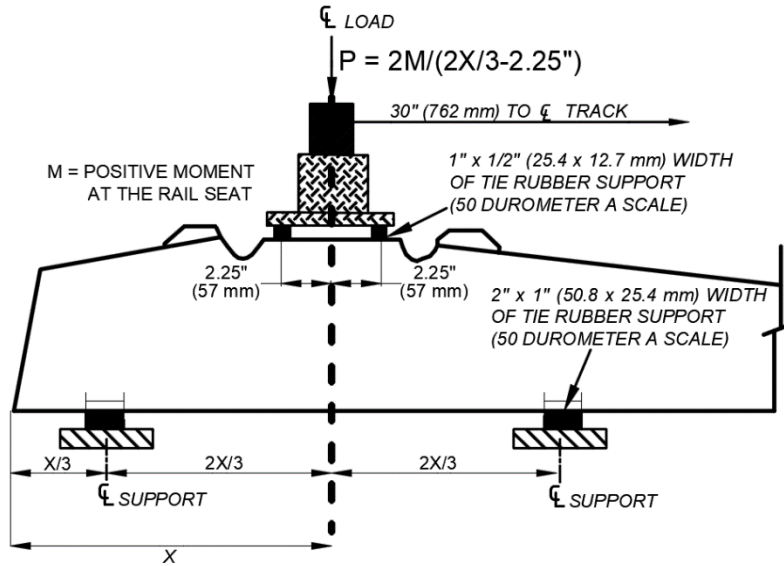
(a) Rail seat positive moment test
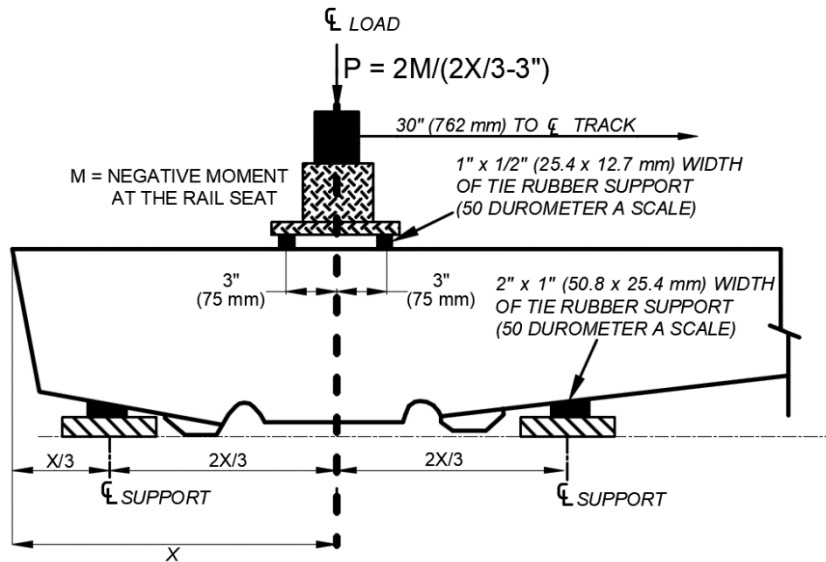
(b) Rail seat negative moment test

Figure 2-6. Vertical load test at seat A (AREMA 2015)
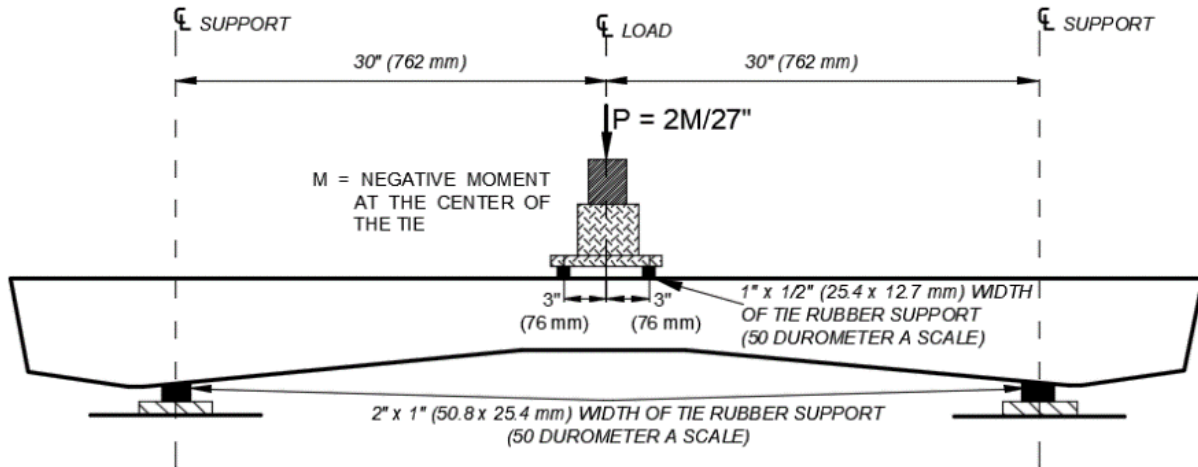
(a) Center negative moment test
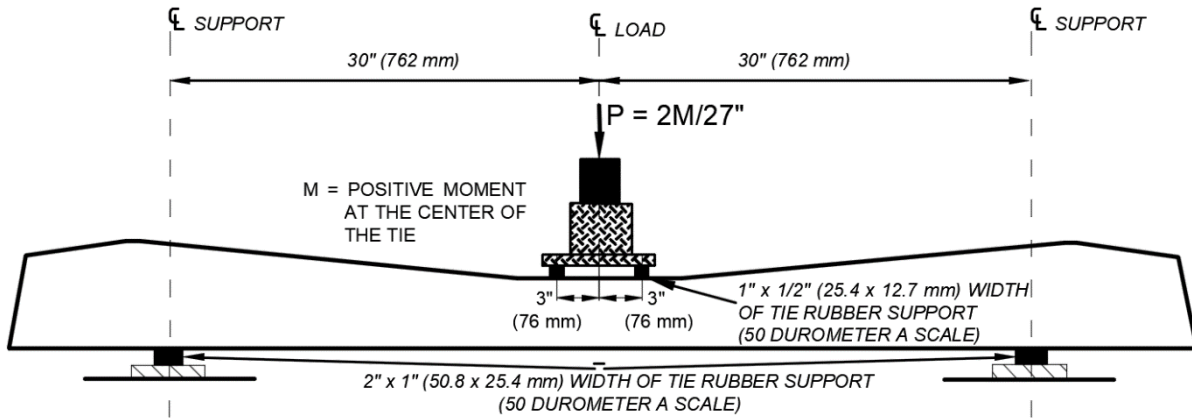
(b) Center positive moment test

Figure 2-7. Center moment test (AREMA 2015)
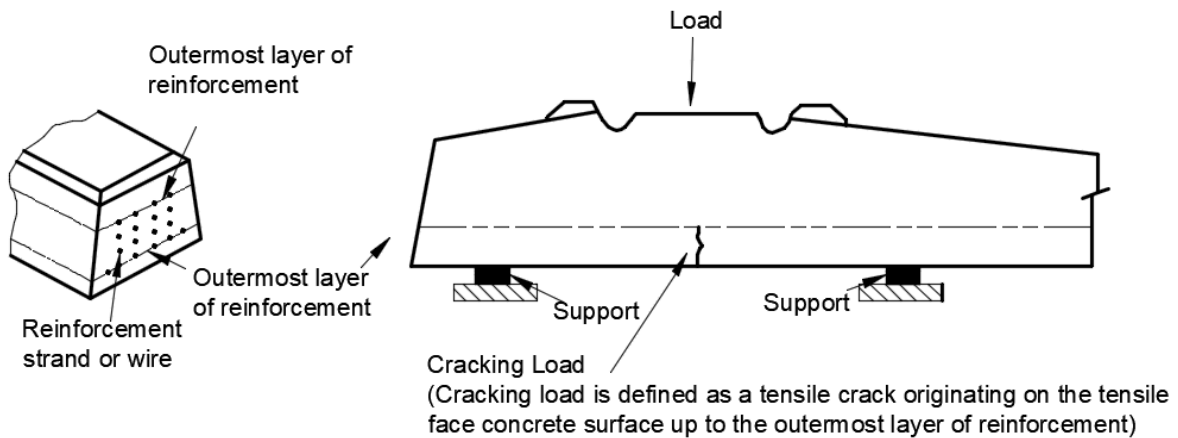
Figure 2-8. Repeated load test at Seat B (AREMA 2015)

When the testing of Tie 1 and Tie 2 is satisfactory, the design is approved and the production begins. Production QC process to assure high-quality products is depicted in Figure 2-9. The process requires sampling one tie from a lot of 200 units or a fraction thereof to (i) verify rail seat configuration and insert locations, (ii) conduct rail seat positive bending moment test shown in Figure 2-6a with a load rate of at least 5 kips/min and held at least one minute after reaching the maximum required load, and (iii) conduct fastening insert test. All 200 ties are accepted if the sample passes QC tests. If the sample fails any of the tests, 2 additional ties are sampled from the same lot and tested. A failure of either of these ties results in rejection or testing of all the remaining ties in the original lot.

AREMA (2015) also specifies stringent material and curing specifications. Deterioration of concrete due to Alkali Silica Reactivity (ASR), Alkali Carbonate Reactivity (ACR), Delayed Ettringnite Formation (DEF), and sulfate reaction has played a key role in shaping the specifications. The use of cement with Na_2O equivalent alkali ($Na_2O + 0.658\ K_2O$) content of less than 0.6% is specified. Concrete mixes with at least 10 years of service record are recommended. The concrete temperature during the preset period is limited to 90 ^{0}F during the first 3 hours and 105 ^{0}F during the first 4 hours. During the accelerated curing, the rate of temperature increase is limited to 35 ^{0}F per hour with a maximum curing temperature of 140 ^{0}F. Curing temperature up to 158 ^{0}F is allowed when the can demonstrate the long-term durability of the material used for fabrication. Automatic measurement of the temperature at the center of the rail seat cross-section is required for one tie in each casting bed.
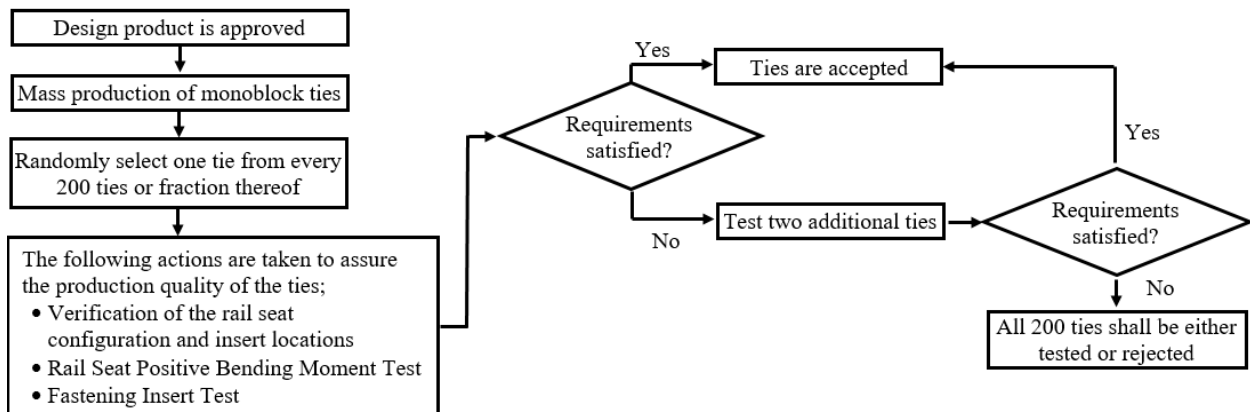
Figure 2-9. Prestressed concrete railway tie production QC process (AREMA 2015)

2.3.3   Load Testing of PC Beams

Load testing is often performed to evaluate the capacity of PC girders when design changes are introduced with new sections, materials, prestressing strand sizes, prestressing strand patters, or a combination thereof. As an example, Spadea et al. (2018) performed a three-point flexural load test to evaluate the service moment capacity of a 66 ft long double tee beam fabricated using self-consolidating concrete (SCC) and carbon-fiber-reinforced polymer (CFRP) tendons. This beam was designed for a pedestrian bridge to support a 100 lb/ft^2 live load, a 3 in. non-integral concrete wearing surface, and safety barriers. The load testing was performed at the precast yard after 26 days following fabrication. The required load of 27 kip was back-calculated after subtracting the beam self-weight moment from the 809 ft-kip maximum service moment. Figure 2-10 shows the beam cross-section and loading at the yard. As shown in the figure, 3 concrete blocks of 9 kip/block were used to load the beam. In this particular case, the calculation of the required load and load placement to generate the maximum service moment at mid-span is straight forward since a non-composite section is used on the bridge.

Figure 2-10. Load testing of a double tee beam at the fabricator's yard (Spadea et al. 2018)

MDOT recently evaluated the service moment capacity of a girder with significant nonconformance. The loading pattern and a close-up of girder bottom flange honeycombs are shown in Figure 2-11. This was a much challenging situation to address at a plant for the following reasons:

(1) girder length more than 100 ft with a significant moment capacity

(2) honeycombs visible at multiple locations along the girder with questionable internal conditions making it harder to identify the weak section

(3) developing a loading pattern to test if service moment stresses can be developed while the service loads are applied on a composite section

(4) placing loads to reach the service stress state while maintaining stability.

(a) A girder with major nonconformance

(b) A close-up view of the bottom flange honeycomb

Figure 2-11. Load testing of a bulb tee beam with bottom flange honeycombs

Load testing is not typically conducted as part of a QA program. A common purpose for load testing is to evaluate the capacity of distress girders. Attanayake and Aktan (2011) evaluated the capacity of a 50-year old beam by using a hydraulic ram with a load configuration developed using the equipment and accessories available at a contractor's yard (Figure 2-12). The primary

challenge with this approach was to develop a significantly large counterweight to balance the hydraulic ram reaction.

Stuedlein and Holtz (2012) presented two experimental loading setups for evaluating load and displacement characteristics of stone columns. Figure 2-13 shows the reaction frame developed with 8 helical piles. The load applied using this frame was 647 kips. A 1,000-kip hydraulic ram with a 20-in. travel was used for this purpose. The service load capacity of a typical PC I-beam under four-point loading can be evaluated with a 50 to 60-kip load at each loading point. If four helical piles are used to develop reaction frames at each load point, the maximum allowable capacity required per pile is 15 kips. A helical pile with a shaft diameter of 2.875 in., driven into cohesive soil with N_{60} of 25 or non-cohesive soil with N_{60} of 20, can develop an ultimate tension capacity of 49.5 kips (i.e. an allowable tension capacity of 24.75 kips with a factor of safety of 2) (HCI 2014). With proper sizing of the helical piles and the extension couplers, customized configurations can be developed for load testing of PC beams in the absence of permanent load frames.

| (a) A view of the load setup | (b) A close-up view of the loading setup |

Figure 2-12. Testing of a deteriorated box beam using a four-point bending load configuration

Figure 2-13. Reaction frame and loading setup for a footing (Stuedlein and Holtz 2012)

2.3.4   Monitoring PC Beam Response During Load Testing

The typical responses monitored during beam load testing are the load, deflection, support settlement, strain, the inception of cracking, crack width, and crack propagation.

2.3.4.1   Measurement of Load

The load is measured by a load cell placed between the hydraulic ram and the loading beam (Figure 2-14, Figure 2-15, and Figure 2-16).
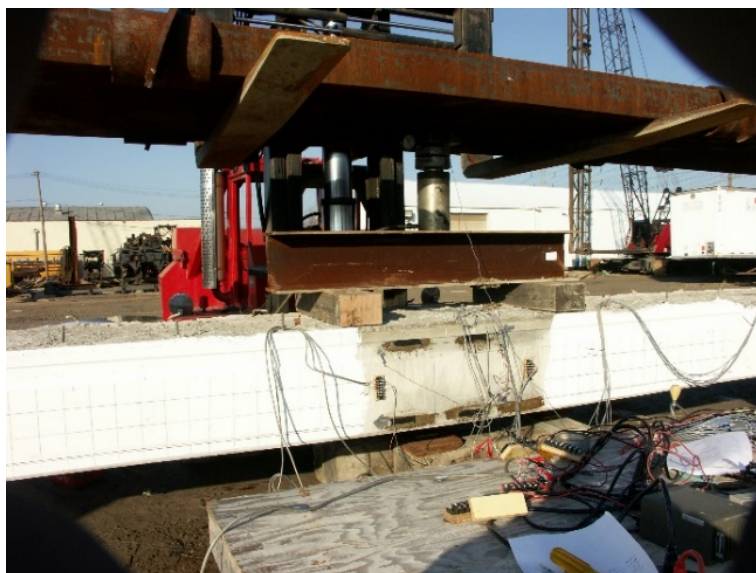
Figure 2-14. Load test setup for four-point bending test

Figure 2-15. A closeup view of the hydraulic ram and load cell

Figure 2-16. A closeup view of the load cell

2.3.4.2   Measurement of Displacements

Commonly used sensors for displacement measurements are cable actuated position sensors (CAPS), linear variable differential transformers (LVDT), and direct current differential transformers (DCDT) (Figure 2-17). The use of CAPS, LVDT, and DCDT requires establishing a reference to mount the sensors. These requirements and the access limitations at sites are considered as major limitations for using these sensors. Hence, noncontact distance measurement technologies such as *Laser Tracker®* shown in Figure 2-18 are popular. Attanayake and Aktan (2019) describe the capabilities of this technology and provide outdoor implementation examples. Laser Tracer can be used to capture beam deflection profile, curvature, and strain during load testing by mounting a series of reflectors along the beam length and depth.

26

(a) CAPS setup for beam deflection measurement   (b Calibration of a DCDT at the site

Figure 2-17. CAPS and DCDT

(a) Leica Laser Tracker   (b) CAPS and Laser Tracker reflector on a beam
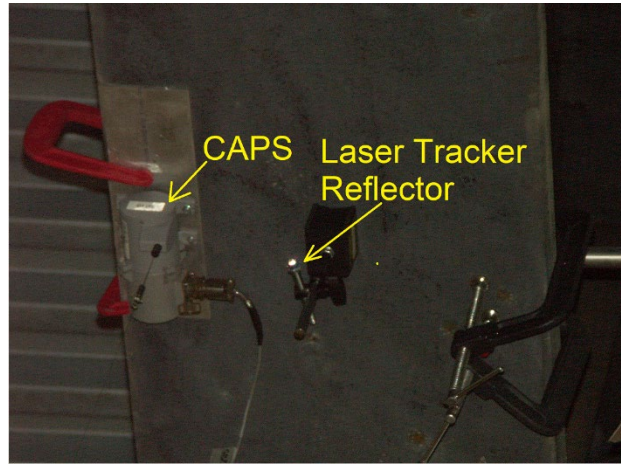
Figure 2-18. Laser Tracker distance measuring system

Additionally, several commercially available optical technologies are used in structural testing. Optotrack Certus HD® is a Dynamic Measuring Machine (DMM) that tracks motion in 6 DOF of specific locations with special targets. Figure 2-19 shows the equipment and accessories. Figure 2-20 and Figure 2-21 show two implementations under indoor conditions. A single unit of the device can monitor an area of 8.9 ft × 12.1 ft and a 35.3 ft^3 volume. With a sampling rate is 4500 targets/sec and a maximum of 512 targets located within the 35.3 ft^3 volume, the device can record deformations under cyclic or rapidly applied loads. However, as with any optical measurement system, the impact of ambient light on measurement accuracy needs to be considered (NDI 2020). Another technology developed for full-field deformation measurement is the digital image correlation (DIC) system (Attanayake 2013). Figure 2-22 shows the monitoring of a webgap deformation under laboratory conditions.

<table>
<tr><td>(a) Optotrack Certus HD</td><td>(b) Targets and a wireless strober</td></tr>
</table>

Figure 2-19. Optotrack Certus HD measuring system (NDI 2020)
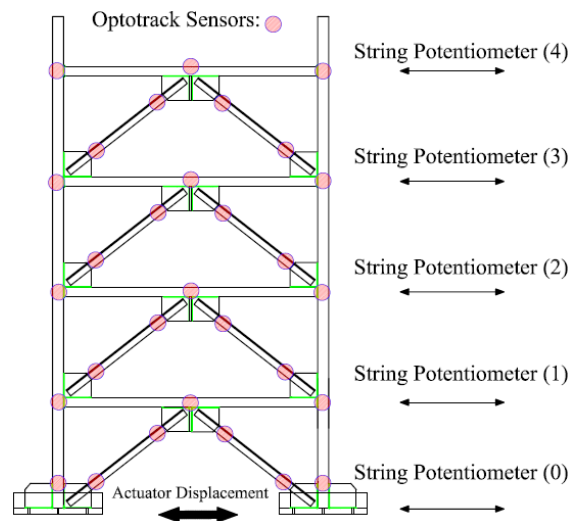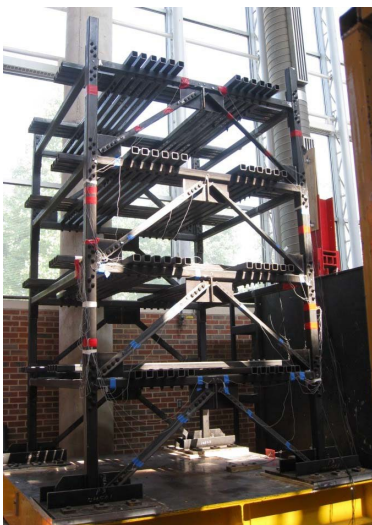
Figure 2-20. Concentrically braced frame under seismic loads (NDI 2020)

Figure 2-21. Reversed cyclic testing of a pile pile (NDI 2020)

(a) Camera system on a mount
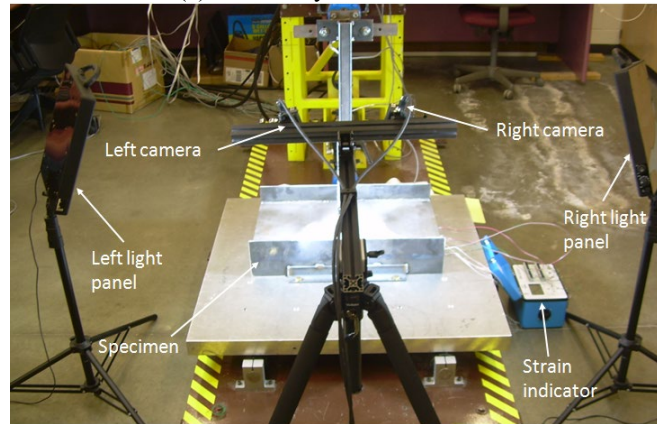
(b) Measurement of a web gap deformation
Figure 2-22. Monitoring webgap deformation using VIC-3D system

2.3.4.3   *Measuring Strain*

Foil strain gauges are typically used to measure strain. Figure 2-23 shows the use of foil gauges for measuring strain within a span and beam end. Optotrack Certus HD® and DIC systems can be used to measure full-field strain distribution. Figure 2-24 shows the strain profile at a webgap measured using the DIC system.
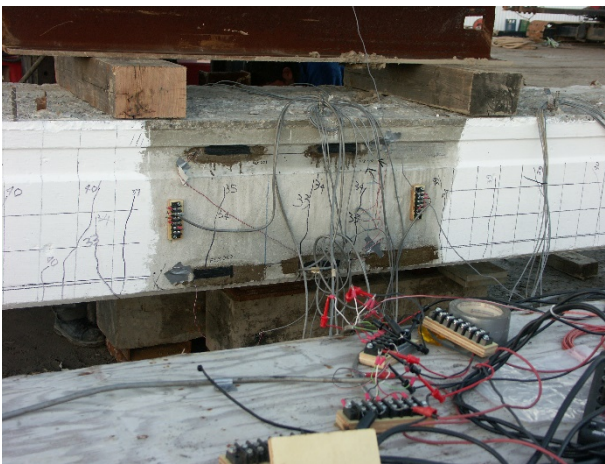
(a) Foil strain gauges at midspan   (b) Foil strain gauge layout at beam end
Figure 2-23. Foil strain gauges

(a) Speckle pattern on the web top surface (b) Close up view of the random speckle pattern

(c) Strain E_{zz} contours (c) Strain E_{xx} contours
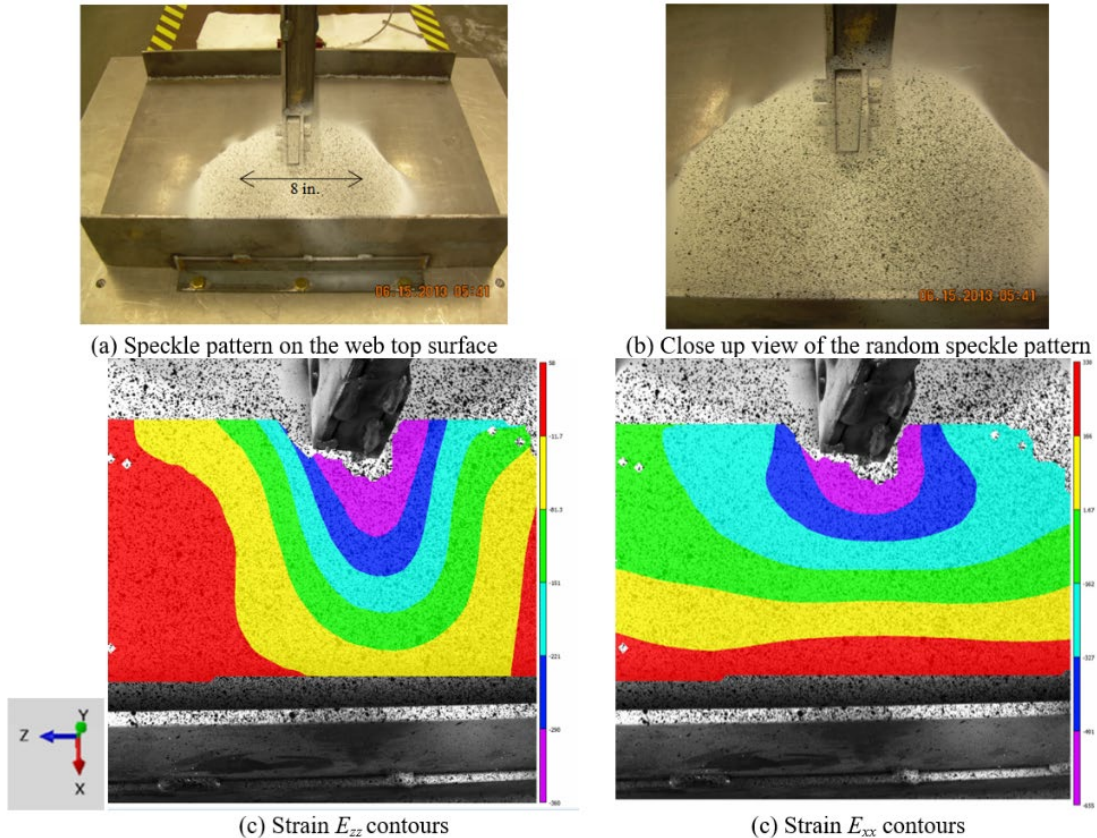
Figure 2-24. Strain profile measured using the DIC system

2.3.4.4 Detection of Crack Initiation and Measurement of Crack Width

Crack width and growth measurement technologies are available. Bruciati et al. (2019) presented an application of radio-frequency identification (RFID) technology based sensors for concrete crack detection. RFID sensors need to be mounted over the surface to detect cracks. This requires knowing the potential crack location, a challenge for monitoring crack initiation in large PC beams. Vibrating wire crackmeters are also available off-the-shelf (Figure 2-23). The standard measurement range of Model 4220 crackmeter is 0.5 in. to 6 in. with a resolution of 0.025% of the full scale (F.S) and an accuracy of +/- 0.1% F.S. The distance between sensor end supports ranges from 12.5 in. to 25.4 in. Therefore, the sensor with the 0.5 in. measurement range can be mounted across a 12.5 in. length to monitor crack width development with an accuracy of 5×10^{-4} in. The standard measurement range of Model 4422 micro crackmeter is 0.16 +/- 0.08 in. The accuracy and resolution of this sensor are +/- 0.1% F.S. and 4×10^{-5} in. The distance between sensor end supports of Model 4422 micro crackmeter is 4.72 in. Even though the sensors are labeled as 'crackmeters', these sensors basically measure the displacement between the supports. These

30

sensors are unable to identify the initiation of a crack. Therefore, the data recorded from these sensors cannot be interpreted as widening or closing of a crack without a knowledge of the crack. Acoustic emission (AE) monitoring sensors can detect crack initiation, location, and progression (BA 86 2006). Implementation of AE technology requires expertise and experience. Once the concrete cracking sound is detected, cracks are often mapped manually with markers. Beam surface can be painted in white before starting load testing to highlight the cracks. Crack width is typically measured using crack comparators and noted next to the crack, as shown in Figure 2-24.

| (a) Model 4220 crackmeter | (b) Model 4422 micro crackmeter |

Figure 2-25. Vibrating wire crackmeter (GEOKON 2020)

Figure 2-26. Flexural crack propagation during load testing

2.4 REQUIRED LEVEL OF ANALYSIS

Typical single girder responses under self-weight are flexure, deflection, and rotation. Curved and/or skewed beams develop additional effects such as torsional St. Venant shear stresses, warping normal stresses, flange lateral bending, load shifting, and twisting deformations (AASHTO/NSBA 2014a). The load response accuracy of beams calculated by structural analysis is dependent on the models used to represent the geometry, boundary conditions, and loads.

31

Solutions using 1D line-girder and 2D grid methods are not sufficiently accurate for bridges with skew, curvature, irregular geometry, or a combination thereof. For this reason, it is important to provide guidelines to establish the Required Level of Analysis (RLOA) for evaluating the member or structural system response.

The structural responses important for constructability analysis of steel I-girder bridge superstructures include major-axis bending stresses, vertical displacements, cross-frame forces, flange lateral bending stresses, and girder layover at bearings. White et al. (2012a), as part of the NCHRP Project 12-79, developed guidelines for selecting the RLOA (i.e. 1D, 2D, or 3D) for representing an accurate behavior of steel I-girder bridge superstructure response under non-composite dead loads. The guidelines presented in Table 2-2 were developed by comparing results of analyses from models with different refinement (i.e. 1D line-girder and 2D-grid methods) with the results obtained from refined 3D finite element models. Column (a) of the table shows the structural responses, and defines the bridge superstructure geometry (curved and skewed) and classification of superstructure behavior in terms of connectivity index (I_C) and skew index (I_S). Columns (b-1 and b-2) show the worst-case scores for 2D-grid and 1D line-girder analyses obtained by comparing the results of associated structural response with 3D finite element analysis (FEA) results. For identifying the analysis model, White et al. (2012a) suggested using the worst-case scores when the bridge under consideration has irregular geometry such as unsymmetrical structural geometry, unequal girder spacing, non-uniform deck width, non-uniform cross-frame spacing, etc. Lastly, columns (c-1 and c-2) present the mode of scores for 2D-grid and 1D line-girder analysis using the same methodology.

The scores in columns (b-1) through (c-2) are described in Table 2-3. Column (a) of the table shows scores that are assigned to approximate methods. Column (b) provides normalized mean error range associated with each score, and column (c) presents the interpretation of the scores.

The connectivity index, shown in Eq. (2-1), is a function of the radius of curvature of bridge centerline (R), number of intermediate cross-frames (n_{cf}), and the span configuration (simple or continuous). Cross-frame spacing and radius of curvature are the key parameters that influence the accuracy of simplified analysis results of curved steel I-girder bridges (White et al. 2012b).

$$I_C = \frac{15000}{R(n_{cf} + 1)m} \qquad (2\text{-}1)$$

In Eq. (2-1), R is measured in feet and the coefficient m is equal to 1 for simple-span and 2 for continuous-span bridges. For continuous bridges, I_C needs to be calculated for each span, and the largest value is assigned as the connectivity index for the bridge (White et al. 2012a).

The skew index, shown in Eq. (2-2), characterizes bridges based on the significance of skew that directly relates to the transverse stiffness and load path (White et al. 2012b). The skew index is a function of the bridge width measured between the centerline of the exterior girders (w_g), skew angle (θ), and span length (L).

$$I_S = \frac{w_g \tan\theta}{L} \tag{2-2}$$

In Eq. (2-2), w_g and L are measured in feet and θ is in degrees. The skew effects may be neglected when the skew index is less than 0.30. Flange lateral bending stresses and cross-frame forces are significantly affected by the skew when the index is between 0.30 and 0.65. For an index greater than 0.65, the impact of skew becomes significant to major axis bending stresses and vertical deflections, in addition to flange lateral bending stresses and cross-frame forces (White et al. 2012b).

White et al. (2012a) considered curved and skewed bridges. When $I_C \leq 0.5$ and $I_S > 0.1$, a bridge can be considered straight but skewed. When $I_C > 0.5$ and $I_S \leq 0.1$, bridges are classified as horizontally curved with no skew. As shown in Table 2-2, 1D and 2D analysis do not provide an accurate estimate of girder behavior under non-composite loads for curved and skewed bridges. This is primarily due to the inability of such modeling techniques to accurately represent the geometry, boundary conditions, and loads to capture the torsional effects due to curvature and skew.

A rational procedure for electing the RLOA for concrete bridges has not been studied. The reasons for the lack of such guidelines are (1) typical prestressed concrete multi-girder curved bridges are built with straight girder sections, (2) web and flange buckling are not of a concern for the typical sections, and (3) a majority of concrete bridges are built using standard procedures and details. Yet, experience-based rule of thumb policies are discussed in state highway agency specifications specifically to address the complications due to skew. As an example, Section 7.01.14 of the MDOT Bridge Design Manual (MDOT 2019a) presents analysis guidelines based on bridge skew (Table 2-4). Such policies apply to the constructability evaluation of concrete bridges.

Table 2-2. Matrix for Deciding the Required Level of Analysis Needed for Steel I-girder Bridges (White et al. 2012a)

Structural Response and I_c ad I_s Limits for Curved and Skewed Geometry (a)	Worst-Case Scores: Traditional 2D-Grid (b-1)	Worst-Case Scores: 1D-Line Girder (b-2)	Mode of Scores: Traditional 2D-Grid (c-1)	Mode of Scores: 1D-Line Girder (c-2)
Major-Axis Bending Stresses: Curved ($I_C \leq 1$)	B	B	A	B
Major-Axis Bending Stresses: Curved ($I_C > 1$)	D	C	B	C
Major-Axis Bending Stresses: Skewed ($I_S < 0.30$)	B	B	A	A
Major-Axis Bending Stresses:	B	C	B	B
Major-Axis Bending Stresses: Skewed ($I_S \geq 0.65$)	D	D	C	C
Major-Axis Bending Stresses: Curved & Skewed ($I_C > 0.5$ & $I_S > 0.1$)	D	F	B	C
Vertical Displacements: Curved ($I_C \leq 1$)	B	C	A	B
Vertical Displacements: Curved ($I_C > 1$)	F	D	F	C
Vertical Displacements: Skewed ($I_S < 0.30$)	B	A	A	A
Vertical Displacements: Skewed ($0.30 \leq I_S < 0.65$)	B	B	A	B
Vertical Displacements: Skewed ($I_S \geq 0.65$)	D	D	C	C
Vertical Displacements: Curved & Skewed ($I_C > 0.5$ & $I_S > 0.1$)	F	F	F	C
Cross-Frame Forces: Curved ($I_C \leq 1$)	C	C	B	B
Cross-Frame Forces: Curved ($I_C > 1$)	F	D	C	C
Cross-Frame Forces: Skewed ($I_S < 0.30$)	NA[a]	NA[a]	NA[a]	NA[a]
Cross-Frame Forces: Skewed ($0.30 \leq I_S < 0.65$)	F[b]	F[c]	F[b]	F[c]
Cross-Frame Forces: Skewed ($I_S \geq 0.65$)	F[b]	F[c]	F[b]	F[c]
Cross-Frame Forces: Curved & Skewed ($I_C > 0.5$ & $I_S > 0.1$)	F[b]	F[c]	F[b]	F[c]
Flange Lateral Bending Stresses: Curved ($I_C \leq 1$)	C	C	B	B
Flange Lateral Bending Stresses: Curved ($I_C > 1$)	F	D	C	C
Flange Lateral Bending Stresses: Skewed ($I_S < 0.30$)	NA[d]	NA[d]	NA[d]	NA[d]
Flange Lateral Bending Stresses: Skewed ($0.30 \leq I_S < 0.65$)	F[b]	F[e]	F[b]	F[e]
Flange Lateral Bending Stresses: Skewed ($I_S \geq 0.65$)	F[b]	F[e]	F[b]	F[e]
Flange Lateral Bending Stresses: Curved & Skewed ($I_C > 0.5$ & $I_S > 0.1$)	F[b]	F[e]	F[b]	F[e]
Girder Layover at Bearings: Curved ($I_C \leq 1$)	NA[f]	NA[f]	NA[f]	NA[f]
Girder Layover at Bearings: Curved ($I_C > 1$)	NA[f]	NA[f]	NA[f]	NA[f]
Girder Layover at Bearings: Skewed ($I_S < 0.30$)	B	A	A	A
Girder Layover at Bearings: Skewed ($0.30 \leq I_S < 0.65$)	B	B	A	B
Girder Layover at Bearings: Skewed ($I_S \geq 0.65$)	D	D	C	C
Girder Layover at Bearings: Curved & Skewed ($I_C > 0.5$ & $I_S > 0.1$)	F	F	F	C

[a] Magnitudes should be negligible for bridges that are properly designed and detailed. The cross-frame design is likely to be controlled by considerations other than gravity-load forces.

[b] Results are highly inaccurate. The improved 2D-grid method discussed in Chapter 6 of NCHRP 12-79 Task 8 report provides an accurate estimate of forces.

[c] Line-girder analysis provides no estimate of cross-frame forces associated with skew.

[d] The flange lateral bending stresses tend to be small. The AASHTO (2017a) Article C.6.10.1 may be used as a conservative estimate of the flange lateral bending stresses due to skew.

[e] Line-girder analysis provides no estimate of girder flange lateral bending stresses associated with skew.

[f] Magnitudes should be negligible for bridges that are properly designed and detailed.

where: I_C = connectivity index I_S = skew index

Table 2-3. Criteria for Assigning the Grades in the Required Level of Analysis Matrix

Grade (a)	Normalized Mean Error (b)	Performance (c)
A	$\mu_e < 6\,\%$	Excellent accuracy
B	$7\,\% < \mu_e < 12\,\%$	Reasonable agreement
C	$13\,\% < \mu_e < 20\,\%$	Significant deviation
D	$21\,\% < \mu_e < 30\,\%$	Poor
F	$\mu_e > 30\,\%$	Unreliable & inadequate

Table 2-4. MDOT Skew Policy (MDOT 2019a)

Skew Angle	Design Requirements
$\theta \leq 30^\circ$	Standard design using approximate methods
$\theta > 30^\circ$	Special design using refined methods*

* *Refined methods shall include using finite element methods of analysis to address girder roll, torsion, bearing restraints, bearing rotations, thermal movement direction and amount, cross-frame loading, camber detailing and deck edge/end reinforcement.*

2.5 CONSTRUCTABILITY EVALUATIONS DURING TRANSPORTATION AND LIFTING

Conventional highway bridge superstructure on-site construction starts with transportation and lifting of girders or girder segments. Such activities, if not properly executed, could result in loads exceeding section capacity or deformations exceeding the tolerances. As a result, girder stability or the quality of the completed structure can be compromised. Thus, the analysis of girders during transportation and lifting need to be a part of a constructability evaluation program. This section documents calculation procedures and practices required to maintain (*i*) capacity of PC girders against cracking and failure, (*ii*) yielding capacity of steel I-girders against local flange stresses, (*iii*) capacity of steel I-girders against lateral torsional buckling and (*iv*) deformations due to rigid-body rotation and cross-sectional twist of steel I-girders within tolerances. Analysis methods, procedures, and tools available in the literature for evaluating these constructability cases are briefly discussed along with their capabilities and limitations.

2.5.1 Lifting of PC and Steel Girders

PC and steel girder lifting procedures depend on highway agency policies and the contractor means and methods developed based on the available equipment, accessories, and experience. Figure 2-27 and Figure 2-28 show the most commonly used lifting devices. For PC girders, MDOT

requires using lifting loops (Figure 2-27a). The MDOT Bridge Design Guide Sections 6.65.14, 6.65.14A, and 6.65.14B specify (*i*) a criterion for selecting the number of strands and size for lifting loops based on PC girder type, size, and weight, (*ii*) the minimum angle of lift, and (*iii*) the minimum and maximum distances from girder ends to lifting points (MDOT 2019b). Regardless of the type, lifting devices do not provide rotational restraint. Thus, with initial eccentricity due to horizontal curvature or sweep, girders are free to rotate about the roll axis (an imaginary line connecting lifting points as shown in Figure 2-29).

(a) PC girder being lifted using lifting loops   (b) PC girder being lifted using basket hitch
Figure 2-27. Lifting devices for PC girders (FHWA 2015)

Figure 2-28. Steel I-girder being lifted using beam clamps (FHWA 2015)
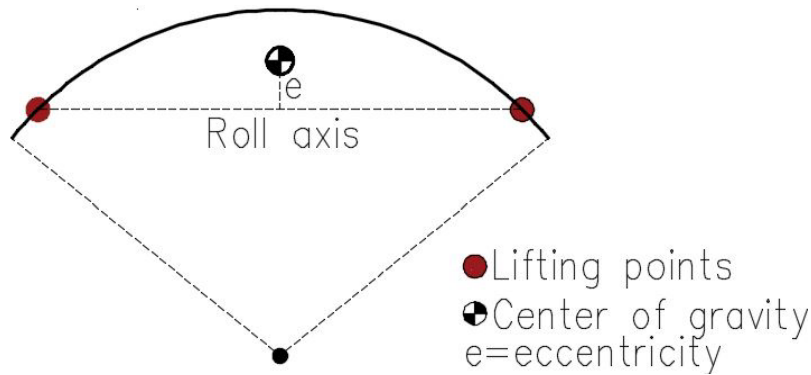
Figure 2-29. Typical lifting scheme of a girder with an initial eccentricity

2.5.2 Capacity of PC Girders Against Cracking and Ultimate Stress

2.5.2.1 Lifting

PC girder sweep results from fabrication tolerances such as deviations in girder cross-section, the lateral eccentricity of prestressing strands, or a combination thereof. When a PC girder with an initial eccentricity due to sweep is lifted, the girder rotates about the roll axis. As a result, the horizontal component of the girder self-weight acts parallel to the major axis of the cross-section and causes lateral deflection. Lateral deflection increases the eccentricity leading into an equilibrium position (Figure 2-30) or moments that could exceed the girder capacity (Mast 1989, 1993). Figure 2-31 shows the position of a rotated PC girder during lifting and forces acting on the girder. The following parameters are defined in the figure to describe the girder behavior:

e_i = initial eccentricity of girder center of mass due to sweep and lifting device placement tolerances, measured parallel to the girder major axis

W = girder self-weight

$W\cos\theta$ = vertical component of self-weight

$W\sin\theta$ = horizontal component of self-weight

y_{cm} = distance between top of girder and center of mass

y_{lift} = distance between lifting point and top of girder

y_r = distance between roll axis and girder center of mass

z = lateral deflection of girder center of mass measured parallel to the girder major axis

θ = girder rotation measured from vertical
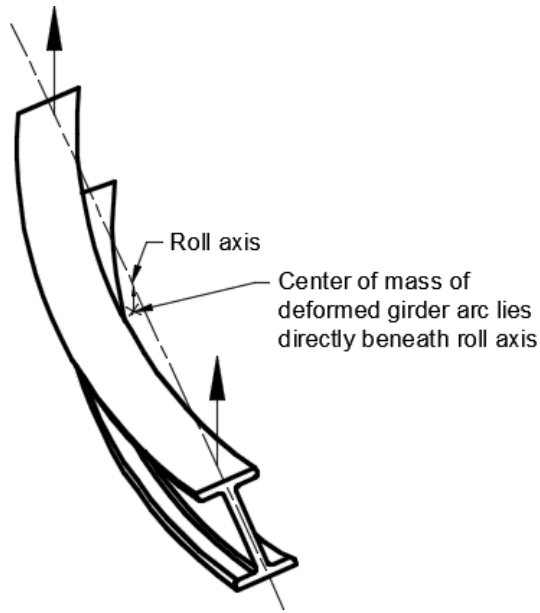
Figure 2-30. Equilibrium position of a rotated PC girder during lifting
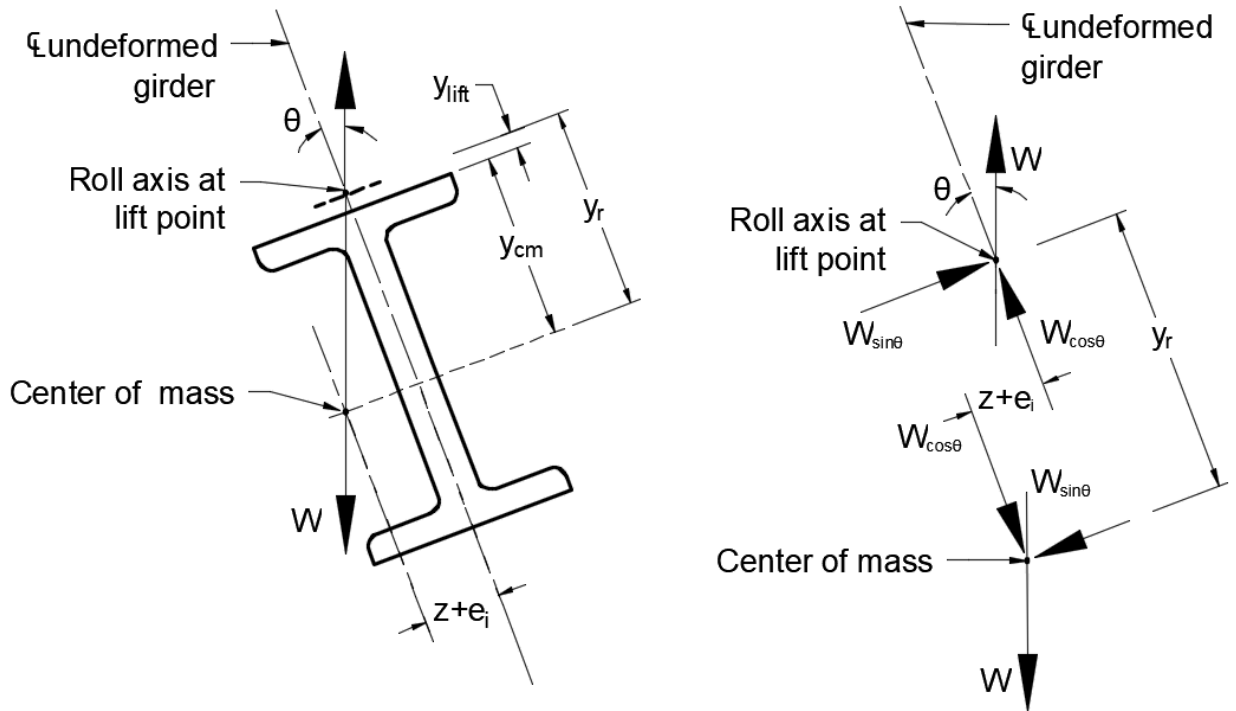
Figure 2-31. Free body diagram of a rotated PC girder during lifting

The lateral deflection of girder centroid (z) is due to the self-weight component parallel to the girder major axis ($Wsin\theta$). To calculate the girder rotation (θ) at equilibrium, z needs to be calculated, which is dependent on the rotation angle θ. Mast (1989) overcomes this issue by considering a fictitious case where the self-weight (W) is applied about the girder minor axis that

38

causes lateral deflection of girder centroid (z_o). Then, z_o is calculated using a series of statics equations with few assumptions, and z is rewritten as $z_o sin\theta$. Based on the studies by Mast (1989, 1993), PCI (2016) recommends using Eqs. (2-3) and (2-4) for calculating factor of safety against cracking (FS_{cr}) and failure (FS_f) of PC girders. PCI (2016) recommends a minimum of 1.0 and 1.5 as the factor of safety against cracking and failure, respectively.

$$FS_{cr} = \frac{M_r}{M_a} = \frac{y_r \theta_{max}}{z_o \theta_{max} + e_i} \geq 1.0 \tag{2-3}$$

$$FS_f = \frac{M_r}{M_a} = \frac{y_r \theta'_{max}}{z_o \theta'_{max}(1 + 2.5\theta'_{max}) + e_i} \geq 1.5 \tag{2-4}$$

where:

    M_a = applied moment
    M_r = resisting moment
    θ_{max} = rotation at which section cracks
    θ'_{max} = the maximum tilt angle for cracked section

2.5.2.2 Transport

Flexible bearings support PC girders during transport. The flexibility of the supports allows a girder with lateral eccentricity to rotate about its longitudinal axis. Rotational stiffness of the truck and slope of the roadway are other parameters included in the analyses. PCI (2016) recommends using Eqs. (2-5) and (2-6) for calculating factor of safety against cracking (FS_{cr}) and rollover (FS_r), respectively. The recommended minimum factor of safety against cracking and girder rollover are 1.0 and 1.5, respectively.

$$FS_{cr} = \frac{M_r}{M_a} = \frac{K_\theta(\theta_{max} - \alpha)}{W[(z_o + y_r)\theta_{max} + e_i]} \geq 1.0 \tag{2-5}$$

$$FS_r = \frac{M_r}{M_a} = \frac{K_\theta(\theta'_{max} - \alpha)}{W[(z_o(1 + 2.5\theta'_{max}) + y_r)\theta'_{max} + e_i]} \geq 1.5 \tag{2-6}$$

where:

    K_θ = rotational spring constant of the trailer
    W self-weight of the girder
    α superelevation of the roadway
    θ'_{max} critical rotation at rollover

    K_θ is often unknown but can be calculated by measuring the twisting angle of the trailer under a known weight and its position on the trailer. The trailer can be forced to twist by placing

a weight at various positions with an offset from the longitudinal axis (PCI 2003). Once the rotations at either side of braces are measured, the rotational spring constant is calculated as the average of the eccentric moment divided by the rotation in radians. In the absence of such a procedure, Article 8.1.0.3 of PCI (2003) suggests using a range of 3,000 to 6,000 kip-in per radian per dual-tire axle for K_θ. As an example, K_θ of a trailer with four dual-tire axles and a single-tire axle can be assumed to have between 13,500 to 27,000 kip-in per radian (i.e., $3,000 \frac{kip-in}{rad} \times 4 +$ $3,000 \frac{kip-in}{rad} \times \frac{1}{2}$ and $6,000 \frac{kip-in}{rad} \times 4 + 6,000 \frac{kip-in}{rad} \times \frac{1}{2}$).

2.5.3 Capacity of Steel I-Girders Against Flange Yielding Stresses

Steel I-girders are often lifted with beam clamps as shown in Figure 2-28. Beam clamps grip girders at bottom of the top flange on either side of the web and top of the top flange. The resulting moment acting on the top flange generates localized stresses (FHWA 2015). These stresses need to be checked against the yield strength of steel to determine the need for adding cover plates to strengthen the flange. FHWA (2015) recommends using Eq. (2-7) to evaluate the flange local bending stress (f_{lb}) due to clamping forces.

$$f_{lb} = \frac{R_c k}{(b_f) + (t_f)^2 / 6} \tag{2-7}$$

where:

b_f = top flange width (in.)
C_L = length of clamp along the top flange (in.)
F_{yf} = specified minimum flange yield stress (ksi)
k = distance from outer face of top flange to web toe of fillet (in.)
R_c = concentrated force at each flange edge (kip)
t_f = top flange thickness (in.)

It should be noted that the clamp forces are equal to half of the total weight when the distance between the girder center of gravity and lifting points is equal (Stith 2010). In such cases, R_c is equal to 1/4th of the girder weight. For other cases, R_c needs to be calculated considering the proposed lifting scheme.

2.5.4 Rotation of Steel I-Girders

The rationale presented in Section 2.5.2.1 for PC girder rotation during lifting also applies to the steel girders. Girder rotation about the roll axis is not expected when lifting straight girders since

the girder center of gravity coincides with the roll axis. However, when lifting a horizontally curved steel girder, the eccentricity between the girder center of gravity and roll axis causes girder rotation (Figure 2-29). Calculation of this rotation concerning a pre-approved lifting scheme and checking against given tolerances help alleviate girder splicing complications. Based on contractors' and engineers' experience documented in a survey conducted by Farris (2008), limiting the maximum girder end rotation to 1.5 degrees reduces the steel I-girder splicing complications.

Curved steel I-girder rotation consists of rigid-body rotation and cross-sectional twist. Rigid-body rotation (θ_{rigid}), which is a function of the girder center of gravity and lifting point locations, can be calculated using Eq. (2-8) (Stith 2010).

$$\theta_{rigid} = tan^{-1}\left(\frac{e}{H + t_{fc} + \bar{H}_{C.G.}}\right) \qquad (2\text{-}8)$$

where:

e = eccentricity between girder center of gravity and roll axis
H = roll axis height measured from top of the top flange
$\bar{H}_{C.G.}$ = distance to girder center of gravity measured from bottom of the top flange
t_{fc} = top flange thickness

A girder that is free to rotate about the roll axis is subjected to torsion due to self-weight, resulting in the twisting of the cross-section. The magnitude of the cross-sectional twist is a function of girder torsional stiffness. For open sections, such as I-girders, the torsional stiffness is the summation of St. Venant and warping stiffnesses. Stith (2010) presented a 1D displacement-based finite element procedure for analyzing cross-sectional twist, and suggested a generalized relationship of cross-sectional stiffness $[K_e]$, nodal displacements (nodal rotation and change of rotation) $\{\varphi\}$, nodal fixed end forces $\{G_{eFE}\}$, and external nodal forces (applied torques) $\{G\}$. This relationship is shown in Eq. (2-9).

$$[K_e]\{\varphi\} = \{G_{eFE}\} + \{G\} \qquad (2\text{-}9)$$

This procedure is implemented in *UT Lift 1.3*, a spreadsheet, for calculating cross-sectional twist and total rotation (UT Lift 2019). Section 2.5.6.2 provides additional details about this tool.

2.5.5 Lateral Torsional Buckling of Steel I-Girders

Steel girders are susceptible to lateral torsional buckling during lifting when unbraced length segments are relatively long. Timoshenko and Gere (1961) proposed Eq. (2-10) for buckling analysis of a straight, doubly-symmetric girder under a uniform moment.

$$M_o = \frac{\pi}{L_b} \sqrt{EI_y GJ + E^2 I_y C_w \left(\frac{\pi^2}{L_b{}^2}\right)} \tag{2-10}$$

where M_o is elastic lateral-torsional buckling capacity, L_b is unbraced length of the girder segment, E is the modulus of elasticity, I_y is minor axis moment of inertia, G is shear modulus, J is the torsional constant of the cross-section, and C_w is warping constant.

Eq. (2-10) is also multiplied by a moment gradient factor (C_b) to account for the non-uniform moment. Buckling analysis of a girder during lifting is not straightforward since the boundary conditions dictated by lifting equipment and the corresponding unbraced lengths are not clearly defined. Farris (2008) and Schuh (2008) performed parametric finite element analyses for investigating the buckling behavior of steel I-girders during lifting and developed moment gradient factors that apply to this problem. The scope of their study includes straight and curved prismatic and non-prismatic steel I-girders. The study indicated that the unbraced length needs to be taken as the full length of the girder and that buckling capacity is maximized when girders are lifted near quarter points. Farris (2008) recommended using the following C_b factors to multiply the elastic lateral torsional buckling capacity, calculated using Eq. (2-10), to account for the non-uniform moments acting on a girder:

$$C_b = 2.0 \; for \; \frac{L_{\overline{Lift}}}{L} \le 0.225 \tag{2-11}$$

$$C_b = 6.0 \; for \; 0.225 < \frac{L_{\overline{Lift}}}{L} < 0.300 \tag{2-12}$$

$$C_b = 4.0 \; for \; 0.300 \le \frac{L_{\overline{Lift}}}{L} \tag{2-13}$$

where:

L = distance from lift points to the girder ends
$L_{\overline{Lift}}$ = length of the girder segment being lifted

For unsymmetrical lifting schemes, $L_{\overline{Lift}}$ is taken as the arithmetic average. The proposed C_b factors can also be used for the buckling analysis of straight or mildly curved (radius of curvature, $R \ge 1800$ ft) prismatic or non-prismatic steel I-girders (Stith et al. 2013).

42

2.5.6 Analysis Methods and Tools

2.5.6.1 *PC Girder Stability and Capacity Analysis during Lifting and Transport*

PCI Girder Stability Subcommittee developed examples encompassing various lifting and transportation cases for PC girders. Chapter 6 of the *PCI Recommended Practice for Lateral Stability of Precast, Prestressed Concrete Bridge Girders* (PCI 2016) presents these examples and associated Mathcad scripts. The Mathcad scripts are based on the methodology and equations presented in Imper and Laszlo (1987) and Mast (1989 and 1993) for evaluating the impact of the following parameters on girder stability and capacity:

- lifting cable configuration (vertical or inclined cables)
- wind loads during lifting and transport
- roadway superelevation during transport
- sweep and camber during lifting or transport
- harped strands on girder stresses
- rotational stiffness of the truck used for girder transport.

The Mathcad script analysis results provide:

- lateral girder eccentricities under self-weight and wind loading
- girder compressive and tensile stresses at harping points against the allowable stress limits
- factor of safety against cracking and failure during lifting
- factor of safety against cracking and rollover during transport.

The analysis procedure incorporates the following assumptions:

- Girder deformations are small enough for the small deflection theory.
- Girders are lifted using two devices.
- The distances from the girder ends to lifting points are equal.
- Girder sweep is due to form misalignment.
- Prestressing strands are placed symmetrically.
- The effect of vertical wind uplift pressure is negligible.

2.5.6.2 *Steel I-Girder Stability and Deformation Analysis during Lifting*

The Texas Department of Transportation (TxDOT) sponsored a project for analyzing stability and deformation of straight and curved steel I-girders during lifting. For this purpose, the project developed a tool on an excel platform. This tool, named as the *UT Lift*, incorporates the equations

and assumptions presented in Stith (2010) and Farris (2008). The tool provides the following capabilities:

- analysis of prismatic and non-prismatic girders
- analysis of girders with up to eight cross-sectional changes along the span
- scale factor to account for the weight of fabricated parts such as shear studs and stiffeners
- incorporating girders with cross-frames attached on the inside, outside, or either side of the girder.

The output of *UT Lift* consists of:

- the center of gravity of the girder segment being lifted
    - the optimum location for lifting points and the required spreader beam length to prevent girder rotation
- reaction forces at beam clamps (i.e. lifting forces)
- girder rigid body rotation and the total rotational response at girder ends and mid-distance between lifting points
- top and bottom flange stresses at lifting points and mid-distance between lifting points
- buckling capacity of the girder and the critical buckling load as per the procedures presented in Farris (2008)
- out-of-plane displacement, rotation, and torsion along the girder length.

The procedures incorporate the following assumptions:

- The girders are lifted at two points with two or a single crane using a spreader beam, the most common methods used by contractors (Farris 2008).
- Cross-frame weights are at a distance of *S/2* from the girder centerline (where *S* is the girder spacing).

The procedures have the following limitations:

- Wind load effects are not considered.
- Girder rotation due to a cross-sectional twist is calculated by 1D linear finite element analysis; thus, it neglects the effect of geometric nonlinearity.
- The critical buckling load calculated by incorporating C_b factors recommended by Farris (2008) is only accurate for straight or mildly curved girders (radius of curvature, $R \geq 1800$ ft) but represents an upper-bound solution for moderately to highly curved girders ($R \leq 1200$ ft).

2.6   CONSTRUCTABILITY EVALUATIONS DURING ERECTION

The challenges faced during the erection of steel and concrete superstructures are primarily related to retaining deformation tolerances and stability of girders or girder systems. Controlling structural geometry during erection is essential for meeting deformation tolerances and constructing the bridge as per project specifications. Moreover, in the absence of a hardened deck, girders or girder systems are susceptible to lateral deformations and instability. This section addresses (*i*) potential constructability cases during erection, (*ii*) available analysis methods and tools for evaluating such cases, (*iii*) capabilities and limitations of the analysis methods and tools, and (*iv*) the assumptions used in such methods and tools.

2.6.1   Vertical and Horizontal Alignment of Concrete and Steel Bridges

Controlling vertical and horizontal alignment of a superstructure is key to constructing the bridge as per project specifications. Thus, the geometry of the partially erected structure should be maintained within the specified vertical and horizontal displacement tolerances during each stage of the erection. Table 2-5 presents the horizontal and vertical alignment tolerances for steel I-girder bridges (AASHTO/NSBA 2014b). Table 2-6 presents the PC girder dimensional tolerances specified by MDOT.

Table 2-5. Horizontal and Vertical Alignment Tolerances for Steel I-Girder Bridges (AASHTO/NSBA 2014b)

The maximum deviation from theoretical horizontal alignment*
= ± 1/8 in. × (total length along girder between supports (ft) / 10)
The maximum deviation from theoretical vertical alignment*
= + 1/4 in. × (total length from the nearest support (ft) / 10)
*Both horizontal and vertical alignments shall be measured under steel dead load at the centerline of the top flange.

Table 2-6. MDOT PC Beam Dimensional Tolerances (MDOT 2012)

Beam Type	Tolerance
Length of I-beams and 1800 beams	$\pm 1/4$ in. / 25 ft, 1 in. max
Length of box beams	$\pm 3/4$ in.
Width of I-beams and 1800 beams	+ 1/2 in., -1/8 in.
Width of box beams	$\pm 1/2$ in.
Height of I-beams, 1800 beams, or box beams	+ 1/4 in., -1/8 in.
Camber deviation from design value (measured within 24 hours of strand release)	1/8 in. / 10 ft
Thickness of top slab of box beams	+ 1/2 in., -1/4 in.
Length of I-beam end blocks	+ 2 ft
Sweep of I-beams and 1800 beams (horizontal deviation of centerline from a straight line between ends measured at both top and bottom)	1/4 in. / 10 ft
Sweep of box beams (horizontal deviation of centerline from a straight line between ends measured at both top and bottom)	3/8 in. up to 60 ft, 1/2 in. over 60 ft
Vertical deviation of side forms between top and bottom of beam	$\leq 1/4$ in. from plan location
Prestress strand	$\leq 1/4$ in. from plan location
Location of conduit for transverse post-tensioning	$\leq 1/2$ in. from plan location
Location of holes for position dowels (I-beams and 1800 beams)	$\leq 1/2$ in. from plan location
Location of holes for position dowels (box beams)	≤ 1 in. from plan location

2.6.1.1 Time-Dependent Deformation of PC Girders

PC girders develop a net upward deflection (camber) under the effect of prestressing force. During design, the camber at transfer and before deck placement are often calculated. Estimating the camber is necessary for quality assurance purposes and adjusting screed elevations before deck placement. When field camber varies from calculated, remedial actions, such as adjustment of girder seats and haunch depth, need to be implemented to achieve the intended deck profile and ride quality. These activities increase construction duration and cost, and for certain cases, the girder design needs to be re-checked against an increased dead load due to the modified haunch and/or deck thickness. Thus, it is critical to maintain the deformations within the tolerances given in Table 2-6.

PC girder camber is affected by many parameters, of which time-dependent concrete properties (i.e. elasticity modulus, concrete shrinkage, creep, etc.) and time-dependent prestressing losses are the dominant parameters. At present, MDOT uses Eq. (2-14) presented in Libby (1997) for calculating PC girder deflection and camber after incorporating appropriate factors and the effects of dead and live loads, creep, shrinkage, and prestress losses. This equation is also used in

the MDOT Bridge Design System (BDS) for calculating the ultimate total load deflection (δ_u) of a composite girder.

$$\delta_u = \delta_p\left[1 - \frac{\Delta P_s}{P_o} + \alpha_s k_r C_u \lambda'\right] + \delta_d[1 + \alpha_s k_r C_u]$$
$$+ \delta_p \frac{I}{I'}\left[-\frac{\Delta P_u - \Delta P_s}{P_o} + k_r C_u(\lambda - \alpha_s \lambda')\right] + \delta_d \frac{I}{I'} k_r C_u(1 - \alpha_s) \qquad (2\text{-}14)$$
$$+ \delta_s\left[1 + \alpha_s k_r C_u \frac{I}{I'}\right] + \delta_{DS} + \delta_L$$

where:

C_u	= ultimate creep ratio
I	= moment of inertia of non-composite girder
I'	= moment of inertia of composite girder
k_r	= factor taken as 1.0 for PC girder
P_o	= prestressing force after transfer (after elastic loss)
α_s	= ratio of the creep ratio for the concrete of the girder at the time the slab is cast to the ultimate ratio
	= $t^c / (d + t^c)$
δ_d	= deflection due to girder self-weight
δ_{DS}	= deflection due to differential shrinkage and creep between girder and slab concrete
δ_L	= deflection due to live load
δ_p	= deflection due to prestressing
δ_s	= deflection due to slab dead load
ΔP_s	= loss of prestress at time the slab is cast (excluding the initial elastic loss)
ΔP_u	= total loss of prestress (excluding the initial elastic loss)
λ	= $1 - (\Delta P_u / 2P_o)$
λ'	= $1 - (\Delta P_s / 2P_o)$

Appertaining to construction means and methods, particular attention should be given to girder storage conditions. PC girders, upon attaining the target release strength, are stripped from beds and stored in the yard. During this period, overhang portions of girders (cantilever parts beyond the temporary supports) induce additional camber because of elastic deflection owing to overhang self-weight and time-dependent deflection due to creep of the overhangs (Honarvar et al. 2015). This phenomenon applies to field storage as well.

PC girders of adjacent box-beam bridges may have unique constructability challenges due to differential camber. In general, the construction sequence of an adjacent box-beam bridge can be summarized as: (1) lifting and placing PC girders on their respective bearings, (2) grouting of shear keys, (3) transverse post-tensioning of the bridge cross-section, and (4) pouring the cast-in-place deck. An excessive differential camber results in misalignment of post-tensioning ducts and non-uniform cast-in-place concrete deck. Thus, misalignment must be corrected before grouting

the shear keys. Typical practice is to place dead loads or barriers on the beam with excessive camber until the differential camber is reduced to the specified tolerances. Since the girder behavior during preloading is linear elastic, the required load and placement can be calculated by the elastic theory of beam deflection. The preloading results in locked-in stresses in the girder-shear key assembly that need to be considered later during load rating.

2.6.1.2 Twist and Detailing of Steel I-Girder Bridges

Individual girders or partially erected superstructure units of curved and/or skewed steel I-girder bridges exhibit torsional displacements (twist) under component self-weight and construction loads. It is important to understand the fundamental difference in skewed and curved bridge behavior that develops torsional displacements.

Girders in skewed I-girder bridges deflect vertically under the gravity loads and do not exhibit torsional displacements before cross-frame installation. As per the AASHTO (2017a) Article 6.7.4.2, cross-frames are placed parallel to skewed support lines when the skew is less than or equal to 20 degrees. In this case, no differential deflection occurs at the end of cross-frames, but the girders twist to maintain rotational continuity with cross-frames between the girders (NSBA 2016). When the skew angle is greater than 20 degrees, the cross-frames are installed normal to the girders. Thus, each cross-frame connects along the girder span at different positions causing the girders to twist under the vertical differential deflection at each end of the cross-frames. Curved I-girder bridges, on the other hand, are subjected to torsion because of the eccentricity between the applied loads and the line of support. Thus, the girder twist is independent of cross-frame installation. In fact, in the absence of cross-frames, torsional displacements tend to be larger due to the lack of internal constraints (NSBA 2016).

Torsional deformations of curved and/or skewed steel I-girder superstructure units create several complications during erection; a few examples are (1) difficulties in assembling girders and cross-frames that may require significant force-fitting, field drilling, field welding, or a combination thereof, (2) locked-in stresses developed in girders and cross-frames that will impact the design capacity of the structure, (3) misalignment between the approach spans and bridge superstructure, and (4) bearing rotation exceeding the design value (NSBA 2016). These complications can be alleviated utilizing appropriate fit conditions for the bridge under consideration. As per the AASHTO (2017a) Article C6.7.2, the common fit conditions are:

- **No Load Fit (NLF):** *Cross-frames or diaphragms are detailed to fit to the girders in their fabricated, plumb, fully cambered position <u>under zero dead load</u>.*

- **Steel Dead Load Fit (SDLF):** *Cross-frames or diaphragms are detailed to fit to the girders in their ideally plum as-deflected positions <u>under the self-weight of the steel</u> after the erection.*

- **Total Dead Load Fit (TDLF):** *Cross-frames or diaphragms are detailed to fit to the girders in their ideally plumb as-deflected positions <u>under the total dead load</u>. The total dead load typically includes the weight of the concrete deck, but not the superimposed dead loads.*

Since the torsion develops from applied loads, the girder web can only be plumb in one particular load condition. Detailing girders and cross-frames for TDLF condition might be seen as the first choice, however, TDL deflections are often significantly greater than SDL deflections (NSBA 2016). Therefore, when TDLF condition is targeted, the contractor may be required to apply substantial loads using cranes, jacks, etc., for facilitating the assembly, especially for bridges with extreme curvature and/or sharp skews. Table 2-7 presents the recommended fit conditions for steel I-girder bridges provided by NSBA (2016). The recommendations are also adopted by AASHTO and included in Article C6.7.2 (AASHTO 2017a). In the table, L is the span length (ft), R is the radius of curvature (ft), θ is the skew angle (deg), and I_S is the skew index calculated as per Eq. (2-2).

Table 2-7. Recommended Fit Conditions for Steel I-Girder Bridges (NSBA 2016)

L/R ratio*, Skew Angle (θ), and Skew Index (I$_S$) Limits	L	Recommended Fit Condition	Acceptable Fit Condition	Fit Conditions to be Avoided
L/R ≤ 0.03; θ ≤ 20°	Any	NLF & SDLF & TDLF	NLF & SDLF & TDLF	-
L/R ≤ 0.03; θ > 20° & I$_S$ ≤ 0.30	Any	SDLF & TDLF	SDLF & TDLF	NLF
L/R ≤ 0.03; θ > 20° & I$_S$ > 0.30	≤ 200 ft	SDLF	TDLF	NLF
	> 200 ft	SDLF	-	TDLF & NLF
L/R > 0.03 & < 0.20; N/A	Any	SDLF	NLF	TDLF
L/R ≥ 0.20; N/A	Any	NLF	SDLF	TDLF

* Use maximum L/R of any span in the bridge

2.6.2 Lateral Stability of PC and Steel Girders

Girders are designed as composite sections for in-service loads. The composite action between the girders and a hardened deck increases the flexural stiffness of the superstructure and provides continuous lateral restraint to the girders. In the absence of the hardened deck, erected girders or girder systems are susceptible to lateral instability. The potential for lateral instability during erection is common to both concrete and steel bridges, however, instability modes often differ. Lateral torsional buckling is the primary instability mode for steel I-girders. Also, a rollover can be a concern for the first erected steel girder due to a lack of bracings. For PC girders, lateral torsional buckling is generally not a concern due to the high torsional stiffness of the girder and the governing instability mode is only girder rollover.

In steel I-girder bridges, bridge geometry (i.e. curvature and skew), wind loading, long unbraced length, or a combination thereof can contribute to the lateral instability. In curved girders, eccentricity between the applied loads and line of support creates an overturning moment that tends to de-stabilize the girders (FHWA 2015). Instability is especially a concern while erecting the first curved girder. Intermediate supports such as shore towers and temporary holding cranes may be required for maintaining the overturning stability. Under wind loads, lateral deflection, flange lateral bending stresses, and overturning moments can result in girder rollover and lateral torsional buckling. Similar to the curvature effect, roll stability under wind loads is critical for the first erected girder in a span.

Lateral torsional buckling capacity is controlled by the unbraced length. In steel I-girder bridges, cross-frames or diaphragms are installed as the erection progresses and provides lateral stabilization to partially erected structures. AASHTO ASD and LFD Bridge Design Specifications limited the maximum spacing of cross-frames to 25 feet (FHWA 2012). This requirement is removed from the current AASHTO LRFD Specifications and allows rational analyses to determine the required cross-frame spacing. As per AASHTO (2017a) Article 6.7.4.1, this analysis should consider the stability of the top flange in compression before curing of the deck, as well as controlling the torsional stresses and rotations due to loads applied to the overhangs during deck placement. In horizontally curved bridges, however, cross-frames and diaphragms are considered as the main load-carrying members and the AASHTO LRFD Specifications limits cross-frame spacing. As per AASHTO (2017a) Article 6.7.4.2 and C6.7.4.2, the spacing of

intermediate cross-frames (L_b) shall satisfy Eq. (2-15) in erected condition. Eq. (2-16) can be used as a guide for preliminary framing of horizontally curved steel I-girder bridges.

$$L_b \leq L_r \leq \frac{R}{10} \tag{2-15}$$

$$L_b = \sqrt{\frac{5}{3} r_\sigma R b_f} \tag{2-16}$$

where, L_r is the limiting unbraced length calculated in feet as per AASHTO (2017a) Eq. 6.10.8.2.3-5, R is the minimum girder radius within the panel (ft), r_σ is the desired bending stress ratio (a maximum value of 0.3 can be used), and b_f is the flange width (ft).

As per AASHTO (2017a) Article A6.3.3, Eq. (2-17) gives the elastic lateral torsional buckling stress (F_{cr}) in units of ksi.

$$F_{cr} = \frac{C_b \pi^2 E}{(L_b/r_t)^2} \sqrt{1 + 0.078 \frac{J}{S_{xc}h}(L_b/r_t)^2} \tag{2-17}$$

where, C_b is moment gradient modifier, E is elasticity modulus of steel (ksi), L_b is unbraced length (in.), r_t is effective radius of gyration (in.), S_{xc} is elastic section modulus about the major axis of the section to the compression flange (in.³), and h is depth between centerline of the flanges (in.).

PC girder rollover is possible due to lateral imperfections (i.e. girder sweep), wind loading, or a combination thereof. Theoretically, girder horizontal curvature is sweep and the eccentricity between the applied loads and support axis generates an overturning moment. Similarly, wind loads generate additional lateral force and overturning moment that must be accounted for in the stability analysis of PC girders. PCI (2016) adopted the procedures developed by Mast (1993) and recommends Eq. (2-6) for calculating a factor of safety against rollover by replacing the rotational spring constant of a trailer with the rotational stiffness of the bearings and superelevation of the roadway with a tilt angle of bearings. Tilt angles can be taken as the maximum transverse seating tolerance from a level position. The procedure developed by Mast (1993) is used by state highway agencies. As an example, FDOT developed a Mathcad script titled Beam Stability (version 2.4) for evaluating the stability and temporary bracing requirements of simple-span PC girders during erection. Unlike the Mathcad scripts developed by PCI (2016) (see Section 2.6.3.3), this script

reflects FDOT policies and practices such as state-specific PC girder inventory and temporary bracing configurations.

2.6.2.1 *Bracing of PC and Steel I-Girders*

Permanent and/or temporary bracings are used during erection to maintain the stability of individual girders or partially completed girder systems. Permanent bracings consist of cross-frames and diaphragms. Temporary bracings, on the other hand, are not well-standardized as cross-frames or diaphragms. This is because their design and use depend on contractor means and methods. Consequently, the bracing can be in various forms depending on availability and experience. Permanent and temporary bracings are both designed or designated from predesigned details. PC girders are braced near girder ends and within the span using temporary bracing systems during erection for holding the girders in place, preventing rollover, and restraining girder twist. End bracings are installed before crane release; intermediate bracings are installed between adjacent girders as the erection progresses.

For PC girders, MDOT specifies cast-in-place (CIP) concrete and steel diaphragms (or cross-frames) (MDOT 2019b). The use of steel intermediate diaphragms and steel end diaphragms at independent backwalls with sliding slabs is preferred as it reduces the construction duration (MDOT 2019a). Yet, MDOT Bridge Design Guide (MDOT 2019b) details CIP concrete diaphragms to be used at piers, independent backwalls without sliding slab, and midspan. However, CIP diaphragms cannot be counted as lateral stability bracings since formwork installation and casting of diaphragms are completed after erecting all the girders in a span or a bridge. Table 2-8 summarizes the MDOT practice on steel diaphragms and cross-frames for PC girders. These diaphragms and cross-frames can serve as stabilizing members when utilized during erection. The common practice is to install bracing just before deck placement. Thus, temporary bracings are critical for maintaining PC girder stability during erection.

Table 2-8. Steel Diaphragm and Cross-frame Alternatives for PC Girders (MDOT 2019b)

Girder Type	Steel Diaphragm / Cross-Frame	Location	Layout
28" through 54" deep PC I-girders	Steel channel diaphragm	Midspan & Independent backwalls with sliding slab	Continuous line for $\theta \leq 10°$ Staggered for $\theta > 10°$
70" deep PC I-girder & MI 1800	Steel X-type cross-frame with a bottom strut		
48" and 54" deep bulb-tee PC girders	Steel channel diaphragm		
60", 66", and 72" deep bulb-tee PC girders	Steel X-type cross-frame		

Figure 2-32a shows a typical TxDOT diagonal bracing system used at the girder ends. To hold the girder in place, irrespective of the direction of loading, a timber block is used as a compression member while a wire acts as a tension member. As per the Texas DOT *Standard Details for Minimum Erection and Bracing Requirements: Prestressed Concrete I-Girders and I-Beams* (TxDOT 2015), diagonal bracing is required at both ends of the first erected girder in a span. In addition to diagonal bracing, top and bottom flange level braces are required in the vicinity of girder ends and within the span. Figure 2-32b shows a TxDOT horizontal bracing system with steel straps that are anchored to the top flange and timber blocks that are in tight fit between the bottom flanges. Alternatively, steel straps can be welded to shear connectors. The TxDOT practice is to place the first horizontal bracing at 4 feet from the girder ends and to limit the maximum spacing of horizontal bracings to 60 feet.

(a) Diagonal bracing details

(b) Horizontal end and intermediate bracing alternative
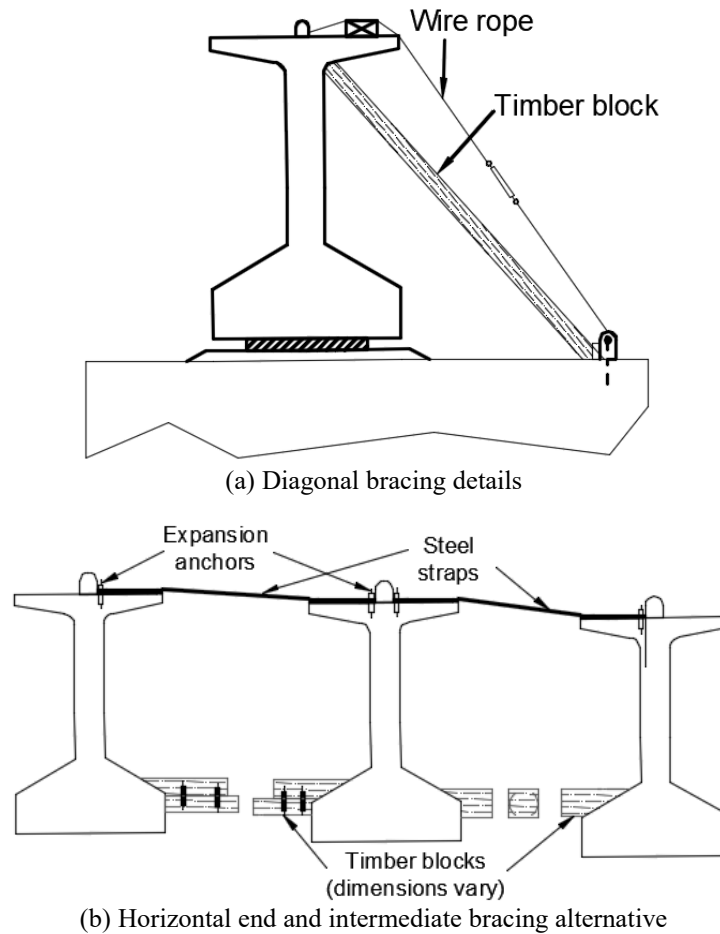
Figure 2-32. TxDOT temporary bracing details for PC girders

Figure 2-33a shows three FDOT anchor bracing alternatives used at piers or abutments of PC girder bridges. The contractor is permitted to use any of these configurations depending on their experience and material availability. Anchor bracings are only used for the first erected girder within the cross-section (FDOT 2013). Cables are often used as tension members (T) while angles or pipes are used as tension and/or compression members (T&C). In addition to anchor bracings, FDOT requires contractors to use temporary bracing for all the girders. Figure 2-33b shows FDOT bracing system alternatives used in the vicinity of girder ends and within the span. The maximum longitudinal distance between end bracings and the bearing centerline is limited to 4 feet (FDOT 2013).

(a) Anchor bracing alternatives

(b) End and intermediate bracing alternatives
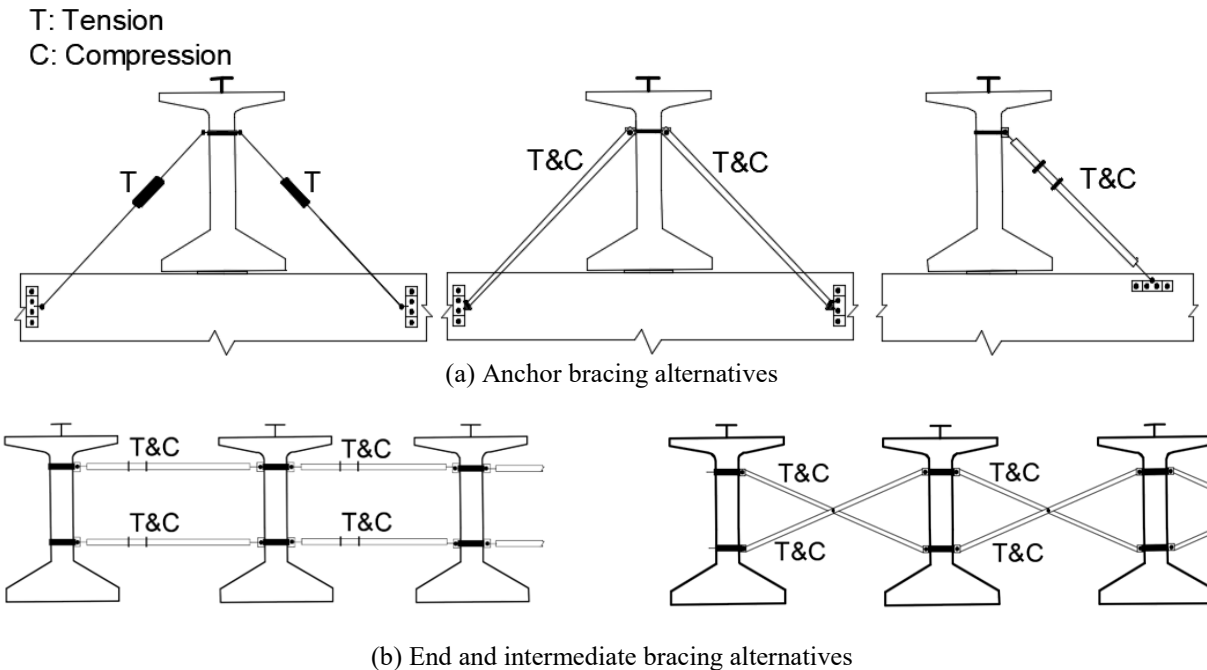
Figure 2-33. FDOT temporary bracing details for PC girders

At PC girder ends, PennDOT specifies primary and secondary temporary bracing systems (Figure 2-34). The primary bracings are hold-down systems. Figure 2-34a shows one such system with threaded bars and a channel. The bars are anchored to the substructure. The channel is placed across the top flange to distribute loads and eliminate local stresses at the flange tips. The secondary bracing, on the other hand, consists of top flange level timber blocks and a cable. The cable connects all girders in the cross-section and is anchored to the substructure. PennDOT requires contractors to use the primary bracings when girders are *inherently unstable* or placed on high load multirotational bearings, whereas the secondary bracing is required for *inherently stable* girders. As per the Pennsylvania DOT *BC-772M Standard Prestressed Concrete Beam Bracing Notes* (PennDOT 2010), a girder is defined as *inherently stable* if the vertical reaction at the girder support under specific load cases is located within the middle 2/3 of the bearing (load cases are shown in Figure 2-35). The reaction is calculated at the girder seat considering moment equilibrium. The first load case in Figure 2-35 is used for evaluating stability before crane release while the second load case is considered for stability during erection. Table 2-9 and Table 2-10 describe the loads, load cases, and their applications.

(a) Primary bracing details

(b) Secondary bracing details
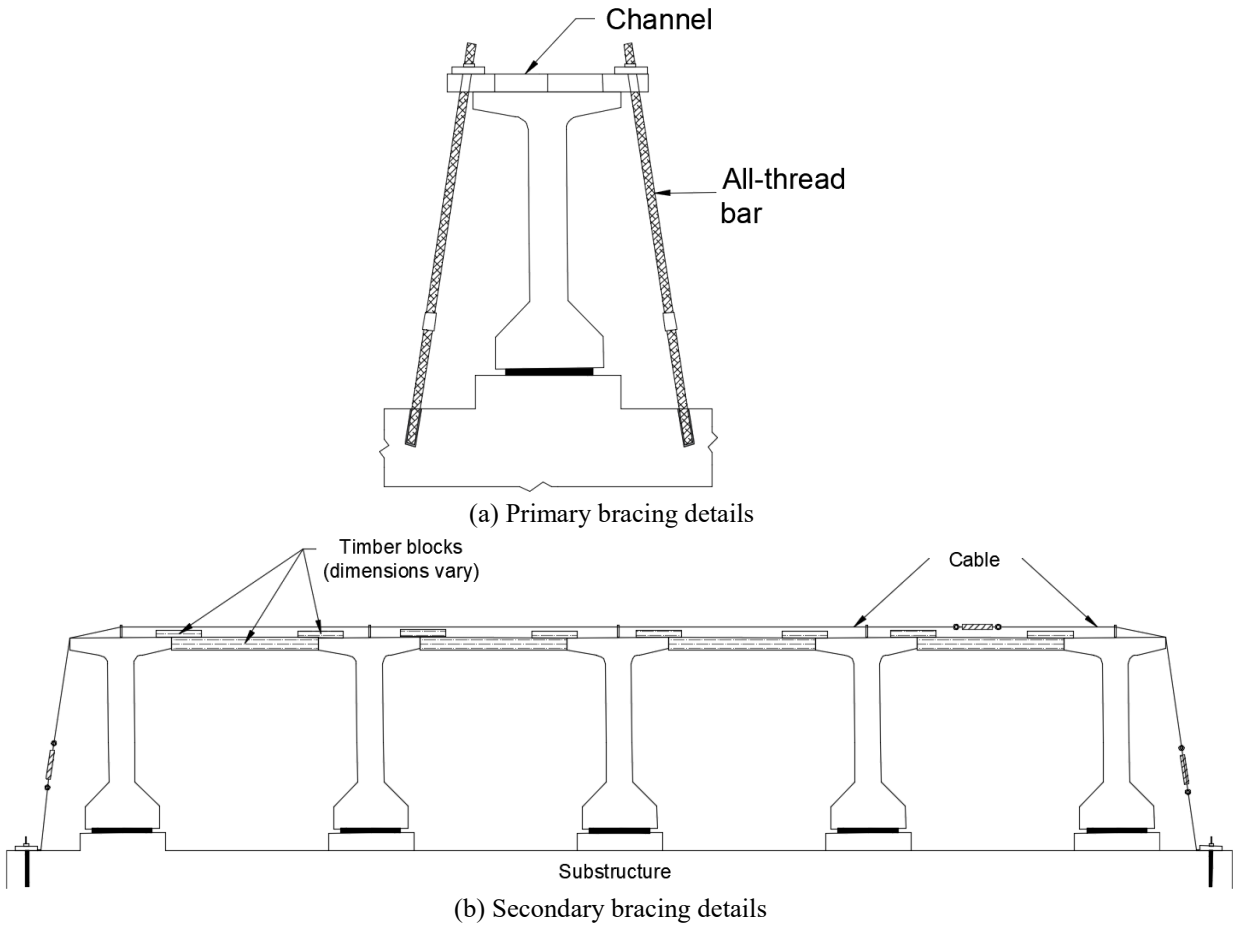
Figure 2-34. PennDOT temporary bracing details for PC girder ends

P = Beam weight reaction
= Beam unit weight/ft x span length/2
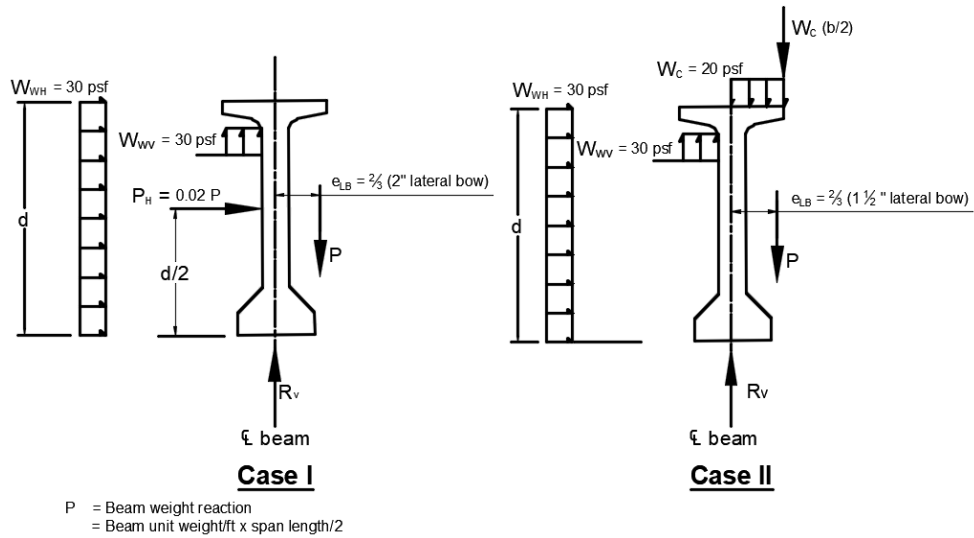
Figure 2-35. PennDOT load cases for girder stability evaluation

Table 2-9. Details of PennDOT Load Case I for Girder Stability Evaluation (PennDOT 2010)

W_{WH} = Horizontal force acting at mid-depth of the girder due to a wind pressure of 30 psf acting horizontally on girder side.
W_{WV} = Vertical force acting upward on one side of the top flange overhang due to a wind pressure of 30 psf. The resultant force acts at mid-point of the load.
P_H = Horizontal load of 0.02P acting at the girder mid-depth due to girder tilt. P is half of the girder weight, see Figure 2-35.
e_{LB} = Eccentricity equals to 2/3 of the 2 in. lateral bow to be used for locating the girder weight reaction. The 2 in. lateral bow is due to 1.5 in. maximum allowable sweep and 0.5 in. solar gain.

Table 2-10. Details of PennDOT Load Case II for Girder Stability Evaluation (PennDOT 2010)

W_{WH} = Horizontal force acting at mid-depth of the girder due to a wind pressure of 30 psf acting horizontally on girder side.
W_{WV} = Vertical force acting upward on one side of the top flange overhang due to a wind pressure of 30 psf. The resultant force acts at mid-point of the load.
W_C = Construction load of 20 psf including overhang system and/or deck pans, acting along half of the girder top flange. The resultant force acts on the flange tip.
e_{LB} = Eccentricity equals to 2/3 of the 1.5 in. lateral bow to be used for locating the girder weight reaction. The 1.5 in. lateral bow is due to 1.0 in. maximum allowable sweep and 0.5 in. solar gain.

As an example, for the first load case, the vertical reaction at the girder seat (R_v) and the location of R_v measured from the bearing centerline (x) are calculated using Eqs. (2-18) and (2-19), respectively.

$$R_v = \frac{w_g L}{2} - \frac{W_{WV} L b}{4} \tag{2-18}$$

$$x = \frac{\dfrac{W_{WH} L d^2}{4} + \dfrac{W_{WV} L b^2}{16} + \dfrac{0.02 w_g L d}{4} + \dfrac{4 w_g L}{6}}{\dfrac{w_g L}{2} - \dfrac{W_{WV} L b}{4}} \tag{2-19}$$

where w_g is girder weight as a line load, L is span length, b is top flange width, and d is girder depth.

In steel I-girder bridges, lateral stability of the partially erected structure is provided by cross-frames or diaphragms that are installed during girder erection. Cross-frame and diaphragm designs and connection details are provided in highway agency manuals, guides, and standard plans. MDOT specifies cross-frames/diaphragms near girder ends and within the span for steel I-girder bridges. As an example, Figure 2-36a shows a K-type cross-frame provided over a pier. Figure 2-36b lists the minimum bottom chord and diagonal member size (angle size) concerning

girder spacing (*L*) and the length of a diagonal member (*S*) for straight and curved girders (MDOT 2019b).

(a) Cross-frame details
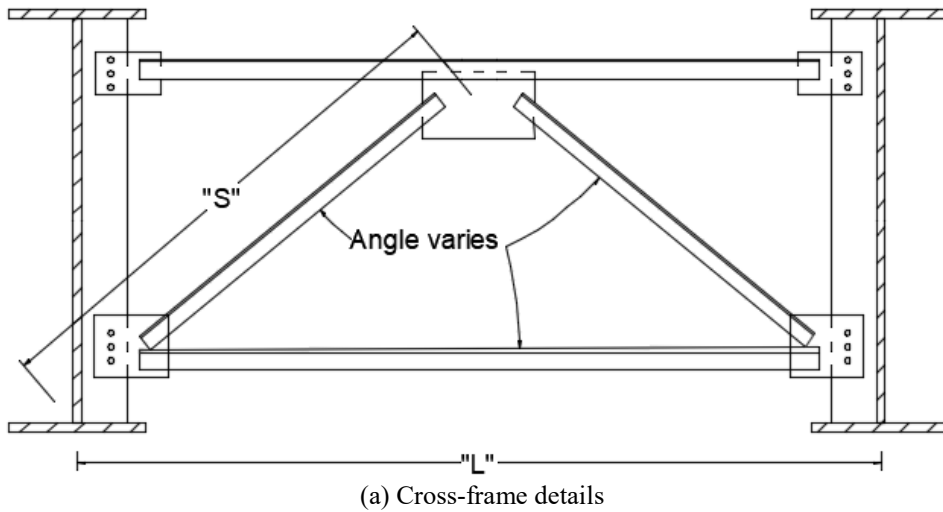
STRAIGHT GIRDERS	
"L" or "S"	Min. Angle Size
Less than 6'-9"	3" × 3" × 5/16"
6'-9" to 9'-3"	4" × 4" × 5/16"
9'-3" to 11'-6"	5" × 5" × 3/8"
11'-6" to 13'-9"	6" × 6" × 3/8"
13'-9" to 18'-6"	8" × 8" × 1/2"
CURVED GIRDERS	
Less than 5'-9"	3" × 3" × 5/16"
5'-9" to 7'-9"	4" × 4" × 5/16"
7'-9" to 9'-9"	5" × 5" × 3/8"
9'-9" to 11'-9"	6" × 6" × 1/2"
11'-9" to 15'-9"	8" × 8" × 5/8"

(b) Minimum member sizes (angle sizes) for cross-frames used in straight and curved I-girder bridges

Figure 2-36. MDOT cross-frame details and minimum member sizes (angle sizes) used in straight and curved I-girder bridges

In addition to cross-frames and diaphragms, temporary bracings are commonly used in steel I-girder bridges to maintain girder stability during construction (FHWA 2015). Figure 2-37 shows two different chain-down configurations for stability and deformation tolerance of steel I-girders during erection. In these configurations, girders are chained to their respective pedestals at piers or abutments. The chain-down system shown in Figure 2-37a consists of a steel chain with load binders. The system shown in Figure 2-37b includes a steel pipe to transfer the compression force due to wind loading and provide necessary resistance for preventing girder rollover. The chain provides resistance to the wind load from the right, whereas the steel pipe is placed for resisting the wind load from the left (FHWA 2015). As shown in the figures below, the chains

58

and the pipe are connected to the pedestals. Alternatively, these can be directly anchored to piers or abutments as shown in Figure 2-38.

(a)   (b)
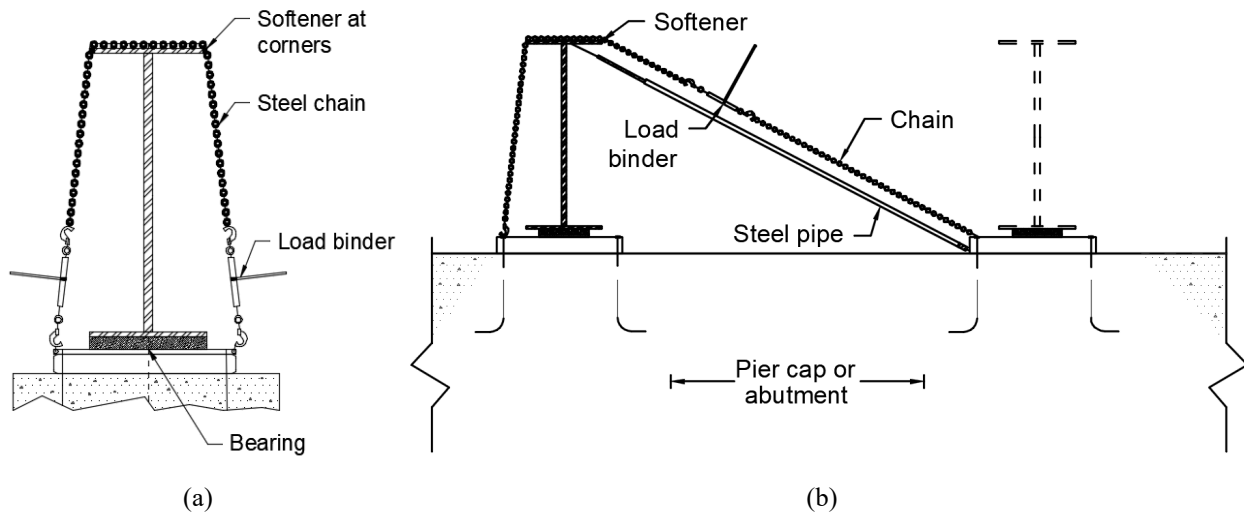
Figure 2-37. Chain-down alternatives for steel I-girders

Figure 2-38. A chain-down system anchored to substructure (Photo courtesy: MDOT)

2.6.3   Analysis Methods and Tools

2.6.3.1   *Approximate Analysis of Curved Steel I-Girder Bridges*

The V-load method, an approximate method for analyzing horizontally curved steel I-girder bridges, was developed by Richardson, Gordon, and Associates (1963). The method was developed as an improvement to the 1D line-girder analysis for evaluating curvature effects in I-girder bridges (White et al. 2012b). In this method, curved girders are modeled as equivalent

59

straight segments (i.e. straight segment length is equal to the girder length), and curvature effects are accounted for by applying self-equilibrating vertical and lateral forces at cross-frame or diaphragm locations. Figure 2-39a shows a representative segment of a two curved I-girder system and the internal forces developed within the system. In this figure, the flange force couples (M_i/h) are due to applied loads. A horizontal load couple (H_i) is introduced to the system to satisfy the equilibrium on flanges at cross-frame locations, (Figure 2-39b). Finally, the cross-frames transfer vertical shear forces (V) to achieve moment equilibrium.

(a) Internal forces develop in a curved I-girder system   (b) A flange segment at a cross-frame
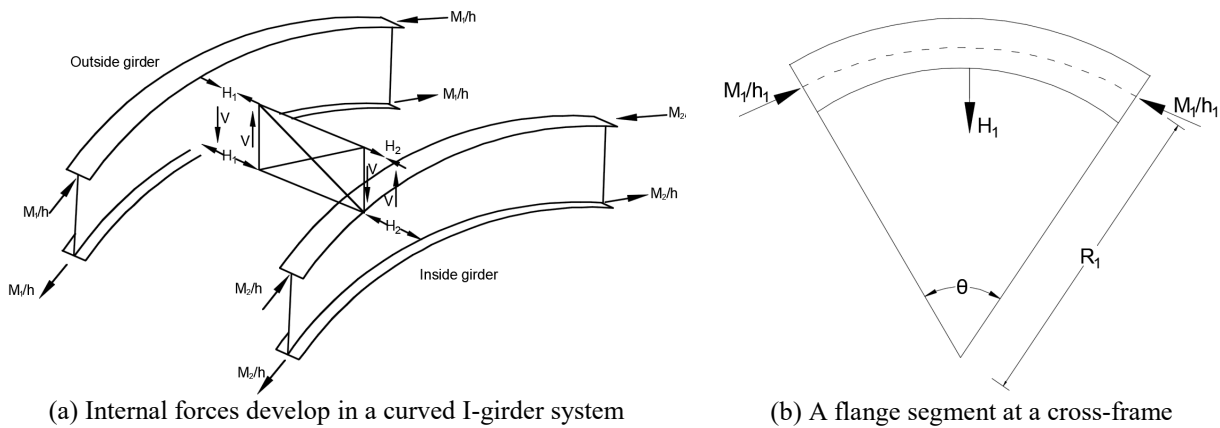
Figure 2-39. A twin curved I-girder system showing the internal forces

The analysis steps of the V-load method are summarized below (Fiechtl et al. 1987; Stith 2010):

1. Calculate bending moments and shear forces along the equivalent straight girders due to applied loads (P-loads).

2. Calculate moments due to P-loads at each cross-frame or diaphragm location.

3. Calculate the vertical shear force (V-loads) at each cross-frame or diaphragm location from Eq. (2-20).

4. Apply V-loads as point loads at each cross-frame or diaphragm locations.

5. Calculate bending moments and shear forces due to applied V-loads.

6. Calculate final moments and shear forces by superposing the results of Step 1 and 5.

$$
V = \begin{cases}
\dfrac{M_{p1} + M_{p2}}{\dfrac{RS}{d}} & N_b = 2 \\[4mm]
\dfrac{\sum_{i=1}^{N_g} M_{pi}}{\dfrac{N_b(N_b + 1)}{6(N_b - 1)} \times \left(\dfrac{RS}{d}\right)} & N_b > 2
\end{cases}
\tag{2-20}
$$

where V is the vertical shear force (V-load) at cross-frame or diaphragm locations, M_{pi} is the moment at cross-frame or diaphragm locations due to the P-load of the ith girder, R is the radius of the curvature, S is the girder spacing, d is the arch length between cross-frames or diaphragms, and N_b is the number of girders in the cross-section. The method is developed with the following assumptions and limitations (AASHTO 2017a, White et al. 2012b):

- Vertical shear forces are distributed linearly across the bridge cross-section, therefore, the method is increasingly accurate for bridges with girders having approximately equal major axis stiffness.

- The method only accounts for the torsion due to curvature.

- Inherently, the method is not capable of addressing skew effects; thus, the method is not applicable for curved bridges with a skew.

- The method is only valid for open-framed systems (i.e. non-composite I-girder systems connected by cross-frames or diaphragms located within the girder webs). The method is not applicable for composite sections as well as the girder systems with lateral bracing between the flanges.

2.6.3.2 *Erection Analysis of Steel I-Girder Bridges*

For analyzing straight, curved, or skewed steel I-girder bridges during erection and deck placement, the TxDOT project developed a 3D finite element software *UT Bridge*. Modeling features that were specifically developed for erection and deck placement analysis makes *UT Bridge* a useful tool for constructability evaluations. Figure 2-40 shows the analysis feature window for the data input process. This window optimizes the data input efforts by allowing the user to select modeling parameters. The user can select the type of analysis (e.g. erection analysis, deck placement analysis, buckling analysis, etc.) from the same window.

Feature	Check
Curved bridge	☐
Skewed supports	☐
Tapered cross-section	☐
Multiple girders	☐
Bridge supports	☐
Splices/ Transitions	☐
Stiffeners	☐
X-frames	☐
K-frames	☐
Lateral trusses	☐
Temporary supports	☐
Dapped ends	☐
Additional reference points	☐
Erection analysis	☐
Placement analysis	☐
Eigenvalue buckling analysis	☐
Point loads	☐
Wind loads	☐
Springs	☐
Special DOF fixities	☐
Large displacement analysis	☐
Modal dynamic analysis	☐
Top flange uniform loads	☐
Thermal loads	☐

Figure 2-40. *UT Bridge* **(v2.2) analysis feature window**

The finite element types available in *UT Bridge* and their applicability to specific bridge elements include:

- nine-node isoparametric displacement-based shell elements to model girder plates (flanges and web) and deck slab
- three-dimensional two-node truss elements to model cross-frames
- three-dimensional two-node beam elements to model stiffeners
- spring elements to model shear stud interaction.

The software analysis and modelling options allow:

- defining first-order structural analysis, large displacement (non-linear) analysis, or eigenvalue buckling analysis
- defining the number of elements through the web depth (4 or 8 elements) and approximate mesh size

- defining prismatic or non-prismatic girder and girder systems

- assigning X- and K-type cross-frames

- defining support and intermediate cross-frame sectional properties separately

- modeling lean-on cross-frame configuration (this feature allows inclusion or exclusion of cross-frames between girders as needed)

- accounting for the reduction in cross-frame stiffness due to bending moment from connection eccentricities

- modeling stiffeners along the girder length and specify stiffener dimensions

- defining applied load and self-weight factors and performing analysis concerning the AASHTO LRFD limit states

- specifying the number of girders to be erected, the corresponding length of the girders, cross-frame installation, and the applied loads in each step of erection

- defining flange level temporary lateral bracings, shore towers, or temporary holding cranes in each step of erection

- specifying the number of pours, start and end locations of each pour along the bridge length, time of each pour (hours), and girders to be involved in each pour during deck placement sequence

- defining shear stud parameters for composite action between the girder and deck slab

- accounting for early stiffness gain of deck slab concrete and the corresponding effects on cross-frame forces, vertical displacement and rotational behavior of girders

- defining the following loads:
  - point loads – the location and direction of the load along the girder and on the cross-section (nodes) can be specified (Figure 2-41).
  - top flange uniform loads (area loads) – construction loads can be defined with this option.
  - wind loads – load magnitude and direction can be defined for specific girders that are expected to be exposed to wind loads.
  - thermal loads – the coefficient of thermal expansion and temperature values can be defined with this option.

The loads may be defined at nine different points on the cross-section:

- the bottom flange left tip (1)
- the bottom flange to web node (2)
- the bottom flange right tip (3)
- the web lower quarter point (4)
- the web mid-depth (5)
- the web upper quarter point (6)
- the top flange left tip (7)
- the top flange to web node (8)
- the top flange right tip (9)

The loads may be applied in the X-direction (1), Y-direction (2), or Z-direction (3).

(a) *UT Bridge* point load definition
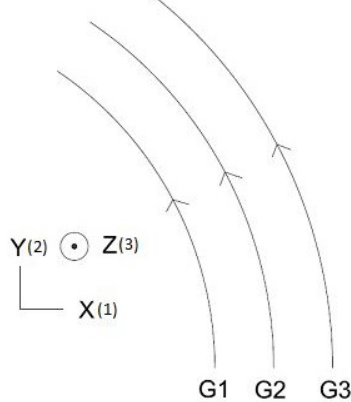
(b) *UT Bridge* global coordinate system

Figure 2-41. *UT Bridge* (v2.2) point load application

Analysis result options are:

- bending moment, shear force, torsion, and top and bottom flange lateral moment diagrams

- displacement and rotation along the girders

- Von Misses and principal stresses

- cross-frame forces

- eigenvalues for buckling analysis.

2.6.3.3   PC Girder Stability and Capacity Analysis during Erection

PCI Girder Stability Subcommittee developed an analysis example for the stability and capacity of single and multiple PC I-girders during erection. The example is developed in the Mathcad script and included in Chapter 6 of the *PCI Recommended Practice for Lateral Stability of Precast, Prestressed Concrete Bridge Girders* (PCI 2016). The analysis is based on the methodology and equations presented in Imper and Laszlo (1987) and Mast (1989 and 1993). The impact of the following parameters on girder stability and capacity is defined:

- wind loads for active and inactive construction cases

- bearing pad rotational stiffness incorporated from the NCHRP (2008)

- slope of transverse seating between girders and bearings

- sweep and camber of girders

- harped strands on girder stresses.

The calculation procedures evaluate:

- lateral girder eccentricities due to self-weight and wind loading

- girder compressive and tensile stresses at harping points against the allowable stress limits

- factor of safety against cracking, failure, and rollover during the erection of single girder

- factor of safety against cracking and failure during the erection of multiple girders

- bearing pad effectiveness under applied loads to determine the need for external bracings

- the required number of external bracings and the resulting bracing forces.

The calculation procedures incorporate the following assumptions:

- Girder deformations are small and based on small deflection theory.

- During the erection of single and multiple girders, active and inactive construction activities are considered, respectively. Wind pressure magnitudes are calculated independently during these activities.

- Effect of vertical wind uplift pressure is neglected for active construction activity (i.e. single girder erection).

- Drag coefficient is taken as 0.3 for calculating uplift pressure during extreme wind effects for inactive construction activity (i.e. multiple girder erections).

- Prestressing strands are placed symmetrically and do not contribute to girder sweep.

- Girder sweep is due to form misalignment.

2.7 CONSTRUCTABILITY EVALUATIONS DURING DECK PLACEMENT

Conventional highway bridges utilize cast-in-place concrete decks. During deck placement, plastic concrete between adjacent girders is often supported by stay-in-place (SIP) forms. For supporting overhang concrete temporary formwork is installed. The overhang formwork is supported on brackets (fascia jacks) placed at specific intervals. Figure 2-42 shows the elevation of a typical supporting system for deck overhang concrete in steel I-girder bridges, including overhang formwork, bracket (bracket beam, diagonal and vertical legs), and hanger rod. The figure

also shows the bracket-bearing point and the distance between the bearing point and top of the bottom flange (H_{br}). Hanger rods, which are either welded or clamped to the exterior girder top flange, support the bracket.
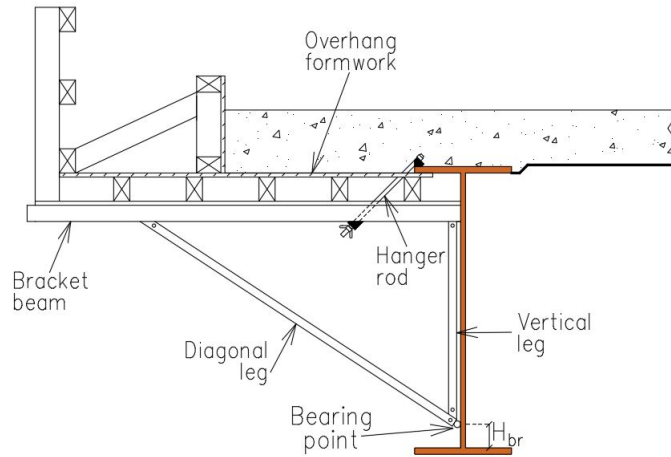
Figure 2-42. A typical overhang bracket and its components

Maintaining deck profile as per the project specifications during deck placement requires knowledge of girder and formwork deformation under wet concrete weight, especially the overhang portion of the formwork. Differential deflection of steel girders, steel exterior girder warping, and web out-of-plane deformation, or a combination thereof impacts deck profile (ODOT 2007a).

Assuming that the overhang formwork and falsework are attached firmly to the exterior girder, the total rotation of an overhang bracket (θ_t) in steel I-girder bridges can be calculated using Eq. (2-21).

$$\theta_t = \theta_d + \theta_w + \theta_{we} \tag{2-21}$$

where:

θ_d = exterior girder rotation due to differential deflection
θ_w = exterior girder rotation due to warping
θ_{we} = exterior girder top flange rotation due to web out-of-plane deformation

Subsequent to the total rotation calculation, the variation in deck profile (Δ_{deck}) due to girder deformations during deck placement is calculated using Eq. (2-22).

$$\Delta_{deck} = \left(\frac{b_{sr}}{2} + b_{ov}\right) tan(\theta_t) \tag{2-22}$$

66

where b_{sr} is the width of screed rail platform and b_{ov} is deck overhang width shown in Figure 2-43. Many state highway agencies define deck profile tolerances in terms of exterior girder rotation or variation in deck profile. Table 2-11 provides a few such policies.

Table 2-11. Highway Agency Tolerances for Exterior Girder Rotation and Deck Profile

Source of Information	Tolerance
KDOT (2016) – Section 16.8	Exterior girder rotation < 1°
MDOT (2017)	$\Delta_{deck} \leq 0.125$ in. / 10 ft
ODOT (2016) – Section 302.2.7.3	$\Delta_{deck} \leq 0.5$ in.
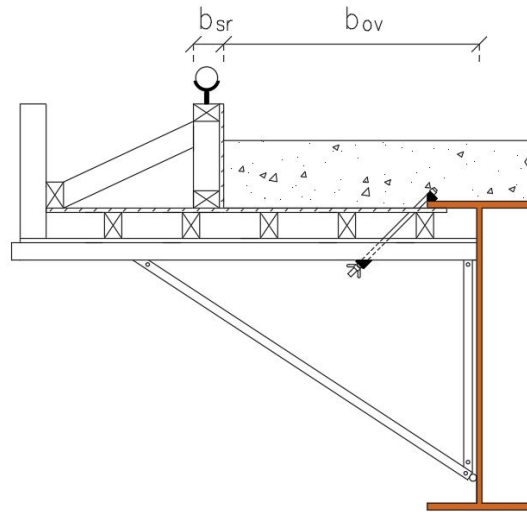
Figure 2-43. Dimensions for calculating the variation in deck profile (Δ_{deck})

2.7.1   Differential Girder Deflection

Girder deflection is a function of loads, boundary conditions, and girder geometry and stiffness. Girder differential deflection is controlled by the connection details of cross-frames and diaphragms. This is because cross-frames and diaphragms define the load transfer mechanisms and boundary conditions. In the absence of a hardened deck, cross-frames (or diaphragms) along with temporary bracing systems control lateral stability of the erected superstructure. For this reason, the common practice is to fully fasten the cross-frames before deck placement. When girders are subjected to differential deflection with fully connected cross-frames, girders rotate about their longitudinal axis. Since screed rails are supported by overhang brackets that are attached to exterior girders, rotation of the exterior girders will impact the intended deck profile as illustrated in Figure 2-44.
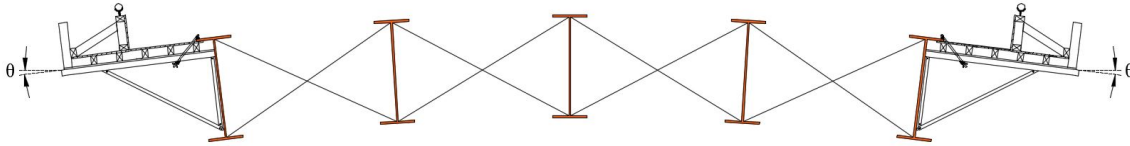
Figure 2-44. Rotation of overhang brackets due to girder differential deflection

According to ODOT (2007a), girder differential deflection is a function of the difference in load magnitudes transferred to individual girders. ODOT (2007a) Section 302.2 states that for a new superstructure, girder rotation due to differential deflection can be neglected when the tributary deck load carried by exterior girders are below 110% of the average deck tributary load carried by the interior girders. During deck replacement, the limit defined for existing bridges is 115%. These recommendations primarily consider the effect of deck overhang width concerning a given girder spacing of bridges with similar girders at equal spacing. Most likely these limits are based on field observations. Rational analysis is required to investigate the impact of boundary conditions, structure geometry, and stiffness characteristics of individual girders.

Girder deflections from non-composite loads are often calculated using 1D line-girder analysis. In line-girder analysis, a girder is isolated from the rest of the structure and analyzed independently. Inherently, 1D line-girder analysis cannot incorporate the effects of cross-frames or diaphragms on structural behavior. The study by Fisher (2006) demonstrated that even in straight steel I-girder bridges, transverse load distribution through cross-frames has an influence on differential girder deflection under non-composite loads. Fisher (2006) measured girder deflections during deck placement of seven simple-span and three continuous-span steel I-girder bridges with skew angles varying from 0 to 62 degrees. Then, 3D finite element models were developed and field measurements were used to calibrate these models. Finally, simplified procedures were developed for predicting girder deflections under non-composite loads. These procedures were adopted by North Carolina DOT for estimating girder deflections during deck placement. Further details are provided in Section 2.7.5.1.

2.7.2 Steel I-Girder Web Out-of-Plane Deformation

The horizontal component of the bracket diagonal leg axial force acts on the exterior girder web as a lateral load at the bearing point (Figure 2-45). The magnitude of steel I-girder web out-of-plane deformation is a function of diagonal leg force magnitude, bearing point location, and web slenderness. The resulting overhang bracket rotation (θ_{we}) is the cause of uneven deck thickness.

68

Consequently, exterior girder web behavior needs to be evaluated before deck placement. Unlike steel I-girders, the web out-of-plane deformation is not a concern for PC I-girders due to the high flexural rigidity of the webs.
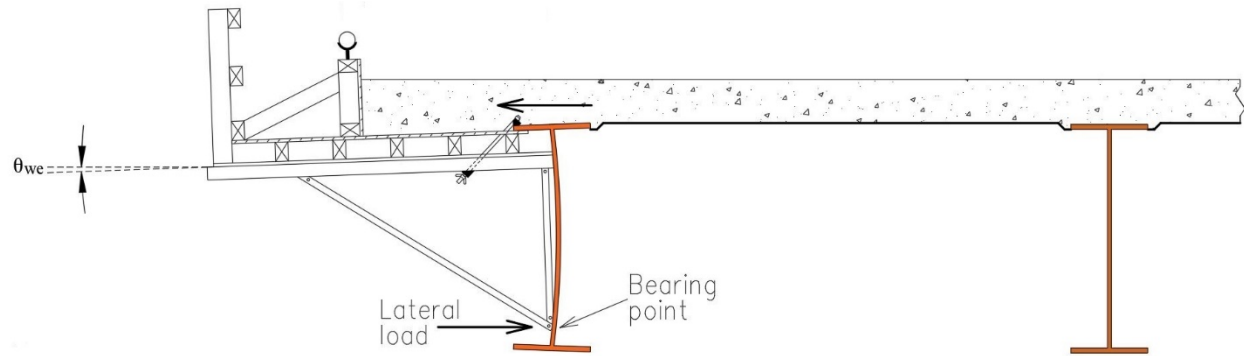
Figure 2-45. Overhang bracket rotation due to web out-of-plane deformation

Several highway agencies provide guidance for controlling web out-of-plane deformation. The most common requirements are related to the bearing point position (H_{br}) with respect to the bottom flange of the exterior girder under consideration. Table 2-12 summarizes the limits for H_{br} specified by agencies that warrant excluding the web out-of-plane deformation and local distortion check. In addition to the limits provided in Table 2-12, Ohio DOT and Pennsylvania DOT provide further guidelines. The ODOT (2007a) Section 302.2.7.2, requires web out-of-plane deformation to be evaluated when the web depth is greater than 84 inches. PennDOT (2015) Article 6.10.3.2.5.2P provides the maximum permissible overhang bracket spacing and the horizontal loads with respect to overhang bracket depths to control web buckling due to out-of-plane deformations (Figure 2-46). The horizontal loads include the weight of concrete, formwork, and screed machine, and other construction loads. The limits provided in Figure 2-46 are valid for the following conditions:

   (i)   girder web depth < 8 ft
   (ii)   overhang width < 4 ft – 9 in.
   (iii)   deck thickness ≤ 10 in.
   (iv)   transverse stiffener spacing < girder depth
   (v) γ_w < 2.5 within the region of interest (see the PennDOT (2015) Article D6.10.1.9.3P for details)
   (vi)   the dead load shear factored with 4.0 is < the buckling shear calculated as per the AASHTO (2017a) Article 6.10.9.3.

69

The maximum permissible horizontal loads by PennDOT (2015) were determined from field measurements and finite element analysis. When the above requirements are not satisfied, the limits for H_{br} are shown in Table 2-12 for PennDOT and other agencies.

Table 2-12. H$_{br}$ Limits from Various Highway Agencies

Source of Information	H$_{br}$ Limits
AASHTO (2017a) – Article C6.10.3.4	$\cong 0$ (at bottom flange web intersection)
FDOT (2018b) – Section 400-4.4	< 6 in.
IDOT (2016) – Section 503.06b	< 6 in.
KDOT (2016) – Section 16.8	$\cong 0$ (at bottom flange web intersection)
ODOT (2016) – Section 508.02	< 8 in.
Oklahoma DOT (2009) – Section 502.04	< 6 in.
PennDOT (2015) – Article 6.10.3.2.5.2P	< 6 in.

Nominal Depth, y (in.)	Maximum Permissible Horizontal Load, h (kip/ft)
36	1.250
56	0.750
76	0.540

Maximum permissible jack spacing is 4 ft.
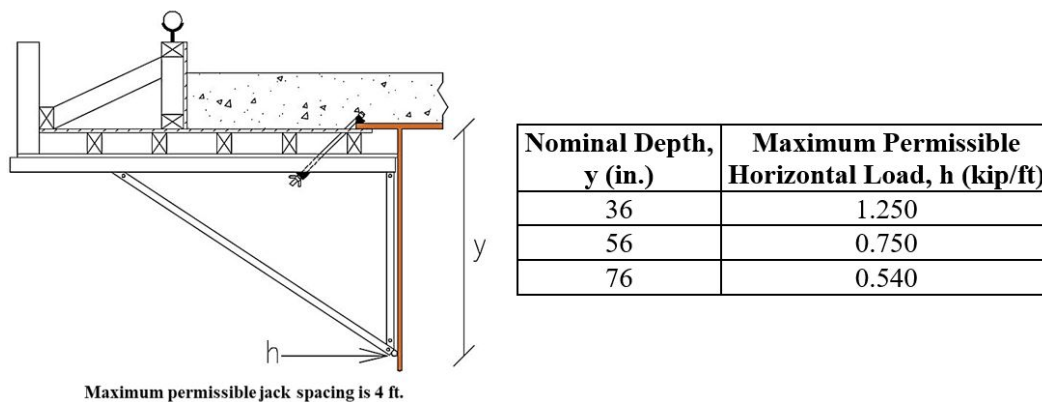
Figure 2-46. Bearing point distance and max. permissible horizontal load (PennDOT 2015)

Web out-of-plane deformation and the corresponding formwork rotation need to be evaluated if the bracket diagonal leg bearing point cannot be placed closer to the bottom flange-web intersection due to site constraints, exterior girder depth, incorrect bracket size, or a combination thereof. Based on similar cases, studies have been reported in the literature for evaluating the web out-of-plane deformation under lateral loads resulting from the bracket diagonal leg. Yang et al. (2010) investigated steel I-girder web out-of-plane deformations under deck overhang loads. The primary parameters considered by Yang et al. (2010) are: girder web slenderness, the position of the bracket-bearing point on the girder web, transverse web stiffeners, and deck overhang width. Additional parameters included girder top flange width, P-delta effects, and initial web imperfections. The study concluded that web slenderness, the position of bracket-bearing point on the web, transverse stiffener spacing, and the overhang width are the dominant

70

parameters influencing web out-of-plane deformations. A computational tool was not provided for analyzing web out-of-plane deformation and the associated overhang bracket rotation.

2.7.3 Steel I-Girder Warping

During deck placement, loads act eccentrically to the exterior girder. With cross-section warping restrained at cross-frame locations, the exterior girder is subjected to non-uniform torsion between consecutive cross-frames as shown in Figure 2-47. The overhang bracket also rotates with the exterior girder and impacts the deck profile. The assumption of full restraint against warping at cross-frame locations is an idealization. The actual warping fixity provided by cross-frames is somewhere between fixed and pinned boundary conditions (KDOT 2016). Unlike in steel I-girders, warping of exterior PC I-girders is not considered due to the high torsional stiffness of the girder.
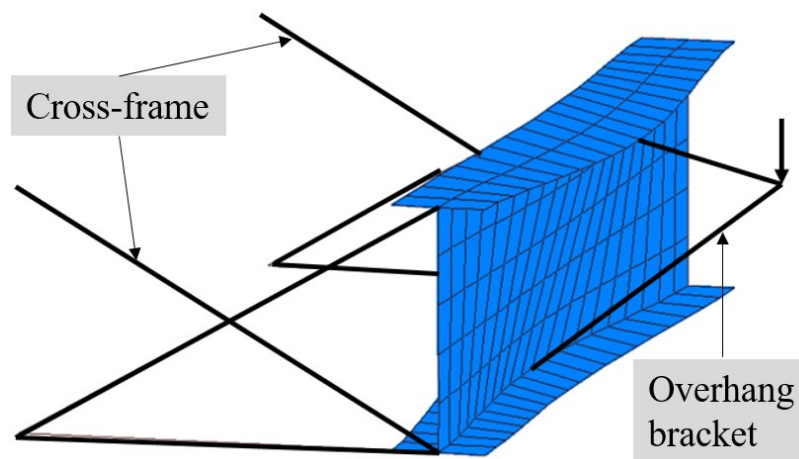
Figure 2-47. Exterior girder behavior under non-uniform torsion (ODOT 2007b)

Approximate solutions and a computer-based analysis tool are available for estimating the rotational response of exterior girders under torsional loading. As per the Idaho DOT's *LRFD Bridge Design Manual* (Idaho DOT 2017) Article 6.10.3.4, torsion applied on an exterior girder can be resolved as a force couple acting on the top and bottom flanges, as illustrated in Figure 2-48. The flanges are then modeled as continuous beams and analyzed under applied lateral loads. Finally, rotation of the exterior girder is calculated by dividing the sum of two resulting flange deflections by the girder depth. Article 6.10.3.4 states that the rotation estimated using this analysis will be approximately 10% greater than refined analysis. Article A6.1 provides an example procedure for calculating the rotation due to exterior girder warping.
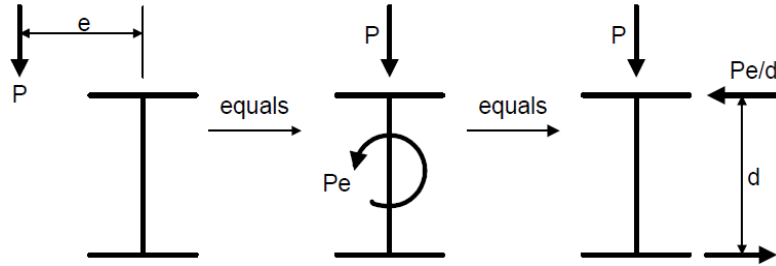
Figure 2-48. The force couple on an exterior girder (Idaho DOT 2017)

KDOT (2016) utilizes the solution of the governing differential equation of torsion for calculating rotation of the exterior girder due to warping. As shown in Eq. (2-23), the total torsional moment (T) resisted by the cross-section restrained against warping, is the summation of St. Venant (T_t) and warping resisting (T_w) moments.

$$T = T_t + T_w = GJ\theta' - EC_w\theta'''$$ (2-23)

where:

C_w = warping constant of the cross-section
E = modulus of elasticity
G = shear modulus of elasticity
J = torsional constant of the cross-section
θ = torsional rotation about the longitudinal axis
θ' = first derivative of the rotation (θ)
θ''' = third derivative of the rotation (θ)

Solutions of Eq. (2-23) under various boundary and loading conditions are provided in the Design Guide 9: Torsional Analysis of Structural Steel Members (AISC 2003). KDOT (2016) provides an example calculation procedure using Eq. (2-23). The example calculates two rotations corresponding to fixed-fixed and pinned-pinned boundary conditions. The final estimate is calculated as the average of the two. Instead of averaging, the two rotations can be presented as upper and lower bounds due to warping.

2.7.4   Custom Overhang Brackets

On rare occasions, contractors use custom bracket configurations. Figure 2-49 shows an example of such a bracket used in the deck placement of a steel I-girder bridge in Michigan. In the figure, the mid-depth of the web is marked by a dashed line. In this case, the bearing point is away from the bottom flange; thus, the web out-of-plane deformation may exceed deck thickness tolerance.

Figure 2-49. A custom overhang bracket for a steel I-girder bridge (Photo courtesy: MDOT)

2.7.5 Tools and Analysis Methods

2.7.5.1 Steel I-Girder Differential Deflection Analysis during Deck Placement

The North Carolina Department of Transportation (NCDOT) sponsored a project for the accurate estimation of girder deflections in steel I-girder bridges under non-composite loads. As a result, Fisher (2006) proposed three different procedures: simplified procedure (SP), alternative simplified procedure (ASP), and single girder line straight line (SGLSL) procedure. The use of the specific procedure is depended on the span type and exterior-to-interior girder load ratios. The exterior-to-interior girder load ratio is the ratio of the loads acting on the exterior and interior girders. For a bridge under consideration, two separate ratios are calculated for each of the exterior girders. If the difference is less than 10%, exterior-to-interior girder load ratios are taken "equal". The simplified procedure is recommended for simple-span bridges with equal exterior-to-interior girder load ratios. For simple-span bridges with unequal exterior-to-interior load ratios, the alternative simplified procedure is recommended. The SGLSL procedure is recommended for calculating deflections in continuous steel I-girder bridges with equal exterior-to-interior load ratios. Fisher (2006) did not provide a procedure for continuous steel I-girder bridges with unequal load ratios.

The procedures developed by Fisher (2006) are subjected to the following limitations:

- Span length < 250 feet
- Girder spacing < 11.5 feet
- Number of girders < 10 (this limit is only for the ASP method)
- Girder spacing to span ratio < 0.08.

73

These limits encompass the majority of steel I-girder bridge stock in the U.S. Thus, the procedures have a broad range of applicability.

In the simplified procedure, exterior girder deflection (Δ'_{ex}) and differential deflection between the adjacent interior girders (Δ_{dif}) are calculated using Eqs. (2-24) and (2-25), respectively. Then, Eq. (2-26) is used for calculating rotation from differential girder deflection.

$$\Delta'_{ex} = [\Delta_{in} - (0.03 - \alpha\theta)(100 - \eta_L)][1 - 0.1\tan(1.2\theta)] \tag{2-24}$$

$$\Delta_{dif} = \frac{\Delta_{in}}{\Delta_{in\_m}}\left[(3 - b\theta)\left(\frac{S}{L} - 0.04\right)(1 + z) - 0.1\tan(1.2\theta)\right] \tag{2-25}$$

$$\theta_d = tan^{-1}\left(\frac{-\Delta_{dif}}{S}\right) \tag{2-26}$$

where:

b $= -0.08$, if $\frac{S}{L} \leq 0.05$
          $= -0.08 + 8(\frac{S}{L} - 0.05)$, if $0.05 < \frac{S}{L} \leq 0.08$
L $=$ span length (ft)
S $=$ girder spacing (ft)
z $= [10(\frac{S}{L} - 0.04) + 0.02](2 - 0.02\eta_L)$
α $= 0.0002$, if $S \leq 8.2$ ft
          $= 0.0002 + 0.000305(S-8.2)$, if 8.2 ft $< S \leq 11.5$ ft
Δ_{dif} $=$ differential deflection between girders (in.)
Δ'_{ex} $=$ exterior girder deflection (in.)
Δ_{in} $=$ interior girder deflection calculated using 1D line-girder analysis (in.)
Δ_{in_m} $=$ interior girder midspan deflection calculated using 1D line-girder analysis (in.)
η_L $=$ exterior-to-interior girder load ratio (%)
θ $=$ skew angle (deg)

The alternative simplified procedure is recommended for simple-span bridges with unequal exterior-to-interior load ratios. Such cases likely come up during phased construction and due to unequal deck overhang widths as discussed in Section 2.8.2.

The SGLSL procedure (for continuous steel I-girder bridges with equal exterior-to-interior load ratios) uses 1D line-girder analysis to calculate exterior girder deflections along the girder at defined locations. The deflections are taken equal to interior girder deflections. In other words, the SGLSL procedure results in a straight-line deflection profile throughout the bridge cross-section, implying no differential deflection between girders. Although the deflected shape of continuous span bridges tends to be flat in general, the SGLSL procedure over-simplifies this

74

behavior. The procedure indirectly indicates that when the difference between the exterior-to-interior girder load ratios is below 10%, or in other words, when exterior girders are subjected to equal loads, differential deflections are negligible. The procedure may be useful as an approximate tool; however, a refined analysis should be required in continuous bridges for estimating rotation of exterior girders under differential girder deflection. Finally, the procedures by Fisher (2006) do not apply to curved or curved and skewed steel I-girder bridges.

UT Bridge is capable of evaluating differential girder deflection in straight, skewed, or curved I-girder bridges during deck placement considering the effect of cross-frames and temporary lateral bracings. Section 2.6.3.2 provides further details.

2.7.5.2   *Steel I-Girder Web Out-of-Plane Deformation Analysis during Deck Placement*

Within the scope of this project, Inceefe (2018) developed an analytical procedure for calculating web out-of-plane deformation and the associated overhang bracket rotation in steel I-girder bridges. Inceefe (2018) approached the problem by isolating a girder segment bounded by flanges and two adjacent transverse stiffeners as a representative module of the girder. The girder segment was analyzed using the theory of thin plates with simply supported edges. Figure 2-50 shows a representative rectangular plate with a thickness of t_w and side lengths of D and d_o, where D and d_o represent web depth and stiffener spacing. The plate flexural rigidity is D_f. A concentrated normal force of P, determined from overhang bracket analysis, is acting at point $(x_1 = D - H_{br}, y_1)$ shown in the figure. Eq. (2-27) is used for calculating deflection at any point (x, y) on a plate surface under a concentrated normal force, assuming the plate is simply supported on all four edges.
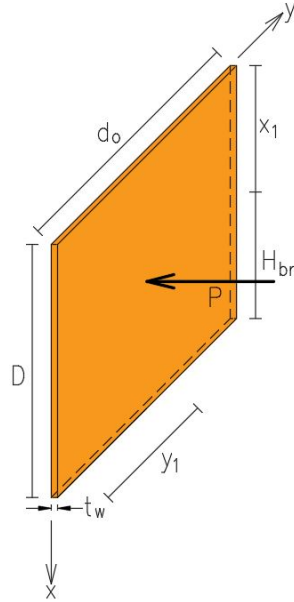
Figure 2-50. A plate under a concentrated load

$$w(x,y) = \frac{4P}{\pi^4 D_f D d_o} \sum_{m}^{\infty} \sum_{n}^{\infty} \frac{sin\left(\frac{m\pi(D - H_{br})}{D}\right) sin\left(\frac{n\pi y_1}{d_o}\right)}{\left[\left(\frac{m}{D}\right)^2 + \left(\frac{n}{d_o}\right)^2\right]^2} sin\left(\frac{m\pi x}{D}\right) sin\left(\frac{n\pi y}{d_o}\right) \qquad (2\text{-}27)$$

Rotation of the bracket and rotation of the top flange will be equal when the bracket and the exterior girder top flange are rigidly connected, and the top flange is unconstrained. When the top flange and web are rigidly connected, top flange rotation at the web-top flange connection will be equal to the web rotation at the connection. Consequently, the bracket rotation will be equal to the web rotation at the flange-web connection. Web rotation is calculated at specific locations along the y-axis; thus, x is the only variable in Eq. (2-27). Hence, as shown in Eq. (2-28), the first derivative of Eq. (2-27) with respect to x at $x = 0$ represents the overhang bracket rotation.

$$\theta_{we} = \frac{\partial w(0)}{\partial x} \qquad (2\text{-}28)$$

Simply supported boundary condition is an idealization and does not account for the constraints provided by the flanges and stiffeners. The rotational fixity provided to the girder web by flanges and stiffeners was investigated by refined FE analysis. Based on the results of the analysis, adjustment factors for various bracket-bearing point locations are given in Table 2-13. The adjustment factors are used with plate theory solutions to estimate the bracket rotation for any girder that is designed following AASHTO (2017a) and AASHTO/NSBA (2016) specifications

76

and procedures. In curved bridges, the spacing between two consecutive transverse stiffeners will be small compared to the girder length. Hence, a model of the exterior girder web that is bounded by flanges and stiffeners can be assumed as straight. In skewed as well as curved bridges, the overhang bracket is placed perpendicular to the flange. In that case, the lateral load at the bearing point acts perpendicular to the web. Consequently, the adjustment factors are also applicable for curved and skewed girders. Inceefe (2018) also concluded that the 6 in. limit stated in Table 2-12 is sufficient for reducing the web out-of-plane deformations in steel I-girder bridges.

Table 2-13. Suggested Adjustment Factors (Inceefe 2018)

Bearing Point Location	Factor, α_c
$0.5D \leq D - H_{br} < 0.6D$	0.300
$0.6D \leq D - H_{br} < 0.7D$	0.275
$0.7D \leq D - H_{br} < 0.8D$	0.250
$0.8D \leq D - H_{br} < 0.9D$	0.200
$0.9D \leq D - H_{br} < D$	0.125

2.7.5.3 Steel I-Girder Warping Analysis during Deck Placement

The Kansas Department of Transportation (KDOT) sponsored a project for evaluating the torsional behavior of exterior girders during deck placement. The project developed a computational tool, described as *Torsional Analysis of Exterior Girders (TAEG),* which became a commonly used tool by the bridge industry. For example, Section 302.2.7.2c of Ohio DOT *Bridge Design Manual* (ODOT 2007a) suggests using *TAEG* for calculating exterior girder rotation due to warping during deck placement and provides data and equations to reflect the ODOT practice. *TAEG* is based on the force method of analysis and spring-supported girder models. User inputs include:

- Structure of cross-frames or diaphragms with cross-sectional area and moment of inertia
- Girder and diaphragm connection details such as bolt number, size, and spacing
- Cross-sectional area of top flange level tie-rods and bottom flange level timber blocks
- Custom overhang bracket geometry, bracket spacing, and weight
- Screed machine wheel spacing
- The following loads:
    - live load on walkway and deck slab
    - formwork and concrete dead load
    - maximum screed machine wheel load
    - maximum top and bottom flange stresses due to non-composite dead loads at positive and negative moment regions. Stresses are either defined at or between

77

cross-frame or diaphragm locations such that torsion stresses are superimposed with non-composite dead load stresses.

The calculation procedures allow evaluating:

- exterior girder top and bottom flange stresses at positive and negative moment regions due to applied torsion and non-composite dead load
- exterior girder top and bottom flange lateral deformations, screed rail vertical deflection, and exterior girder rotation due to warping
- overhang bracket component, and permanent and temporary lateral support forces.

The calculation procedures incorporate the following assumptions:

- Self-equilibrating concrete and formwork loads on the interior side of the exterior girder are neglected as shown in Figure 2-51.
- Screed machine is operated on eight wheels (four wheels on each side).
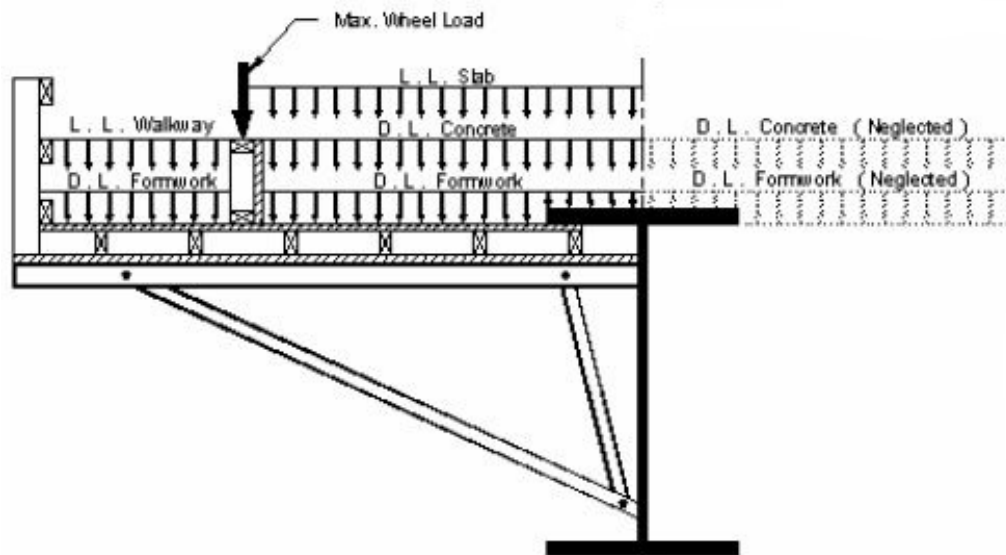
Figure 2-51. Exterior girder loading configuration in *TAEG* (Roddis and Kulseth 2005)

The calculation procedures have the following limitations:

- Top and bottom flange stresses due to non-composite dead loads need to be calculated to input to *TAEG*.
- Analysis is limited to prismatic girders.
- Loads are not factored.
- Curved girders and the associated torsional effects are excluded.

- Skew effects are neglected for skew angle less than 20 degrees. When the angle is greater than 20 degrees, skew effects are incorporated by unsymmetrical loading.

- Non-uniform cross-frame or diaphragm spacing is not considered.

- The maximum number of temporary lateral supports between two consecutive cross-frames or diaphragms is limited to three.

2.8   CONSTRUCTABILITY EVALUATIONS IN PHASED CONSTRUCTION

Phased construction, also called part-width construction, refers to a procedure where one portion or phase of the structure is in service while the other portion is under construction. Phased construction is implemented for deck replacement, superstructure replacement, or widening projects. The constructability cases outlined in the previous sections are equally applicable to phased construction. However, phased construction possesses unique constructability aspects that need to be evaluated for assuring structural safety and retaining deformation tolerances and stability. This section discusses (1) the capacity evaluation of in-service structures, (2) vertical and horizontal misalignment of phases due to differential deflection, the twist of bridge cross-section, foundation settlement, or a combination thereof, and (3) global lateral torsional buckling instability of steel I-girder systems.

2.8.1   Capacity Evaluation of the In-Service Structure

As per MDOT (2019a) Section 7.01.17, the structural performance of the in-service structure needs to be evaluated when phased construction is utilized. This assessment is often performed by a load rating analysis for the portion of the bridge that will remain in service. Load rating for phased construction is a complex analysis and requires documenting the current condition of structural elements, time-dependent material properties, and locked-in stresses (if exist) in the structure. Also, the designer needs to be aware of the historical perspective of design criteria, such as live loads, allowable stresses, etc. (SCDOT 2006). Additionally, if live load analysis is performed using the approximate methods given in the AASHTO LRFD Specifications (e.g. application of the load distribution factors), the designer should consider the applicability of the associated equations.

Some DOTs have standardized load rating procedures for phased construction. As an example, Figure 2-52 shows the flowchart used by FDOT describing the load rating procedure for assessing the structural performance in widening or rehabilitation projects. Further details of this

procedure are explained in FDOT (2018c) Section 7.1.1. The procedure used by FDOT recognizes the need for structural performance evaluation during phased construction, addresses the historical design perspective of the structure, and provides options to the engineer if the capacity of the structure is insufficient.
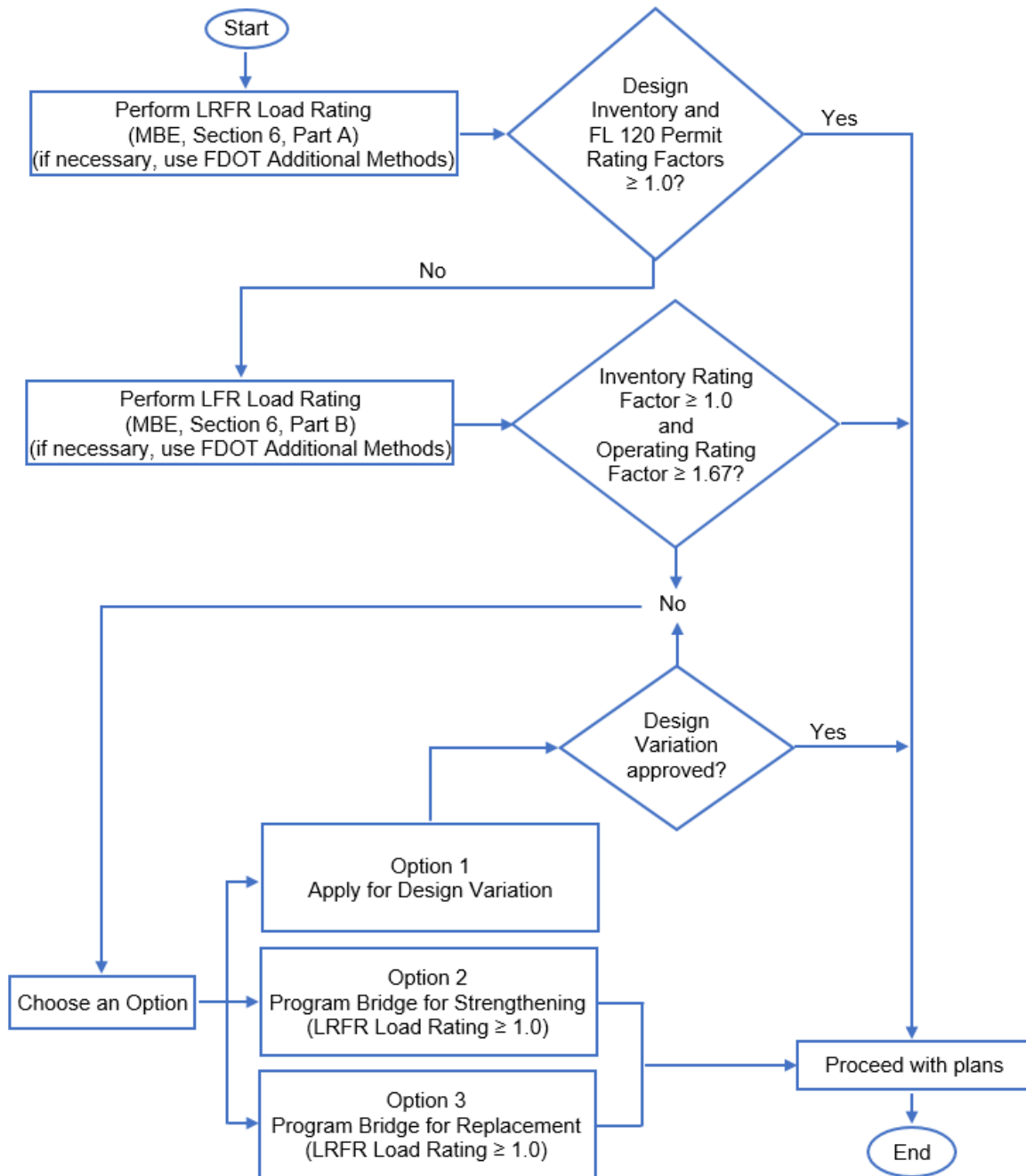
Figure 2-52. Load rating procedures for bridge widening and rehabilitation (FDOT 2018c)

2.8.2 Vertical and/or Horizontal Misalignment between Phases

In phased construction, each phase is constructed as an independent structure. The completed phases are connected for securing structural integrity. Common methods of combining phases include detailing a longitudinal expansion joint in the corresponding portion of the deck or by a closure pour. The expansion joints often create bridge maintenance problems, and a potential safety hazard if located within the clear roadway (CALTRANS 2010, SCDOT 2006). Thus, a closure pour is typically specified to connect the two phases.

Width of closure pour is often detailed in a way to provide the required development length for reinforcing bars, preclude effects of superstructure differential elevation differences, and provide a smooth transition between the phases. Several highway agencies have provided limits on the closure pour width in design specifications and guidelines. For example, Utah DOT (2017) and Iowa DOT (2019) specify a minimum closure width of 3 ft, whereas Louisiana DOT (2019) and INDOT (2013) require a minimum width of 30 in. and 20 in., respectively.

An elevation difference of the structures needs to be managed within a specified tolerance before a closure pour so that a smooth transition between the phases and the intended deck profile is maintained. The elevation difference is a result of the structural performance of the phases (stiffness, loads, and support conditions), foundation settlement, or a combination thereof. The elevation difference leads to complexities in deck formwork and cross-frame installation, deck transverse reinforcement splicing, and/or maintaining the deck profile. Even though slotted-holes can be used to overcome the cross-frame installation challenges, the magnitude of deformation tolerance that can be accommodated is limited by the length of the slotted holes. AASHTO (2017a) Table 6.13.2.4.2-1 provides the maximum permissible hole sizes for various hole types. Relevant information from the AASHTO table is provided in Table 2-14. For example, the length of a long slot cannot exceed 2.5 in. for a 1 in. diameter bolt. Also, the use of oversized or slotted holes is not allowed in horizontally curved bridges as per AASHTO (2017a) Article 6.13.1.

Table 2-14. Maximum Hole Sizes (AASHTO 2017a)

Bolt Diameter (d) (in.)	Short Slot Width × Length (in.)	Long Slot Width × Length (in.)
0.625	0.688 × 0.875	0.688 × 1.563
0.750	0.812 × 1.000	0.813 × 1.875
0.875	0.938 × 1.125	0.938 × 2.188
1.000	1.125 × 1.313	1.125 × 2.500
≥ 1.125	(d+0.125) × (d+0.375)	(d+0.125) × (2.5d)

Superstructure units of each phase may be subjected to unbalanced torsional loading from unequal overhang widths and eccentric construction loads. In other words, when the sum of the torsional moments about the shear center of each cross-section is not zero, the resultant deformations cause vertical and horizontal misalignment between the phases (Yang et al. 2010). Figure 2-53 shows a twin steel I-girder system in widening an existing bridge. In this case, the system is torsionally unbalanced since part of the interior overhang concrete load during the placement is transferred to the existing structure. The exterior overhang concrete during placement is primarily supported by the twin I-girder system.

Unbalanced torsional loading may appear also during deck and superstructure replacements. Individual phases may have unequal overhang widths before the closure pour, deck reinforcement lapping, or cross-frame installation as per the project specifications. As an example, CALTRANS (2010) and SCDOT (2006) require removing a part of the overhang concrete of existing structures to accommodate the required lap length of the deck reinforcement to maintain continuity. Thus, in the presence of unequal overhang widths, torsional analysis of individual phases is required for calculating vertical and horizontal displacements and their impact on the closure pour.
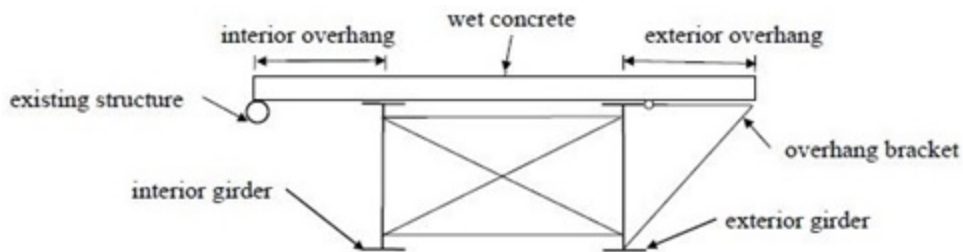
Figure 2-53. A twin I-girder system subjected to unbalanced loading (Yang et al. 2010)

Phased construction can cause differential settlement within a single substructure unit, i.e., pier or abutment (UDOT 2017). This can occur due to changes in load acting on the substructure during construction phases, soil consolidation differences, or a combination thereof. Chapter 17

of the Utah Structures Design and Detailing Manual (UDOT 2017) provides limits for settlement allowances that need to be considered during design. However, there are no clear guidelines on developing remedies when the allowable settlement limits are exceeded.

These cases require a system-level evaluation and cannot be accurately analyzed with 1D line-girder methods. Also, state-of-the-art literature does not provide any explicit methods or tools for displacement analysis during phased construction. Analyses can be performed using general-purpose software with 2D or 3D modeling features.

2.8.3   Global Buckling of Steel Multi-Girder Systems

For widening projects, it is common to add a new superstructure unit with a limited number of girders. Often, the girder assemblage will have a large span to width ratio. Lateral torsional buckling of individual steel girders can be effectively controlled by cross-frames, however, superstructure units with large span-to-width ratios are susceptible to global lateral buckling. Global buckling mode is relatively insensitive to cross-frames spacing since the assemblage behaves as a unit (Figure 2-54).

Literature documents construction failures due to global lateral buckling of girder systems. As an example, Marcy pedestrian bridge structure of a single trapezoidal steel tub-girder collapsed during construction due to global lateral buckling. The section behaved as a double I-girder system with the absence of top flange bracing before deck hardening. In another instance, a two I-girder assemblage with several cross-frames used in a widening project in the state of Texas twisted during deck placement (Yura et al. 2008).

(a) Individual girder buckling

(b) Global system buckling
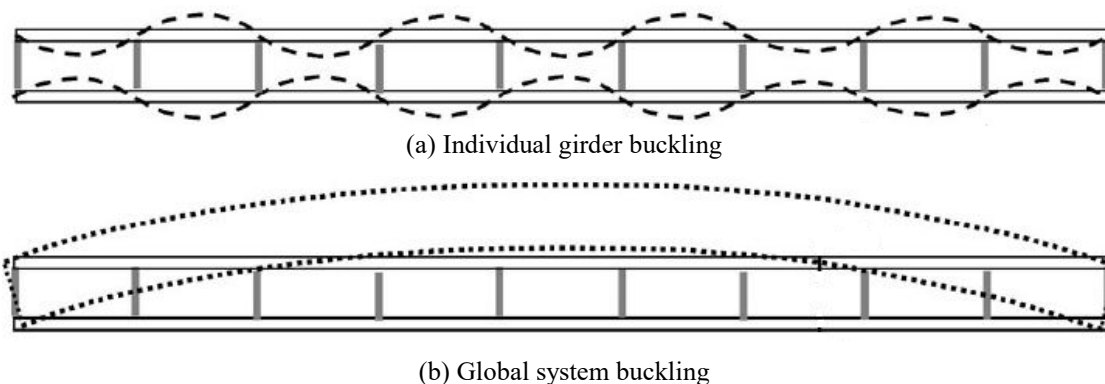
Figure 2-54. Lateral buckling modes for girders and girder systems (Yura et al. 2008)

AASHTO (2017a) Article 6.10.3.4.2 states that the sum of the largest total factored girder moments developed within the span during deck placement should not exceed 70% of the elastic

global lateral torsional buckling resistance. The resistance of the system, M_{gs}, is calculated using Eq. (2-29), which was developed by Yura et al. (2008) and presented in AASHTO (2017a) as Eq. 6.10.3.4.2-1.

$$M_{gs} = C_{bs} \frac{\pi^2 w_g E}{L^2} \sqrt{I_{eff} I_x} \tag{2-29}$$

in which

C_{bs} = system moment gradient modifier
     = 1.1 for simply-supported units
     = 2.0 for continuous-span units
I_{eff} = I_y for doubly-symmetric girders
     = $I_{yc} + \frac{t}{c} I_{yt}$ for singly-symmetric girders

where c is the distance from the centroid of the noncomposite steel section under consideration to the centroid of the compression flange (in.), I_x is the noncomposite moment of inertia about the horizontal centroidal axis of a single girder within the span under consideration (in.^{4}), and I_{yc} and I_{yt} are moments of inertia of the compression and tension flange, respectively. The article states that provisions apply to straight steel I-girder bridge units with three or fewer girders under the following conditions:

- *The unit is not braced by other structural units and/or by external bracing within the span.*

- *The unit does not contain any flange level lateral bracing or lateral bracing from a hardened composite deck within the span.*

2.9 CONSTRUCTION LOADS AND LOAD COMBINATIONS

The loads need to be clearly defined for constructability cases associated with capacity, deformation, and stability during various stages of construction. This section describes the loads acting on bridge superstructure during each stage of construction and appropriate LRFD load combinations for evaluating the stresses and deformations.

2.9.1 Construction Loads

The loads, boundary conditions, and structural elements and system configurations change throughout the construction process. Figure 2-55 presents the type of loads to be considered during lifting, erection, and deck placement analysis.

Lifting	**Erection**	**Deck Placement**

• Component Loads (DC)
  Girders
  Cross-frames/diaphragms (if exists)
• Wind Load (WS)
	• Component Loads (DC)
	  Girders
	  Cross-frames/diaphragms
	• Wind Load (WS)
		• Component Loads (DC)
		  Girders
		  Cross-frames/diaphragms
		  Deck concrete
		  SIP form
		• Construction Dead Loads (CDL)
		  Overhang formwork and bracket
		  Walkway
		• Construction Live Loads (CLL)
		  Construction live load
		  Screed machine
		• Wind Load (WS)

Figure 2-55. Loads for constructability analyses during lifting, erection, and deck placement

During lifting, girders are subjected to component loads (DC) and wind loads (WS). Component loads include girder self-weight and cross-frame and/or diaphragm weight if such members are connected to the girder during lifting. Wind load magnitude depends on parameters such as girder geometry, type, position in the bridge cross-section, girder spacing to depth ratio, and construction duration. Wind load needs to be calculated for each girder, considering the stage of construction. Wind loads are calculated in terms of wind pressure (P_z). Eq. (2-30) is widely used for calculating P_z (AASHTO 2017c).

$$P_z = \rho V^2 R^2 K_z G C_D \tag{2-30}$$

where ρ is a constant related to the air density, V is 3-second design gust wind speed, R is wind speed reduction factor, K_z is pressure exposure and elevation coefficient accounting for the effect of the elevation of the bridge or bridge component, site topography, and surrounding obstructions to wind action, G is gust effect factor accounting for the distribution of wind pressure on the surface and/or dynamic effects, and C_D is drag coefficient accounting for the effect of the structural element shape on wind pressure. A Mathcad script is included in Appendix C for calculating the wind loads during various stages of construction following the procedures given in the *AASHTO Guide Specifications for Wind Loads on Bridges during Construction* (AASHTO 2017c).

Erection analyses also include components and wind load calculations. In steel bridges, cross-frames and/or diaphragms are installed as the erection progresses; thus, component loads include the weight of cross-frames. For concrete bridges with CIP diaphragms, the diaphragm weight is not included since formwork installation and concrete placement for these members are

completed after girders are fully erected. The weight of temporary components such as lateral bracings is usually small and can be neglected.

During cast-in-place deck construction, girders are subjected to construction loads in addition to component loads (such as girder weight, cross-frames or diaphragms, deck concrete in a plastic state, and SIP forms). As per AASHTO (2017a) Article C3.4.2.1, construction loads include the weights of material, removable formworks, the live load of workers and construction equipment such as screed machines, and any loads applied to the structure through falsework or temporary supports.

Guidelines and recommendations on the load magnitudes and applications are presented in the literature (AASHTO 2017b, Consolazio and Edwards 2014, FDOT 2018c, INDOT 2013, KDOT 2016, McPheron et al. 2012, MDOT 2019a). Highway Agencies show an overall agreement on the component loads, but there is no consensus on the magnitude and application procedures of such loads. This is primarily because construction procedures are handled by the contractors' means and methods.

As per AASHTO (2017b) Article 2.3.3.1, the combined load of normal weight concrete, reinforcing and prestressing steel, and formwork shall not be taken less than 160 pcf. Unlike AASHTO, DOTs separate the weight of concrete and formwork. FDOT (2018c) and INDOT (2013) specify the weight of concrete as 150 pcf. INDOT (2013) and MDOT (2019a) indicate the weight of SIP forms as 15 psf. Additionally, FDOT (2018c) specifies the combined weight of overhang formwork and overhang bracket as 15 psf. These load magnitudes represent a conservative estimate of the combined weight of concrete and formwork provided in AASHTO (2017b).

AASHTO (2017b) defines different construction live loads for the design of falsework and formwork. As per Article 2.3.3.2.1, construction live load for falsework design includes the weight of equipment to be supported, a uniform load of 20 psf applied over the area supported by the falsework, and a 75 plf load applied at the outside edge of deck overhang. On the other hand, for the design of formwork, Article 3.2.1 states that construction live load shall not be taken less than 50 psf. Construction live loads are transferred to superstructure when falsework or formwork is supported by the superstructure. Highway agencies define construction live loads for the design of falsework or formwork specified in AASHTO (2017b) for the constructability analyses of the superstructure. Overhang brackets, a component of falsework, are supported by girders and

subjected to direct and non-redundant load distribution (KDOT 2016). Conservative estimation of displacements is a contradiction during construction, however, deck finish tolerances are provided for the worst-case calculations. Consequently, in the absence of a comprehensive and accurate state-specific construction load database, conservative assumptions for construction live load for overhang bracket design and displacement analysis are appropriate.

The total weight of a screed machine is defined by the machine size and components. The accurate weight of a machine can be obtained from the manufacturer. Several highway agencies specify the weight of the screed machine to be used in the absence of more accurate information. INDOT (2013) specifies the screed machine weight as 4500 lbs, whereas FDOT (2018c) standardizes the load magnitude with respect to the bridge width. The total weight of the screed machine differs based on the machine size, so the FDOT's guidance is more appropriate.

Table 2-15 provides a summary of component loads, construction dead loads, and construction live loads for deck placement analyses documented in AASHTO (2017b), FDOT (2018c), INDOT (2013), KDOT (2016), and MDOT (2019a). It should be noted that the weight of girders and cross-frames (or diaphragms) and wind loads are also considered during deck placement. Figure 2-56 illustrates the application of the loads given in Table 2-15 on an exterior steel I-girder with concrete, SIP forms, combined overhang formwork and bracket, and walkway loads. Construction live load is applied across bridge width and the walkway. Lastly, half of the screed machine load is applied on each screed rail.

Table 2-15. Vertical Loads for Deck Placement Analyses

Load and Magnitude	Source
Component Loads (DC): Concrete = 150 pcf	FDOT (2018c) INDOT (2013)
Component Loads (DC): SIP form = 15 psf	INDOT (2013) MDOT (2019a)
Construction Dead Loads (CDL): Overhang formwork + bracket = 15 psf	FDOT (2018c)
Construction Dead Loads (CDL): Walkway =15 psf	INDOT (2013)
Construction Live Load (CLL) = 50 psf	AASHTO (2017b) KDOT (2016)
Construction Live Load (CLL): Screed Machine = 7 kips, if 26 ft ≤ Bridge Width ≤ 32 ft	FDOT (2018c)
Construction Live Load (CLL): Screed Machine = 11 kips, if 32 ft < Bridge Width ≤ 56 ft	FDOT (2018c)
Construction Live Load (CLL): Screed Machine = 13 kips, if 56 ft < Bridge Width ≤ 80 ft	FDOT (2018c)
Construction Live Load (CLL): Screed Machine = 16 kips, if 80 ft < Bridge Width ≤ 120 ft	FDOT (2018c)
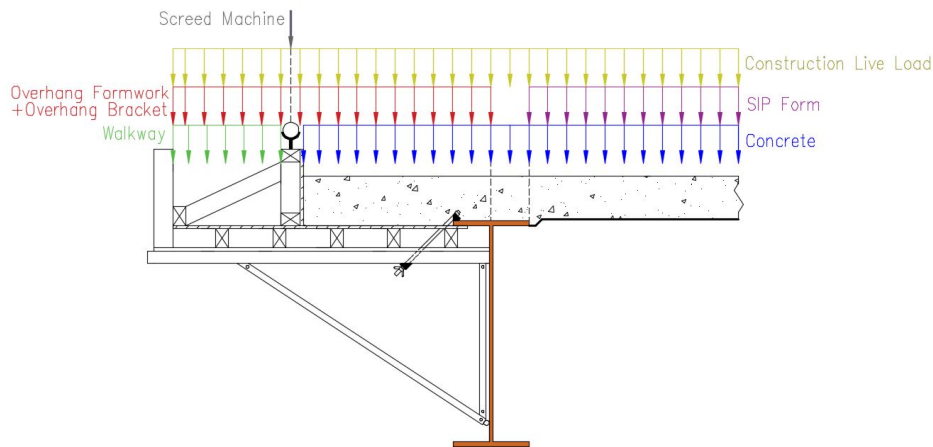
Figure 2-56. Gravity loads acting on an exterior steel I-girder during deck placement

2.9.2   Load Combinations

AASHTO (2017a) Article 3.4.2 presents the load factors for construction analyses. AASHTO Article 3.4.2.1 states that the load factors for a dead load of structural elements and appurtenances, *DC* and *DW*, shall not be taken less than 1.25 for the construction stages using Strength I and Strength III limit states. Additionally, construction loads, including the dynamic effects, shall be factored with a minimum of 1.5 for Strength I limit state. For the Strength III limit state, however, construction loads and the wind load during construction shall be factored with a minimum of 1.25. Further, AASHTO (2017a) considers an additional load combination to amplify the effects of component and construction loads in the absence of service loads. In this particular load

88

combination, a minimum factor of 1.4 shall be applied to a dead load of structural elements and construction loads, including the dynamic effects. Also, AASHTO Article 3.4.2.2 states that the deflections during construction shall be evaluated using Service I limit state with a load factor of 1.00. Table 2-16 summarizes the load combinations to be considered for the constructability analysis cases discussed above.

Table 2-16. Load Combinations for Construction Analyses

Limit State	Load Combination	AASHTO Article
Service I	1.00(*DC*) + 1.00(*CDL+CLL*)	Article 3.4.2.2
Strength I	1.25(*DC*) + 1.50(*CDL+CLL*)	Article 3.4.2.1
Strength III	1.25(*DC*) + 1.25(*CDL+CLL*) + 1.25(*WS*)	Article 3.4.2.1
Additional load combination	1.40(*DC*) + 1.40(*CDL+CLL*)	Article 3.4.2.1

where:
  CDL = construction dead loads
  CLL = construction live loads
  DC = dead load of structural elements
  WS = wind load on structure

Note: Dead load of wearing surfaces and utilities (*DW*) does not exist during construction stages; thus, it is excluded from the load combinations above.

2.10 SUMMARY

Primary parties involved in a bridge construction include the Contractor and highway agency Engineer and Inspector. The Contractor is responsible for selecting suppliers to provide materials and structural elements, developing the means and methods, submitting construction plans and associated calculations to the engineer prior to construction, and completing and delivering the project in compliance with the specifications. The contractor's calculations often include, but not limited to, girder stability and displacement checks during lifting, stability and deformation analysis of partially erected structures, and displacement analysis of the bridge frame under component and construction loads. Also, the Contractor may request changes to pre-approved construction plans depending on the material and equipment availability and other constraints. The Engineer reviews and approves the contractor submittals and perform supplemental calculations, when needed. The Inspector reviews the approved construction plans and verifies construction activities primarily by visual inspection, and consult the Engineer when the activities deviate from the approved construction plans.

Developing construction plans and performing associated constructability analyses are the contractor's responsibility. Yet, the Engineer needs to be well-informed on (*i*) potential PC girder

quality issues that affect capacity and durability (*ii*) potential superstructure constructability cases for the specific bridge, (*iii*) the required level of analysis for accurate evaluation of these cases, (*iv*) methods and tools available for performing as needed analyses, and (*v*) geometry, boundary conditions, construction loads, and load combinations appropriate to evaluate these cases. Also, the Inspector's productivity can be enhanced with guidelines, tools, and checklists for assuring that the fabricated elements and the constructed bridge are complying with the tolerances and details provided in the construction plans and project specifications.

A comprehensive literature review was conducted to document the information required for developing a toolkit to assist engineers and inspectors to evaluate constructability. As shown in Figure 2-57, with the help of these tools, the constructability of a bridge is accomplished by a collective effort of the Engineer, Contractor, and Inspector. Chapter 3 presents guidelines, tools, and procedures for PC girder capacity assessment during QA verification inspection at precast concrete fabrication facilities. The *Constructability Analysis Cases Form* was developed from the framework presented in Figure 2-1 to identify the potential constructability cases based on bridge type (PC or Steel), bridge geometry (straight, skewed and/or curved), and the construction type (complete bridge superstructure construction or phased construction). The *Required Level of Analysis (RLOA) Selection Tools* provide the level of analysis required for evaluating the cases given in the *Constructability Analysis Cases Form.* The *Structural Analysis Tools* for evaluating constructability cases include *UT Lift* (Section 2.5.6.2), *UT Bridge* (Section 2.6.3.2), *TAEG* (Section 2.7.5.3), and Mathcad scripts developed as part of this project. Chapter 4 presents the details of these tools. Three inspector checklists were developed and presented in Chapter 5.
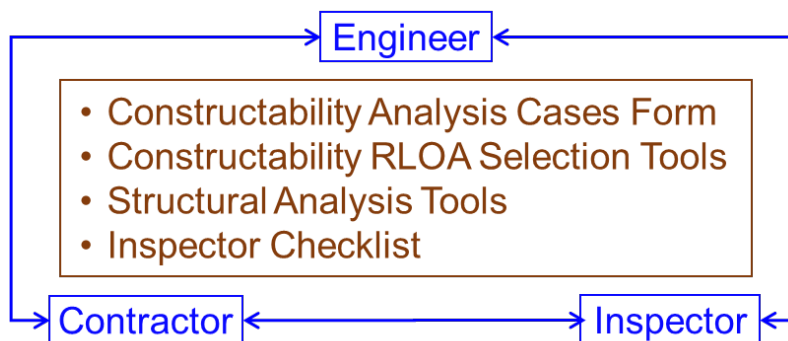
Figure 2-57. Constructability evaluation toolkit for engineers and inspectors to assess contractor means and methods

3   ASSESSMENT OF PC BEAM PERFORMANCE EXPECTATIONS

3.1   OVERVIEW

The PC beams, manufactured and produced under stringent quality control requirements, are expected to improve buildability, cost-effectiveness, durability, and maintainability. Constructability cases for conventional highway bridges are shown in Figure 2-1. As shown in the figure, the capacity and durability performance of the manufactured beams need to be evaluated. MDOT PC beam QA/QC process is described in Section 2.3.1. As a requirement of the current QA/QC process, the compressive strength of match cured cylinders is evaluated and beam cracking and surface defects are documented through visual inspection. The strength and visual inspection data are required for accepting (with full or reduced payment) or rejecting the beams. The current practice is to evaluate cylinder strength, not the beam concrete strength. Concrete durability properties (such as permeability) and beam internal conditions (honeycombs and voids) are not directly evaluated.

When deficiencies are detected, either from strength tests on match cured cylinders or the visual inspection, the QAI need to notify the Fabricator and Engineer. The Engineer engages the Engineer of Record (EOR) in girder structural capacity related decisions. The capacity of beams with various deficiencies is sporadically evaluated through load testing. The final decision regarding beams with deficiencies is at the Engineer's discretion. Hence, the following changes are suggested to improve the QA process for PC beam performance assessment:

(1) define a non-destructive testing toolkit to assess in-situ strength, cracks (length, width, depth, and orientation), surface defects, and internal defects to provide quantitative data for decision making and performance evaluation.

(2) define a PC beam capacity assessment procedure to evaluate safety.

The process of defining a non-destructive testing toolkit is beyond the scope of this project. This chapter presents a procedure to calculate the loading for the physical PC girder testing. The loading is calculated to verify that the PC beam can achieve the flexural tensile stress limit at and near the midspan.

3.2 PC BEAM CAPACITY ASSESSMENT PROCEDURE

The PC beam design is based on stresses at release and in service being at or below the respective AASHTO defined stress limits. The capacity assessment procedure determines the load level required for the manufactured PC beam to reach the critical stress limit. The calculation procedure uses a sign convention where tensile stress is negative.

3.2.1 Midspan Stress State at Release

Top and bottom fiber stresses of the noncomposite beam section under a prestressing force and the beam's self-weight should be below the allowable tension and compression stress limits. These limitations are formulated below as Condition 1 and 2.

Condition 1: Beam top fiber tensile stress check at release

$$\frac{F_i}{A_b} - \frac{F_i e_{pg}}{S_t} + \frac{M_{gr}}{S_t} \geq \left(-\bar{f}_{ti}\right)$$

$$-\frac{F_i}{A_b} + \frac{F_i e_{pg}}{S_t} - \frac{M_{gr}}{S_t} \leq \bar{f}_{ti}$$

LRFD Table 5.9.4.1.2-1

where,

F_i = prestressing force at release (kip)
A_b = area of beam cross-section (in.^{2})
e_{pg} = eccentricity of strands with respect to girder centroid (in.)
S_t = section modulus for top fiber (in.^{3})
M_{gr} = moment due to beam weight at release (kip-ft)
$\bar{f}_{ti}$ = allowable concrete tensile stress at release (ksi)

Condition 2: Beam bottom fiber compression stress check at release

$$\frac{F_i}{A_b} + \frac{F_i e_{pg}}{S_b} - \frac{M_{gr}}{S_b} \leq \bar{f}_{ci}$$

LRFD Art. 5.9.4.1.1

where,

S_b = section modulus of noncomposite beam for bottom fiber (in.^{3})
$\bar{f}_{ci}$ = allowable concrete compressive stress at release (ksi)

3.2.2 Midspan Stress State of a Beam During Construction and in Service

In addition to the stress conditions at release, the following conditions are considered to verify the stress limits of beams during construction and in service:

- Moment due to beam, cast-in-place deck, and haunch weight on the noncomposite section.
- Moment due to the non-structural elements (barrier and future wearing surface) weight and live load on the composite section.

92

These limits are formulated and shown as Condition 3, Condition 4, and Condition 5.

Condition 3: Beam top fiber compression stress check under effective prestress and permanent loads

$$\frac{\eta F_i}{A_b} - \frac{\eta F_i e_{pg}}{S_t} + \frac{(M_g + M_D)}{S_t} + \frac{(M_b + M_{ws})}{S_{tc}} \le \bar{f}_{cpl} \qquad \text{LRFD Table 5.9.4.2.1-1}$$

where,

η = ratio of effective stress after losses to prestressing steel stress before transfer

M_g = moment due to beam weight (kip-in)

M_D = moment due to deck and haunch weight (kip-in)

M_b = moment due to barrier weight (kip-in)

M_{ws} = moment due to future wearing surface (kip-in)

S_{tc} = section modulus of composite beam for beam top fiber (in.^{3})

$\bar{f}_{cpl}$ = allowable compressive stress for concrete subjected to effective prestress and permanent loads (ksi)

Condition 4: Beam top fiber compression stress check under effective prestress, permanent loads, and transient loads

$$\frac{\eta F_i}{A_b} - \frac{\eta F_i e_{pg}}{S_t} + \frac{(M_g + M_D)}{S_t} + \frac{(M_b + M_{ws} + M_{LT} + M_{LL})}{S_{tc}} \le \bar{f}_{ctl} \qquad \text{LRFD Table 5.9.4.2.1-1}$$

where,

$\bar{f}_{ctl}$ = allowable compressive stress for concrete subjected to effective prestress, permanent loads, and transient loads (ksi)

M_{LT} = moment due to design truck or axle load (kip-in)

M_{LL} = moment due to design lane load (kip-in)

Condition 5: Beam bottom fiber tension stress check under effective prestress, permanent loads, and transient loads

$$\frac{\eta F_i}{A_b} + \frac{\eta F_i e_{pg}}{S_b} - \frac{(M_g + M_D)}{S_b} - \frac{(M_b + M_{ws} + 0.8 M_{LT} + 0.8 M_{LL})}{S_{bc}} \ge (-\bar{f}_{ts})$$

$$-\frac{\eta F_i}{A_b} - \frac{\eta F_i e_{pg}}{S_b} + \frac{(M_g + M_D)}{S_b}$$

$$+ \frac{(M_b + M_{ws} + 0.8 M_{LT} + 0.8 M_{LL})}{S_{bc}} \le \bar{f}_{ts}$$

LRFD Table 5.9.4.2.2-1

where,

S_{bc} = section modulus of the composite beam for bottom fiber (in.^{3})

$\bar{f}_{ts}$ = allowable tensile stress for concrete with bonded steel and subjected to not worse than moderate corrosion condition (ksi)

For calculating the required prestressing force and associated eccentricity from the midspan stress checks, the five inequality conditions given above are merged graphically to demonstrate the iterative approach of the design. In this process, the five conditions are rearranged to represent the relationship between eccentricity (e_{pg}) and initial prestressing force ($F_i = f_{pi}A_{ps}N$, where A_{ps} is the area of a prestressing strand and N is the number of strands). In addition to the five conditions, a sixth condition is defined limiting the eccentricity of the prestressing strands to be bounded by the depth of the concrete cover. A 2 in. concrete cover is typically used in standard beam sections. All six conditions are summarized and shown below:

Condition 1:
$$e_{pg} \leq k_b + \left[\frac{1}{F_i}\right](M_{gr} + \bar{f}_{ti}S_t)$$

Condition 2:
$$e_{pg} \leq k_t + \left[\frac{1}{F_i}\right](M_{gr} + \bar{f}_{ci}S_b)$$

Condition 3:
$$e_{pg} \geq k_b + \left[\frac{1}{\eta F_i}\right]\left[(M_g + M_D) + \frac{(M_b + M_{ws})S_t}{S_{tc}} - \bar{f}_{cpl}S_t\right]$$

Condition 4:
$$e_{pg} \geq k_b + \left[\frac{1}{\eta F_i}\right]\left[(M_g + M_D) + \frac{(M_b + M_{ws} + M_{LT} + M_{LL})S_t}{S_{tc}} - \bar{f}_{ctl}S_t\right]$$

Condition 5:
$$e_{pg} \geq k_t + \left[\frac{1}{\eta F_i}\right]\left[(M_g + M_D) + \frac{(M_b + M_{ws} + 0.8M_{LT} + 0.8M_{LL})S_b}{S_{bc}} - \bar{f}_{ts}S_b\right]$$

Condition 6:
$$e_{pg} \leq y_b - 2 \text{ in.}$$

k_t = distance from the centroid to upper limit of kern = $-S_b/A_b$
k_b = distance from the centroid to lower limit of kern = S_t/A_b
y_b = distance from the centroid to the extreme bottom fiber of the noncomposite precast beam (in.)

These six inequalities are illustrated graphically in Figure 3-1. The highlighted area represents the 'feasibility domain' of the prestressing force (F_i) and strand eccentricity (e_{pg}) combinations that will not violate the five stress limits and the maximum allowable eccentricity limit.
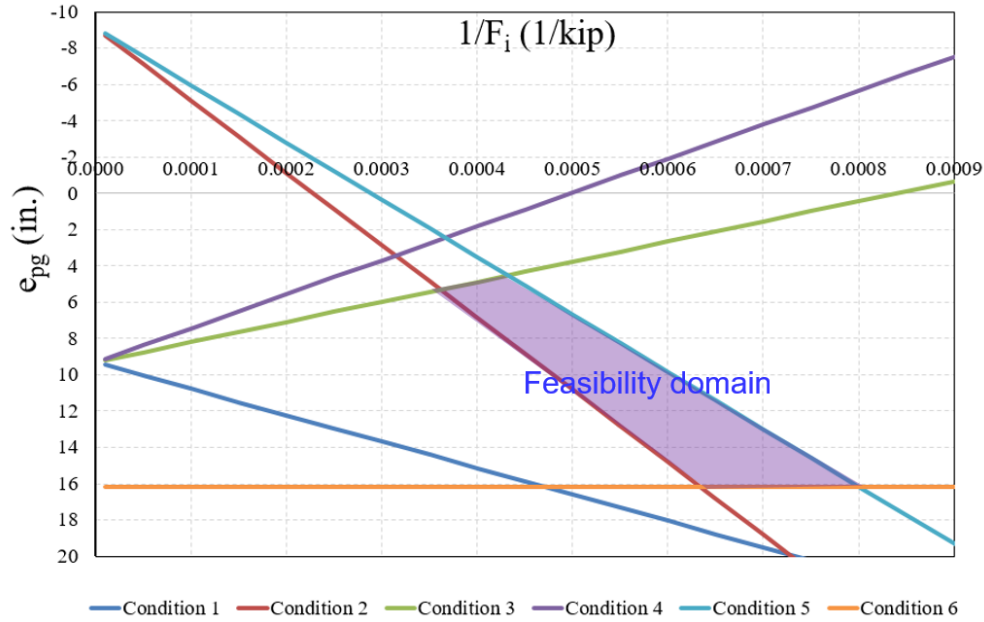
Figure 3-1. Feasibility domain of e_{pg} and F_i at midspan

3.2.3 Beam Failure Mode and Loads

Using the stress inequalities as the basis, an excel spreadsheet (*Quality Assurance Load Testing.xlsx*) was developed as part of this project to identify the failure mode and to calculate the load magnitude required to reach the design stress limits. The spreadsheet (i) checks for PC beam capacity against the stress limits defined in the AASHTO LRFD (2017a), (ii) identifies the flexural failure mode during load testing, and (iii) calculates the force magnitude required for load testing using either a 3-point or 4-point loading configuration.

The service moments under dead and live loads, e_{pg} and F_i at midspan, and cross sectional properties of the beam to be tested represent the input data for the spreadsheet. At the completion of data input, the graphical representation of stress inequalities and the coordinates representing e_{pg} and F_i at midspan are displayed as shown in Figure 3-2. The 'Final Design', located within the 'feasibility domain', represents the e_{pg} and F_i at midspan of the beam. For the specific beam, the spreadsheet calculates the governing flexural failure mode by gradually increasing the moment at midspan until the stress limit is reached (Figure 3-3). The spreadsheet also calculates the forces required to achieve the stress limit for 3-point and 4-point loading. Increasing the moment at midspan changes the slope of stress inequality relationships for condition 3, 4, and 5. The position of the original and new stress inequality relationships under increasing moment are graphically presented as shown in Figure 3-4. For the example represented in Figure 3-3, the beam bottom

95

fiber stress reaches the allowable stress limit ($\bar{f}_{ts}$) under the applied moment; thus, in this case Condition 5 represents the critical failure mode.
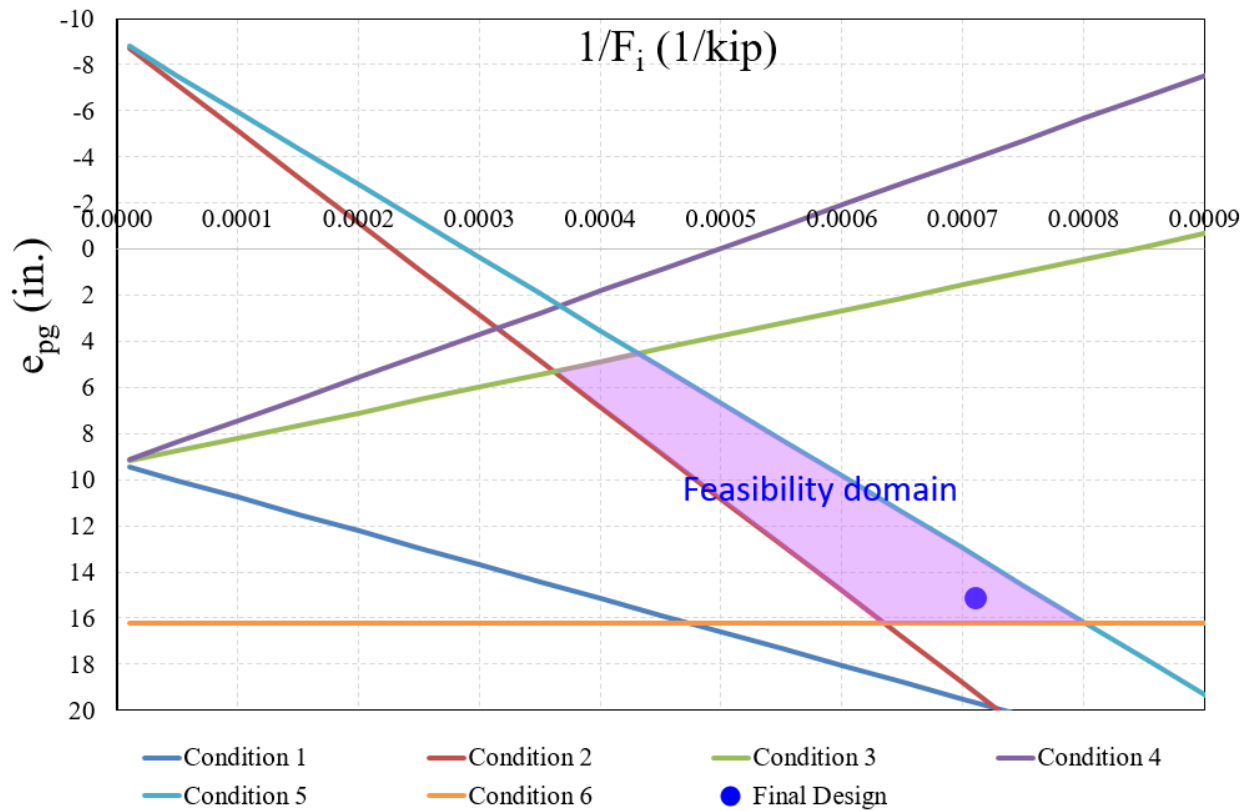
Figure 3-2. Location of e_{pg} and F_i of the selected beam
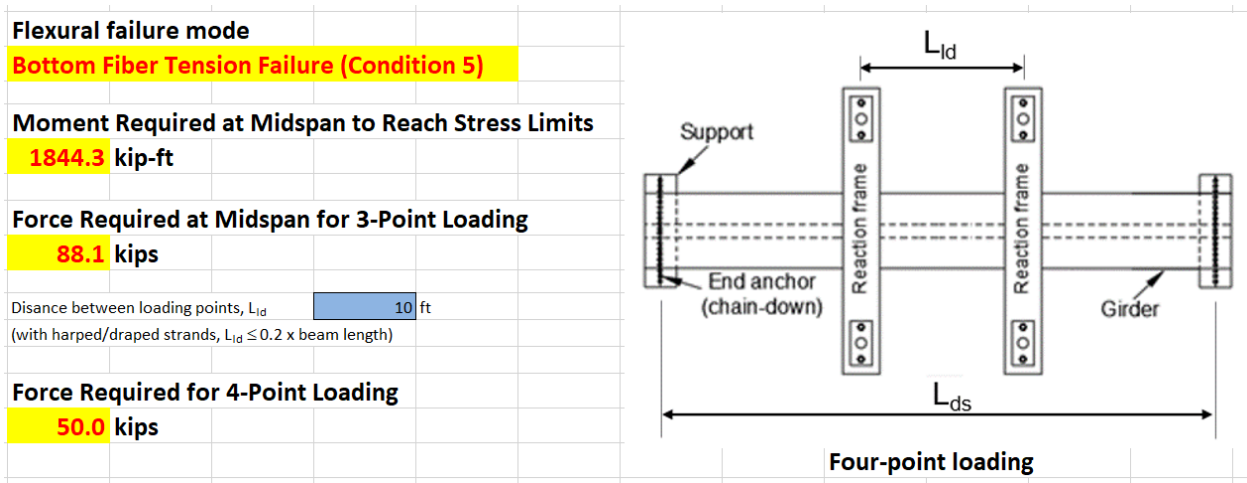
Figure 3-3. Flexural mode of failure and the required loads for testing
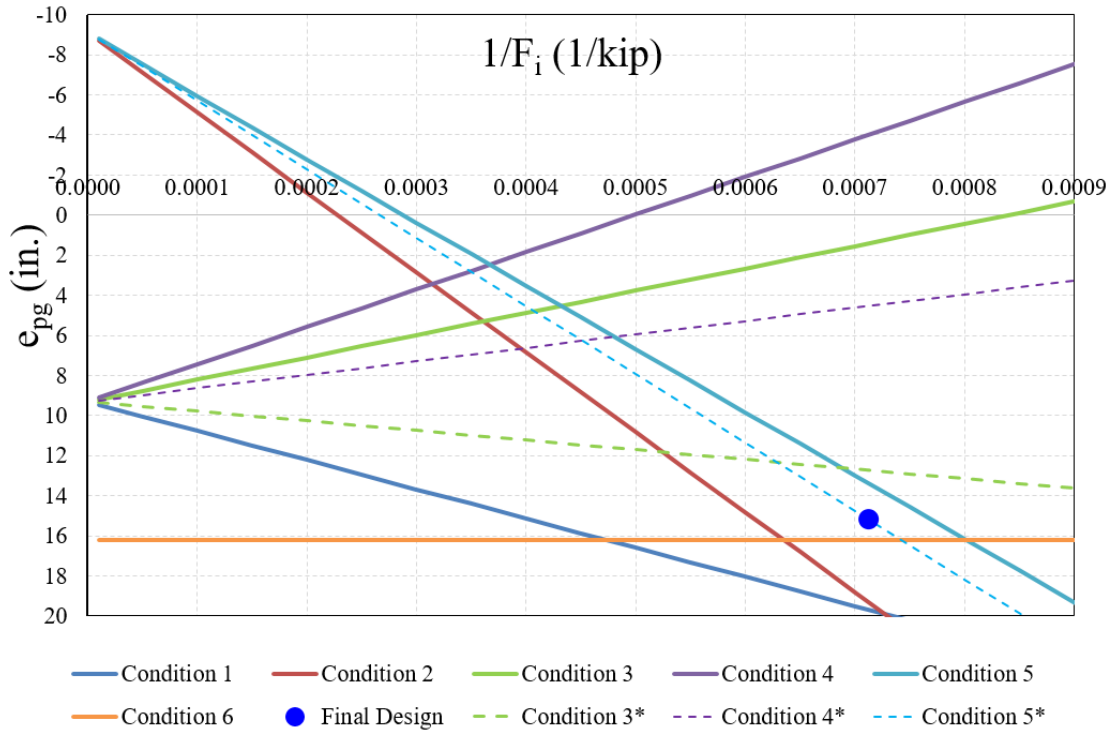
Figure 3-4. Condition 5 is the critical mode of failure with the application of an additional moment at midspan

3.3 LOAD TESTING AND BEAM RESPONSE MONITORING

Section 2.3 presented various options for potential apparatus for load testing and beam response monitoring. Load configurations can often be developed with the equipment and accessories available at a contractor's yard. The service load capacity of a typical PC I-beam under four-point loading can be evaluated with a 50 to 60-kip load at each loading point. With proper sizing of the helical piles and the extension couplers, customized reaction frames can be developed for load testing of PC beams at the fabrication facilities. The use of such reaction frames improves the safety and control of loading rate and magnitudes.

During beam load testing, the typical responses that require monitoring are the load, deflection, support settlement, strain, initiation of cracking, crack width, and crack propagation. Section 2.3.4 listed numerous state-of-the practice technologies for the monitoring of beam responses. The load, deflection, support settlement, and strain measurement technologies are quite common and can be economically acquired. The detection of crack initiation is very important when a beam capacity is evaluated against the allowable stress limits. Hence, the development and implementation of an acoustic emission (AE) based monitoring system to detect concrete cracking and crack propagation is recommended.

97

4   CONSTRUCTABILITY EVALUATION TOOLS FOR ENGINEERS

4.1   CONSTRUCTABILITY ANALYSIS CASES FORM

The *Constructability Analysis Cases Form*, a Microsoft Excel spreadsheet with Visual Basic for Applications (VBA) language, was developed as part of this project. The purpose of this form is to identify a list of potential constructability analysis cases during all stages of construction that would require the engineer's involvement. Figure 4-1 shows a screen image of the form. The form provides fields for inputting project name, engineer's name, and date. The form requires input for three parameters to execute the VBA code. The input parameters and the option are shown in Table 4-1. The appropriate option for each parameter is selected from the drop-down lists provided in the spreadsheet.

CONSTRUCTABILITY ANALYSIS CASES FORM

Project:			Analyzed by:		Date:
INPUT			**Potential Analysis Cases During**		
Bridge type					
Bridge geometry					
Construction type					
Submit	Clear				
Note: Clear the form before submitting another case					

Figure 4-1. Constructability Analysis Cases Form

Table 4-1. Input Parameters of the Constructability Analysis Cases Form

Input Parameter	Options
Bridge type	PC I-girder Steel I-girder
Bridge geometry	Straight Curved Skewed Curved and Skewed
Construction type	Complete superstructure construction Phased construction

Following the entry of input parameters, the VBA code is executed by clicking on the *Submit* button. The scope of analysis of typical PC I-girder curved bridges is limited to those constructed using straight girders. Hence, a message (shown in Figure 4-2) appears to inform the user about this limitation when the curved or curved and skewed option is selected as the bridge geometry for the PC I-girder bridge type.
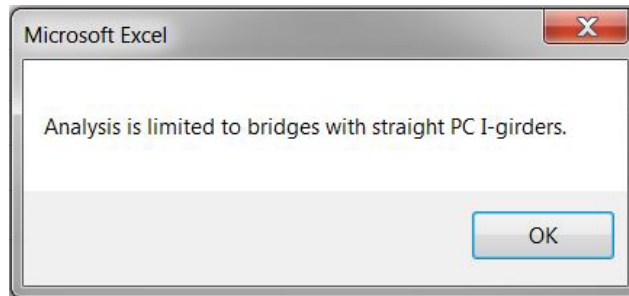
Figure 4-2. Pop-up message showing the PC I-girder geometry used in the analysis of curved or curved and skewed PC-I girder bridges

Figure 4-3 shows the full list of constructability analysis cases that need to be considered for PC I-girder bridge construction. These cases are grouped under lifting, erection, and phased construction. The number of analysis cases required for straight and skewed PC I-girder bridges is the same because:

- Lifting scheme includes only straight girders.
- Skew effects are observed with lateral load paths developed by the diaphragms (or cross-frames), and these elements are included in the superstructure after the girders are fully erected.
- Phased construction cases are equally applicable.

Potential Analysis Cases During
Lifting
Capacity against cracking and ultimate stress
Erection
Time-dependent deformation of girders
Lateral instability of girders
Phased Construction
Capacity of the in-service structure
Elevation difference between phases due to differential deflection
Elevation difference between phases due to foundation settlement
Cross-sectional twist of phases

Figure 4-3. Constructability analysis cases for PC I-girder bridges

Figure 4-4 shows the full list of constructability cases that require analysis for curved steel I-girder bridges. As it was described in Section 2.6.2 that bridge geometry (i.e. curvature and skew), wind loading, long unbraced length, or a combination thereof contribute to the lateral instability of I-girders. Each of these loads and attributes, when applicable, are included in girder

99

stability evaluation. Thus, lateral torsional buckling stability during erection is included as a single constructability case.

Potential Analysis Cases During
Lifting
Capacity against flange yielding stress
Rigid-body rotation and cross-sectional twist
Lateral torsional buckling capacity of girders
Erection
Girder twist and detailing
Lateral torsional buckling capacity of girders
Deck Placement
Unintended deck profile due to differential deflection
Unintended deck profile due to exterior girder warping
Unintended deck profile due to exterior girder web out-of-plane deformation
Phased Construction
Capacity of the in-service structure
Elevation difference between phases due to differential deflection
Elevation difference between phases due to foundation settlement
Cross-sectional twist of phases
Global lateral torsional buckling capacity of multi-girder systems (widening projects)

Figure 4-4. Constructability analysis cases for curved steel I-girder bridges

It is important to indicate that the constructability cases form lists those requiring analysis for the specific bridge project. In other words, all these cases may not be warranted for every bridge project and construction. As an example, controlling the deck profile due to exterior girder web out-of-plane deformation is excluded if the overhang bracket-bearing point is located near the bottom flange-web intersection. The descriptions in Chapter 2 of this report will help discriminate the nature of constructability cases listed.

4.2 REQUIRED LEVEL OF ANALYSIS (RLOA) FOR CONSTRUCTABILITY EVALUATION

A set of Microsoft Excel spreadsheets with embedded VBA codes were developed in this project for the engineer to determine the level of analysis required for modeling the constructability cases. These spreadsheets are labeled as the *Required Level of Analysis (RLOA) Selection Tools* and cover only a subset of constructability cases listed in the *Constructability Analysis Cases Form*. This is due to practical difficulties in developing tools for all the cases listed in the form. Two RLOA

selection tools were developed for steel and PC I-girder bridges. The following sections summarize structural modeling options, methodology, and rationale of developing RLOA selection tools, and the Structural Analysis Tools for analyzing constructability cases.

4.2.1 Constructability Cases Structural Modeling Options

The RLOA selection tools developed for steel I-girder bridges are based on Table 2-2 and the supplementary discussions provided in the NCHRP 12-79 project report. Table 2-2 compares the analysis results of 1D line-girder and 2D-grid models with refined 3D finite element models (White et al. 2012b).

A single girder or a girder segment is isolated from the rest of the structure and analyzed as a discrete element with the 1D line-girder models, the interaction between girders and bracings is ignored or considered using simplified assumptions. The loads acting on the girders are calculated from the tributary area or member cross-section. The construction stages that involve a single girder, such as lifting or erection of the first girder in a span, can be accurately analyzed using the 1D line-girder models. However, a 1D model is not suitable for modeling of girder systems that are affected by stiffness and secondary load paths provided by cross-frames, skew, curvature, structural asymmetry, or a combination thereof (FHWA 2015). Supplementary methods with 1D models can be used - such as V-Load analysis (see Section 2.6.3.1), the SP method given in Fisher (2006) (see Section 2.7.5.1), or AASHTO (2017a) Eq. C6.10.3.4.1-2 for calculating the flange lateral bending moment with the overhang brackets. These supplementary methods extend the capabilities of the 1D girder model to approximate the interaction of a girder system when skew, curvature, structural asymmetry, etc., are limited.

The common 2D methods used for the analysis of highway bridges are the traditional 2D-grid (also known as a "plane grid" or "grillage method"), the generalized grid (also known as a "2D-frame method"), and the plate and eccentric beam analysis (AASHTO/NSBA 2014a, White et al. 2012b). In the 2D-grid analysis, girders and cross-frames (or diaphragms) are modeled as line elements on the same plane as shown in Figure 4-5. These elements often have three degrees of freedom (dof) at each node; one translational and two rotational (White et al. 2012b). The translational dof (u_1 and u_4) represent vertical displacement, and the rotational dofs (u_2, u_5 and u_3, u_6) represent major axis bending and torsional responses, respectively as shown in Figure 4 6. The 2D-grid analysis model cannot explicitly incorporate the depth of a girder. Girders and cross-

101

frames connections are modeled as common nodes on the centroidal axis of the girders. Boundary conditions are also defined at the level of the centroidal axis.
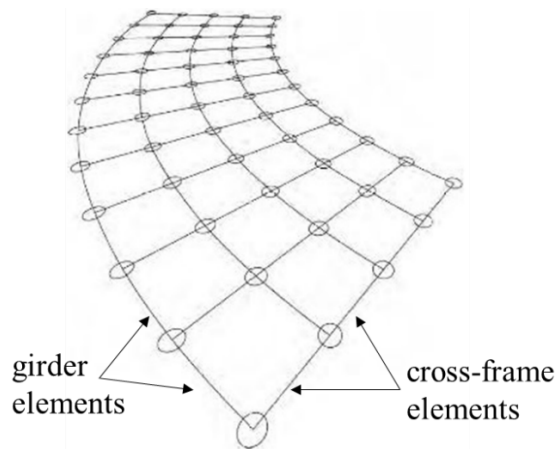
Figure 4-5. Analytical model of a curved bridge developed using the traditional 2D-grid method (AASHTO/NSBA 2014a)
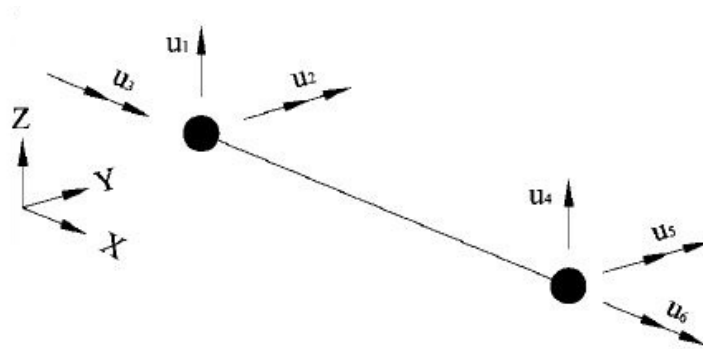
Figure 4-6. Line elements for modeling girders and cross-frames in the traditional 2D-grid method (White et al. 2012b)

The generalized grid analysis shown in Figure 4-7 is a variation of the 2D-grid analysis with line elements and six dof at each node. The dof shown in red in Figure 4-7 represent those common to the 2D-grid method while the dof shown in black represent those specific to the generalized grid analysis. The additional dofs provide refinement in modeling such as shear-deformable cross-frames (or diaphragms), physical girder supports, etc. (AASHTO/NSBA 2014a). In principle, the generalized grid analysis is practically identical to the traditional 2D-grid method when line elements are defined on the same plane, neglecting the position of bridge elements with respect to the vertical axis (White et al. 2012b). Thus, the NCHRP 12-79 project classified the generalized grid method under 2D-grid analysis.

102
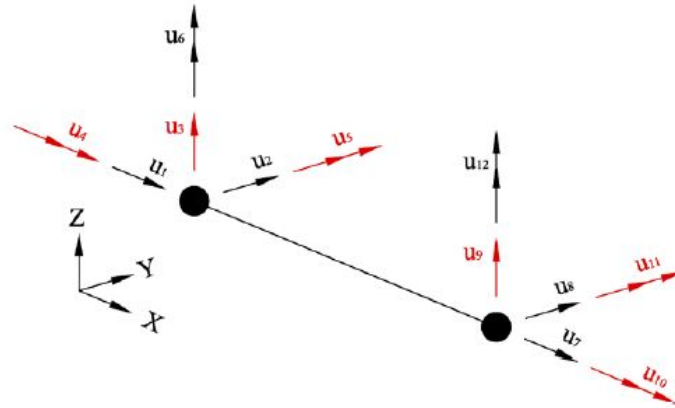
Figure 4-7. Line elements for modeling girders and cross-frames in the generalized grid method (White et al. 2012b)

The plate and eccentric beam analysis is a variation of the 2D-grid. In this method, the concrete deck is modeled by plate or shell elements and connected to the girder elements with rigid links with an offset equal to the distance between the centroids of the deck and girders, as shown in Figure 4-8. The plate and eccentric beam model is often used for the analysis of in-service structures. Thus, the NCHRP 12-79 project did not consider this method in their evaluation. Consequently, this method is not included in the matrix of the RLOA in Table 2-2 (White et al. 2012b).
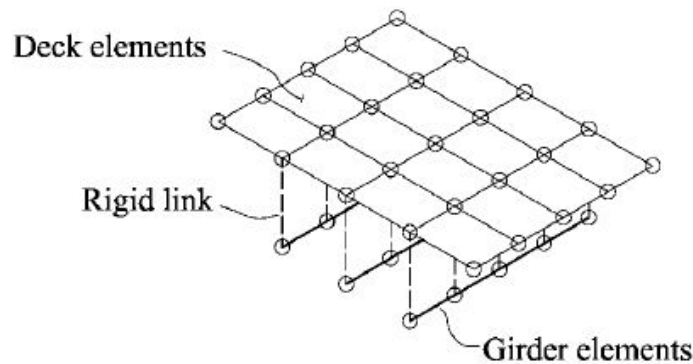
Figure 4-8. Bridge analytical model: plate and eccentric beam method (White et al. 2012b)

According to AASHTO/NSBA (2014a), 3D finite element analysis (FEA) refers to any computer-based matrix analysis in which:

- *the structure is modeled in three dimensions,*
- *the girder flanges are modeled using line, beam, plate, shell, or solid elements,*
- *the girder webs are modeled using plate, shell, or solid elements,*
- *the cross-frames and diaphragms are modeled using line, beam, plate, shell, or solid elements as appropriate, and*
- *the deck is modeled using plate, shell, or solid elements.*

103

The NCHRP 12-79 project adopted the same definition. Also, the *UT Bridge* program (see Section 2.6.3.2) complies with this definition.

The tool for PC I-girder bridges adopted the same terminology and definitions for the analysis methods.

4.2.2   RLOA Selection Tool for Steel I-Girder Bridges

The *RLOA Selection Tool for Steel I-Girder Bridges* is a Microsoft Excel spreadsheet with embedded VBA codes. The input parameters shown in Figure 4-9 are required for executing the VBA codes. Input parameter definitions are provided in Table 4-2. The blue cells require direct user input. The green cells are calculated based on user input. These input parameters are needed for (*i*) establishing potential constructability cases, (*ii*) calculating the connectivity and skew indices, (*iii*) describing the use of the *mode of scores* or *worst-case scores* given in Table 2-2, and (*iv*) defining the recommended fit conditions. A parameter definition can be displayed by moving the cursor to the cell corner marked in red, shown in Figure 4-9. If there are missing inputs, a warning message is displayed directing the user to complete the input data, as shown in Figure 4-10.

INPUT	
L (ft)	250
w_g (ft)	100
R (ft)	No
θ (deg)	10
n_{cf}	5
m	1
Is phased construction employed?	Yes
Does the structure have an irregular geometry?	No
L/R	0.00
Connectivity Index, I_C	0.00
Skew Index, I_S	0.07

Clear   Submit

Figure 4-9. Input parameters in Constructability RLOA Tool for steel I-girder bridges

Table 4-2. Input Parameters and Definitions for the RLOA Selection Tool for Steel I-Girder Bridges

Input Parameters	Definitions
L	Length of the span under consideration (ft)
w_g	Width of the structural unit measured between centerline of exterior girders (ft)
R	Radius of curvature of bridge centerline (ft) **Select** *No* for straight girders
θ	Skew angle (deg) **Input *0*** for straight bridges
n_{cf}	Number of intermediate cross-frames within the span
m	Factor for span type **Select** *1* for simple-span bridges *2* for continuous-span bridges
Construction Type	**Select** *Yes* for phased construction *No* for complete superstructure construction
Irregular Geometry	**Select** *No* if the structure has symmetry, constant girder spacing, constant deck width, relatively uniform cross-frame spacing, etc. *Yes* to represent other geometries

Microsoft Excel ✕

Input parameter(s) is missing.

OK

Figure 4-10. Warning message for incomplete input

Upon executing the spreadsheet, the constructability analysis cases are displayed with the minimum RLOA for each case, associated analysis tool, and supplemental analysis tools (if needed). Figure 4-11 shows output screen examples of the RLOA Selection Tool for a straight bridge and a curved and skew bridge. For the cases where the matrix in Table 2-2 is used, a minimum score of "B" (see Table 2-3) is appropriate for the RLOA. The sections below describe the background in designating the RLOA for each constructability case.

The blue text in the output window displays the analysis tools that are hyperlinked. Among the analysis tools, UT Lift is a spreadsheet (see Section 2.5.6.2 for more details.) The other tools include Mathcad scripts developed as part of this project and presented in Appendices C to J. Recommended fit conditions are also provided as supplemental information in the output window in Figure 4-11b associated with the *girder twist and detailing* listed under *erection*.

105

Cases during	RLOA	Analysis Tool	Supplemental
Lifting			
Capacity against flange yielding stress	1D	Top Flange Stress Analysis	UT Lift
Lateral torsional buckling capacity of girders	1D	UT Lift	
Erection			
Lateral torsional buckling capacity of girders	1D	UT Bridge	Wind Load Calculation
Deck Placement			
Unintended deck profile due to differential deflection	1D	UT Bridge	Differential Deflection Analysis
Unintended deck profile due to exterior girder warping	1D	TAEG	
Unintended deck profile due to exterior girder web out-of-plane deformation	3D	Web Out-of-Plane Deformation Analysis	Overhang Bracket Analysis
Phased Construction			
Capacity of the in-service structure	N/A	MDOT Load Rating Procedures	
Elevation difference between phases due to differential deflection	N/A	N/A	
Elevation difference between phases due to foundation settlement	N/A	N/A	
Cross-sectional twist of phases	3D	UT Bridge	
Global lateral torsional buckling capacity of multi-girder systems	1D	Global LTB Analysis	

(a) Straight bridge

Cases during	RLOA	Analysis Tool	Supplemental
Lifting			
Capacity against flange yielding stress	1D	Top Flange Stress Analysis	UT Lift
Rigid-body rotation and cross-sectional twist of girders	1D	UT Lift	
Lateral torsional buckling capacity of girders	1D	UT Lift	
Erection			
Girder twist and detailing	3D	UT Bridge	Recommended fit condition(s): NLF
Lateral torsional buckling capacity of girders	3D	UT Bridge	Wind Load Calculation
Deck Placement			
Unintended deck profile due to differential deflection	3D	UT Bridge	
Unintended deck profile due to exterior girder warping	3D	UT Bridge	Overhang Bracket Analysis
Unintended deck profile due to exterior girder web out-of-plane deformation	3D	Web Out-of-Plane Deformation Analysis	Overhang Bracket Analysis
Phased Construction			
Capacity of the in-service structure	N/A	MDOT Load Rating Procedures	
Elevation difference between phases due to differential deflection	N/A	N/A	
Elevation difference between phases due to foundation settlement	N/A	N/A	
Cross-sectional twist of phases	3D	UT Bridge	
Global lateral torsional buckling capacity of multi-girder systems	3D	UT Bridge	

(b) Curved and skew bridge

Figure 4-11. Sample screenshot of the *RLOA Selection Tool for Steel I-girder Bridges*

4.2.2.1   Lifting Analysis

Lifting of steel I-girders deals with top flange local bending stress, rotational deformation of curved girders, and lateral torsional buckling. The typical practice is to lift a single girder or a girder segment at a time. So, 1D line-girder models can be used to evaluate the stresses and deformations.

The top flange stress is evaluated for yielding near the lifting points. Eq. (2-7) or the *UT Lift* discussed in Section 2.5.6.2 is recommended for this purpose. Also, *UT Lift* can be used to perform the rotational displacement and lateral torsional buckling stability analyses. *UT Lift* calculates the total rotational response using the 1D model described in Stith (2010). Buckling analysis is performed using the procedure discussed in Farris (2008), in which the recommended C_b factors developed by Timoshenko and Gere (1961) are applied to the classical buckling solution.

4.2.2.2   Erection Analysis

Steel I-girder erection covers (i) twisting and detailing of curved and/or skewed bridges and (ii) lateral torsional buckling instability due to curvature and/or skew, wind loading, long unbraced length, or a combination thereof.

The total normal stress in steel I-girders of curved and/or skewed bridges is the summation of axial stress, major axis bending stress, lateral bending stress, and warping stress, as shown in Figure 4-12. Warping stress is induced by torsion and the associated distortion of the cross-section (AASHTO 2017a). Warping stress distribution is similar to flange lateral bending stress distributions. Thus, the RLOA for lateral flange bending stress can also be the ROLA for warping stresses.
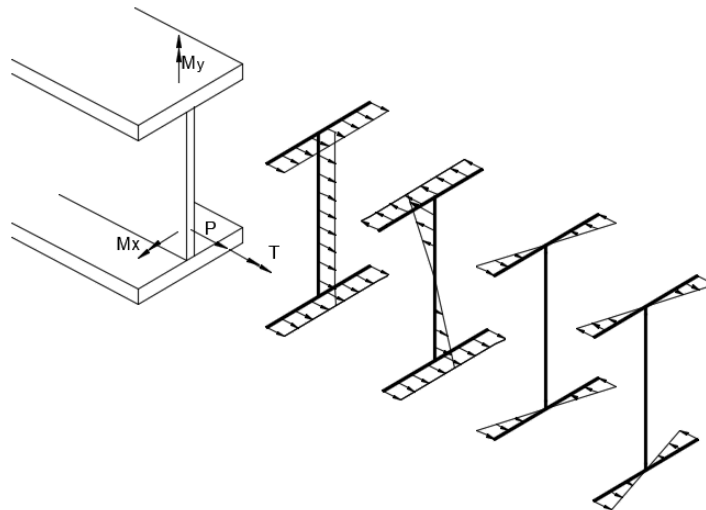
$$Total\ Normal\ Stress = \sigma = \frac{P}{A} + \frac{M_x y}{I_x} + \frac{M_y x}{I_y} + Warping\ Stress$$

Figure 4-12. Normal stresses in I-girders of curved and/or skewed steel bridges (AASHTO/NSBA 2014a)

In skew bridges, cross-frames are either placed perpendicular to the girders (non-skewed cross-frames) or parallel to support skew. The distances between each girder end to the connecting points of non-skewed cross-frames will vary. Differential displacement of cross-frame connecting points on the adjacent girders and cross-frame orientation and high in-plane stiffness subjects the cross-frames to an in-plane rotation rather than shear deformation (AASHTO/NSBA 2014a). The cross-frame forces resulting from in-plane rotation create torsion in the girder, which generates warping stresses. Skewed cross-frames, on the other hand, are connected at points along the

Bridge Structural Analyses for Staged Construction and Constructability Reviews

adjacent girders where girder vertical deflections and major-axis bending rotations are equal. As a result, the cross-frames rotate with the girders. Since the skewed cross-frame rotation axis is not perpendicular to the major axis of the girders, the cross-frames will tend to rack (AASHTO/NSBA 2014a). Again, the high in-plane stiffness of the cross-frames generates in-plane rotation rather than racking and thus, the girders will be subjected to torsion. As a result, warping stresses develop.

It is important to note that Table 2-2 reflects the relationship between cross-frame forces and flange lateral bending stresses. For example, in curved bridges, in the analysis of cross-frame forces and flange lateral bending stresses, the worst-case and mode of scores given in Table 4-3 for 1D line-girder and 2D-grid analysis are identical. In slightly skewed bridges (i.e. $I_S < 0.30$), the footnotes (a) and (d) signify that cross-frame forces and flange lateral bending stresses will be small and negligible. When the skew effect is significant on a structural response (i.e. $0.30 \leq I_S < 0.65$ and $I_S > 0.65$), the footnotes (c) and (e) signify that 1D line-girder analysis will not capture the skew effects. Moreover, the footnote (b) states that the traditional 2D-grid analysis will be inaccurate in estimating cross-frame forces and flange lateral bending stresses. In the traditional 2D-grid analysis, the torsional stiffness of I-girders is often incorporated only in the St. Venant torsional stiffness (GJ/L_b) term (AASHTO 2017a, White et al. 2012b). In this case, actual girder stiffness will be underestimated since open sections, such as I-girders, resist torsion primarily by warping stiffness.

Table 4-3. RLOA for Cross-Frame Forces and Flange Lateral Bending Stress Calculations (White et al. 2012a)

Structural Response and I_c ad I_s Limits for Curves and Skewed Geometry (a)	Worst-Case Scores: Traditional 2D-Grid (b-1)	Worst-Case Scores: 1D-Line Girder (b-2)	Mode of Scores: Traditional 2D-Grid (c-1)	Mode of Scores: 1D-Line Girder (c-2)
Cross-Frame Forces: Curved ($I_C \le 1$)	C	C	B	B
Cross-Frame Forces: Curved ($I_C > 1$)	F	D	C	C
Cross-Frame Forces: Skewed ($I_S < 0.30$)	NA[a]	NA[a]	NA[a]	NA[a]
Cross-Frame Forces: Skewed ($0.30 \le I_S < 0.65$)	F[b]	F[c]	F[b]	F[c]
Cross-Frame Forces: Skewed ($I_S \ge 0.65$)	F[b]	F[c]	F[b]	F[c]
Cross-Frame Forces: Curved & Skewed ($I_C > 0.5$ & $I_S > 0.1$)	F[b]	F[c]	F[b]	F[c]
Flange Lateral Bending Stresses: Curved ($I_C \le 1$)	C	C	B	B
Flange Lateral Bending Stresses: Curved ($I_C > 1$)	F	D	C	C
Flange Lateral Bending Stresses: Skewed ($I_S < 0.30$)	NA[d]	NA[d]	NA[d]	NA[d]
Flange Lateral Bending Stresses: Skewed ($0.30 \le I_S < 0.65$)	F[b]	F[e]	F[b]	F[e]
Flange Lateral Bending Stresses: Skewed ($I_S \ge 0.65$)	F[b]	F[e]	F[b]	F[e]
Flange Lateral Bending Stresses: Curved & Skewed ($I_C > 0.5$ & $I_S > 0.1$)	F[b]	F[e]	F[b]	F[e]

[a] Magnitudes should be negligible for bridges that are properly designed and detailed. The cross-frame design is likely to be controlled by considerations other than gravity-load forces.

[b] Results are highly inaccurate. The improved 2D-grid method discussed in Chapter 6 of NCHRP 12-79 Task 8 report provides an accurate estimate of forces.

[c] Line-girder analysis provides no estimate of cross-frame forces associated with skew.

[d] The flange lateral bending stresses tend to be small. The AASHTO (2017a) Article C.6.10.1 may be used as a conservative estimate of the flange lateral bending stresses due to skew.

[e] Line-girder analysis provides no estimate of girder flange lateral bending stresses associated with skew.

As shown in Figure 4-11, the *RLOA Selection Tool for Steel I-girder Bridges* guides the users to consider recommended fit conditions given in Table 2-7. This is because the accuracy of the approximate analysis methods is also affected by the specified fit conditions. The 1D line-girder method provides an accurate estimation of major-axis bending stresses and vertical displacements in skewed bridges only if the loading condition matches with the targeted fit condition (i.e., total dead load for TDLF detailing or steel dead load for SDLF detailing) (White et al. 2012b). Moreover, large cross-frame forces and flange lateral bending stresses are expected for bridges with $I_S > 0.30$. Since the cross-frame contributions cannot be represented in 1D-girder analysis, dead load detailing effects in skewed bridges cannot be captured. Similarly, the V-load method fails to capture the locked-in forces developed in cross-frames of horizontally curved bridges with SDLF or TDLF conditions (White et al. 2012b). It should also be recalled from Table 2-7 that NLF is the recommended fit condition for curved bridges. The traditional 2D-grid analysis

cannot accurately estimate the dead load fit cross-frame forces with I-girder torsional stiffness underestimated (White et al. 2012b).

The stability analysis of I-girder, as per the *AASHTO LRFD Specifications*, requires an accurate estimation of the normal stress in the cross-section. AASHTO (2017a) Article 6.10.1.6 states that lateral torsional buckling evaluation requires:

- f_{bu} – the largest value of the compressive stress in the flange without consideration of flange lateral bending
- M_u – the largest value of the major-axis bending moment causing compression in the flange
- f_l – the largest value of the stress due to lateral bending in the flange.

Thus, the accuracy of stability analysis is controlled by how accurately the major-axis bending stress and flange lateral bending stress are calculated. Table 4-4 presents the RLOA for these two stress components. Both 1D line-girder and 2D-grid models provide equally accurate results for the major-axis bending stress. Flange lateral bending stress calculated with both models become inaccurate with increasing skew or skew and curvature. Hence, the RLOA is recommended based on the scores associated with the accuracy of flange lateral bending stresses.

Table 4-4. RLOA for Major-Axis and Flange Lateral Bending Stress Calculations (White et al. 2012a)

Structural Response and I_c ad I_s Limits for Curved and Skewed Geometry (a)	Worst-Case Scores: Traditional 2D-Grid (b-1)	Worst-Case Scores: 1D-Line Girder (b-2)	Mode of Scores: Traditional 2D-Grid (c-1)	Mode of Scores: 1D-Line Girder (c-2)
Major-Axis Bending Stress: Curved ($I_C \leq 1$)	B	B	A	B
Major-Axis Bending Stress: Curved ($I_C > 1$)	D	C	B	C
Major-Axis Bending Stress: Skewed ($I_S < 0.30$)	B	B	A	A
Major-Axis Bending Stress: Skewed ($0.30 \leq I_S < 0.65$)	B	C	B	B
Major-Axis Bending Stress: Skewed ($I_S \geq 0.65$)	D	D	C	C
Major-Axis Bending Stress: Curved & Skewed ($I_C > 0.5$ & $I_S > 0.1$)	D	F	B	C
Flange Lateral Bending Stress: Curved ($I_C \leq 1$)	C	C	B	B
Flange Lateral Bending Stress: Curved ($I_C > 1$)	F	D	C	C
Flange Lateral Bending Stress: Skewed ($I_S < 0.30$)	NA[d]	NA[d]	NA[d]	NA[d]
Flange Lateral Bending Stress: Skewed ($0.30 \leq I_S < 0.65$)	F[b]	F[e]	F[b]	F[e]
Flange Lateral Bending Stress: Skewed ($I_S \geq 0.65$)	F[b]	F[e]	F[b]	F[e]
Flange Lateral Bending Stress: Curved & Skewed ($I_C > 0.5$ & $I_S > 0.1$)	F[b]	F[e]	F[b]	F[e]

[b] Results are highly inaccurate. The improved 2D-grid method discussed in Chapter 6 of NCHRP 12-79 Task 8 report provides an accurate estimate of forces.

[d] The flange lateral bending stresses tend to be small. The AASHTO (2017a) Article C.6.10.1 may be used as a conservative estimate of the flange lateral bending stresses due to skew.

[e] Line-girder analysis provides no estimate of girder flange lateral bending stresses associated with skew.

As mentioned, 1D line-girder analysis will not provide an accurate estimate of flange lateral bending stresses associated with skew (AASHTO/NSBA 2014a, White et. al 2012b). However, in slightly skewed bridges ($I_S < 0.30$) these stresses will be small, and the AASHTO LRFD provisions can be followed. AASHTO (2017a) Article C6.10.1 states that in the absence of a refined analysis, the total unfactored flange lateral bending stress (f_l) is taken as:

- 10.0 ksi for interior girders and 7.5 ksi for exterior girders at a cross-frame (or diaphragm) location due to the use of discontinuous cross-frame (or diaphragm) lines at or near supports, but not along the entire bridge length

- 10.0 ksi for interior and 2.0 ksi for exterior girders at a cross-frame (or diaphragm) location due to the use of discontinuous cross-frame (or diaphragm) lines over the entire bridge.

In a traditional 2D-grid analysis, the torsional stiffness of I-girders only considers the St. Venant torsional stiffness. For that reason, for bridges with $I_S \geq 0.30$, flange lateral bending stresses calculated using the 2D-grid analysis will not be accurate. Approximate methods are available for calculating the flange lateral bending stress of curved bridge girders. For curved girders, White et al. (2012b) recommend using Eq. (4-1) for calculating flange lateral bending stress (f_l) at cross-frame locations. The equation can be used for both 1D line-girder and 2D-grid analyses.

$$f_l = \frac{ML_b^2}{12RhS_{yf}} \tag{4-1}$$

where:

h	= distance between flange centroids
L_b	= cross-frame spacing
M	= total major axis bending moment due to gravity loads and V-loads (see Section 2.6.3.1)
R	= radius of curvature
S_{yf}	= flange elastic section modulus about the weak axis of the I-section

Eq. (4-1) becomes identical to AASHTO (2017a) Eq. C4.6.1.2.4b-1, when the stress is expressed in terms of lateral bending moment and the constant N in the AASHTO equation is taken as 12. Alternatively, girder stability can be evaluated using eigenvalue buckling analysis. Eigenvectors represent the associated buckling modes. The first mode corresponding to the lowest eigenvalue is often critical. A target eigenvalue that guarantees girder stability depends on the magnitude of the applied loads. FHWA (2015) recommends limiting eigenvalues to a range of 1.5 to 1.75 for deck placement analysis. However, the erection analysis uses the self-weight of

structural elements, which is relatively accurate compared to other construction loads involved in deck placement analysis. Thus, for girder stability analysis during erection eigenvalues lower than 1.5 can be allowed. *UT Bridge*, discussed in Section 2.6.3.2, has eigenvalue buckling analysis capability.

4.2.2.3   Deck Placement Analysis

The primary expectation from this analysis is to have the intended deck profile maintained. The analysis evaluates (*i*) girder differential deflection, (*ii*) exterior girder warping, and (*iii*) exterior girder web out-of-plane deformation.

Table 4-5 shows the relevant section of Table 2-2 with the accuracy scores of approximate analysis methods for vertical displacement calculation. The *RLOA Selection Tool for Steel I-girder Bridges*, shown in Figure 4-11, suggests the analysis models for differential girder deflection based on Table 4-5.

Table 4-5. RLOA for Vertical Displacement Calculation (White et al. 2012a)

Structural Response and I_c ad I_s Limits for Curved and Skewed Geometry (a)	Worst-Case Scores: Traditional 2D-Grid (b-1)	Worst-Case Scores: 1D-Line Girder (b-2)	Mode of Scores: Traditional 2D-Grid (c-1)	Mode of Scores: 1D-Line Girder (c-2)
Vertical Displacements: Curved ($I_C \leq 1$)	B	C	A	B
Vertical Displacements: Curved ($I_C > 1$)	F	D	F	C
Vertical Displacements: Skewed ($I_S < 0.30$)	B	A	A	A
Vertical Displacements: Skewed ($0.30 \leq I_S < 0.65$)	B	B	A	B
Vertical Displacements: Skewed ($I_S \geq 0.65$)	D	D	C	C
Vertical Displacements: Curved & Skewed ($I_C > 0.5$ & $I_S > 0.1$)	F	F	F	C

Large cross-frame forces and flange lateral bending stresses develop in high skew bridges (i.e., $I_S \geq 0.65$). 1D-girder analysis model cannot account for the contribution of cross-frame effects and will not be suitable for accurate estimation of the vertical displacements (White et al. 2012b). The procedure developed by Fisher (2006) (discussed in Section 2.7.5.1) extends the capabilities of the line-girder analysis to account for skew effects. However, this methodology is not included in Table 2-2.

In curved bridges with $I_C > 1$, for estimating vertical displacements, the 1D line-girder analysis provides better accuracy than the traditional 2D-grid analysis. This is unusual since one would expect that a more rigorous analysis provides better accuracy. White et al. (2012b) explains this fact by a 2D-grid model of a curved I-girder. Figure 4-13 shows an isolated curved I-girder

segment subjected to a uniform bending moment of M. The girder segment is modeled as four straight-line elements between two consecutive cross-frames. The moment resolves into a major axis bending moment and torsion at each end. The major-axis moment in each element again resolves into both major-axis moment and torsion to satisfy the equilibrium at intermediate nodes. Twisting of the straight elements not only twists the next element but also creates major axis bending moments and vertical displacements from the change in element orientation. Since the traditional 2D-grid analysis underestimates the accurate torsional stiffness of I-girders (see Section 4.2.2.2), twisting deformations and vertical displacements will be overestimated.
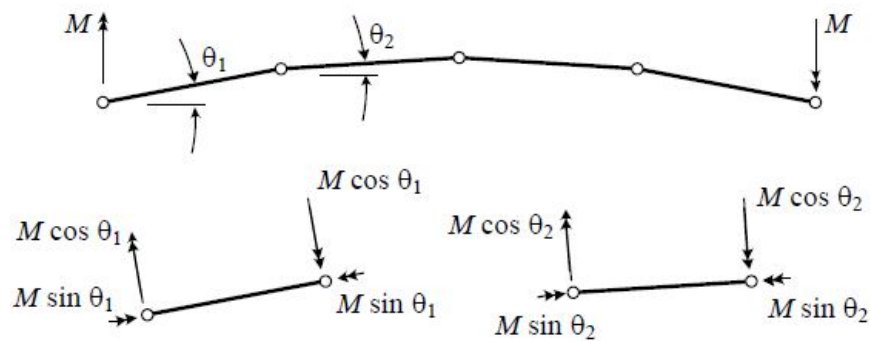
Figure 4-13. A 2D-grid model of a curved I-girder segment located between two cross-frames (White et al. 2012b)

Warping analysis of an exterior steel I-girder under eccentric overhang bracket loads requires defining the loading (externally applied torsion) and boundary conditions. To calculate the torsion of an exterior girder of a straight bridge under the loads acting on the bracket, boundary conditions at cross-frame locations can be assumed as pinned-pinned or fixed-fixed. For curved and/or skewed bridges, however, this analysis also needs to consider cross-frame forces and the resulting internal torsion and flange lateral bending stresses. Therefore, the discussion regarding twisting of curved and/or skewed bridges during erection, presented in Section 4.2.2.2, equally applies to warping analysis.

As discussed in Section 2.7.5.3, *TAEG* is recommended for evaluating the torsional response of straight exterior I-girders under overhang bracket loads. The analysis model used in *TAEG* cannot be classified as 1D line-girder or 2D-grid. *TAEG* is not a general structural analysis software and was specifically developed for calculating the torsional response of I-girders (Roddis and Kulseth 2005). The top and bottom flange stresses from maximum dead load moments need to be calculated and entered as an input to TAEG. Ashiquzzaman et al. (2017) investigated *TAEG* for evaluating skew effects. Exterior girder rotations were compared to eccentric bracket loads

obtained by *TAEG* and 3D FEA. The rotations were significantly different for an 80 feet long simple-span bridge with a skew angle of 30°. For this reason, the *RLOA Selection Tool for Steel I-girder Bridges* recommends *TAEG* only for straight and slightly skewed bridges (i.e., $I_S < 0.30$). To perform warping analysis of other bridge geometries (i.e. high skew, curved, or curved and skew bridges), *UT Bridge* is suitable. Although *UT Bridge* does not include an input field for defining overhang brackets, the torsion applied on an exterior girder can be resolved into a force couple acting on the top and bottom flanges, as shown earlier in Chapter 2, Figure 2-48. Then, these forces can be applied to the cross-section nodes also as shown earlier in Figure 2-41a.

The deck profile from overhang bracket rotation and exterior girder web out-of-plane deformation can be calculated using the analytical procedure presented in Section 2.7.5.2. The procedure is based on the small deformation theory of thin plates for modeling the girder web and incorporates adjustment factors to account for the fixity provided by flanges and transverse stiffeners. The adjustment factors were developed by 3D FE analyses using 3D shell elements for modeling girder plates. Therefore, the tool is designated as 3D in the RLOA tool.

4.2.2.4 Phased Construction Analysis

The analysis cases listed in the *RLOA Selection Tool for Steel I-girder Bridges* are *(i)* capacity of the in-service structure, *(ii)* misalignment between phases due to differential deflection, foundation settlement, or a combination thereof, *(iii)* cross-sectional twist of each phase, and *(iv)* global lateral torsional buckling capacity of multi-girder systems.

The capacity of the in-service structure needs to be evaluated by load rating. This analysis is performed by imposing the state-specific legal truck loads and accounting for the current condition of structural elements. For calculating the capacity of the in-service structure, the *RLOA Selection Tool for Steel I-girder Bridges* suggests the use of *MDOT Load Rating Procedures*.

In phased construction, by definition, one of the phases remain in service prior to pouring the closure joint. Thus, calculation of elevation difference between phases due to differential deflection requires at least the analysis of the two phases under service loads and under-construction under dead loads. Methods and models for the analysis of in-service structure under service loads and differential foundation settlement to determine the elevation difference between phases is not within the scope of this project.

A cross-sectional twist from unequal overhang widths between the phases, eccentric construction loads, or a combination needs to be evaluated. Such cases require a system-level analysis accounting for the contribution of girders and cross-frames to the overall system stiffness and load transfer path. Also, modeling should be capable of defining the depth of structural elements, such as the location of the girder or girder system shear center relative to the center of gravity of girders or the system. The inability of 1D and 2D analysis methods for evaluating the torsion-governed cases discussed in Section 4.2.2.2 is equally applicable to the analysis of cross-sectional twisting of phases. Because of these reasons, regardless of the bridge geometry, the *RLOA Selection Tool for Steel I-girder Bridges* suggests 3D modeling. Consequently, *UT Bridge* is recommended as the analysis tool.

Global lateral torsional buckling (LTB) is often a concern where limited numbers of I-girder assemblages are used to widen the existing superstructure. Global LTB capacity of straight narrow I-girder bridge assemblages that comply with the conditions stated in Section 2.8.3, can be calculated using AASHTO (2017a) Eq. 6.10.3.4.2-1. I-girder systems with curvature, skew, asymmetry, or a combination thereof may have increased lateral-torsional displacements. Increased lateral-torsional displacements will reduce the elastic buckling capacity (White et al. 2012b). As per AASHTO (2017a) Article C6.10.3.4.2, these cases can be analyzed by eigenvalue or global second-order load-deflection analysis. *UT Bridge* provides this capability. The RLOA tool recommends 1D models for symmetrical straight bridges and 3D models for other bridge configurations.

4.2.3 RLOA Tool for PC I-Girder Bridges

The *RLOA Selection Tool for PC I-Girder Bridges* is another Microsoft Excel spreadsheet developed by this project. A screen image of the output window is shown in Figure 4-14. The tool lists constructability analysis cases associated with PC I-girder bridges, the RLOA recommendations, analysis tools, and supplemental tools for calculating parameters that are required as input to analysis tools.

Cases during	RLOA	Analysis Tool	Supplemental
Lifting			
Capacity against cracking and ultimate stress	1D	Lifting Analysis of PC I-Girders	Wind Load Calculation
Erection			
Time-dependent deformation of girders	N/A	MDOT BDS	
Lateral instability of girders	1D	Erection Analysis of PC I-Girders	Wind Load Calculation
Phased Construction			
Capacity of the in-service structure	N/A	MDOT Load Rating Procedures	
Elevation difference between phases due to differential deflection	N/A	N/A	
Elevation difference between phases due to foundation settlement	N/A	N/A	
Cross-sectional twist of phases	3D	N/A	

Figure 4-14. Output window of the RLOA Selection Tool for PC I-Girder Bridges

The *RLOA Selection Tool for PC I-Girder Bridges* is more compact since girder curvature and skew are not parameters.

During lifting, girder capacity against cracking and ultimate stresses need to be verified. This analysis can be performed using the procedure given in PCI (2016) and discussed in Section 2.5.6.1. PCI (2016) procedure employs a 1D line-girder model. As part of this project, a comprehensive Mathcad script was developed specifically for the MDOT inventory and practices. Mathcad script and particulars are given in Appendix I.

During an erection, time-dependent deformations and lateral stability analyses of girders are performed. For calculating time-dependent deformations MDOT uses Eq. (2-14), which is also incorporated into the MDOT Bridge Design System software (BDS). Thus, the *RLOA Selection Tool for PC I-Girder Bridges* lists MDOT BDS as the analysis tool without an RLOA recommendation. The stability analysis of PC I-girders during erection can be performed using the procedure given in PCI (2016). As discussed in Section 2.6.3.3, PCI (2016) procedures employ a 1D line-girder model. In this project, a Mathcad script is developed and presented following PCI (2016) procedures for MDOT girder sections and practices. Mathcad script is given in Appendix J. Skew angle is not considered as a parameter for stability analysis of PC girders. The skew effects are introduced by lateral load paths provided by the diaphragms. The MDOT practice requires casting (or installing) diaphragms after all the girders are placed on bearings. The stability is maintained until then with temporary bracings as needed.

For deck placement, analysis cases are not included in the RLOA tool. The analysis cases associated with deck placement of steel I-girder bridges are not considered for PC I-girder bridges for the following reasons:

- PC girders have relatively high torsional stiffness.

- End and intermediate diaphragms are placed before deck placement. Diaphragms with in-plane stiffness control out-of-plane girder deformations.

Phased construction of PC I-girder bridge analysis cases listed by the RLOA tool include *(i)* capacity evaluation of the in-service structure, *(ii)* misalignment between phases due to differential deflection, foundation settlement, or a combination thereof, and *(iii)* cross-sectional twist of phases. The phased construction cases of steel I-girder bridges presented in Section 4.2.2.4 are the same for PC girder bridges as well. Also, skew effects should be included in phased construction analyses of PC girder bridges. The MDOT skew policy given in Table 2-4 represents a guideline for such cases.

4.3   STRUCTURAL ANALYSIS TOOLS

The *RLOA Selection Tools* recommend structural analysis tools for evaluating constructability cases in a bridge project. The recommendations include *UT Lift* (Section 2.5.6.2), *UT Bridge* (Section 2.6.3.2), *TAEG* (Section 2.7.5.3), and the Mathcad scripts developed in this project. Figure 4-15 shows an output example for a straight bridge generated by the *RLOA Selection Tool for Steel Bridges*. The column "Analysis Tool" displays the primary tool recommended, whereas the column "Supplemental" includes tools either as an alternative to the primary tool or for calculating a required variable for input to the primary tool. Microsoft Excel or Mathcad (.xmcd files) analysis tools are hyperlinked to the *RLOA Selection Tool* in blue colored fonts (Figure 4-15).

Appendices C to J provide the Mathcad scripts (.xmcd files) developed as part of this project. Mathcad script descriptions include assumptions and limitations of the procedures utilized.

It should be noted that the RLOA recommendation may not always match the analysis type utilized in the recommended analysis tool. As an example, Figure 4-15 in Chapter 4 shows the RLOA as 1D for lateral torsional buckling capacity analysis of girders during erection, whereas *UT Bridge* is a 3D FEA tool. Thus, the tools listed will provide the most accurate analysis.

117

Cases during	RLOA	Analysis Tool	Supplemental
Lifting			
Capacity against flange yielding stress	1D	Top Flange Stress Analysis	UT Lift
Lateral torsional buckling capacity of girders	1D	UT Lift	
Erection			
Lateral torsional buckling capacity of girders	1D	UT Bridge	Wind Load Calculation
Deck Placement			
Unintended deck profile due to differential deflection	1D	UT Bridge	Differential Deflection Analysis
Unintended deck profile due to exterior girder warping	1D	TAEG	
Unintended deck profile due to exterior girder web out-of-plane deformatio	3D	Web Out-of-Plane Deformation Analysis	Overhang Bracket Analysis

Figure 4-15. An output example of the *RLOA Selection Tool for Steel I-Girder Bridges*

Table 4-6 summarizes the use and applicability of the structural analysis tools recommended by the *RLOA Selection Tools*.

Table 4-6. Structural Analysis Tools Recommended by the *RLOA Selection Tools*

Analysis Tool	Construction Stage	Purpose	Applicability
UT Lift (S)	Lifting	• Calculate girder rotational deformations • Evaluate lateral torsional buckling capacity of girders • Calculate beam clamping forces to be used in *Top Flange Stress Analysis.xmcd*	Straight and Curved Girders
Top Flange Stress Analysis.xmcd (S)	Lifting	• Evaluate capacity against top flange yielding stresses due to beam clamping forces	Straight and Curved Girders
PC Girder Lifting Analysis.xmcd (PC)	Lifting	• Evaluate capacity of girders against cracking and ultimate stress	Straight Girders
PC Girder Erection Analysis.xmcd (PC)	Erection	• Evaluate capacity of girders against lateral instability	Straight Girders
UT Bridge (S)	Erection, Deck Placement, and Phased Construction	• Calculate girder twisting deformations (erection) • Evaluate lateral torsional buckling capacity of girders (erection) • Calculate variation in deck profile due to differential girder deflection (deck placement) • Calculate variation in deck profile due to exterior girder warping (deck placement) • Calculate cross-sectional twist of phases (phased construction) • Evaluate capacity of multi-girder systems against global lateral torsional buckling (phased construction)	Straight, Curved, Skewed, and Curved and Skewed Bridges
TAEG (S)	Deck Placement	• Calculate variation in deck profile due to exterior girder warping	Straight and Slightly Skewed Bridges
Differential Deflection Analysis.xmcd (S)	Deck Placement	• Calculate variation in deck profile due to differential girder deflection	Straight and Skewed Bridges
Web Out-of-Plane Deformation Analysis.xmcd (S)	Deck Placement	• Calculate variation in deck profile due to exterior girder web out-of-plane deformation	Straight and Curved Girders
Overhang Bracket Analysis.xmcd (S)	Deck Placement	• Calculate horizontal component of bracket diagonal leg axial force acting on exterior girder web to be used in *Web Out-of-Plane Deformation Analysis.xmcd* • Calculate force couple acting on top and bottom flanges to be used in *UT Bridge*	Straight and Curved Girders
Wind Load Calculation.xmcd (PC&S)	Lifting and Erection	• Calculate wind loads acting on girders to be used in *UT Bridge, PC Girder Lifting Analysis.xmcd,* and *PC Girder Erection Analysis.xmcd*	Straight and Curved Girders
Global LTB Analysis.xmcd (S)	Phased Construction	• Evaluate global lateral torsional buckling capacity of multi-girder systems	Straight Bridges

S – Steel girder bridge

PC – Prestressed concrete girder bridge

5 CHECKLISTS FOR INSPECTORS

Checklists for inspectors were developed for the evaluation of the constructability of prestressed concrete and steel I-girder bridges. An additional checklist is suggested to document comments and observations during the post-construction review. Figure 5-1, Figure 5-3, and Figure 5-5 show the suggested layout and content of the checklists. Figure 5-2 and Figure 5-4 show the supplementary information included with the inspector checklists. These checklists are formatted to be suitable for adoption by MDOT simply by assigning form numbers. Hence, these formatted copies are included in Appendix K. The first two checklists are to be completed during a visual inspection with the use of limited tools.

The checklists were developed based on the constructability cases listed in Figure 2-1. Hence, Section 5.1 and 5.2 provide a brief overview, the rationale behind the checklist, and the relationship to the constructability cases listed in Figure 2-1.

Michigan Department Of
Transportation
Form **** (2020)

CONTROL SECTION, JOB NUMBER

CONSTRUCTABILITY CHECKLIST FOR INSPECTORS
PRESTRESSED CONCRETE BRIDGES

PROJECT DESCRIPTION:

☐ Girders are supported during storage as per the plans.

☐ Girders are lifted using lifting loops. Otherwise, MDOT Engineer is consulted.

☐ Structural Fabrication Unit is consulted if cracks greater than 0.006 in. develop during storage and lifting.

☐ Girders and bearing pads are in full contact. Bearing surface flatness tolerance is met (0.125 in. per 12 in.).

☐ Girders are properly braced using hold-downs in their final position.

☐ Girders meet dimensional tolerances given in **Table 1** as girder sweep, the differential camber of adjacent box beams, etc.

☐ Strands exposed on the top flanges are cut before deck placement.

☐ Girder spacing is as intended prior to placing of the diaphragms and deck slab.

Figure 5-1. Constructability checklist for inspectors – prestressed concrete bridges

CONTROL SECTION, JOB NUMBER

CONSTRUCTABILITY CHECKLIST FOR INSPECTORS
PRESTRESSED CONCRETE BRIDGES (SUPPLEMENTARY)

Table 1 Dimensional Tolerances for Concrete Beams

Beam Type	Tolerance
Length of I-Beams and 1800 Beams	±¼ in/25 ft, 1 in max
Length of Box Beams	±¾ in
Width of I-Beams and 1800 Beams	+½ in, -⅛ in
Width of Box Beams	±½ in
Height of I-Beams, 1800 Beams, or Box Beams	+¼ in, -⅛ in
Camber Deviation From Design Value (Measured Within 24 h of Strand Release)	⅛ in/10 ft
Thickness of Top Slab of Box Beam	+½ in, -¼ in
Length of I-Beam End Blocks	+2 ft, -0 in
Sweep of I-Beams and 1800 Beams (Horizontal Deviation of Centerline from a Straight Line Between Ends Measured at Both Top and bottom)	¼ in/10 ft
Sweep of Box Beams (Horizontal Deviation of Centerline from a Straight Line Between Ends Measured at Both Top and Bottom)	⅜ in up to 60 ft, ½ in over 60 ft
Vertical Deviation of Side Forms Between Top and Bottom of Beam	≤¼ in from plan location
Prestress Strand	≤¼ in from plan location
Location of Conduit for Transverse Post Tensioning	≤½ in from plan location
Location of Holes for Position Dowels (I-beams and 1800 Beams)	≤½ in from plan location
Location of Holes for Position Dowels Box Beams	≤1 in from plan location

Figure 5-2. Constructability checklist for inspectors – PC bridges (supplementary)

CONTROL SECTION, JOB NUMBER

CONSTRUCTABILITY CHECKLIST FOR INSPECTORS
STEEL I-GIRDER BRIDGES

PROJECT DESCRIPTION: _____

_____

_____

☐ Girders are lifted near quarter points.

☐ Girders are erected per the fabrication detailing. Recommended fit conditions are provided in **Table 1**.

☐ Sufficient horizontal stabilization is provided by bolting girders to substructure units, installing cross-frames as the erection progresses, placing falsework, or a combination thereof.

☐ The maximum deviation from the theoretical horizontal alignment in a span does <u>not</u> exceed ± 0.125 in. × (total length along girder between supports (ft) / 10).

☐ The maximum deviation from the theoretical vertical alignment in a span does <u>not</u> exceed + 0.25 in. × (total length from the nearest support (ft) / 10).

☐ The overhang bracket-bearing point is located close to the exterior girder bottom flange (≥ 0.9D measured from the bottom of the top flange).

☐ Wet depth measurements meet deck finish tolerances (0.125 in. per 10 ft).

Figure 5-3. Constructability checklist for inspectors – steel I-girder bridges

Bridge Structural Analyses for Staged Construction and Constructability Reviews

CONSTRUCTABILITY CHECKLIST FOR INSPECTORS
STEEL I-GIRDER BRIDGES (SUPPLEMENTARY)

Table 1 Recommended Fit Conditions for Steel I-Girder Bridges

L/R*	Skew (θ) and Skew Index (I_S)	Span Length	Recommended Fit Condition
≤ 0.03	θ ≤ 20°	N/A	NLF & SDLF &TDLF
	θ > 20° & I_S ≤ 0.30	N/A	SDLF & TDLF
	θ > 20° & I_S > 0.30	≤ 200 ft	SDLF & TDLF
		> 200 ft	SDLF
> 0.03	N/A	N/A	NLF & SDLF

* Maximum L/R of any span in the bridge

Notations:

I_S = Skew index = $\dfrac{w_g \tan\theta}{L}$

L = Span length (ft)

w_g = Bridge width measured between exterior girder centerlines (ft)

NLF = No Load Fit

R = Radius of curvature (ft)

SDLF = Steel Dead Load Fit

TDLF = Total Dead Load Fit

θ = Skew angle (deg)

Definitions:

NLF = Cross-frames or diaphragms are detailed to fit to the girders in their fabricated, plumb, fully cambered position under <u>zero dead load</u>.

SDLF = Cross-frames or diaphragms are detailed to fit to the girders in their ideally plum as-deflected positions under <u>the self-weight of the steel</u> at the completion of the erection.

TDLF = Cross-frames or diaphragms are detailed to fit to the girders in their ideally plumb as-deflected positions under <u>the total dead load</u>. The total dead load typically includes the weight of the concrete deck, but not the weight of any superimposed dead loads.

Figure 5-4. Constructability checklist for inspectors – steel I-girder bridges (supplementary)

CONTROL SECTION, JOB NUMBER

POST-CONSTRUCTION REVIEW FORM FOR INSPECTORS

PROJECT DESCRIPTION: _____

_____

_____

☐ Construction plan is reviewed.
Describe anticipated difficulties, if any:

_____

_____

_____

_____

☐ MDOT Engineer is consulted for the contractor change requests.
Describe the change requests:

_____

_____

_____

_____

☐ The bridge is constructed as per the approved construction plans.
If not, describe the changes and associated reasons:

_____

_____

_____

_____

Figure 5-5. Constructability checklist for inspectors – post-construction review

5.1   CONSTRUCTABILITY CHECKLIST FOR PC I-GIRDER BRIDGES

The checklist items are numbered from *a* to *h* as shown below. A brief description is provided with each item. Table 5-1 shows the relationship between the constructability cases listed in Figure 2-1 and the constructability checklist for prestressed concrete bridges. As shown in the table, the checklist includes at least one item to address the constructability cases associated with PC girder bridges.

a. **Girders are supported during storage as per the plans.**

Girder stress analysis at release uses the support conditions given in the approved construction plans. Also, as discussed in Section 2.6.1.1, there is a potential for excessive and/or differential camber during erection when girders are not stored as specified.

b. **Girders are lifted using lifting loops. Otherwise, MDOT Engineer is consulted.**

As per the MDOT Bridge Design Guide (MDOT 2019b), PC girders shall be lifted using lifting loops; the use of other means to lift the PC girders could violate the analysis and design assumptions. As an example, lifting analysis is performed assuming a zero distance between the lifting device rigid extension and the girder top, which may not be the case if other lifting devices are used.

c. **Structural Fabrication Unit is consulted if cracks greater than 0.006 in. develop during storage and lifting.**

The given tolerance from the MDOT Wiki E-Construction Section 708 represents the maximum allowable structural crack size. If the allowable limit is exceeded, the cause and structural impact of such cracking need to be evaluated.

d. **Girders and bearing pads are in full contact. Bearing surface flatness tolerance is met (0.125 in. per 12 in.).**

Erection and deck placement analyses use idealized support conditions assuming that bearing and girder surfaces are in full contact. Also, the eccentricity between the girder center of gravity and reaction forces causes an overturning moment that could be a concern for girder stability. The given MDOT tolerance warrants idealized support conditions.

e. **Girders are properly braced using hold-downs in their final position.**

Roll instability of PC girders due to sweep, wind load, or a combination thereof is prevented with temporary end and intermediate bracings. Hold-downs should consist of

compression and tension members to resist the lateral load effects. See Section 2.6.2.1 for more details on the bracings.

f. Girders meet dimensional tolerances given in Table 1 as girder sweep, the differential camber of adjacent box beams, etc.

The given MDOT tolerances assure retaining vertical and horizontal alignment during erection. Table 1 referenced in the checklist is shown in Figure 5-2.

g. Strands exposed on the top flanges are cut before deck placement.

PC girders may include cut strands at the top for controlling girder end stresses at release and/or during shipping and handling. These strands are expected to be cut before placing the deck. This checklist item is included as a reminder that the strands are cut as detailed in the plans.

h. Girder spacing is as intended prior to placing of the diaphragms and deck slab.

Achieving intended girder spacing is one of the expectations in retaining lateral deformation tolerances and horizontal structural alignment. Further, achieving intended girder spacing will alleviate challenges during the installation of intermediate diaphragms. This is also applicable to phased construction cases.

Table 5-1. Constructability Cases for PC I-Girder Bridges and Relevant Checklist Items

Activity	Constructability Cases for PC Bridges	Checklist Item
Transportation and Lifting	Capacity against Cracking and Ultimate Stress	a, b, c
Erection	Vertical and/or Horizontal Misalignment: Time-dependent Deformation of Girders	a, f, g, h
Erection	Lateral Instability of Girders: Impact of Girder Fabrication Tolerances	d, e
Erection	Lateral Instability of Girders: Impact of Wind Loading	d, e
Phased Construction	Capacity of the In-service Structure	-
Phased Construction	Vertical and/or Horizontal Misalignment of Phases: Twist of Bridge Cross-Section	f, h
Phased Construction	Vertical and/or Horizontal Misalignment of Phases: Foundation Settlement	h

Bridge Structural Analyses for Staged Construction and Constructability Reviews

5.2 CONSTRUCTABILITY CHECKLIST FOR STEEL I-GIRDER BRIDGES

The checklist items are numbered from a to g as shown below. A brief description is provided for each item. Table 5-2 shows the relationship between the constructability cases listed in Figure 2-1 and the constructability checklist items for steel I-girder bridges. As shown in the table, the checklist includes items to address the constructability cases associated with steel I- girder bridges.

a. **Girders are lifted near quarter points.**

   Lifting steel I-girders in the vicinity of quarter points maximizes lateral torsional buckling capacity. See Section 0 for more details about the lateral torsional buckling capacity calculation.

b. **Girders are erected per the fabrication detailing. Recommended fit conditions are provided in Table 1.**

   The recommended fit conditions are given in Table 1 to help meeting deformation tolerances and structural alignment. Table 1 referenced in the checklist is shown in Figure 5-4. Section 2.6.1.2 defines fit conditions.

c. **Sufficient horizontal stabilization is provided by bolting girders to substructure units, installing cross-frames as the erection progresses, placing falsework, or a combination thereof.**

   Lateral instability due to girder curvature, long unbraced length, wind load, or a combination thereof is prevented by employing permanent and/or temporary bracings and support systems. See Section 2.6.2.1 for more details on the bracings.

d. **The maximum deviation from the theoretical horizontal alignment in a span does not exceed ± 0.125 in. × (total length along girder between supports (ft)/10).**

   The tolerance recommended by AASHTO/NSBA (2014b) warrants maintaining the horizontal alignment of the structure and constructing the bridge as per the project specifications. The specified tolerance applies to phased construction as well.

e. **The maximum deviation from the theoretical vertical alignment in a span does not exceed + 0.25 in. × (total length from the nearest support (ft) / 10).**

   The tolerance recommended by AASHTO/NSBA (2014b) warrants maintaining the vertical alignment of the structure and constructing the bridge as per the project specifications. The specified tolerance applies to phased construction as well.

f. The overhang bracket-bearing point is located close to the exterior girder bottom flange (≥ 0.9D measured from the bottom of the top flange).

Locating bracket-bearing points within the recommended range eliminates the web out-of-plane deformation and the resulting bracket rotation. Web depth is defined as D. Sections 2.7.2 and 2.7.5.2 describe the impact of web out-of-plane deformation on the cast-in-place deck profile, calculation procedures to quantify the deformations, and potential methods for controlling web out-of-plane deformation.

g. Wet depth measurements meet deck finish tolerances (0.125 in. per 10 ft).
This checklist item is to assure that the variation in deck profile due to differential girder deflection, exterior girder warping, web out-of-plane deformation, or a combination thereof is maintained within the MDOT specified tolerance.

Table 5-2. Constructability Cases for Steel I-Girder Bridges and Relevant Checklist Items

Activity	Constructability Cases for Steel I-Girder Bridges	Checklist Item
Transportation and Lifting	Capacity against Flange Bending Stress	-
Transportation and Lifting	Rotational Behavior: Cross-Sectional Twist	-
Transportation and Lifting	Rotational Behavior: Rigid-body Rotation	-
Transportation and Lifting	LTB Capacity of Girders	a
Erection	Vertical and/or Horizontal Misalignment: Girder Twist and Detailing	b, c, d, e
Erection	Lateral Instability of Girders: Impact of Girder Geometry	c
Erection	Lateral Instability of Girders: Impact of Wind Loading	c
Erection	Lateral Instability of Girders: Impact of Long Unbraced Length	c
Deck Placement	Differential Girder Deflection	g
Deck Placement	Exterior Girder Web Out-of-plane Deformation	f, g
Deck Placement	Warping of Exterior Girder	g
Phased Construction	Capacity of the In-service Structure	-
Phased Construction	Vertical and/or Horizontal Misalignment of Phases: Twist of Bridge Cross-Section	c, d, e
Phased Construction	Vertical and/or Horizontal Misalignment of Phases: Foundation Settlement	d, e
Phased Construction	Global LTB Capacity of Multi-Girder Systems	-

6   SUMMARY AND IMPLEMENTATION RECOMMENDATIONS

6.1   SUMMARY

During the design of highway bridges, constructability requirements need to be addressed. Whereas, the typical bridge design practice is to consider the limit state stresses in structural elements of a structure that is completed as per the project specifications. Analysis of construction stages is the contractor's ("the Contractor") responsibility since the means and methods for construction are based on their experience and available equipment. Nevertheless, the agency engineer ("the Engineer") needs to review and approve the contractor submittals. A lack of detailed response evaluation of structural elements and systems during construction by both parties may lead to: rejection by MDOT, change requests by the contractor, construction delays, and sometimes, to safety issues. Also, the Contractor selects qualified suppliers to provide materials and structural elements for the bridge. The Quality Assurance Inspector (QAI) conducts quality assurance (QA) verification inspection, and nonconformance identified during an inspection could affect project schedule, constructability, capacity, and durability of the structure. Subsequently, there is a need to develop a framework that encompasses PC girder nonconformance issues, constructability analysis cases during every stage of construction, as well as guidelines and tools for performing required calculations and inspections.

This project was organized into seven tasks: (1) review of literature and state-of-the-art practices, (2) collect input from MDOT Design, Field Services, and Construction staff and the review of typical MDOT bridge project plans and construction methods, (3) develop PC beam performance assessment guidelines and procedures, (4) identify common design and construction review scenarios that require documented guidelines, (5) develop frameworks to address the common scenarios and the Mathcad scripts, (6) develop standalone constructability review and staged construction design guidelines, and (7) produce final research deliverables.

A comprehensive literature review was conducted to document the constructability cases associated with capacity, deformation, stability, and durability of superstructure elements. These cases were grouped under each construction activity and discussed for production and manufacturing, transportation and lifting, erection, and deck placement stages. Also, phased construction scenarios and the associated constructability cases were documented. The design and construction best practices implemented by state highway agencies were also documented. Available methods and tools for analyzing the identified constructability cases including the

129

associated capabilities, assumptions, and limitation were discussed. Later, the documented cases were discussed with the MDOT Research Advisory Panel (RAP). The documented cases and additional cases recommended by the RAP were incorporated to develop a constructability framework for prestressed concrete (PC) and steel (S) girder bridges. Together with the first and second tasks, the MDOT involvement warranted the success of this project and completion of the fourth task, which was to identify common design and construction review scenarios that need documented guidelines.

The PC beams are manufactured and produced under stringent quality control requirements. The final decision regarding beams with deficiencies is at the Engineer's discretion. As a fulfilment of the third task, an excel spreadsheet (*Quality Assurance Load Testing.xlsx*) was developed evaluate PC beam capacity against the stress limits defined in the AASHTO LRFD (2017), identify the controlling flexural failure mode, and calculate the force magnitude required for load testing using either a 3-point or 4-point loading configuration.

The fifth and sixth tasks were to identify the common constructability cases and develop constructability review and design guidelines. Microsoft Excel spreadsheets with embedded VBA codes and Mathcad analysis scripts for engineers were developed. Two constructability checklists for inspectors and a post-construction review form were developed.

The *Constructability Analysis Cases Form*, a spreadsheet with embedded VBA codes, was developed to identify the constructability cases based on the bridge type, bridge geometry, and the construction type. The *Constructability Required Level of Analysis (RLOA) Selection Tools*, also a spreadsheet with embedded VBA codes, was developed to identify the required level of analysis (1D, 2D, or 3D) for evaluating the cases in the *Constructability Analysis Cases Form*. Eight Mathcad scripts were developed and linked to the *Constructability Required Level of Analysis (RLOA) Selection Tools*. These tools provide a platform to assure the constructability of a bridge through a collective effort of the engineer, contractor, and inspector. The Mathcad scripts are included in the appendices. All the digital copies of spreadsheets and Mathcad scripts were submitted to MDOT as part of the project deliverables.

6.2   IMPLEMENTATION RECOMMENDATIONS

MDOT Bridge Design Manual (BDM) Section 2.05 describes the bridge design quality assurance and quality control (QA/QC) procedures employed by MDOT to ensure that the bridge design final contract documents are prepared with no errors and omissions. The *Structural Precast Concrete QAI Manual* describes the QA/QC process of precast concrete members.   The tools and recommendations developed in this project can be seamlessly integrated into these procedures to achieve the QA/QC program objectives.

1) Employ the *Quality Assurance Load Testing* spreadsheet with data to check for PC beam capacity against the stress limits defined in the AASHTO LRFD (2017), identify the critical flexural failure mode, and (iii) calculate the force magnitude required for load testing using either a 3-point or 4-point loading configuration. This spreadsheet can be integrated into PC beam QA process for checking the failure mode and load capacity of PC beams with major nonconformance.

2) As per BDM Section 2.05.03A., "the Designers, Checkers, and Reviewers are key personnel providing well-designed, accurate, and constructible plans for use in the construction of bridges." The Designers, Checkers, and Reviewers can use the *Constructability Analysis Cases Form* to identify analysis cases that need to be considered during PC I- and steel I-girder bridge construction. These cases are listed under lifting, erection, deck placement and phased construction. The design, checking, and review processes can be standardized using this form.

3) BDM Section 2.05.03C5 indicates that the Designers and Checkers face significant challenges due to the complexity of the software programs used for bridge structural analysis and design. Also, Checkers and Reviewers are challenged with the content and formats of submittals for review. Such challenges can be managed by providing (i) direction on the Required Level of Analysis (RLOA) and (ii) tools for independent verification of submitted calculations. The *Constructability Required Level of Analysis (RLOA) Selection Tools* and Mathcad scripts developed during this project will serve that purpose. Also, MDOT can expect bridge design consultants to comply with the required level of analysis guidelines. For this purpose, MDOT can provide access to the *Constructability Required Level of Analysis (RLOA) Selection Tools*.

4) According to BDM Section 2.05.03D6, Program Level Quality Assurance (PLQA) is performed by the Bridge Design Supervising Engineer (BDSE). The objective of performing

131

PLQA is "to promote consistency and uniformity between MDOT working units and between MDOT in-house and consultant designers." The *Constructability Analysis Cases Form* is such a tool to promote consistency in constructability related calculations and organization of the submittals.

5) Two constructability checklists were developed for inspectors. BDM Section 2.02.18 describes the process for the final constructability review. These two lists can be linked to BDM Section 2.02.18 to ensure that items are addressed in the plans and adequate descriptions and associated notes are provided. Also, MDOT Form 5616 *Pre and Post Pour Inspection Checklist* can be updated using items in *Constructability Checklist for Inspectors - Prestressed Concrete Bridges* provided in Appendix K. The checklist for prestressed concrete bridges can be linked to the Wiki E-Construction Section 708. The checklist for steel I-girder bridges can be linked to Wiki E-Construction Section 707. Additionally, checklist items related to structural stability can be incorporated into the construction staging section of the Form 1960.

6) BDM Section 2.04.04 indicates the need for documenting project history. The *Constructability Checklist for Inspectors - Post-Construction Review* form in Appendix K can be used to document the errors/omissions in the plans, contractor change requests, and any nonconformities with the approved construction plans. The compilation of such information helps to convert tacit knowledge into explicit knowledge that can be used to enhance the QA/QC program outcome.

The deliverables of this project can be implemented as describe below to identify and evaluate (i) the capacity and failure mode of a beam with major nonconformance and (ii) potential constructability cases as a result of the contractor-proposed means and methods and change requests:

1) Employ the *Quality Assurance Load Testing* spreadsheet with data to identify the failure mode of the beam with major nonconformance and to calculate the load magnitude required to reach the design stress limits during load testing.

2) Employ the *Constructability Analysis Cases Form* with data to identify the potential constructability cases that require analysis and development of design details. The output of this form can evaluate the need for additional analysis and check if contractor submittals

include necessary calculations for all the required analysis and design. The input data required for this form is the bridge type, bridge geometry, and the construction type.

3) Employ the *Required Level of Analysis (RLOA) Selection Tools* to suggest the required level of analysis (i.e., 1D, 2D, or 3D) for analyzing the cases from the *Constructability Analysis Cases Form* output. This tool helps evaluate the models and tools used by the contractor in representing the stress state of structural elements included in the analysis.

4) Employ the *Required Level of Analysis (RLOA) Selection Tools* to access structural analysis tools for verifying the calculations given in contractor submittals.

7 REFERENCES

AASHTO. (2000). *Constructability Review Best Practices Guide,* American Association of State Highway and Transportation Officials (AASHTO) Subcommittee on Construction, Washington, DC.

AASHTO. (2017a). *LRFD Bridge Design Specifications*, Customary U.S. Units, 8th Ed., American Association of State Highway and Transportation Officials, Washington, DC.

AASHTO. (2017b). *Guide Design Specifications for Bridge Temporary Works,* 2nd Ed., American Association of State Highway and Transportation Officials, Washington, DC.

AASHTO. (2017c). *Guide Specifications for Wind Loads on Bridges during Construction,* 1st Ed., American Association of State Highway and Transportation Officials, Washington, DC.

AASHTO/NSBA. (2014a). *G13.1 Guidelines for Steel Girder Bridge Analysis*, 2nd Ed., American Association of State Highway and Transportation Officials/National Steel Bridge Alliance Steel Bridge Collaboration, Washington, DC.

AASHTO/NSBA. (2014b). *S10.1 Steel Bridge Erection Guide Specification*, American Association of State Highway and Transportation Officials/National Steel Bridge Alliance Steel Bridge Collaboration, Washington, DC.

AASHTO/NSBA. (2016). *G12.1 Guidelines to Design for Constructability,* American Association of State Highway and Transportation Officials/National Steel Bridge Alliance Steel Bridge Collaboration, Washington, DC.

AISC. (2003). *Design Guide 9: Torsional Analysis of Structural Steel Members,* 2nd Ed., American Institute of Steel Construction, Chicago, Illinois.

Aktan, H. and Attanayake, U. (2013). *Improving Bridges with Prefabricated Precast Concrete Systems,* MDOT RC-1602, the Michigan Department of Transportation, Lansing, Michigan.

AREMA. (2015). *AREMA Manual for Railway Engineering,* the American Railway Engineering and Maintenance-of-Way Association, Lanham, Maryland, 20706.

Ashiquzzaman, M., Schmeltz, J., Ibrahim, A., Lindquist, W., and Hindi, R. (2017). "Assessment of the Rotation of Exterior Bridge Girders Due to Construction Loading Using TAEG Software", Modern Civil and Structural Engineering, Vol. 1, No. 1, October.

Attanayake, U., and Aktan, H. (2011). "Capacity evaluation of a severely distressed and deteriorated 50-year-old box beam with limited data", J. Perform. Const. Facil., 25(4), 299-308.

Attanayake, U. (2013). "Simulation and Measurement of Web Gap Strain in a Steel Girder for Developing a SHM System – A Laboratory Study," the 4th International Conference on Structural Engineering and Construction Management 2013, December 13-15.

Attanayake, U. B., and Aktan, H. (2019). "Non-contact Measurement of Bridge Load Response using He-Ne Modulated Lasers," BEENG-S-18-00319, ASCE Journal of Bridge Engineering, Special Online Collection of Non-contact Sensing Technologies for Bridge Structural Health Assessment, Vol. 24, Issue 11, November.

BA 86. (2006). Volume 3 Highway Structures – Inspection and Maintenance, Design Manual for Roads and Bridges, the Highways Agency, UK.

Bruciati, B., Jang, S., and Fils, P. (2019). "RFID-Based Crack Detection of Ultra High-Performance Concrete Retrofitted Beams," Sensors, 19, 1573; doi:10.3390/s19071573.

CALTRANS. (2006). *PS&E Constructability Review Checklist,* the California Department of Transportation, Sacramento, California.

CALTRANS. (2010). *Memo to Designers 9-3: Widening Existing Bridges,* the California Department of Transportation, Sacramento, California.

ConnDOT. (2011). *Design/Constructability Plan Review Guidelines,* the Connecticut Department of Transportation, Newington, Connecticut.

Consolazio, G. and Edwards, S. (2014). *Determination of Brace Forces Caused by Construction Loads and Wind Loads During Bridge Construction*, the Florida Department of Transportation, Tallahassee, Florida.

Farris, J. F. (2008). *Behavior of Horizontally Curved Steel I-Girders During Construction*, Master's Thesis, the University of Texas at Austin, Austin, Texas.

FDOT. (2013). *Design Standards,* the Florida Department of Transportation, Tallahassee, Florida.

FDOT. (2018a). *Construction Project Administration Manual,* the Florida Department of Transportation, Tallahassee, Florida.

FDOT. (2018b). *Standard Specifications for Road and Bridge Construction,* the Florida Department of Transportation, Tallahassee, Florida.

FDOT. (2018c). *Structures Design Guidelines* the Florida Department of Transportation, Tallahassee, Florida.

FHWA. (2012). *Steel Bridge Design Handbook – Stringer Bridges: Making the Right Choices,* the Federal Highway Administration, Washington, DC.

FHWA. (2015). *Engineering for Structural Stability in Bridge Construction,* the National Highway Institute (NHI) Course Number 130102 Reference Manual, Federal Highway Administration, Washington, DC.

Fiechtl, A. L., Fenves, G. L. and Frank, K. H. (1987). *Approximate Analysis of Horizontally Curved Girder Bridges*, Center for Transportation Research, the University of Texas at Austin, Austin, Texas.

Fisher, S.T (2006). *Development of a Simplified Procedure to Predict Dead Load Deflections of Skewed and Non-Skewed Steel Plate Girder Bridges*, Master's Thesis, Civil Engineering, North Carolina State University, Raleigh, North Carolina.

GEOKON. (2020). https://www.geokon.com/Displacement-Transducers (Last accessed: April 22, 2020).

HCI. (2014). Design Technical Manual, Helical Concepts, Inc., 710 Cooper Drive, P.O. Box 1238, Wylie, TX 75098. http://www.helicalpier.com/engineering/ (Last accessed: April 22, 2020).

Honarvar, E., Nervig, J., He, W., Rouse, J. and Sritharan, S. (2015). *Improving the Accuracy of Camber Predictions for Precast Pretensioned Concrete Beams*, Bridge Engineering Center, Iowa State University, Ames, Iowa.

Idaho DOT. (2011). *Constructability Review Guidelines,* the Idaho Department of Transportation, Boise, Idaho.

Idaho DOT. (2017). *LRFD Bridge Design Manual,* the Idaho Department of Transportation, Boise, Idaho.

IDOT. (2016). *Standard Specifications for Road and Bridge Construction,* the Illinois Department of Transportation, Springfield, Illinois.

Imper, R. and Laszlo, G. (1987). "Handling and Shipping of Long Span Bridge Beams", Precast/Prestressed Concrete Institute, PCI Journal, V.32, No.6, 86-101, Chicago, IL.

Inceefe, A. N. (2018). *Maintaining Deck Profile in Steel I-Girder Bridges during Deck Placement*, Master's Thesis, Department of Civil and Construction Engineering, Western Michigan University, Kalamazoo, Michigan.

INDOT. (2010). *Constructability Guide Book,* the Indiana Department of Transportation, Indianapolis, Indiana.

INDOT. (2013). *Design Manual*, the Indiana Department of Transportation, Indianapolis, Indiana.

Iowa DOT. (2019). *LRFD Bridge Design Manual*, the Iowa Department of Transportation-Office of Bridges and Structures, Ames, Iowa.

KDOT. (2016). *Design Manual Volume III-Bridge Section,* the Kansas Department of Transportation, Topeka, Kansas.

Libby, J. R. (1977). *Modern Prestressed Concrete: Design Principles and Construction Methods*, 2nd Ed., Van Nostrand Reinhold Company, New York City, New York.

Louisiana DOT. (2019). *Bridge Design and Evaluation Manual Chapter 6-Design Policy for Bridge Rehabilitation/Repair Projects*, the Louisiana Department of Transportation & Development, Baton Rouge, Louisiana.

Mast, R.F. (1989). "Lateral Stability of Long Prestressed Concrete Beams - Part 1." Precast/Prestressed Concrete Institute, PCI Journal, V.34, No.1, 34-53, Chicago, IL.

Mast, R.F. (1993). "Lateral Stability of Long Prestressed Concrete Beams - Part 2", Precast/Prestressed Concrete Institute, PCI Journal, V.38, No.1, 70-88, Chicago, IL.

McPheron, D., McCullouch, B., and Bowman, M. (2012). *Structural Impact of Construction Loads,* Joint Transportation Research Program, Purdue University, West Lafayette, Indiana.

MDOT. (2009). *Form 1961 – Checklist for Constructability Review Early Project Scoping,* the Michigan Department of Transportation, Lansing, Michigan.

MDOT. (2010). *Form 1960 – Checklist for Constructability Review Project Development Phase,* the Michigan Department of Transportation, Lansing, Michigan.

MDOT. (2012). *Standard Specification for Construction*, the Michigan Department of Transportation, Lansing, Michigan.
https://mdotcf.state.mi.us/public/specbook/2012/main.cfm (Last accessed: March 07, 2020).

MDOT. (2017). *Bridge Deck Construction Inspection Checklist 0395,* the Michigan Department of Transportation, Lansing, Michigan.

MDOT. (2018). *Materials Quality Assurance Procedures Manual (MQAP)*, the Michigan Department of Transportation, Lansing, Michigan.
https://www.michigan.gov/mdot/0,4616,7-151-9622_11044_11367-207980--,00.html (Last accessed: March 07, 2020).

MDOT. (2019a). *Bridge Design Manual,* the Michigan Department of Transportation, Lansing, Michigan.

Bridge Structural Analyses for Staged Construction and Constructability Reviews

MDOT. (2019b). *Bridge Design Guides,* the Michigan Department of Transportation, Lansing, Michigan.

MDOT. (2019c). *Materials Source Guide*, the Michigan Department of Transportation, Lansing, Michigan. https://www.michigan.gov/mdot/0,4616,7-151-9622_11044_11367_68095---,00.html (Last accessed: March 07, 2020).

MDOT. (2019d). *Special Provision for Quality Control and Acceptance of Structural Precast Concrete*, 12SP-708C-02, the Michigan Department of Transportation, Lansing, Michigan. https://mdotcf.state.mi.us/public/dessssp/spss_source/12SP-708C-02.pdf (Last accessed: March 07, 2020).

MDOT. (2019e). *Structural Precast Concrete QAI Manual,* 2019 Interim, Structural Fabrication Unit, Bureau of Bridges and Structures, the Michigan Department of Transportation, Lansing, Michigan.
https://www.michigan.gov/documents/mdot/Structural_Precast_Concrete_QAI_Manual_611733_7.pdf (Last accessed: March 07, 2020).

MDOT (2020a). MDOT Construction Forms, https://mdotjboss.state.mi.us/webforms/ConstrManualForms.htm (Last accessed: March 07, 2020).

MDOT. (2020b). *MDOT Supplier Qualification Standard for Prestressed Concrete Beams*, the Michigan Department of Transportation, Lansing, Michigan.

NCHRP. (2008). *Rotation Limits for Elastomeric Bearings*, NCHRP Report 596, National Cooperative Highway Research Program, Washington, D.C.

NCHRP. (2008). *Rotation Limits for Elastomeric Bearings Appendixes*, NCHRP Report 596, National Cooperative Highway Research Program, Washington, D.C.

NDI (2020). Optotrack Certus HD®: Dynamic Measuring Machine (DMM), Northern Digital Inc. https://www.ndigital.com/ (Last accessed: April 04, 2020).

NJDOT. (2016). *Capital Project Procedures – Constructability Manual,* the New Jersey Department of Transportation, Ewing Township, New Jersey.

NSBA. (2016). *Skewed and Curved Steel I-Girder Bridge Fit,* National Steel Bridge Alliance, Chicago, Illinois.

NYSDOT. (2017). *Bridge Manual,* the New York State Department of Transportation, Albany, New York.

ODOT. (2007a). *Bridge Design Manual*, the Ohio Department of Transportation, Columbus, Ohio.

ODOT. (2007b). "Deck Issues: Design Perspective."
<http://www.dot.state.oh.us/Divisions/Engineering/Structures/standard/State%20of%20practice%20for%20highly%20skewed%20bridges/skew/crossframes/Printable/Deck%20Issues-Construction%20Perspective.ppt > (June 9, 2018)

ODOT. (2016). *Construction and Material Specifications,* the Ohio Department of Transportation, Columbus, Ohio.

Oklahoma DOT. (2009). *Standard Specifications Book,* the Oklahoma Department of Transportation, Oklahoma City, Oklahoma.

PCI. (2003). *Bridge Design Manual,* 2nd Ed., the Precast/Prestressed Concrete Institute (PCI), Chicago, Illinois.

PCI. (2016). *Recommended Practice for Lateral Stability of Precast, Prestressed Concrete Bridge Girders,* 1st Ed., the Precast/Prestressed Concrete Institute (PCI), Chicago, Illinois.

PennDOT. (2010). *BC-772M – Standard Prestressed Concrete Beam Bracing Notes,* the Pennsylvania Department of Transportation, Harrisburg, Pennsylvania.

PennDOT. (2015). *Design Manual Part 4 – Structures,* the Pennsylvania Department of Transportation, Harrisburg, Pennsylvania.

Roddis, K., and Kulseth, P. (2005). *Torsional Analysis for Exterior Girders (TAEG) 2.1 – User's Manual*, Department of Civil, Environmental & Architectural Engineering, the University of Kansas, Lawrence, Kansas.

SCDOT. (2006). *Bridge Design Manual,* the South Carolina Department of Transportation, Columbia, South Carolina.

Schuh, A. C. (2008). *Behavior of Horizontally Curved Steel I-Girders during Lifting,* Master's Thesis, the University of Texas at Austin, Austin, Texas.

Spadea, S., Rossini, M., and Nanni, A. (2018). "Design analysis and experimental behavior of precast concrete double-tee girders prestressed with carbon-fiber- reinforced polymer strands", PCI Journal, V. 63, No. 1, January-February, pp. 72-84.

Stamatiadis, N., Goodrum, P., Shocklee, E., and Wang, C. (2013). *Tools for Applying Constructability Concepts to Project Development (Design) – Interim Report,* Report Number: KTC-13-15 / FRT 190-11-1F, Kentucky Transportation Cabinet, Frankfort, Kentucky.

Stith. J. C. (2010). *Predicting the Behavior of Horizontally Curved I-Girders during Construction*, Ph.D. Dissertation, the University of Texas at Austin, Austin, Texas.

Stith, J. C., Helwig, T. A., Williamson, E. B., Frank, K. H., Engelhardt, M. D., Schuh, A. C., Farris,J. F., and Petruzzi, B. J. (2013). "Behavior of Horizontally Curved I-Girders during Lifting." Journal of Structural Engineering, 139(4), 481-490.

Stuedlein, A. W. and Holtz, R. D. (2012). "Analysis of Footing Load Tests on Aggregate Pier Reinforced Clay", J. Geotech. Geoenviron. Eng., 138(9): 1091-1103.

Timoshenko, S. P., and Gere, J. M. (1961). *Theory of Elastic Stability*, 2nd Ed., McGraw-Hill Book Company Inc., New York City, New York.

TxDOT. (2015). *Standard Details for Minimum Erection and Bracing Requirements: Prestressed Concrete I-Girders and I-Beams,* the Texas Department of Transportation, Austin, Texas.

UT Lift. (2019). "*UT Lift 1.3*– a spreadsheet provided as a tool to an engineer when deciding the safety of lifting a horizontally curved steel I-girder with one crane and two lift clamps." <https://fsel.engr.utexas.edu/facilities/software/software> (Last accessed: Sept. 9, 2019).

Utah DOT. (2017*). Structures Design and Detailing Manual Chapter 16 and 17*, the Utah Department of Transportation, Salt Lake City, Utah.

VDOT. (2007). *Concurrent Engineering Constructability Review Guidelines,* the Virginia Department of Transportation, Richmond, Virginia.

White, D. W., Coletti, D., Chavel, B. W., Sanchez, A., Ozgur, C., Chong, J. M. J, Leon, R. T., Medlock, R. D., Cisneros, R. A., Galambos, T. V., Yadlosky, J. M., Gatti, W. J., and Kowatch, G. T. (2012a). *Guidelines for Analysis Methods and Construction Engineering of Curved and Skewed Steel Girder Bridges*, *NCHRP Report 725*, the National Cooperative Highway Research Program, the Transportation Research Board, Washington, DC.

White, D. W., Sanchez, A., Ozgur, C., and Chong, J. M. J. (2012b). *Evaluation of Analytical Methods for Construction Engineering of Curved and Skewed Steel Girder Bridges*, *NCHRP Report 725 Appendix C*, the National Cooperative Highway Research Program, the Transportation Research Board, Washington, DC.

Yang, S., Helwig, T., Klinger, R., Engelhardt, M., and Fasl, J. (2010). *Impact of Overhang Construction on Girder Design*, Center for Transportation Research, the University of Texas at Austin, Austin, Texas.

Yura, J., Helwig, T., Herman, R., and Zhou, C. (2008). "Global Lateral Buckling of I-Shaped Girder Systems." Journal of Structural Engineering, 134(9), 1487-1494.

ADDITIONAL REFERENCES

The American Concrete Institute (ACI). (2013). *Guide for Widening Highway Bridges*, 345.2R-13, Farmington Hills, Michigan.

Meadow Burke. (2017). "'Bridge Technical Manual" <http://meadowburke.com/techmanuals/bridge.pdf> (Last accessed: June 9, 2018)

Mohammadi, A., Yakel, A., and Azizinamini, A. (2014). *Phase and Widening Construction of Steel Bridges,* the Florida Department of Transportation, Tallahassee, Florida.

PennDOT. (2016). *BD-620M – Standard Steel Girder Bridges Lateral Bracing Criteria and Details,* the Pennsylvania Department of Transportation, Harrisburg, Pennsylvania.

Plaut, R. H. and Moen, C. D. (2013). "Analysis of Elastic, Doubly Symmetric, Horizontally Curved Beams during Lifting." Journal of Structural Engineering, 139(1), 39-46.

TxDOT. (2018). *Bridge Design Guide*, the Texas Department of Transportation, Austin, Texas.

Weyers, R. E., Prowell, B. D., Sprinkel, M. M. and Vorster, M. (1993). *Concrete Bridge Deck Protection, Repair, and Rehabilitation Relative to Reinforcement Corrosion: A Methods Application Manual,* SHRP-S-360, Strategic Highway Research Program, National Academy of Sciences, Washington, DC.

Yeoh, O. H. (1993). "Some forms of the strain energy function for rubber", Rubber Chemistry and Technology Journal, November, Vol. 66, No. 5, 754-771, Akron, Ohio.

APPENDIX A:
ABBREVIATIONS

A

AASHTO	American Association of State Highway and Transportation Officials
AISC	American Institute of Steel Construction
ASCE	American Society of Civil Engineers
ASD	Allowable Stress Design
ASP	Alternative Simplified Procedure

B

BDS	Bridge Design System
BDSE	Bridge Design Supervising Engineer
BDM	Bridge Design Manual

C

CALTRANS	California Department of Transportation
CDL	Construction Dead Loads
CIP	Cast-In-Place
CLL	Construction Live Loads
ConnDOT	Connecticut Department of Transportation

D

DOT	Department of Transportation
DC	Component Loads
DW	Dead Load of Wearing Surfaces and Utilities

F

FDOT	Florida Department of Transportation
FE	Finite Element
FEA	Finite Element Analysis
FHWA	Federal Highway Administration

I

INDOT	Indiana Department of Transportation

K

KDOT	Kansas Department of Transportation

L

LFD	Load Factor Design
LRFD	Load and Resistance Factor Design

LRFR	Load and Resistance Factor Rating
LTB	Lateral Torsional Buckling
M	
MBE	Manual for Bridge Evaluation
MDOT	Michigan Department of Transportation
N	
NCDOT	North Carolina Department of Transportation
NCHRP	National Cooperative Highway Research Program
NHI	National Highway Institute
NJDOT	New Jersey Department of Transportation
NLF	No Load Fit
NSBA	National Steel Bridge Alliance
NYSDOT	New York State Department of Transportation
O	
ODOT	Ohio Department of Transportation
P	
PC	Prestressed Concrete
PCI	Prestressed Concrete Institute
PennDOT	Pennsylvania Department of Transportation
PLQA	Program Level Quality Assurance
Q	
QA	Quality Assurance
QAI	Quality Assurance Inspector
QA/QC	Quality Assurance and Quality Control
R	
RAP	Research Advisory Panel
RLOA	Required Level of Analysis
R.O.W.	Right of Way
S	
SCDOT	South Carolina Department of Transportation
SDL	Steel Dead Load
SDLF	Steel Dead Load Fit

SGLSL	Single Girder Line Straight Line
SIP	Stay-In-Place
SP	Simplified Procedure
T	
TAEG	Torsional Analysis of Exterior Girders
TDL	Total Dead Load
TDLF	Total Dead Load Fit
TxDOT	Texas Department of Transportation
T&C	Tension and/or Compression
U	
UDOT	Utah Department of Transportation
UT	University of Texas
V	
VBA	Visual Basic for Applications
VDOT	Virginia Department of Transportation
W	
WS	Wind Loads

APPENDIX B:
CONSTRUCTABILITY CHECKLIST ITEMS

This appendix provides a brief description of constructability checklist items presented in Table 2-1.

- **Access:** Evaluates access conditions for the surroundings and public services during and after construction.
- **Bases and Pavements:** Evaluates various aspects of pavement and subbase applications for roadways.
- **Constructability:** Evaluates appropriateness of existing site conditions to proposed construction activities.
- **Construction Staging:** Evaluates each step of construction sequence considering various aspects.
- **Detours:** Evaluates various aspects of alternative transportation paths to be used during construction.
- **Drainage:** Evaluates existing and proposed temporary or permanent drainage structures in construction site and their related aspects.
- **Earthwork:** Evaluates various aspects of earthwork activities (cut and fill), material disposal and removal plans, and clearing and grubbing of trees.
- **Environmental:** Evaluates the impact of the proposed construction plan to the environment, evaluates and requests needed environmental permissions.
- **Erosion Control/Landscaping:** Evaluates the need and implementation of erosion control activities and landscape plans near the construction site.
- **Future Work/Maintenance:** Evaluates various aspects of projects considering the potential maintenance actions.
- **General/Incidentals:** Evaluates various aspects of project. Check items under these categories are generally either too broad or not appropriate for other categories.
- **Guardrail:** Evaluates various aspects of guardrail installations.
- **Maintenance of Traffic:** Evaluates various aspects of maintaining traffic during construction.
- **Pay Items:** Evaluates the accuracy and the completeness of pay items in project plans.
- **Plan Content:** Evaluates accuracy and completeness of project plan content.
- **Railroad:** Evaluates various aspects of railroad construction projects.

- **Reconstructability:** Evaluates various aspects of projects with respect to implementation easiness in case of the same project is reconstructed in future.
- **Removal/Demolition:** Evaluates construction site for the demolition, and the impacts of the demolition to the surroundings.
- **Right of Way:** Evaluates the agreement between proposed site and existing right of way.
- **Roadway:** Evaluates accuracy and completeness of roadway plans.
- **Schedule:** Evaluates the proposed schedule of construction.
- **Signs/Signals/Electrical:** Evaluates the need and implementation of signs, signals, and temporary control devices during and after the construction.
- **Site Investigation:** Evaluates the agreement between project plans and current site conditions that may impact construction.
- **Sound Walls:** Evaluates the need and implementation of sound walls.
- **Special Materials/Conditions:** Evaluates the use of special materials and technologies needed for the contract, as well as the existence of hazardous materials.
- **Staffing:** Evaluates the need for specialized personnel and the cost.
- **Structure Rehabilitation:** Evaluates various aspects of structure rehabilitation projects.
- **Structures:** Evaluates the impact of bridges, culverts, walls, and their components on construction activities.
- **Surveying:** Evaluates needs and completeness of site surveys.
- **Utilities:** Evaluates the need of utility management and coordination.
- **Vertical Construction:** Evaluates various aspects of vertical construction projects. Bridge and culvert projects are classified as horizontal construction.

APPENDIX C:
WIND LOAD CALCULATION

Calculation of Wind Loads during Construction

MDOT

Project:

Checked by:

Date:

Legend: *The following formats and color coding are used to identify commentary, input variables, references, and results and design checks presented in this document.*

Commentary   Input Variables   **References**   Results & Design Checks

References

Primary reference(s)

AASHTO. (2017). *Guide Specifications for Wind Loads on Bridges During Construction*, 1st Edition, the American Association of State Highway and Transportation Officials, Washington, D.C.

Assumptions and Limitations

▼ Assumptions and Limitations

▲ Assumptions and Limitations

Notes

Input Variables

$h := 60 \cdot in$ *girder depth*

$S := 8 \cdot ft$ *girder spacing*

$Z := 60 \cdot ft$ *height of the member from ground surface*

Construction_Stage :=   *select construction stage from the pull down menu*

| Erection at Active Work Zone ⌄ |

Ground_Surface_Roughness :=   *select ground surface roughness at the site*

| Category D ⌄ |

Wind_Exposure_Category := Ground_Surface_Roughness   *wind exposure categories are selected based on the ground surface roughness, types of bridge structures*

Construction_Duration :=   *select an estimated construction duuration (first six of them considered in erected inactive work zone, lifting and active work zone erection shall be selected seperately from last two option)*

| >1-2 years ⌄ |

Girder_Type :=   *select girder section*

| Concrete I-Girders ⌄ |

Girder_for_Wind_Pressure_Analysis := 1   *select a girder for wind pressure analysis during erection. For lifting phase number of intended girder is 1.*

$G := 1$ *gust effect factor determined using a structure specified study, otherwise use 1.0*

Wind Pressure Coefficients

▼ Calculations

$$V := \begin{cases} 20 \cdot \text{mph} & \text{if Construction\_Stage} = 1 \lor \text{Construction\_Stage} = 2 \\ 115 \cdot \text{mph} & \text{otherwise} \end{cases}$$

AASHTO(2017) Figure 4.1.2.1

design for a 3-second gust wind speed as determined. 20 mph is selected for an active zone.

$$R := \begin{cases} 1.0 & \text{if Construction\_Duration} = 7 \lor \text{Construction\_Duration} = 8 \\ 1.0 & \text{if Construction\_Duration} = 6 \\ 0.65 & \text{if Construction\_Duration} = 1 \\ 0.73 & \text{if Construction\_Duration} = 2 \\ 0.75 & \text{if Construction\_Duration} = 3 \\ 0.77 & \text{if Construction\_Duration} = 4 \\ 0.84 & \text{otherwise} \end{cases}$$

AASHTO(2017) Table 4.2.1.1

wind speed reduction factor during construction

$$K_Z := \begin{cases} 0.71 & \text{if Wind\_Exposure\_Category} = 1 \land Z \le 33 \cdot \text{ft} \\ 1 & \text{if Wind\_Exposure\_Category} = 2 \land Z \le 33 \cdot \text{ft} \\ 1.15 & \text{if Wind\_Exposure\_Category} = 3 \land Z \le 33 \cdot \text{ft} \\ \dfrac{\left(2.5 \cdot \ln\left(\dfrac{Z}{0.9834 \cdot \text{ft}}\right) + 6.87\right)^2}{345.6} & \text{if Wind\_Exposure\_Category} = 1 \land Z > 33 \cdot \text{ft} \\ \dfrac{\left(2.5 \cdot \ln\left(\dfrac{Z}{0.0984 \cdot \text{ft}}\right) + 7.35\right)^2}{478.4} & \text{if Wind\_Exposure\_Category} = 2 \land Z > 33 \cdot \text{ft} \\ \dfrac{\left(2.5 \cdot \ln\left(\dfrac{Z}{0.0164 \cdot \text{ft}}\right) + 7.65\right)^2}{616.1} & \text{if Wind\_Exposure\_Category} = 3 \land Z \land 33 \cdot \text{ft} \\ \text{"Mistake"} & \text{otherwise} \end{cases}$$

AASHTO(2017) Eqn. 4.2.1-2
AASHTO(2017) Eqn. 4.2.1-3
AASHTO(2017) Eqn. 4.2.1-4

wind pressure exposure and elevation coefficient

$$C_{D.base} := \begin{cases} 2.2 & \text{if } Girder\_Type = 1 \\ 2.0 & \text{if } Girder\_Type = 2 \\ \text{"Check for Other Types of Girders Sections in AASHTO"} & \text{otherwise} \end{cases}$$

AASHTO(2017) Table 4.2.1.2

wind base drag coefficient

$$C_D := \begin{cases} C_{D.base} & \text{if } Construction\_Stage = 1 \lor Girder\_for\_Wind\_Pressure\_Analysis = 1 \\ 0 & \text{if } Girder\_for\_Wind\_Pressure\_Analysis = 2 \\ 0.5 \cdot C_{D.base} & \text{if } Girder\_for\_Wind\_Pressure\_Analysis = 3 \land \frac{S}{h} > 3 \\ 0.25 \cdot C_{D.base} & \text{if } Girder\_for\_Wind\_Pressure\_Analysis = 3 \land \frac{S}{h} \le 3 \\ 0.5 \cdot C_{D.base} & \text{if } Girder\_for\_Wind\_Pressure\_Analysis = 4 \land \frac{S}{h} > 3 \\ 0.25 \cdot C_{D.base} & \text{if } Girder\_for\_Wind\_Pressure\_Analysis = 4 \land \frac{S}{h} \le 3 \\ 0.5 \cdot C_{D.base} & \text{otherwise} \end{cases}$$

AASHTO(2017) Table 4.2.1.3

wind drag coefficient

$V = 20 \cdot mph$ $\quad\quad$ $R = 0.75$ $\quad\quad$ $K_Z = 1.287$ $\quad\quad$ $C_D = 2$

▲ Calculations

Wind Pressure Acting on the Girder

$$P_z := 2.56 \cdot 10^{-6} \cdot ksf \cdot \left(\frac{V}{mph}\right)^2 \cdot R^2 \cdot K_Z \cdot G \cdot C_D \cdot h = 7.415 \cdot plf$$ $\quad\quad$ *lateral wind load*

$$W_{pressure} := 2.56 \cdot 10^{-6} \cdot ksf \cdot \left(\frac{V}{mph}\right)^2 \cdot R^2 \cdot K_Z \cdot G \cdot C_D = 1.483 \cdot psf$$ $\quad\quad$ *lateral wind pressure*

APPENDIX D:

TOP FLANGE BENDING STRESS ANALYSIS DURING LIFTING

Top Flange Bending Stress Analysis during Lifting

MDOT

Project:

Checked by:

Date:

Legend: *The following formats and color coding are used to identify commentary, input variables, references, and results and design checks presented in this document.*

Commentary   Input Variables   **References**   Results & Design Checks

References

Primary reference(s)

FHWA. (2015). *Engineering for Structural Stability in Bridge Construction*, NHI Course Number 130102 Reference Number, the Federal Highway Administration, Washington, D.C.

▼ Supplemental Reference(s)

Stith, J. C. (2010a). *Predicting the Behavior of Horizontally Curved I-Girders during Construction*, Doctoral Dissertation, Department of Civil, Architectural, and Environmental Engineering, the University of Texas at Austin, Austin, Texas.

UT Lift. (2019). "UT Lift 1.3-a spreadsheet provided as a tool to an engineer when deciding the safety of lifting a horizontally curved steel I-girder with one crane and two lift clamps." <https://fsel.engr.utexas.edu/facilities/software/software>(Last accessed: Sept. 9, 2019)

▲ Supplemental Reference(s)

Assumptions and Limitations

▼ Assumptions and Limitations

- Beam clamps grip the girder at each side of the top flange.
- Bending stress is distributed over an effective flange length. The corresponding region is analyzed as a cantilever beam **(FHWA 2015).**
- The procedure provides a conservative estimation that aids for minimizing top flange distortion **(FHWA 2015).**

▲ Assumptions and Limitations

Notes

Input Variables

$b_f := 11.5 \cdot in$ *top flange width*

$C_L := 3 \cdot in$ *length of beam clamp along top flange*

$F_{yf} := 50 \cdot ksi$ *specified minimum flange yield stress*

$k := 1.44 \cdot in$ *distance from outer face of top flange to web toe fillet*

$R_c := 28.4 \cdot kip$ *beam clamp force*
Note: clamp forces are equal to half of the total weight if the distance between girder center of gravity and lifting points is equal **(Stith 2010a)**. *Use* **(UT Lift 2019)** *to estimate clamp forces for other cases.*

$t_f := 0.74 \cdot in$ *top flange thickness*

Top Flange Bending Stresses

$$f_{lb} := 1.25 \frac{\dfrac{R_c}{2} \cdot k}{\left[\dfrac{(b_f + C_L) \cdot t_f^2}{6}\right]} = 19.314 \cdot ksi$$ *flange local bending stress factored for Strength Load Combinations*   **FHWA (2015)**

$$Check\_f_{lb} := if\left(f_{lb} \leq F_{yf}, \text{"OK"}, \text{"ADD COVER PLATE"}\right) = \text{"OK"}$$

APPENDIX E:

STEEL I-GIRDER DIFFERENTIAL DEFLECTION ANALYSIS AT

THE END OF DECK PLACEMENT

Steel I-Girder Differential Deflection Analysis at the end of Deck Placement

MDOT

Project:

Checked by:

Date:

Legend: *The following formats and color coding are used to identify commentary, input variables, references, and results and design checks presented in this document.*

Commentary   Input Variables   **References**   Results & Design Checks

References

Primary reference(s)

Fisher, S.T. (2006). *Development of a Simplified Procedure to Predict Dead Load Deflections of Skewed and Non-Skewed Steel Plate Girder Bridges*, Master's Thesis, North Carolina State University, Raleigh, North Carolina.

▼ Supplemental Reference(s)

AASHTO. (2017). *Guide Design Specifications for Bridge Temporary Works*, 2nd Edition, the American Association of State Highway and Transportation Officials, Washington, D.C.

MDOT. (2019). *Bridge Design Manual,* the Michigan Department of Transportation, Lansing, Michigan.

▲ Supplemental Reference(s)

Assumptions and Limitations

▼ Assumptions and Limitations

- A simple-span bridge with a regular geometry (i.e., symmetry, constant girder spacing, constant deck width, uniform cross-frame spacing, etc.).
- Span length (L) < 250 feet
- Girder spacing (S) < 11.5 feet
- Girder spacing to span ratio (S/L) < 0.08
- The difference between exterior to interior girder load ratios < %10.

▲ Assumptions and Limitations

Notes

Input Variables

Bridge and Girder Geometry

$A_g := 115.94 \cdot in^2$ *cross-sectional area of girder* $b_{ov} := 36 \cdot in$ *deck overhang width* $L := 150 \cdot ft$ *span length*

$I_x := 122079 \cdot in^4$ *major axis moment of inertia* $S := 10 \cdot ft$ *girder spacing* $t_s := 9 \cdot in$ *deck thickness*

$x := 75 ft$ *distance from the support to the location along girder span at which the deflection is calculated* $\theta := 20 \cdot deg$ *skew angle*

Bridge and Girder Geometry

Material, Falsework, Formwork, and Equipment Data

$b_{sr} := 4 \cdot in$ *width of screed rail platform* $b_{wa} := 24 \cdot in$ *walkway width*

$E := 29000 \cdot ksi$ *steel elasticity modulus* $s_b := 50 \cdot in$ *overhang bracket spacing*

Material, Falsework, Formwork, and Equipment Data

Component and Construction Loads

$w_c := 150 \cdot pcf$ *unit weight of concrete*

$w_{CLL} := 50 \cdot psf$ *construction live load*   **AASHTO (2017)**

$w_g := 490 \cdot pcf$ *unit weight of steel*

$w_{of} := 15 \cdot psf$ *combined weight of overhang formwork and bracket*

$w_{SIP} := 15 \cdot psf$ *weight of stay-in-place (SIP) formwork*   **MDOT (2019)**

$w_{wa} := 15 \cdot psf$ *weight of walkway*

Component and Construction Loads

Step 1: Interior Girder Deflection Analysis

▼ Step 1 Calculations

$q_{c\_int} := w_c \cdot t_s \cdot S = 1.125 \cdot klf$ *concrete load on a girder*

$q_{CLL\_int} := w_{CLL} \cdot S = 0.5 \cdot klf$ *construction live load on a girder*

$q_g := w_g \cdot A_g = 0.395 \cdot klf$ *self-weight of a girder*

$q_{SIP\_int} := w_{SIP} \cdot S = 0.15 \cdot klf$ *SIP formwork load on a girder*

$q_{T\_int} := q_{c\_int} + q_{CLL\_int} + q_g + q_{SIP\_int} = 2.17 \cdot klf$ *total load on a girder*

$\Delta_{in} := \dfrac{q_{T\_int} \cdot x}{24 \cdot E \cdot I_x} \cdot \left(L^3 - 2 \cdot L \cdot x^2 + x^3 \right) = 6.98 \, in$ *deflection of an interior girder at the point of interest*

$\Delta_{in.max} := \dfrac{5 \cdot q_{T\_int} \cdot L^4}{384 \cdot E \cdot I_x} = 6.98 \, in$ *midspan deflection of an interior girder*

▲ Step 1 Calculations

Step 2: Exterior Girder Deflection Analysis

▼ Step 2 Calculations

$q_{c\_ext} := w_c \cdot t_s \cdot \left(\dfrac{S}{2} + b_{ov} \right) = 0.9 \cdot klf$ *concrete load on the girder*

$q_{CLL\_ext} := w_{CLL} \cdot \left(\dfrac{S}{2} + b_{ov} + b_{sr} + b_{wa} \right) = 0.517 \cdot klf$ *construction live load on the girder*

$q_{of} := w_{of} \cdot \left(b_{ov} + b_{sr} + b_{wa} \right) = 0.08 \cdot klf$ *combined load of overhang formwork and bracket on the girder*

$q_{SIP\_ext} := w_{SIP} \cdot \dfrac{S}{2} = 0.075 \cdot klf$ *SIP formwork load on the girder*

$q_{wa} := w_{wa} \cdot b_{wa} = 0.03 \cdot klf$ *walkway load on the girder*

$q_{T\_ext} := q_{c\_ext} + q_{CLL\_ext} + q_g + q_{of} + q_{SIP\_ext} + q_{wa} = 1.996 \cdot klf$ *the total load on the girder*

$$\alpha := \begin{vmatrix} 0.0002 & \text{if } S \le 8.2 \cdot ft \\ 0.0002 + 0.000305 \left(S \cdot \dfrac{1}{ft} - 8.2 \right) & \text{if } 8.2 \cdot ft < S \le 11.5 \cdot ft \end{vmatrix}$$
correction factor   **Fisher (2006)**

$$\eta_L := \frac{q_{T\_ext}}{q_{T\_int}} \cdot 100 = 92.011 \qquad \textit{exterior-to-interior girder load ratio (\%)}$$

▲ Step 2 Calculations

$$\Delta'_{ex} := \left[\frac{\Delta_{in}}{in} - \left(0.03\alpha \cdot \frac{\theta}{deg} \right) \cdot \left(100 - \eta_L \right) \right] \cdot (1 - 0.1 \cdot \tan(1.2\theta)) \cdot in = 6.666 \cdot in$$
exterior girder deflection at the location of interested

Step 3: Differential Deflection between Girders

▼ Step 3 Calculations

$$b := \begin{vmatrix} -0.08 & \text{if } \dfrac{S}{L} \le 0.05 \\ -0.08 + 8 \cdot \left(\dfrac{S}{L} - 0.05 \right) & \text{if } 0.05 < \dfrac{S}{L} \le 0.08 \end{vmatrix} = 0.053 \quad \textit{correction factor}$$
    Fisher (2006)

$$z := \left[10 \cdot \left(\frac{S}{L} - 0.04 \right) + 0.02 \right] \cdot \left(2 - 0.02 \cdot \eta_L \right) = 0.046 \qquad \textit{correction factor} \qquad \textbf{Fisher (2006)}$$

▲ Step 3 Calculations

$$\Delta_{dif} := \frac{\Delta_{in}}{\Delta_{in.max}} \cdot \left[\left(3 - b \cdot \frac{\theta}{deg} \right) \cdot \left(\frac{S}{L} - 0.04 \right) \cdot (1 + z) - 0.1 \cdot \tan(1.2 \cdot \theta) \right] \cdot in = 0.009 \, in$$

differential deflection between the exterior girder and the adjacent interior girder. Positive result indicates that the interior girder deflects more than the exterior girder.

$$\theta_d := \text{atan}\left(\frac{-\Delta_{dif}}{S} \right) = -0.004 \cdot deg \qquad \textit{overhang bracket rotation due to differential deflection}$$

$$\Delta_{deck\_d} := \left(\frac{b_{sr}}{2} + b_{ov} \right) \cdot \tan(\theta_d) = -0.003 \cdot in \qquad \textit{variation in deck profile due to differential deflection}$$

APPENDIX F:

EXTERIOR STEEL I-GIRDER WEB OUT-OF-PLANE

DEFORMATION ANALYSIS

Exterior Steel I-Girder Web Out-of-Plane Deformation Analysis

MDOT

Project:

Checked by:

Date:

Legend: *The following formats and color coding are used to identify commentary, input variables, references, and results and design checks presented in this document.*

Commentary　　Input Variables　　**References**　　Results & Design Checks

References

Primary reference(s):

Inceefe, A. (2018). *Maintaining Deck Profile in Steel I-Girder Bridges during Deck Placement*, Master's Thesis, Department of Civil and Construction Engineering, Western Michigan University, Kalamazoo, Michigan.

Assumptions and Limitations

▼ Assumptions and Limitations

- Exterior girder is designed as per the *AASHTO LRFD Specifications* and *AASHTO/NSBA G12.1 Guidelines*.
- Overhang bracket and exterior girder top flange are rigidly connected, and rotation of the bracket is equal to the rotation of top flange.
- The lateral load (P) at the bracket bearing point acts perpendicular to the web.
- Girder web complies the theory of thin plates with small deformations and Kirchhoff hypotheses.
- The representative analysis module of the girder is the web bounded by flanges and transverse stiffeners.
- Boundary conditions provided by flanges and stiffeners are considered by the adjustment factors suggested by **Inceefe (2018)**.
- Spacing between two consecutive transverse stiffeners is small compared to the girder length, and the curvature of the representative girder web is negligible.

▲ Assumptions and Limitations

Notes

Input Variables

$b_{ov} := 36 \cdot in$ *deck overhang width*

$b_{sr} := 4 \cdot in$ *width of screed rail platform*

$D := 79.25 \cdot in$ *web depth*

$d_o := 100 \cdot in$ *transverse stiffener spacing*

$E := 29000 \cdot ksi$ *steel elasticity modulus*

$H_{br} := 15.85 \cdot in$ *bracket bearing point measured from top of the bottom flange*

$P := 1976.724 \cdot lbf$ *lateral load acting on the exterior girder web at bracket bearing point. Use "Overhang Bracket Analysis.xmcd" to calculate the load.*

$t_w := 0.75 \cdot in$ *web thickness*

$y_1 := 50 \cdot in$ *position of bracket along y-axis*

$\upsilon := 0.3$ *Poisson's ratio of steel*
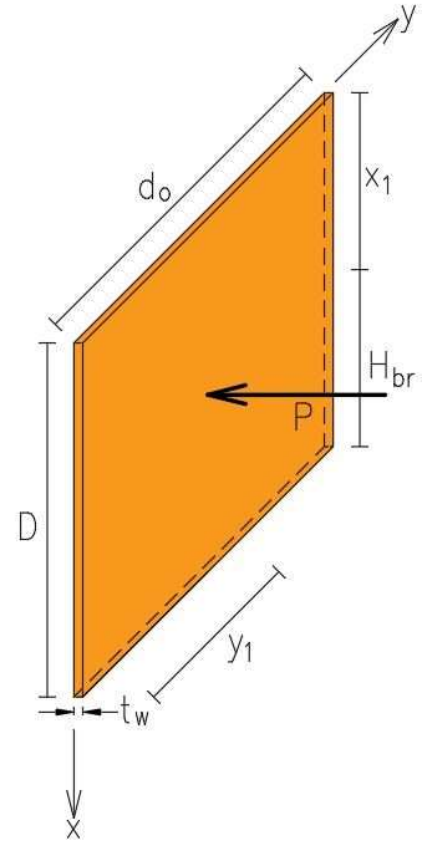
Web out-of-plane Deformation

$$D_f := \frac{E \cdot t_w^3}{12\left(1 - \upsilon^2\right)} = 1120.364 \cdot kip \cdot in \qquad \text{\textit{plate flexural rigidity}}$$

$$w(x) := \frac{4 \cdot P}{\pi^4 \cdot D_f \cdot D \cdot d_o} \cdot \sum_{m=1}^{10} \sum_{n=1}^{10} \left[\frac{\sin\left[\frac{m \cdot \pi \cdot \left(D - H_{br}\right)}{D}\right] \cdot \sin\left(\frac{n \cdot \pi \cdot y_1}{d_o}\right)}{\left[\left(\frac{m}{D}\right)^2 + \left(\frac{n}{d_o}\right)^2\right]^2} \cdot \sin\left(\frac{m \cdot \pi \cdot x}{D}\right) \cdot \sin\left(\frac{n \cdot \pi \cdot y_1}{d_o}\right) \right]$$

exterior girder web out-of-plane deformation along the web depth

$$\alpha_p := \begin{array}{|l l}
0.3 & \text{if } 0.5 \cdot D \le D - H_{br} < 0.6D \\
0.275 & \text{if } 0.6 \cdot D \le D - H_{br} < 0.7D \\
0.25 & \text{if } 0.7 \cdot D \le D - H_{br} < 0.8D \\
0.2 & \text{if } 0.8 \cdot D \le D - H_{br} < 0.9D \\
0.125 & \text{if } 0.9 \cdot D \le D - H_{br} < D
\end{array}$$

$= 0.2$ *adjustment factors accounting for boundary conditions provided by flanges and stiffeners*   **Inceefe (2018)**

$$\theta_{we}(x) := \alpha_p \cdot \frac{d}{dx} w(x)$$

$\theta_{we}(0) = 0.026 \cdot deg$ *overhang bracket rotation due to web out-of-plane deformation*

$$\Delta_{deck\_we} := \left(\frac{b_{sr}}{2} + b_{ov} \right) \cdot \tan\left(\theta_{we}(0) \right) = 0.017 \, in$$ *variation in deck profile due to web out-of-plane deformation*

APPENDIX G:

OVERHANG BRACKET ANALYSIS FOR STEEL I-GIRDER BRIDGES

Overhang Bracket Analysis for Steel I-Girder Bridges

MDOT

Project:
Checked by:
Date:

Legend: *The following formats and color coding are used to identify commentary, input variables, references, and results and design checks presented in this document.*

Commentary   Input Variables   **References**   Results & Design Checks

References

The primary reference(s):

Inceefe, A.N. (2018). *Maintaining Deck Profile in Steel I-Girder Bridges during Deck Placement*, Master's Thesis, Department of Civil and Construction Engineering, Western Michigan University, Kalamazoo, Michigan.

▼ Supplementary Reference(s)

AASHTO. (2017). *Guide Design Specifications for Bridge Temporary Works*, 2nd Edition, the American Association of State Highway and Transportation Officials, Washington, D.C.

FDOT. (2018). *Structures Design Guidelines*, the Florida Department of Transportation, Tallahassee, Florida.

MDOT. (2019). *Bridge Design Manual*, the Michigan Department of Transportation, Lansing, Michigan.

Meadow Burke. (2017). "'Bridge Technical Manual'"
<http://meadowburke.com/techmanuals/bridge.pdf> (Last accessed: June 9, 2018)

▲ Supplementary Reference(s)

Assumptions and Limitations

▼ Assumptions and Limitations

- Hanger rod, bracket diagonal and vertical legs are modeled as axially loaded members, whereas bracket beam is modeled as a flexural element.
- The angle between hanger rod and bracket is 45 degrees.
- Exterior girder web and bracket beam interface is contact-free, thus, boundary condition is not defined at the interface.
- Pin supports are defined at the top flange tip and bracket bearing point.
- Loads are caculated using tributary area. Use the maximum bracket spacing (s_b) if (s_b) is non-uniform.
- Conservatively, self-equilibrating component and construction loads on the interior side of the exterior girder are not considered.
- Screed machine load per bracket (P_{sm}) is calculated using the factors given in **Meadow Burke (2017)**.

▲ Assumptions and Limitations

Notes

Input Variables

Bridge and Girder Geometry

$b_{ov} := 36 \cdot in$ *deck overhang width* $b_{fc} := 28.25 \cdot in$ *top flange width* $D := 79.25 \cdot in$ *web depth*

$N_b := 6$ *number of girders* $S := 10 \cdot ft$ *girder spacing* $t_{fc} := 1 \cdot in$ *top flange thickness*

$t_s := 9 \cdot in$ *deck thickness* $W := (N_b - 1) \cdot S + 2 \cdot b_{ov} = 56 \cdot ft$ *bridge width*

Falsework, Formwork and Equipment Data

$b_{sm} := 3 \cdot ft$ *screed machine wheel spacing* $b_{sr} := 4 \cdot in$ *width of screed rail platform*

$b_{wa} := 24 \cdot in$ *walkway width* $n_w := 8$ *number of screed machine wheels*

$s_b := 50 \cdot in$ *overhang bracket spacing* $H_{br} := 15.85 \cdot in$ *bracket bearing point measured from the top of bottom flange*

Component and Construction Loads

$w_c := 150 \cdot pcf$ *weight of concrete*

$w_{SIP} := 15 \cdot psf$ *weight of stay-in-place (SIP) form*   **MDOT (2019)**

$w_{of} := 15 \cdot psf$ *combined weight of overhang formwork and bracket*

$w_{wa} := 15 \cdot psf$ *weight of walkway*

$w_{CLL} := 50 \cdot psf$ *construction live load*   **AASHTO (2017)**

$$P_{tsm} := \begin{vmatrix} 7 \cdot kip & if & 26 \cdot ft \le W < 32 \cdot ft \\ 11 \cdot kip & if & 32 \cdot ft \le W < 56 \cdot ft \\ 13 \cdot kip & if & 56 \cdot ft \le W < 80 \cdot ft \\ 16 \cdot kip & if & 80 \cdot ft \le W < 120 \cdot ft \end{vmatrix}$$ *total weight of screed machine, where W is the screed machine width*   **FDOT (2018)**

$$f_{sm} := \begin{vmatrix} 1 & if & \dfrac{s_b}{b_{sm}} \le 1 \\\\ 1.25 & if & 1 < \dfrac{s_b}{b_{sm}} \le 1.5 \\\\ 1.5 & if & 1.5 < \dfrac{s_b}{b_{sm}} \le 2.5 \\\\ 1.75 & otherwise \end{vmatrix}$$ *factor for the maximum screed machine load per bracket*   **Meadow Burke (2017)**

▲ Component and Construction Loads

Bracket Analysis

▼ Analysis Calculations

$P_c := w_c \cdot t_s \cdot b_{ov} \cdot s_b = 1.41 \cdot kip$ *concrete load per bracket*

$P_{CLL} := w_{CLL} \cdot (b_{ov} + b_{sr} + b_{wa}) \cdot s_b = 1.11 \cdot kip$ *construction live load per bracket*

$P_{of} := w_{of} \cdot (b_{ov} + b_{sr} + b_{wa}) \cdot s_b = 0.33 \cdot kip$ *combined overhang formwork and bracket load per bracket*

$P_{wa} := w_{wa} \cdot b_{wa} \cdot s_b = 0.13 \cdot kip$ *walkway load per bracket*

$P_{sm} := \dfrac{P_{tsm}}{n_w} \cdot f_{sm} = 2.03 \cdot kip$ *screed machine load per bracket*

$$R_{A\_x} := \dfrac{\dfrac{P_c \cdot b_{ov}}{2} + \dfrac{(P_{CLL} + P_{of}) \cdot (b_{ov} + b_{sr} + b_{wa})}{2} + P_{sm} \cdot \left(\dfrac{b_{sr}}{2} + b_{ov}\right) + P_{wa} \cdot \left(\dfrac{b_{wa}}{2} + b_{sr} + b_{ov}\right)}{\dfrac{b_{fc}}{2} + D + t_{fc} - H_{br}}$$ *horizontal reaction at the top flange*

▲ Analysis Calculations

$R_{A\_x} = 1.98\,kip$ *horizontal reaction at the top flange*

$R_{B\_x} := -R_{A\_x} = -1.98\cdot kip$ *horizontal reaction at the bracket bearing point*

$R_{A\_y} := R_{A\_x} = 1.98\,kip$ *vertical reaction at the top flange*

$R_{B\_y} := P_c + P_{CLL} + P_{of} + P_{wa} + P_{sm} - R_{A\_y} = 3.03\,kip$ *vertical reaction at the bracket bearing point*

APPENDIX H:
GLOBAL LATERAL TORSIONAL BUCKLING ANALYSIS OF I-GIRDER ASSEMBLIES

Global Lateral Torsional Buckling Analysis of I-Girder Assemblies

MDOT

Project:

Checked by:

Date:

Legend: *The following formats and color coding are used to identify commentary, input variables, references, and results and design checks presented in this document.*

Commentary   Input Variables   **References**   Results & Design Checks

References

Primary reference(s)

AASHTO. (2017). *LRFD Bridge Design Specifications*, Customary U.S. Units, 8th Edition, the American Association of State Highway and Transportation Officials, Washington, D.C.

▼ Supplemental Reference(s)

Yura, J., Helwig, T., Herman, R., and Zhou, C. (2008). "Global Lateral Buckling of I-Shaped Girder Systems." J. Struct. Eng., 134 (9), pp. 1487-1494.

▲ Supplemental Reference(s)

Assumptions and Limitations

▼ Assumptions and Limitations

- The procedure applies to straight steel I-girder assemblies with three or fewer girders.
- The assembly is not braced by other structural units and/or by external bracings within the span.
- Flange level lateral bracings are not provided.
- Girder flanges are not restrained by a hardened concrete deck.
- Girder section shall be remained the same along the span.

▲ Assumptions and Limitations

Notes

Input Variables

$b_{fc} := 13in$ *top flange width*

$b_{ft} := 13in$ *bottom flange width*

$t_{fc} := 0.75in$ *top flange thickness*

$t_{ft} := 0.75in$ *bottom flange thickness*

$D := 62in$ *web height*

$t_w := \dfrac{5}{8}in$ *web thickness*

$L := 39.94ft$ *length of the span under consideration*

$w_g := 388.5in$ *distance between the exterior girders*

$C_{bs} := 1.1$ *system moment gradient modifier for the assembly.*   **AASHTO (2017) Article 6.10.3.4.2**
1.1 for simply-supported spans, 2.0 for continuous spans.

$M_u := 30000ft \cdot kip$ *sum of the largest total factored girder moments within the span*

$E := 29000 \cdot ksi$ *steel elasticity modulus*

$$y_0 := \frac{b_{fc} \cdot t_{fc} \cdot \left(t_{ft} + D + \dfrac{t_{fc}}{2}\right) + b_{ft} \cdot t_{ft} \cdot \dfrac{t_{ft}}{2} + D \cdot t_w \cdot \left(t_{ft} + \dfrac{D}{2}\right)}{b_{fc} \cdot t_{fc} + b_{ft} \cdot t_{ft} + D \cdot t_w} = 31.75\,in$$

girder center of gravity measured from bottom fiber

$$I_x := \left\|\begin{array}{l} \dfrac{t_w \cdot D^3}{12} + 2 \cdot \left[\dfrac{b_{fc} \cdot t_{fc}^3}{12} + b_{fc} \cdot t_{fc} \cdot \left(\dfrac{D}{2} + \dfrac{t_{fc}}{2}\right)^2\right] \quad \text{if } b_{fc} = b_{ft} \wedge t_{fc} = t_{ft} \\[3em] \left\|\begin{array}{l} \dfrac{t_w \cdot D^3}{12} + t_w \cdot D \cdot \left[\left|y_0 - \left(t_{ft} + \dfrac{D}{2}\right)\right|\right]^2 + \dfrac{b_{fc} \cdot t_{fc}^3}{12} \dots \\[2em] + b_{fc} \cdot t_{fc} \cdot \left[\left|\left(t_{ft} + D + \dfrac{t_{fc}}{2}\right) - y_0\right|\right]^2 \dots \\[2em] + \dfrac{b_{ft} \cdot t_{ft}^3}{12} + b_{ft} \cdot t_{ft} \cdot \left(\left|y_0 - \dfrac{t_{ft}}{2}\right|\right)^2 \end{array}\right. \quad \text{if } b_{fc} \neq b_{ft} \vee t_{fc} \neq t_{ft} \end{array}\right. = 31609.45 \cdot in^4$$

moment of inertia about the horizontal centroidal axis of a single girder

$$I_{eff} := \left\|\begin{array}{l} \dfrac{D \cdot t_w^3}{12} + \dfrac{t_{fc} \cdot b_{fc}^3}{12} + \dfrac{t_{ft} \cdot b_{ft}^3}{12} \quad \text{if } b_{fc} = b_{ft} \wedge t_{fc} = t_{ft} \\[3em] \dfrac{t_{fc} \cdot b_{fc}^3}{12} + \dfrac{\left|y_0\right|}{\left|t_{ft} + D + t_{fc} - y_0\right|} \cdot \dfrac{t_{ft} \cdot b_{ft}^3}{12} \quad \text{if } b_{fc} \neq b_{ft} \vee t_{fc} \neq t_{ft} \end{array}\right. = 275.89 \cdot in^4$$

effective moment of inertia about the vertical centroidal axis of a single girder

Step 1: Global LTB Analysis

▼ Step 1: Calculations

$$M_{gs} := C_{bs} \cdot \frac{\pi^2 \cdot w_g \cdot E}{L^2} \cdot \sqrt{I_{eff} \cdot I_x} = 131037.38 \ \text{ft} \cdot \text{kip}$$ *the elastic global lateral-torsional buckling resistance of the girder assembly*   **AASHTO (2017) Eq. 6.10.3.4.2-1**

▲ Step 1: Calculations

$$\text{Check\_M} := \text{if}\left(M_u \leq 0.7 M_{gs}, \text{"OK"}, \text{"Not OK"}\right) = \text{"OK"}$$ *the factored moment check with global buckling resistance moment*

If $M_u > 0.7 M_{gs}$ the following alternatives can be considered;   **AASHTO (2017) Article 6.10.3.4.2**

- *adding flange level lateral bracings adjacent to the span supports.*   **AASHTO (2017) Article 6.7.5.2**
- *revising girder section to increase system stiffness.*
- *amplifying second-order displacements of the span during deck placement may be evaluated to verify that they are within tolerances permitted by the Owner.*

APPENDIX I:

PC I-GIRDER LIFTING ANALYSIS

Lifting Analysis of PC I-Girders

MDOT

Project:

Checked by:

Date:

Legend: *The following formats and color coding are used to identify commentary, input variables, references, and results and design checks presented in this document.*

Commentary Input Variables **References** Results & Design Checks

References

Primary reference(s):

PCI. (2016). *Recommended Practice for Lateral Stability of Precast, Prestressed Concrete Bridge Girders*, 1st Edition, the Precast/Prestressed Concrete Institute, Chicago, Illinois.

▼ Supplemental Reference(s)

AASHTO. (2017). *LRFD Bridge Design Specifications*, Customary U.S. Units, 8th Edition, the American Association of State Highway and Transportation Officials, Washington, D.C.

Mast, R.F. (1989). "Lateral Stability of Long Prestressed Concrete Beams - Part 1", The Precast/Prestressed Concrete Institute, PCI Journal, V.34, No.1, 34-53, Chicago, IL.

Mast, R.F. (1993). "Lateral Stability of Long Prestressed Concrete Beams - Part 2", The Precast/Prestressed Concrete Institute, PCI Journal, V.38, No.1, 70-88, Chicago, IL.

Imper, R. and Laszlo, G. (1987). "Handling and Shipping of Long Span Bridge Beams", The Precast/Prestressed Concrete Institute, PCI Journal, V.32, No.6, 86-101, Chicago, IL.

MDOT. (2019). *Bridge Design Guides*, the Michigan Department of Transportation, Lansing, Michigan.

MDOT. (2012). *Standard Specifications for Construction*, the Michigan Department of Transportation, Lansing, Michigan

▲ Supplemental Reference(s)

Assumptions and Limitations

▼ Assumptions and Limitations

- Equations use small deflection theory.
- Girders are lifted with two lifting devices.
- Lifting analysis is performed for symmetrical lifting configuration, i.e. equal distances from girder ends to lifting points.
- Calculations assume that girder sweep (e_i) occurs due to form misalignment, not due to eccentric prestressing.
- Effect of vertical wind uplift pressure is neglected.
- Factor of safety against cracking (FS_{cr}) ≥ 1.0. Factor of safety against failure (FS_f) ≥ 1.5. $FS_f = FS_{cr}$ if $FS_f < FS_{cr}$ **(Mast 1993)**.

▲ Assumptions and Limitations

Notes

Input Variables

▼ Girder Geometry

$\text{SectionData} :=$

SectionTable.xlsx

$\text{SectionType} :=$ [BT 66 x 49 ▼]   *select the section type*

The area below is needed for extracting geometrical properties of the selected section type. Do not attempt to expand this area since Mathcad does not allow expanding/collapsing of external and internal areas independently.

▶

$L := 100\,\text{ft}$ *girder length* $\Delta := 2.5\,\text{in}$ *midspan camber* $e_i := 0\,\text{in}$ *girder sweep at midspan. Type 0 if unknown.*

$$e_i := \begin{vmatrix} e_i & \text{if } e_i \neq 0 \cdot \text{in} \\ \left(\dfrac{L}{10 \cdot \text{ft}} \cdot \dfrac{1}{4} \cdot \dfrac{1}{2} \cdot \text{in} \right) & \text{if } e_i = 0 \cdot \text{in} \end{vmatrix}$$ $= 0.03$ *the sweep tolerance is used if e_i is unknown*   **MDOT (2012) Table 708-1**

▲ Girder Geometry

▼ Girder Section Properties

$A = 1118.3\,\text{in}^2$ *cross-sectional area of the girder* $h = 66\,\text{in}$ *girder depth* $b_{fc} = 49\,\text{in}$ *top flange width*

$b_{ft} = 40\,\text{in}$ *bottom flange width* $y_b = 32.9\,\text{in}$ *distance from girder centroid to the extreme bottom fiber*

$y_t = 33.1\,\text{in}$ *distance from girder centroid to the extreme top fiber* $I_x = 680229\,\text{in}^4$ *major axis moment of inertia*

$I_y = 104063.6 \, in^4$ *minor axis moment of inertia* $S_{xt} = 20550.73 \, in^3$ *major axis section modulus for top fiber*

$S_{xb} = 20675.65 \, in^3$ *major axis section modulus for bottom fiber* $S_{yt} = 4247.49 \, in^3$ *minor axis section modulus for top fiber*

$S_{yb} = 5203.18 \, in^3$ *minor axis section modulus for bottom fiber*

🔼 Girder Section Properties

🔽 Material Properties

$f'_c := 5 \, ksi$ *concrete compressive strength* $w_c := 0.145 \cdot \dfrac{kip}{ft^3}$ *unit weight of concrete* $w_g = 0.12 \, klf$ *girder weight*

$K_1 := 1$ *correction factor for the source of aggregate*   **AASHTO (2017) Article 5.4.2.4**

$$E_c := (120000 \cdot ksi) \cdot K_1 \left[\left(\dfrac{w_c}{\frac{kip}{ft^3}} \right)^2 \right] \cdot \left(\dfrac{f'_c}{ksi} \right)^{0.33} = 4291.19 \, ksi$$ *concrete modulus of elasticity*   **AASHTO (2017) Eq. 5.4.2.4-1**

$f_{ci} := 0.65 f'_c = 3.25 \, ksi$ *allowable concrete compressive stress*   **AASHTO (2017) Article 5.9.2.3.1a**

$f_{ti} := -0.24 \cdot \sqrt{f'_c \cdot ksi} = -0.54 \, ksi$ *allowable concrete tensile stress*   **AASHTO (2017) Table 5.9.2.3.1b-1**

$f_r := f_{ti} = -0.54 \, ksi$ *concrete modulus of rupture*   **AASHTO (2017) Article 5.4.2.6**

🔼 Material Properties

🔽 Lifting Parameters

$\theta_{lift} := 90 \, deg$ *lift angle from horizontal. Take 90 deg for vertical lifting. The minimum θ_{lift} shall be 60 deg.*   **MDOT (2019) Section 6.65.14B**

$W_{pressure} := 0 \, psf$ *lateral wind pressure. Use "Calculation of Wind Loads.xmcd" to estimate the value.*

$w_{wind} := W_{pressure} \cdot h = 0 \cdot plf$ *lateral wind force per unit length*

$L_{pick} := 3 \, ft$ *distance from girder ends to lifting points*

$y_{lift} := 0 \, in$ *length of lifting device rigid extension measured from top of the top flange. Use 0 in. for lifting loops.*

$e_{conn} := 0.25 \, in$ *lifting loop placement tolerance with respect to the girder centerline. Use 0.25 in. if unknown.*   **PCI (2016)**

🔼 Lifting Parameters

$N_s := 20$ *number of strands at midspan*

$e_{ps.mid} := 30in$ *eccentricity of prestressing force with respect to the girder centroid at midspan*

$f_{pu} := 270ksi$ *ultimate tensile strength of prestressing strands*

$f_{pi} := 0.70 \cdot f_{pu} = 189\,ksi$ *prestressing steel stress immediately after transfer*   **AASHTO (2017) C5.9.3.2.3a**

$A_{ps} := 0.217in^2$ *area of one strand* $d_b := 0.6in$ *diameter of one strand*

$E_{ps} := 28500 \cdot ksi$ *elasticity modulus of prestressing strands*

$f_{cgp} := \dfrac{f_{pi} \cdot N_s \cdot A_{ps}}{A} + \dfrac{f_{pi} \cdot N_s \cdot A_{ps} \cdot (e_{ps.mid})^2}{I_x} - \dfrac{w_g \cdot L^2 \cdot (e_{ps.mid})}{8 \cdot I_x} = 1.74\,ksi$ *concrete stress at the center of gravity of strands due to all applied loads*

$F_e := \left(f_{pi} \cdot A_{ps} \cdot N_s - \dfrac{E_{ps}}{E_c} \cdot f_{cgp} \cdot A_{ps} \cdot N_s \right) = 770.06 \cdot kip$ *effective prestressing force after elastic shortening loss is included*   **AASHTO (2017) Eq. 5.9.3.2.3a-1**

Girder_Strand_Pattern :=

| Straight Strands without Debonding ▼ | *choose the girder strand pattern as per design*

$L_{debonded} := 34.5ft$ *distance to end of all debonding from girder end if strands are debonded*

The area below is needed to determine the critical moment location. Do not attempt to expand this area since Mathcad does not allow expanding/collapsing of external and internal areas independently.

▶

$X = 3 \cdot ft$ *critical moment location along the girder*

Step 1: Girder Eccentricities

$P_{cr} := \dfrac{\pi^2 \cdot E_c \cdot I_y}{\left(L - 2 \cdot L_{pick} \right)^2} = 3463.84\,kip$ *critical Euler buckling load about minor axis*

$P_h := w_g \cdot \dfrac{L}{2} \tan\left(90 \cdot deg - \theta_{lift} \right) = 0\,kip$ *horizontal component of the lifting force*

$$e_{mod} := \cfrac{1}{1 - \cfrac{P_h}{P_{cr}}} = 1 \qquad \textit{lateral deflection modifier for P-}\Delta\textit{ effect}$$

$$R_e := \left(\frac{L - 2L_{pick}}{L}\right)^2 - \frac{1}{3} = 0.55 \qquad \textit{eccentricity reduction factor} \qquad \textbf{Mast (1993)}$$

$$e_{i.total} := \left(e_i \cdot R_e + e_{conn}\right) \cdot e_{mod} = 0.94 \text{ in} \qquad \textit{eccentricity due to initial sweep, lifting loop placement tolerance, and lifting angle}$$

$$y_r := \left(h - y_b - R_e \cdot \Delta\right) + y_{lift} = 31.72 \text{ in} \qquad \textit{distance to girder center of gravity measured from the roll center for the girder seated on bearings}$$

$$y_w := \frac{h}{2} + y_{lift} - R_e \cdot \Delta = 31.62 \text{ in} \qquad \textit{distance to girder midheight measured from the roll center for the girder seated on bearings}$$

$$z_{wind} := \frac{w_{wind} \cdot e_{mod}}{12 \cdot E_c \cdot I_y \cdot L} \cdot \left[\frac{1}{10} \cdot \left(L - 2L_{pick}\right)^5 - L_{pick}^2 \cdot \left(L - 2L_{pick}\right)^3 \dots \atop + 3 \cdot L_{pick}^4 \cdot \left(L - 2L_{pick}\right) + \frac{6}{5} \cdot L_{pick}^5 \right] = 0 \cdot \text{in} \qquad \textit{eccentricity of the lifted girder due to lateral wind deflection} \qquad \textbf{Mast (1989)}$$

$$z_0 := \frac{w_g \cdot e_{mod}}{12 \cdot E_c \cdot I_y \cdot L} \cdot \left[\frac{1}{10} \cdot \left(L - 2L_{pick}\right)^5 - L_{pick}^2 \cdot \left(L - 2L_{pick}\right)^3 \dots \atop + 3 \cdot L_{pick}^4 \cdot \left(L - 2L_{pick}\right) + \frac{6}{5} \cdot L_{pick}^5 \right] = 0.27 \text{ in} \qquad \textbf{Mast (1989)}$$

lateral deflection of the girder seated on bearings due to girder weight acting in the weak axis direction

$$e_{wind} := \frac{w_{wind} \cdot y_w}{w_g} = 0 \cdot \text{in} \qquad \textit{lateral eccentricity due to wind load}$$

▲ Step 1 Calculations

Step 2: Girder Stresses

▼ Step 2 Calculations

$$M_g := \frac{w_g \cdot L}{2} \cdot \left(X - L_{pick}\right) - \frac{w_g \left(X^2\right)}{2} = -0.52 \cdot \text{kip} \cdot \text{ft} \qquad \textit{major axis moment due to self-weight at harping point}$$

$$M_{wind} := \frac{w_{wind} \cdot L}{2} \cdot \left(X - L_{pick}\right) - \frac{w_{wind} X^2}{2} = 0 \cdot \text{kip} \cdot \text{ft} \qquad \textit{minor axis moment due to wind load at harping point}$$

$$f_{t.wr} := F_e \cdot \left(\frac{1}{A} - \frac{e_{ps.mid}}{S_{xt}}\right) + \frac{M_g}{S_{xt}} + \frac{M_{wind}}{S_{yt}} + P_h \cdot \left(\frac{1}{A} + \frac{y_r}{S_{xt}}\right) = -0.44 \text{ ksi} \qquad \textit{stress in extreme top fiber at harping point for wind from right}$$

$$f_{t.wl} := F_e \cdot \left(\frac{1}{A} - \frac{e_{ps.mid}}{S_{xt}} \right) + \frac{M_g}{S_{xt}} - \frac{M_{wind}}{S_{yt}} + P_h \cdot \left(\frac{1}{A} + \frac{y_r}{S_{xt}} \right) = -0.44 \, ksi$$

stress in extreme top fiber at harping point for wind from left

$$f_{b.wr} := F_e \cdot \left(\frac{1}{A} + \frac{e_{ps.mid}}{S_{xb}} \right) - \frac{M_g}{S_{xb}} - \frac{M_{wind}}{S_{yb}} + P_h \cdot \left(\frac{1}{A} - \frac{y_r}{S_{xb}} \right) = 1.81 \, ksi$$

stress in extreme bottom fiber at harping point for wind from right

$$f_{b.wl} := F_e \cdot \left(\frac{1}{A} + \frac{e_{ps.mid}}{S_{xb}} \right) - \frac{M_g}{S_{xb}} + \frac{M_{wind}}{S_{yb}} + P_h \cdot \left(\frac{1}{A} - \frac{y_r}{S_{xb}} \right) = 1.81 \, ksi$$

stress in extreme bottom fiber at harping point for wind from left

$$e_{h.pick} := \left[\left(\frac{L - 2 \cdot L_{pick}}{L} \right)^2 - \left(\frac{L - 2 \cdot X}{L} \right)^2 \right] = 0$$

lateral eccentricity of the horizontal component of the tension force from the roll axis to the harping point

$$\theta_{eq.wr} := \frac{e_{i.total} - z_{wind} + e_{wind}}{y_r - z_0} = 0.03 \cdot rad$$

girder rotation at equilibrium for wind from right

$$e_{h.wr} := e_{conn} \cdot e_{mod} + \left(e_i \cdot R_e \cdot e_{mod} - z_{wind} \right) \cdot e_{h.pick} = 0.25 \, in$$

eccentricity of lateral deflection for wind from right

$$f_{b.f.wr} := f_{b.wr} + \frac{\left(M_g + P_h \cdot z_0 \right) \cdot \theta_{eq.wr}}{S_{yb}} + \frac{P_h \cdot e_{h.wr}}{S_{yb}} = 1.81 \, ksi$$

stress in extreme bottom fiber at harping point including rotational effects for wind from right

$$f_{t.f.wr} := f_{t.wr} - \frac{\left(M_g + P_h \cdot z_0 \right) \cdot \theta_{eq.wr}}{S_{yt}} - \frac{P_h \cdot e_{h.wr}}{S_{yt}} = -0.44 \, ksi$$

stress in extreme top fiber at harping point including rotational effects for wind from right

$$\theta_{eq.wl} := \frac{e_{i.total} + z_{wind} - e_{wind}}{y_r - z_0} = 0.03 \cdot rad$$

girder rotation at equilibrium for wind from left

$$e_{h.wl} := e_{conn} \cdot e_{mod} + \left(e_i \cdot R_e \cdot e_{mod} + z_{wind} \right) \cdot e_{h.pick} = 0.25 \, in$$

eccentricity of lateral deflection for wind from left

$$f_{b.f.wl} := f_{b.wl} + \frac{\left(M_g + P_h \cdot z_0 \right) \cdot \theta_{eq.wl}}{S_{yb}} + \frac{P_h \cdot e_{h.wl}}{S_{yb}} = 1.81 \, ksi$$

stress in extreme bottom fiber at harping point including rotational effects for wind from left

$$f_{t.f.wl} := f_{t.wl} - \frac{\left(M_g + P_h \cdot z_0 \right) \cdot \theta_{eq.wl}}{S_{yt}} - \frac{P_h \cdot e_{h.wl}}{S_{yt}} = -0.44 \, ksi$$

stress in extreme top fiber at harping point including rotational effects for wind from left

---

▲ Step 2 Calculations

$$Check\_f_b := if\left(\max\left(f_{b.f.wr}, f_{b.f.wl} \right) \leq f_{ci}, "OK", "Not\ OK" \right) = "OK"$$

extreme bottom fiber (compression) stress check

$$Check\_f_t := if\left(\min\left(f_{t.f.wr}, f_{t.f.wl} \right) \geq f_{ti}, "OK", "Not\ OK" \right) = "OK"$$

extreme top fiber (tension) stress check

Step 3: Factor of Safety Against Cracking

▼ Step 3 Calculations

$M_{lat.wr} := (f_{t.wr} - f_r) \cdot S_{yt} - P_h \cdot e_{h.wr} = 35.68 \cdot kip \cdot ft$ *lateral moment to cause cracking for wind from right*

$M_{lat.wl} := (f_{t.wl} - f_r) \cdot S_{yt} - P_h \cdot e_{h.wl} = 35.68 \cdot kip \cdot ft$ *lateral moment to cause cracking for wind from left*

$\theta_{cr.wr} := \dfrac{M_{lat.wr}}{|M_g| + P_h \cdot z_0} = 68.07 \cdot rad$ *rotation at cracking due to lateral deflection for wind from right*

$\theta_{cr.wl} := \dfrac{M_{lat.wl}}{|M_g| + P_h \cdot z_0} = 68.07 \cdot rad$ *rotation at cracking due to lateral deflection for wind from left*

$FS_{cr.wr} := \dfrac{y_r \cdot (\theta_{cr.wr})}{z_0 \cdot \theta_{cr.wr} - z_{wind} + e_{wind} + e_{i.total}} = 110.66$ *factor of safety against cracking for wind from right*   **Mast (1993)**

$FS_{cr.wl} := \dfrac{y_r \cdot (\theta_{cr.wl})}{z_0 \cdot \theta_{cr.wl} + z_{wind} - e_{wind} + e_{i.total}} = 110.66$ *factor of safety against cracking for wind from left*   **Mast (1993)**

▲ Step 3 Calculations

$FS_{cr} := \begin{cases} \text{"Crack Check is Not Applicable"} & \text{if } M_{lat.wr} \le 0 \lor M_{lat.wl} \le 0 \\ \min(FS_{cr.wr}, FS_{cr.wl}) & \text{otherwise} \end{cases} = 110.66$

minimum factor of safety against cracking. Note: if the tensile (top fiber) stress exceeds the allowable limit, FS_{cr} is not applicable.

$Check\_FS_{cr} := \begin{cases} \text{"OK"} & \text{if } FS_{cr} \ge 1.0 \\ \text{"Not OK"} & \text{if } FS_{cr} < 1.0 \end{cases} = \text{"OK"}$

factor of safety check against cracking. Read the above note related to FS_{cr} check.

Step 4: Factor of Safety Against Failure

▼ Step 4 Calculations

$\theta_{wr} := 0.4 \cdot rad$ *asuumed maximum girder rotation during lifting*

Given

$FS_{f.wr}(\theta_{wr}) := \dfrac{y_r \cdot (\theta_{wr})}{[z_0 \cdot (\theta_{wr}) - z_{wind} + e_{wind}] \cdot [1 + 2.5 \cdot (\theta_{wr})] + e_{i.total}}$ *factor of safety against failure for wind from right*   **Mast (1993)**

$0 \cdot rad \le \theta_{wr} \le 0.4 \cdot rad$ *allowable limit of girder rotation angle*

$\theta_{max.ult.wr} := \text{Maximize}\left(FS_{f.wr}, \theta_{wr}\right) = 0.4 \cdot rad$ *rotation angle for maximum factor of safety for wind from right*

$$\theta_{max.ult.wr.check} := \sqrt{\frac{e_{i.total} - z_{wind} + e_{wind}}{2.5 \cdot z_0}} = 1.17 \cdot rad$$ *rotation angle for wind from right*

$$FS_{f.wr} := \frac{y_r\left(\theta_{max.ult.wr}\right)}{\left[z_0 \cdot \left(\theta_{max.ult.wr}\right) - z_{wind} + e_{wind}\right] \cdot \left[1 + 2.5 \cdot \left(\theta_{max.ult.wr}\right)\right] + e_{i.total}} = 10.98$$ *factor of safety against failure for wind from right*

Given

$\theta_{wl} := 0.4 \cdot rad$ *a random value defined to support functioning of the following equation*

$$FS_{f.wl}\left(\theta_{wl}\right) := \frac{y_r\left(\theta_{wl}\right)}{\left[z_0 \cdot \left(\theta_{wl}\right) + z_{wind} - e_{wind}\right] \cdot \left[1 + 2.5 \cdot \left(\theta_{wl}\right)\right] + e_{i.total}}$$ *factor of safety against failure for wind from left*   **Mast (1993)**

$0 \cdot rad \le \theta_{wl} \le 0.4 \cdot rad$ *rotation angle range*

$\theta_{max.ult.wl} := \text{Maximize}\left(FS_{f.wl}, \theta_{wl}\right) = 0.4 \cdot rad$ *rotation angle for maximum factor of safety for wind from left*

$$\theta_{max.ult.wl.check} := \sqrt{\frac{e_{i.total} + z_{wind} - e_{wind}}{2.5 \cdot z_0}} = 1.17 \cdot rad$$ *rotation angle check for wind from left*

$$FS_{f.wl} := \frac{y_r\left(\theta_{max.ult.wl}\right)}{\left[z_0 \cdot \left(\theta_{max.ult.wl}\right) + z_{wind} - e_{wind}\right] \cdot \left[1 + 2.5 \cdot \left(\theta_{max.ult.wl}\right)\right] + e_{i.total}} = 10.98$$ *factor of safety against failure for wind from left*

▲ Step 4 Calculations

$$FS_{f.mod} := \begin{vmatrix} \min\left(FS_{cr.wr}, FS_{cr.wl}\right) & \text{if } \min\left(FS_{f.wr}, FS_{f.wl}\right) \le \min\left(FS_{cr.wr}, FS_{cr.wl}\right) \\ \min\left(FS_{f.wr}, FS_{f.wl}\right) & \text{if } FS_{cr} = \text{"Crack Check is Not Applicable"} \\ \min\left(FS_{f.wr}, FS_{f.wl}\right) & \text{otherwise} \end{vmatrix}$$ *modified FS$_f$ if required*   **Mast (1993)**

$\text{Check\_FS}_f := \text{if}\left(FS_{f.mod} \ge 1.5, \text{"OK"}, \text{"Not OK"}\right) = \text{"OK"}$ *factor of safety check against failure*

APPENDIX J:
PC I-GIRDER ERECTION ANALYSIS

MDOT

Project:

Checked by:

Date:

Legend: *The following formats and color coding are used to identify commentary, input variables, references, and results and design checks presented in this document.*

Commentary   Input Variables   **References**   Results & Design Checks

References

Primary reference(s):

PCI. (2016). *Recommended Practice for Lateral Stability of Precast, Prestressed Concrete Bridge Girders*, 1st Edition, the Precast/Prestressed Concrete Institute, Chicago, Illinois.

▼ Supplemental Reference(s)

AASHTO. (2017). *LRFD Bridge Design Specifications*, Customary U.S. Units, 8th Edition, the American Association of State Highway and Transportation Officials, Washington, D.C.

NCHRP. (2008). *Rotation Limits for Elastomeric Bearings*, NCHRP Report 596, the National Cooperative Highway Research Program, Washington, D.C.

NCHRP. (2008). *Rotation Limits for Elastomeric Bearings Appendixes*, NCHRP Report 596, the National Cooperative Highway Research Program, Washington, D.C.

Mast, R.F. (1989). "Lateral Stability of Long Prestressed Concrete Beams - Part 1", The Precast/Prestressed Concrete Institute, PCI Journal, V.34, No.1, 34-53, Chicago, IL.

Mast, R.F. (1993). "Lateral Stability of Long Prestressed Concrete Beams - Part 2", The Precast/Prestressed Concrete Institute, PCI Journal, V.38, No.1, 70-88, Chicago, IL.

Imper, R. and Laszlo, G. (1987). "Handling and Shipping of Long Span Bridge Beams", The Precast/Prestressed Concrete Institute, PCI Journal, V.32, No.6, 86-101, Chicago, IL.

Yeoh, O. H. (1993). "Some forms of the strain energy function for rubber", Rubber Chemistry and Technology Journal, November, Vol. 66, No. 5, 754-771, Akron, Ohio.

MDOT. (2019). *Bridge Design Guides*, The Michigan Department of Transportation, Lansing, Michigan.

MDOT. (2012). *Standard Specifications for Construction*, The Michigan Department of Transportation, Lansing, Michigan.

▲ Supplemental Reference(s)

Assumptions and Limitations

- Equations use small deflection theory.
- Wind pressure on a single girder is considered during active construction.
- Wind pressure on multiple girders is considered during inactive construction.
- Effect of vertical wind uplift pressure is neglected during active construction (Single girder seating)**(PCI 2016)**.
- The drag coefficient of 0.3 is used to calculate uplift pressure during extreme wind effects **(PCI 2016)**.
- Calculations assume that girder sweep (e_i) occurs due to form misalignment, not due to eccentric prestressing.
- Factor of safety against cracking (FS_{cr}) ≥ 1.0. Facto of safety against failure (FS_f) ≥ 1.5. $FS_f = FS_{cr}$ if $FS_f <$ FS_{cr}, **(Mast 1993)**.

Notes

Input Variables

▼ Girder Geometry

SectionData :=
SectionTable.xlsx

SectionType := BT 54 x 61 ▾   *select the girder*

The area below is needed for extracting geometrical properties of the selected girder cross-section. Do not attempt to expand this area since Mathcad does not allow expanding/collapsing of external and internal areas independently.

▶

$L := 100 \cdot ft$ *girder length* $b_{chamfer} := 0.75 \cdot in$ *bottom flange chamfer*

$n_{girders} := 6$ *number of girders in the span* $e_i := 0 \cdot in$ *girder sweep at midspan. Type 0 if unknown.*

$\Delta := 2.5 \cdot in$ *midspan camber when the girder is seated on bearings*

$e_i := \begin{vmatrix} e_i & \text{if } e_i \neq 0 \cdot in \\ \left(\dfrac{L}{10 \cdot ft} \cdot \dfrac{1}{4} \cdot \dfrac{1}{2} \cdot in \right) & \text{if } e_i = 0 \cdot in \end{vmatrix}$ $= 0.03$ *the sweep tolerance is used if e_i is unknown*   **MDOT (2012) Table 708-1**

,

$e_{i.total} := 1 \cdot in + e_i = 2.25 \ in$ *assumed lateral deflection of girder (1 in. plus full sweep tolerance)*

▲ Girder Geometry

▼ Girder Section Properties

$A = 1076.4 \ in^2$ *cross-sectional area of the girder* $h = 54 \ in$ *girder depth* $b_{fc} = 61 \ in$ *top flange width*

$b_{ft} = 40 \ in$ *bottom flange width* $y_b = 28.2 \ in$ *distance from girder centroid to the extreme bottom fiber*

$y_t = 25.8 \ in$ *distance from girder centroid to the extreme top fiber* $I_x = 443668 \ in^4$ *major axis moment of inertia*

$I_y = 143899.8 \ in^4$ *minor axis moment of inertia* $S_{xt} = 17196.43 \ in^3$ *major axis section modulus for top fiber*

$S_{xb} = 15732.91 \ in^3$ *major axis section modulus for bottom fiber* $S_{yt} = 4718.03 \ in^3$ *minor axis section modulus for top fiber*

$S_{yb} = 7194.99 \ in^3$ *minor axis section modulus for bottom fiber*

▲ Girder Section Properties

▼ Material Properties

$f'_c := 8 \cdot ksi$ *concrete compressive strength*

$K_1 := 1$ *correction factor for the source of aggregate*   **AASHTO (2017) Article 5.4.2.4**

$w_g = 1.11 \ klf$ *girder weight* $w_c := 0.145 \cdot \dfrac{kip}{ft^3}$ *unit weight of concrete*

$E_c := (120000 \cdot ksi) \cdot K_1 \left[\left(\dfrac{w_c}{\frac{kip}{ft^3}} \right)^2 \right] \cdot \left(\dfrac{f'_c}{ksi} \right)^{0.33} = 5011.14 \ ksi$ *concrete modulus of elasticity*   **AASHTO (2017) Eq. 5.4.2.4-1**

$f_{ci} := 0.65 f'_c = 5.2 \, ksi$ *allowable concrete compressive stress*   **AASHTO (2017) Article 5.9.2.3.1a**

$f_{ti} := -0.24 \cdot \sqrt{f'_c \cdot ksi} = -0.68 \, ksi$ *allowable concrete tensile stress*   **AASHTO (2017) Table 5.9.2.3.1b-1**

$f_r := f_{ti} = -0.68 \, ksi$ *concrete modulus of rupture*   **AASHTO (2017) Article 5.4.2.6**

🔺 Material Properties
_____

🔽 Wind Loads
_____

$W_{active} := 2.65 \cdot psf$ *lateral wind pressure acting on a single unbraced girder seated on bearings. Use "Calculation of Wind Loads.xmcd" to calculate the wind pressure for active construction.*

$w_{wind.s} := W_{active} \cdot h = 11.93 \cdot plf$ *lateral force due to wind acting on a single girder*

$W_{inactive} := 46.46 \cdot psf$ *lateral wind pressure acting on multiple girders (girder assembly) seated on bearings. Use "Calculation of Wind Loads.xmcd" to calculate wind pressure for inactive construction.*

$w_{wind.m} := W_{inactive} \cdot h = 209.07 \cdot plf$ *lateral force due to wind acting on the girder assembly*

$w_{wind.up.m} := 50 \cdot plf$ *vertical (uplift) force due to wind*

$w_{wind.global.m} := w_{wind.m} \cdot \dfrac{n_{girders} + 1}{2} = 0.73 \, klf$ *total wind load resisted by the assembly (full wind on windward girder and half wind on sheltered beams).*

🔺 Wind Loads
_____

🔽 Bearing Pad Properties

$d_{brg} := 10 \cdot in$ *distance from end of girder to center of bearing* $W_{brg} := 20 \cdot in$ *length of bearing pad parallel to axis of rotation*

$n_{ri} := 6$ *number of interior elastomer layers in a bearing* $L_{brg} := 12 \cdot in$ *length of bearing pad perpendicular to the axis of rotation*

$h_{ri} := 0.5 \cdot in$ *thickness of an interior elastomer layers* $h_{brg} := 3.844 \cdot in$ *total bearing height*

$K_{bp} := 450 \cdot ksi$ *elastomer bulk modulus*   **Yeoh (1993)**

$G_{bp} := 127.5 psi$ *elastomer shear modulus (it may be taken as $E_{elastomer}/3$)*   **NCHRP-596 (2008)**

$\alpha_{cr} := 0.35$ *elastomer creep coefficient*

$S_{brg} := \dfrac{W_{brg} \cdot L_{brg}}{2 \cdot h_{ri} \cdot (W_{brg} + L_{brg})} = 7.5$ *bearing shape factor*   **NCHRP-596 (2008)**

$$I_{brg} := \frac{L_{brg} \cdot W_{brg}^{3}}{12} = 8000 \, in^{4} \qquad \text{\textit{bearing moment of inertia about its major axis}} \qquad \textbf{\textcolor{brown}{NCHRP-596 (2008)}}$$

$$\lambda := S_{brg} \cdot \sqrt{3 \cdot \frac{G_{bp}}{K_{bp}}} = 0.22 \qquad \text{\textit{bearing compressibility index}} \qquad \textbf{\textcolor{brown}{NCHRP-596 (2008)}}$$

$A_r := 1 \qquad \text{\textit{dimensionless constant for bearing rotational stiffness calculation (use}}$ \qquad \textbf{\textcolor{brown}{NCHRP-596 (2008) Appendix E}}
$\text{\textit{4/3 for infinite strip bearing)}}$

$$B_r := (0.24 - 0.024 \cdot \lambda) \, ... \qquad\qquad = 0.86 \qquad \textbf{\textcolor{brown}{NCHRP-596 (2008) Appendix F}}$$
$$+ (1.15 - 0.89 \cdot \lambda) \cdot \left[1 - e^{\left(-0.64 \cdot \frac{W_{brg}}{L_{brg}} \right)} \right] \qquad \text{\textit{dimensionless constant for bearing rotational stiffness calculation}}$$

$$K_r := 2 \cdot \frac{3 \cdot G_{bp} \cdot I_{brg}}{n_{ri} \cdot h_{ri} \cdot (1 + \alpha_{cr})} \cdot \left(A_r + B_r \cdot S_{brg}^{2} \right) = 74725.21 \cdot in \cdot kip \qquad \text{\textit{bearing rotational stiffness}} \qquad \textbf{\textcolor{brown}{NCHRP-596 (2008) Appendix F}}$$

$e_{brg} := 0.5in \qquad \text{\textit{bearing tolerance from center of girder to center of support for a single girder or the girder assembly.}}$
$\text{\textit{Use 0.5 in. if unknown.}}$

$\alpha_{seat} := 0.005 \, \dfrac{ft}{ft} \qquad \text{\textit{maximum slope angle of transverse seating tolerance beetween}}$ \qquad \textbf{\textcolor{brown}{NCHRP-596 (2008) Appendix F}}
$\text{\textit{girder and bearings}}$

▲ Bearing Pad Properties

▼ Prestressing Properties

$N_s := 30 \qquad \text{\textit{number of strands at midspan}}$

$e_{pg.mid} := 24.133 \cdot in \qquad \text{\textit{eccentricity of prestressing force with respect to the girder centroid at midspan}}$

$f_{pu} := 270ksi \qquad \text{\textit{ultimate tensile strength of prestressing strands}}$

$f_{pi} := 0.70 \cdot f_{pu} = 189 \, ksi \qquad \text{\textit{prestressing steel stress immediately after transfer}} \qquad \textbf{\textcolor{brown}{AASHTO (2017) Table 5.9.2.2-1}}$

$d_b := 0.6in \qquad \text{\textit{diameter of one strand}} \qquad A_{ps} := 0.217in^{2} \qquad \text{\textit{area of one strand}}$

$E_{ps} := 28500 \cdot ksi \qquad \text{\textit{elasticity modulus of prestressing strands}}$

$$f_{cgp} := \frac{f_{pi} \cdot N_s \cdot A_{ps}}{A} + \frac{f_{pi} \cdot N_s \cdot A_{ps} \cdot \left(e_{pg.mid} \right)^{2}}{I_x} - \frac{w_g \cdot L^{2} \cdot \left(e_{pg.mid} \right)}{8 \cdot I_x} = 1.85 \cdot ksi \qquad \text{\textit{concrete stress at the center of gravity}}$$
$$\text{\textit{of strands due to all apllied loads}}$$

$$F_e := f_{pi} \cdot A_{ps} \cdot N_s - \frac{E_{ps}}{E_c} \cdot f_{cgp} \cdot A_{ps} \cdot N_s = 1161.86 \, kip \qquad \text{\textit{Effective prestressing force after elastic}} \qquad \textbf{\textcolor{brown}{AASHTO (2017) Eq.}}$$
$$\text{\textit{shortening loss is included}} \qquad \textbf{\textcolor{brown}{5.9.3.2.3a-1}}$$

Girder_Strand_Pattern :=

Straight Strands with Debonding   *choose the girder strand pattern as per design*

$L_{debonded} := 15ft$ *distance to end of all debonding from girder end if strands are debonded*

The area below is needed to determine the critical moment location. Do not attempt to expand this area since Mathcad does not allow expanding/collapsing of external and internal areas independently.

▶

$X = 18 \cdot ft$ *critical moment location along the girder*

▲ Prestressing Properties

Eccentricities and Moments on Seated Girders

▼ Step 1 Calculations

$y_{seat} := \dfrac{h_{brg}}{2} = 1.92\,in$ *height from roll center to girder seat*

$a_{seat} := d_{brg} = 10\,in$ *distance from girder end to bearing center*

$offset_{seat} := \left(\dfrac{L - 2 \cdot a_{seat}}{L}\right)^2 - \dfrac{1}{3} = 0.63$ *eccentricity reduction factor for girders seated on bearings*   **Mast (1993)**

$e_{seat} := e_{i.total} \cdot offset_{seat} = 1.43\,in$ *eccentricity of lateral deflection (sweep) and tolerance at the time girder is seated on bearings*

$y_r := y_{seat} + y_b + offset_{seat} \cdot \Delta = 2.64 \cdot ft$ *distance to girder center of gravity measured from the roll center for the girder seated on bearings*

$y_{mid} := y_{seat} + \dfrac{h}{2} + offset_{seat} \cdot \Delta = 2.54 \cdot ft$ *distance to girder midheight measured from the roll center for the girder seated on bearings*

$z_0 := \dfrac{w_g}{12 \cdot E_c \cdot I_y \cdot L} \cdot \left[\dfrac{1}{10} \cdot \left(L - 2a_{seat}\right)^5 - a_{seat}^2 \cdot \left(L - 2a_{seat}\right)^3 + 3 \cdot a_{seat}^4 \cdot \left(L - 2a_{seat}\right) + \dfrac{6}{5} \cdot a_{seat}^5\right] = 2.04\,in$

lateral deflection of the girder seated on bearings due to girder weight acting in the weak axis direction

A Single Seated Girder:

$z_{wind.s} := \dfrac{w_{wind.s}}{12 \cdot E_c \cdot I_y \cdot L} \cdot \left[\dfrac{1}{10} \cdot \left(L - 2a_{seat}\right)^5 - a_{seat}^2 \cdot \left(L - 2a_{seat}\right)^3 + 3 \cdot a_{seat}^4 \cdot \left(L - 2a_{seat}\right) + \dfrac{6}{5} \cdot a_{seat}^5\right] = 0.02\,in$

eccentricity of the girder seated on bearings due to lateral wind deflection

$M_{g.s} := \dfrac{w_g \cdot L}{2} \cdot \left(X - a_{seat}\right) - \dfrac{w_g X^2}{2} = 774.32\,ft \cdot kip$ *moment about the major axis of the girder due to gravity load*

$$M_{wind.s} := \frac{w_{wind.s} \cdot L}{2} \cdot \left(X - a_{seat}\right) - \frac{w_{wind.s} X^2}{2} = 8.3 \cdot kip \cdot ft$$ *moment about the weak axis of the girder due to wind*

$$M_{ot.s} := L \cdot w_{wind.s} \cdot y_{mid} = 3.03 \, ft \cdot kip$$ *overturning moment on the girder due to wind. If bracing is needed see step A.4 for the overturning moment resisted by bracing for a girder on bearings*

Multiple Seated Girders:

$$z_{wind.m} := \frac{w_{wind.m}}{12 \cdot E_c \cdot I_y \cdot L} \cdot \left[\frac{1}{10} \cdot \left(L - 2a_{seat}\right)^5 - a_{seat}^2 \cdot \left(L - 2a_{seat}\right)^3 + 3 \cdot a_{seat}^4 \cdot \left(L - 2a_{seat}\right) + \frac{6}{5} \cdot a_{seat}^5\right] = 0.38 \, in$$

eccentricity due to lateral wind deflection on the girder assembly seated on bearings

$$M_{g.m} := \frac{w_g \cdot L}{2} \cdot \left(X - a_{seat}\right) - \frac{w_g X^2}{2} = 774.32 \, ft \cdot kip$$ *moment on a girder in the assembly due to gravity load*

$$M_{wind.up.m} := \frac{w_{wind.up.m} \cdot L}{2} \cdot \left(X - a_{seat}\right) - \frac{w_{wind.up.m} X^2}{2} = 34.82 \, ft \cdot kip$$

uplift moment on a girder in the assembly due to wind

$$M_{wind.m} := \frac{w_{wind.m} \cdot L}{2} \cdot \left(X - a_{seat}\right) - \frac{w_{wind.m} X^2}{2} = 145.58 \cdot kip \cdot ft$$ *lateral moment an a girder in the assembly due to wind*

$$M_{ot.m} := L \cdot w_{wind.m} \cdot y_{mid} = 53.15 \, ft \cdot kip$$ *overturning moment on a girder in the assembly due to wind*

▲ Step 1 Calculations

A. Stress and Factor of Safety Checks for A Single Girder Seating

A.1 Girder Stress Check

▼ Step A.1 Calculations

$$f_{t.s} := F_e \cdot \left(\frac{1}{A} - \frac{e_{pg.mid}}{S_{xt}}\right) + \frac{M_{g.s}}{S_{xt}} - \frac{M_{wind.s}}{S_{yt}} = -0.03 \, ksi$$ *girder extreme top fiber stress*

$$f_{b.s} := F_e \cdot \left(\frac{1}{A} + \frac{e_{pg.mid}}{S_{xb}}\right) - \frac{M_{g.s}}{S_{xb}} + \frac{M_{wind.s}}{S_{yb}} = 2.28 \, ksi$$ *girder extreme bottom fiber stress*

$$\theta_{eq.s} := \frac{K_r \cdot \alpha_{seat} + w_g \cdot L \cdot (z_{wind.s} + e_{seat}) + M_{ot.s}}{K_r - w_g \cdot L \cdot (y_r + z_0)} = 0.01 \cdot rad$$ *vertical girder rotation at equilibrium*

$$f_{b.f.s} := f_{b.s} + \frac{M_{g.s} \cdot \theta_{eq.s}}{S_{yb}} = 2.3 \, ksi$$ *stress in extreme bottom fiber at equilibrium*

$$f_{t.f.s} := f_{t.s} - \frac{M_{g.s} \cdot \theta_{eq.s}}{S_{yt}} = -0.05 \, ksi$$ *stress in extreme top fiber at equilibrium*

🔺 Step A.1 Calculations

$$\text{Check\_f}_b := if(max(f_{b.f.s}) \le f_{ci}, \text{"OK"}, \text{"Not OK"}) = \text{"OK"}$$ *extreme bottom fiber (compression) stress check*

$$\text{Check\_f}_t := if(min(f_{t.f.s}) \ge f_{ti}, \text{"OK"}, \text{"Not OK"}) = \text{"OK"}$$ *extreme top fiber (tension) stress check*

A.2 Factor of Safety Against Cracking

🔽 Step A.2 Calculations

$$M_{lat.s} := (f_{t.s} - f_r) \cdot S_{yt} = 254.35 \cdot kip \cdot ft$$ *lateral moment to cause cracking at girder top flange*

$$\theta_{cr.s} := \frac{M_{lat.s}}{|M_{g.s}|} = 0.33 \cdot rad$$ *tilt angle at cracking due to lateral deflection for a girder seated on bearings*

$$FS_{cr.s} := \frac{K_r \cdot (\theta_{cr.s} - \alpha_{seat})}{w_g \cdot L \cdot [(z_0 + y_r) \cdot \theta_{cr.s} + z_{wind.s} + e_{seat} + e_{brg}] + M_{ot.s}} = 16.27$$ **(Mast 1993)**

factor of safety against cracking for a girder seated on beaarings

🔺 Step A.2 Calculations

FS Against Cracking for Single Seated Girder:

$$FS_{cr} := \begin{vmatrix} \text{"Crack Check is Not Applicable"} & \text{if } M_{lat.s} \le 0 & = 16.27 \\ FS_{cr.s} & \text{otherwise} \end{vmatrix}$$

minimum factor of safety against cracking. Note: if the tensile (top fiber) stress exceeds the allowable limit, FS_{cr} is not applicable.

$$\text{Check\_FS}_{cr} := \begin{vmatrix} \text{"OK"} & \text{if } FS_{cr} \ge 1.0 & = \text{"OK"} \\ \text{"Not OK"} & \text{if } FS_{cr} < 1.0 \end{vmatrix}$$

factor of safety check against cracking. Read the above note related to FS_{cr} check.

A.3 Factor of Safety Against Failure

$\theta_s := 0.4 \cdot rad$ *assumed maximum girder rotation on bearings*

Given

$$FS_{f.s}(\theta_s) := \frac{K_r \cdot (\theta_s - \alpha_{seat})}{w_g \cdot L \cdot \left[\left[z_0 \cdot (\theta_s) + z_{wind.s}\right] \cdot \left[1 + 2.5 \cdot (\theta_s)\right] + 3.347 ft \cdot \theta_s + e_{seat} + e_{brg}\right] + M_{ot.s}}$$ **Mast (1993)**

factor of safety against failure for a girder seated on bearings

$0 \cdot rad \le \theta_s \le 0.4 \cdot rad$ *allowable limits of girder*

$\theta_{max.ult.s} := Maximize(FS_{f.s}, \theta_s) = 0.4 \cdot rad$ *rotation angle corresponding to the maximum factor of safety against failure*

$$FS_{f.s} := \frac{K_r \cdot (\theta_{max.ult.s} - \alpha_{seat})}{w_g \cdot L \cdot \left[\left[z_0 \cdot (\theta_{max.ult.s}) + z_{wind.s}\right] \cdot \left[1 + 2.5 \cdot (\theta_{max.ult.s})\right] + y_r \cdot \theta_{max.ult.s} + e_{seat} + e_{brg}\right] + M_{ot.s}} = 15.98$$

Mast (1993)

factor of safety against failure

$FS_{f.mod} := \begin{cases} FS_{cr} & \text{if } FS_{f.s} \le FS_{cr.s} \\ FS_{f.s} & \text{if } FS_{cr} = \text{"Crack Check is Not Applicable"} \\ FS_{f.s} & \text{otherwise} \end{cases}$ *criteria for selecting the critical factor of safety for the check*   **Mast (1993)**

$Check\_FS_f := if(FS_{f.mod} \ge 1.5, \text{"OK"}, \text{"Not OK"}) = \text{"OK"}$ *factor of safety check against failure.*

A.4 Factor of Safety Against Rollover (Cracked) for Single Girder

$z_{max} := \frac{W_{brg}}{6} - b_{chamfer} = 2.58\,in$ *horizontal distance from roll axis to the kern point of bearing pad*

$h_{roll} := \frac{h_{brg}}{2} = 1.92\,in$ *height of roll center above bearing pedestal for a girder seated on bearings*

$M_{roll} := M_{ot.s} = 3.03\,ft \cdot kip$ *overturning moment of a girder seated on bearings due to weight*

$\theta_{max.p.s} := \frac{w_g \cdot L \cdot (z_{max} - h_{roll} \cdot \alpha_{seat} - e_{brg}) + M_{roll}}{K_r} + \alpha_{seat} = 0.01$ *tilt angle at maximum resisting arm for a girder seated on bearings*

$$z_{0.p} := z_0 \cdot \left(1 + 2.5 \cdot \theta_{max.p.s}\right) = 0.17 \cdot ft$$ *lateral deflection of a girder seated on bearings due to tilt angle $\theta_{max.p.s}$*

$$FS_{roll} := \frac{K_r \cdot \left(\theta_{max.p.s} - \alpha_{seat}\right)}{w_g \cdot L \cdot \left[\left(z_{0.p}\right) \cdot \theta_{max.p.s} + y_r \cdot \theta_{max.p.s} + e_{seat} + e_{brg}\right] + M_{ot.s}} = 0.94$$

factor of safety against rollover

$$M_{ot.bs} := \frac{w_g \cdot L \cdot \left[\left(z_{0.p}\right) \cdot \theta_{max.p.s} + y_r \cdot \theta_{max.p.s} + e_{seat} + e_{brg}\right] + M_{ot.s}}{2} = 11.78 \, ft \cdot kip$$

overturning moment resisted by bracing for a girder seated on bearings

▲ Step A.4 Calculations

$$\text{Check\_FS}_{roll} := if\left(FS_{roll} \geq 1.2, \text{"OK"}, \text{"Add Bracing"}\right) = \text{"Add Bracing"}$$ *factor of safety against rollover*

B. Stress and Factor of Safety Checks for Multiple Seated Girder

B.1 Exterior Girder Stress Check

▼ Step B.1 Calculations

$$f_{t.m} := F_e \cdot \left(\frac{1}{A} - \frac{e_{pg.mid}}{S_{xt}}\right) + \frac{M_{g.m} - M_{wind.up.m}}{S_{xt}} - \frac{M_{wind.m}}{S_{yt}} = -0.41 \, ksi$$ *girder extreme top fiber stress*

$$f_{b.m} := F_e \cdot \left(\frac{1}{A} + \frac{e_{pg.mid}}{S_{xb}}\right) - \frac{M_{g.m} - M_{wind.up.m}}{S_{xb}} + \frac{M_{wind.m}}{S_{yb}} = 2.54 \, ksi$$ *girder in extreme bottom fiber stress*

$$\theta_{eq.m} := \frac{K_r \cdot \alpha_{seat} + w_g \cdot L \cdot \left(z_{wind.m} + e_{seat}\right) + M_{ot.m}}{K_r - w_g \cdot L \cdot \left(y_r + z_0\right)} = 0.02 \cdot rad$$ *vertical girder rotation at equilibrium*

$$f_{b.f.m} := f_{b.m} + \frac{M_{g.m} \cdot \theta_{eq.m}}{S_{yb}} = 2.56 \, ksi$$ *stress in extreme bottom fiber at equilibrium*

$$f_{t.f.m} := f_{t.m} - \frac{M_{g.m} \cdot \theta_{eq.m}}{S_{yt}} = -0.44 \, ksi$$ *stress in extreme top fiber at equilibrium*

▲ Step B.1 Calculations

$$\text{Check\_f}_b := if\left(\max\left(f_{b.f.m}\right) \leq f_{ci}, \text{"OK"}, \text{"Not OK"}\right) = \text{"OK"}$$ *extreme bottom fiber (compression) stress check*

$$\text{Check\_f}_t := if\left(\min\left(f_{t.f.m}\right) \geq f_{ti}, \text{"OK"}, \text{"Not OK"}\right) = \text{"OK"}$$ *extreme top fiber (tension) stress check*

B.2 Factor of Safety Against Cracking

Step B.2 Calculations

$$M_{lat.m} := \left(f_{t.m} - f_r\right) \cdot S_{yt} = 107.51 \cdot kip \cdot ft \qquad \text{\textit{lateral moment to cause cracking at girder top flange}}$$

$$\theta_{cr.m} := \frac{M_{lat.m}}{\left|M_{g.m}\right|} = 0.14 \cdot rad \qquad \text{\textit{tilt angle at cracking due to lateral deflection for the girder assembly seated on bearings}}$$

$$FS_{cr.m} := \frac{K_r \cdot \left(\theta_{cr.m} - \alpha_{seat}\right)}{w_g \cdot L \cdot \left[\left(z_0 + y_r\right) \cdot \theta_{cr.m} + z_{wind.m} + e_{seat} + e_{brg}\right] + M_{ot.m}} = 7.07 \qquad \textbf{\textcolor{red}{(Mast 1993)}}$$

<div align="center">factor of safety against cracking</div>

Step B.2 Calculations

$$FS_{cr.m} := \begin{array}{|l} \text{"Crack Check is Not Applicable"} \quad \text{if } M_{lat.m} \le 0 \quad = 7.07 \\ FS_{cr.m} \quad \text{otherwise} \end{array}$$

minimum factor of safety against cracking. Note: if the tensile (top fiber) stress exceeds the allowable limit, FS_{cr} is not applicable.

$$\text{Check\_FS}_{cr.m} := \begin{array}{|l} \text{"OK"} \quad \text{if } FS_{cr} \ge 1.0 \quad = \text{"OK"} \\ \text{"NOT OK"} \quad \text{if } FS_{cr} < 1.0 \end{array}$$

factor of safety check against cracking. Read the above note related to FS_{cr} check.

B.3 Factor of Safety Against Failure

Step B.3 Calculations

$$\theta_m := 0.4 \cdot rad \qquad \text{\textit{assumed maximum girder rotation on bearings}}$$

Given

$$FS_{f.m}\left(\theta_m\right) := \frac{K_r \cdot \left(\theta_m - \alpha_{seat}\right)}{w_g \cdot L \cdot \left[\left(z_0 \cdot \theta_m + z_{wind.m}\right) \cdot \left[1 + 2.5 \cdot \left(\theta_m\right)\right] + y_r \cdot \theta_m + e_{seat} + e_{brg}\right] + M_{ot.m}} \qquad \textbf{\textcolor{red}{Mast (1993)}}$$

<div align="right">factor of safety against failure</div>

$$0 \cdot rad \le \theta_m \le 0.4 \cdot rad \qquad \text{\textit{allowable limit of girder rotation angle}}$$

$$\theta_{max.ult.m} := \text{Maximize}\left(FS_{f.m}, \theta_m\right) = 0.4 \cdot rad \qquad \text{\textit{rotation angle corresponding to the maximum factor of safety against failure}}$$

$$FS_{f.m} := \frac{K_r \cdot \left(\theta_{max.ult.m} - \alpha_{seat}\right)}{w_g \cdot L \cdot \left[\left(z_0 \cdot \theta_{max.ult.m} + z_{wind.m}\right) \cdot \left[1 + 2.5 \cdot \left(\theta_{max.ult.m}\right)\right] + y_r \cdot \theta_{max.ult.m} + e_{seat} + e_{brg}\right] + M_{ot.m}} = 11.67$$ **Mast (1993)**

factor of safety against failure

FS Against Failure for Multiple Seated Girders :

$$FS_{f.mod} := \begin{array}{|l} FS_{cr} \ \text{if} \ FS_{f.m} \le FS_{cr.m} \\ FS_{f.m} \ \text{if} \ FS_{cr} = \text{"Crack Check is Not Applicable"} \\ FS_{f.m} \ \text{otherwise} \end{array}$$

criteria for selecting the critical factor of safety for the check   **Mast (1993)**

$$\text{Check\_FS}_f := \text{if}\left(FS_{f.mod} \ge 1.5, \text{"OK"}, \text{"NOT OK"}\right) = \text{"OK"}$$

factor of safety check against failure.

B.4 Bearing Pad Effectiveness under Service Loads

$$\theta_{bp} := 0.01 \cdot rad$$ *assumed girder rotation on bearing pad*

Given

$$1 = \frac{K_r \cdot \left(\theta_{bp} - \alpha_{seat}\right)}{w_g \cdot L \cdot \left[\left(z_0 + z_{wind.m}\right) \cdot \theta_{bp} + y_r \cdot \theta_{bp} + e_{seat} + e_{brg}\right] + M_{ot.m}}$$

make factor of safety equals to 1 to calculate θ_{bp} (tilt angle at service loads)

$$\theta_{bp} := \text{Find}\left(\theta_{bp}\right) = 0.02 \cdot rad$$ *rotation angle for determining bearing pad effectiveness under service laods*

$$SL_{bp} := \frac{W_{brg}}{6 \cdot 1.2} = 2.78 \ in$$ *maximum eccentricity at service point for the girder aseembly seated on bearings*

$$e_{bp} := \frac{w_g \cdot L \cdot \left[\left(z_0 + z_{wind.m} + y_r\right) \cdot \theta_{bp} + e_{seat} + e_{brg}\right] + M_{ot.m}}{w_g \cdot L} = 8.25 \ in$$

maximum girder eccentricity

$$\text{Check\_Full}_{brg} := \text{if}\left(SL_{bp} \ge e_{bp}, \text{"OK"}, \text{"Add Bracing"}\right) = \text{"Add Bracing"}$$

bearing pad check under service loads

B.5 Design of Bracing

▼ Step B.5 Calculations

$n_{braces} :=$

| 2 (only end bracings) ▾ |

number of bracings for a girder in the assembly seated on bearings

$e_{brace} := 0.25 \cdot in$ *imperfection (play) in each bracing. Use 0.25 in. if unknown.*

The area below is needed for determining the location where the critical moment occurs. Do not attempt to expand this area since Mathcad does not allow expanding/collapsing of external and internal areas independently.

▶

$$e_{wind.m} := \frac{\dfrac{w_{wind.m}}{12 \cdot E_c \cdot I_y \cdot L} \cdot \left[\dfrac{1}{10} \cdot (L - 2a_{seat})^5 - a_{seat}^2 \cdot (L - 2a_{seat})^3 + 3 \cdot a_{seat}^4 \cdot (L - 2a_{seat}) + \dfrac{6}{5} \cdot a_{seat}^5 \right]}{n_{girders}} \; ... = 0.69\,in$$

$$+ \frac{(n_{girders} - 1)}{2} \cdot 0.25in$$

average girder deflection in the girder assembly due to wind pressure load

$e_{total.wind} := e_{seat} + e_{wind.m} + e_{brg} = 2.61\,in$ *total girder eccentricity in the assembly*

$M_{mod} = 1$ *effective moment coefficient due to bracing, 1.0 if only end bracings are used.*

$F_{mod} = 2$ *effective resistance of bracing*

$$M_{wind.m.bracing} := M_{mod} \cdot \left[\frac{w_{wind.m} \cdot L}{2} \cdot (X - a_{seat}) - \frac{w_{wind.m} X^2}{2} \right] = 145.58 \cdot kip \cdot ft$$

lateral girder moment in the assembly due to wind loading

$$M_{ot.m.bracing} := \frac{F_{mod} \cdot \left[w_g \cdot L \cdot (z_0 \cdot \theta_{eq.m} + y_r \cdot \theta_{eq.m} + e_{seat} + e_{brg}) + M_{ot.m} \right]}{n_{braces}} = 152.67\,ft \cdot kip$$

overturning moment to be resisted by a bracing

$$F_{m.brace} := \frac{F_{mod} \cdot w_{wind.m} \cdot L}{n_{braces}} = 41.81\,kip$$ *horizontal bracing force*

Check Girder Stress with Installed Bracings

$$f_{t.m.bracing} := F_e \cdot \left(\frac{1}{A} - \frac{e_{pg.mid}}{S_{xt}} \right) + \frac{M_{g.m} - M_{wind.up.m}}{S_{xt}} - \frac{M_{wind.m.bracing}}{S_{yt}} = -0.41\,ksi$$

girder extreme top fiber stress

$$f_{b.m.bracing} := F_e \cdot \left(\frac{1}{A} + \frac{e_{pg.mid}}{S_{xb}} \right) - \frac{M_{g.m} - M_{wind.up.m}}{S_{xb}} + \frac{M_{wind.m.bracing}}{S_{yb}} = 2.54\,ksi$$

girder extreme bottom fiber stress

$\text{Check } f_b := \text{if}\left(\max\left(f_{b.m.bracing}\right) \le f_{ci}, \text{"OK"}, \text{"NOT OK"}\right) = \text{"OK"}$ *extreme bottom fiber (compression) stress check*

$\text{Check } f_t := \text{if}\left(\min\left(f_{t.m.bracing}\right) \ge f_{ti}, \text{"OK"}, \text{"NOT OK"}\right) = \text{"OK"}$ *extreme top fiber (tension) stress check*

APPENDIX K:

CHECKLISTS AND POST-CONSTRUCTION REVIEW FORM FOR INSPECTORS

Michigan Department Of
Transportation
Form **** (2020)

CONSTRUCTABILITY CHECKLIST FOR INSPECTORS
PRESTRESSED CONCRETE BRIDGES

PROJECT DESCRIPTION:

☐ Girders are supported during storage as per the plans.

☐ Girders are lifted using lifting loops. Otherwise, MDOT Engineer is consulted.

☐ Structural Fabrication Unit is consulted if cracks greater than 0.006 in. develop during storage and lifting.

☐ Girders and bearing pads are in full contact. Bearing surface flatness tolerance is met (0.125 in. per 12 in.).

☐ Girders are properly braced using hold-downs in their final position.

☐ Girders meet dimensional tolerances given in **Table 1** as girder sweep, the differential camber of adjacent box beams, etc.

☐ Strands exposed on the top flanges are cut before deck placement.

☐ Girder spacing is as intended prior to placing of the diaphragms and deck slab.

Michigan Department Of
   Transportation
Form **** (2020)

CONTROL SECTION, JOB NUMBER

CONSTRUCTABILITY CHECKLIST FOR INSPECTORS
PRESTRESSED CONCRETE BRIDGES (SUPPLEMENTARY)

Table 1 Dimensional Tolerances for Concrete Beams

Beam Type	Tolerance
Length of I-Beams and 1800 Beams	±¼ in/25 ft, 1 in max
Length of Box Beams	±¾ in
Width of I-Beams and 1800 Beams	+½ in, -⅛ in
Width of Box Beams	±½ in
Height of I-Beams, 1800 Beams, or Box Beams	+¼ in, -⅛ in
Camber Deviation From Design Value (Measured Within 24 h of Strand Release)	⅛ in/10 ft
Thickness of Top Slab of Box Beam	+½ in, -¼ in
Length of I-Beam End Blocks	+2 ft, -0 in
Sweep of I-Beams and 1800 Beams (Horizontal Deviation of Centerline from a Straight Line Between Ends Measured at Both Top and bottom)	¼ in/10 ft
Sweep of Box Beams (Horizontal Deviation of Centerline from a Straight Line Between Ends Measured at Both Top and Bottom)	⅜ in up to 60 ft, ½ in over 60 ft
Vertical Deviation of Side Forms Between Top and Bottom of Beam	≤¼ in from plan location
Prestress Strand	≤¼ in from plan location
Location of Conduit for Transverse Post Tensioning	≤½ in from plan location
Location of Holes for Position Dowels (I-beams and 1800 Beams)	≤½ in from plan location
Location of Holes for Position Dowels Box Beams	≤1 in from plan location

Michigan Department Of
Transportation
Form **** (2020)

CONSTRUCTABILITY CHECKLIST FOR INSPECTORS
STEEL I-GIRDER BRIDGES

PROJECT DESCRIPTION:

☐ Girders are lifted near quarter points.

☐ Girders are erected per the fabrication detailing. Recommended fit conditions are provided in **Table 1**.

☐ Sufficient horizontal stabilization is provided by bolting girders to substructure units, installing cross-frames as the erection progresses, placing falsework, or a combination thereof.

☐ The maximum deviation from the theoretical horizontal alignment in a span does <u>not</u> exceed ± 0.125 in. × (total length along girder between supports (ft) / 10).

☐ The maximum deviation from the theoretical vertical alignment in a span does <u>not</u> exceed + 0.25 in. × (total length from the nearest support (ft) / 10).

☐ The overhang bracket-bearing point is located close to the exterior girder bottom flange (≥ 0.9D measured from the bottom of the top flange).

☐ Wet depth measurements meet deck finish tolerances (0.125 in. per 10 ft).

Michigan Department Of
Transportation
Form **** (2020)

CONTROL SECTION, JOB NUMBER

CONSTRUCTABILITY CHECKLIST FOR INSPECTORS
STEEL I-GIRDER BRIDGES (SUPPLEMENTARY)

Table 1 Recommended Fit Conditions for Steel I-Girder Bridges

L/R*	Skew (θ) and Skew Index (Is)	Span Length	Recommended Fit Condition
≤ 0.03	θ ≤ 20°	N/A	NLF & SDLF &TDLF
	θ > 20° & Is ≤ 0.30	N/A	SDLF & TDLF
	θ > 20° & Is > 0.30	≤ 200 ft	SDLF & TDLF
		> 200 ft	SDLF
> 0.03	N/A	N/A	NLF & SDLF

Maximum L/R of any span in the bridge

Notations:

I_S = Skew index = $\dfrac{w_g \tan\theta}{L}$

L = Span length (ft)
w_g = Bridge width measured between exterior girder centerlines (ft)
NLF = No Load Fit
R = Radius of curvature (ft)
SDLF = Steel Dead Load Fit
TDLF = Total Dead Load Fit
θ = Skew angle (deg)

Definitions:

NLF = Cross-frames or diaphragms are detailed to fit to the girders in their fabricated, plumb, fully cambered position under <u>zero dead load</u>.

SDLF = Cross-frames or diaphragms are detailed to fit to the girders in their ideally plum as-deflected positions under <u>the self-weight of the steel</u> at the completion of the erection.

TDLF = Cross-frames or diaphragms are detailed to fit to the girders in their ideally plumb as-deflected positions under <u>the total dead load</u>. The total dead load typically includes the weight of the concrete deck, but not the weight of any superimposed dead loads.

Michigan Department Of
Transportation
Form **** (2020)

CONTROL SECTION, JOB NUMBER

POST-CONSTRUCTION REVIEW FORM FOR INSPECTORS

PROJECT DESCRIPTION:

☐ Construction plan is reviewed.
Describe anticipated difficulties, if any:

☐ MDOT Engineer is consulted for the contractor change requests.
Describe the change requests:

☐ The bridge is constructed as per the approved construction plans.
If not, describe the changes and associated reasons: